



ICPEAC 2017

XXX INTERNATIONAL CONFERENCE ON PHOTONIC,
ELECTRONIC AND ATOMIC COLLISIONS

CONFERENCE PROGRAM

Cairns, Tropical Queensland, Australia
26 July – 1 August, 2017

icpeac30.edu.au





Points of Interest

1 - Esplanade Lagoon

Public pool with lifeguards, barbecue facilities, WiFi and live music

2 - Reef Fleet Terminal

Tours depart to the Great Barrier Reef

3 - City Place

Assorted retail shops, tour booking, Internet access, restaurants, free entertainment

4 - Pier Market Place

Fashion labels, swimwear, precious gemstone jewellery

5 - Information Centre

Visitor information and tour booking

Conference Preferred Hotels

6 - Pullman Cairns International

7 - Park Regis City Quays

8 - Piermonde Apartments

9 - Rydges Plaza Cairns

10 - Gilligan Backpackers Hotel & Resort

11 - Novotel Cairns Oasis Resort

For more information on accommodation and rates please visit:

<http://icpeac30.edu.au/accommodation.php>

WELCOME MESSAGE



**International Conference on Photonic,
Electronic and Atomic Collisions
Message from the Minister for Tourism, Major
Events and the Commonwealth Games
The Hon. Kate Jones MP**

It is my pleasure to welcome you to the 30th International Conference on Photonic, Electronic and Atomic Collisions.

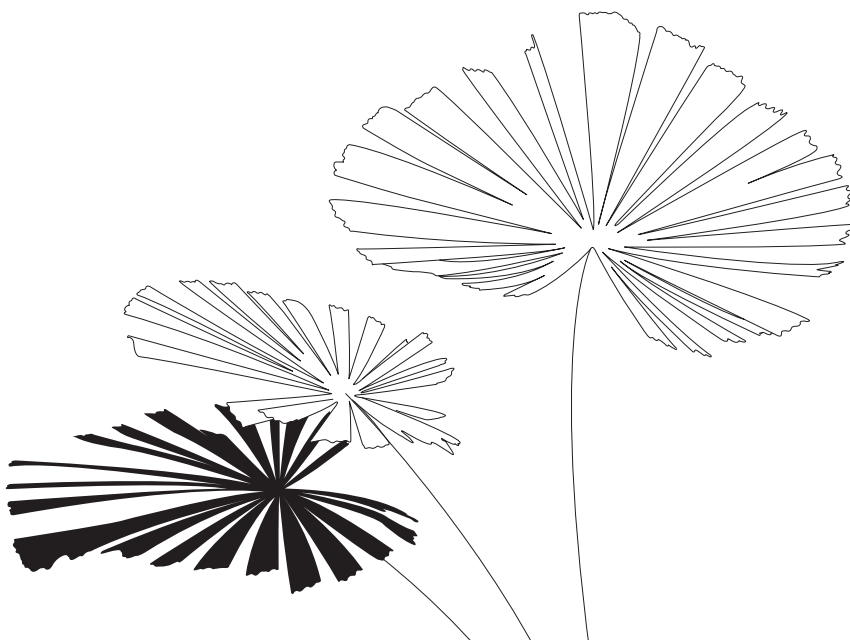
The Palaszczuk Government, through Tourism and Events Queensland, is proud to support this biennial conference in 2017 as part of our Business Events portfolio.

Bringing together hundreds of scientists from around the world for a week of plenary lectures and an exciting social program, this conference promises to be a great success.

Set amongst the mountains right on the doorstep of the Great Barrier Reef, Cairns is the perfect location for this conference, offering a range of world-class visitor experiences.

I trust you will enjoy your time in Tropical North Queensland and I wish you the best for a rewarding conference.

The Hon. Kate Jones MP
**Minister for Tourism,
Major Events and the
Commonwealth Games**



CAIRNS CONVENTION CENTRE

Conference Venue

Cairns Convention Centre,
Sheridan St & Wharf St,
Cairns City, QLD 4870
P: +61 7 4042 4200
www.cairnsconvention.com.au

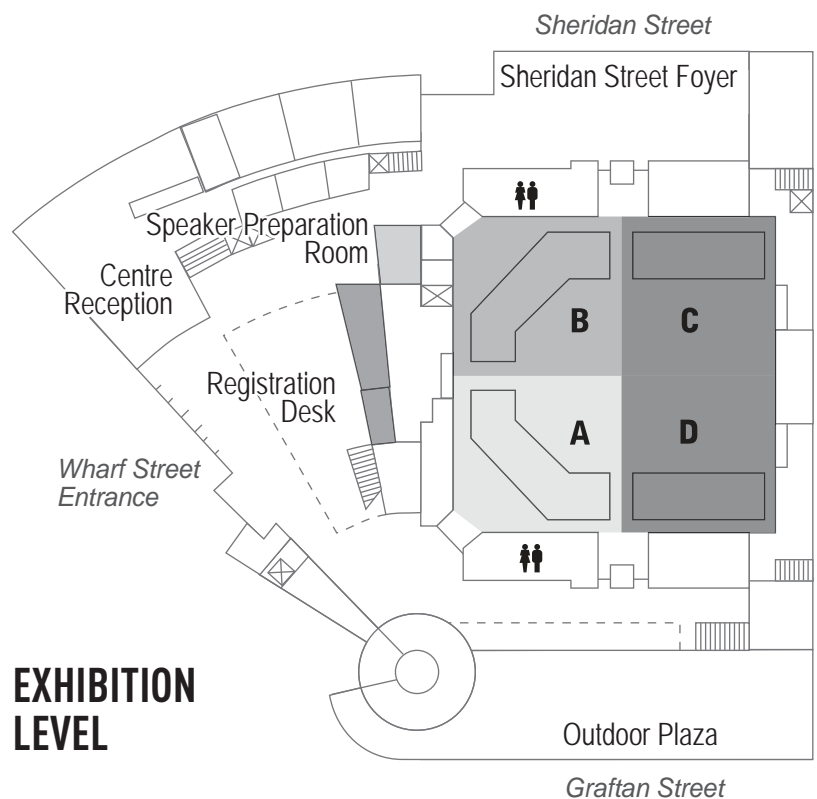
Registration Desk

The registration desk will be
open and contactable on
+61 498 435 169

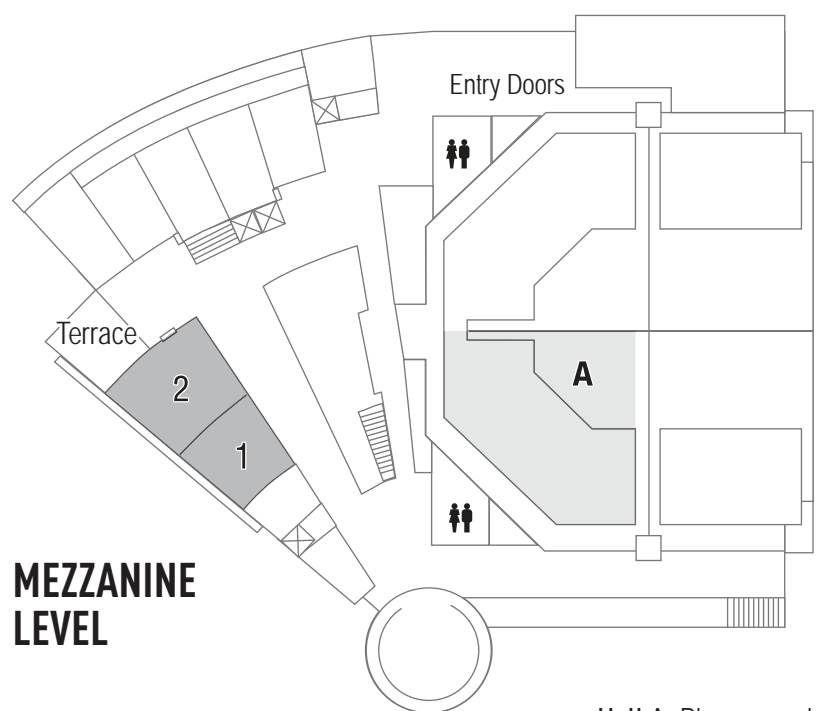
Tuesday 25 July - 13:00 – 19:00
Wednesday 26 July - 8:00 – 19:30
Thursday 27 July - 8:30 – 17:00
Friday 28 July - 8:30 – 17:00
Monday 31 July - 8:30 – 19:15
Tuesday 1 August - 8:30 – 17:00

Conference Secretariat

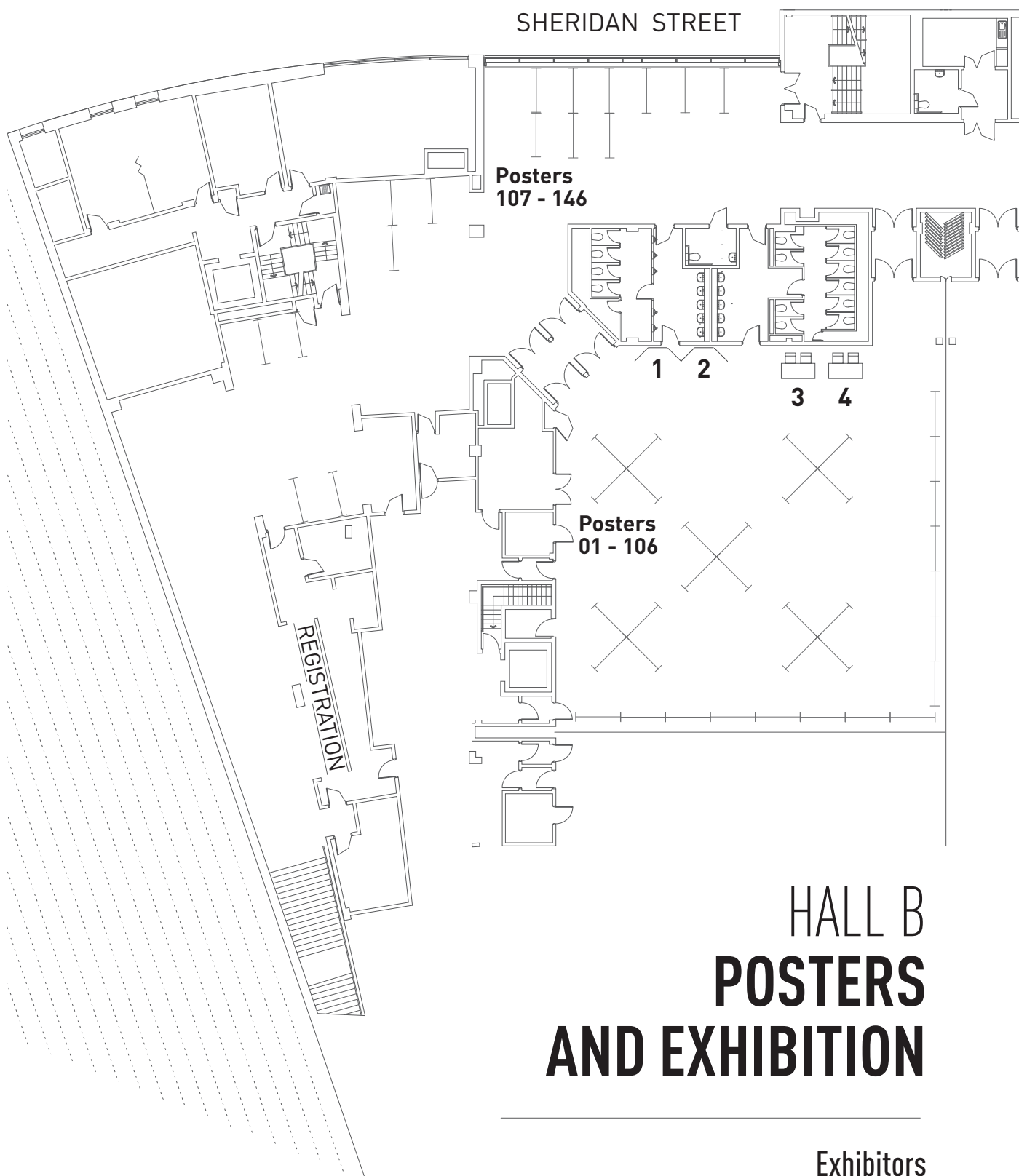
Conference Logistics
PO Box 6150
Kingston ACT 2604
phone:
+61 2 6281 6624
email:
icpeac30@conlog.com.au
web:
www.conferencelogistics.com.au



Hall A: Plenary and Parallel Sessions (A)
Hall B: Posters and Exhibition
Hall C-D: Conference Dinner



Hall A: Plenary and
Parallel Sessions (A)
Room 1-2: Parallel Sessions (B)



Exhibitors

1. Beam Imaging Solutions
2. Journal of Physics B
3. American Physical Society
4. Springer Nature

GENERAL INFORMATION

• Conference Program

Please refer to the noticeboard each morning for notification of any changes to the program. The session chair will also notify delegates of any program changes. The conference organisers cannot be held responsible for any program changes due to external or unforeseen circumstances.

• Catering

Morning and afternoon teas will be held in the exhibition area as well as in the foyers. Lunch is not included, however there are plenty of options nearby for delegates to go and purchase their lunch, a food map will be available at the registration desk.

Dietary requests will be catered for to the best of the venue's ability, please see the catering staff for assistance. Individuals with severe allergies are requested to advise Conference Logistics prior to the conference of their requirements, and bring any allergy medication (EpiPen, Phenergan, etc) as prescribed by your doctor to the conference and any associated function. Whilst due care is taken by the organisers and venue, individuals must take primary responsibility for their own health.

• Delegate List

The delegate list was emailed before and will be emailed again after the conference to all participants. Those delegates who did not give permission on their registration form have not been included.

• Internet Access

Network: CCC Convention

Password: ICPEAC17

• Luggage Cloak Room

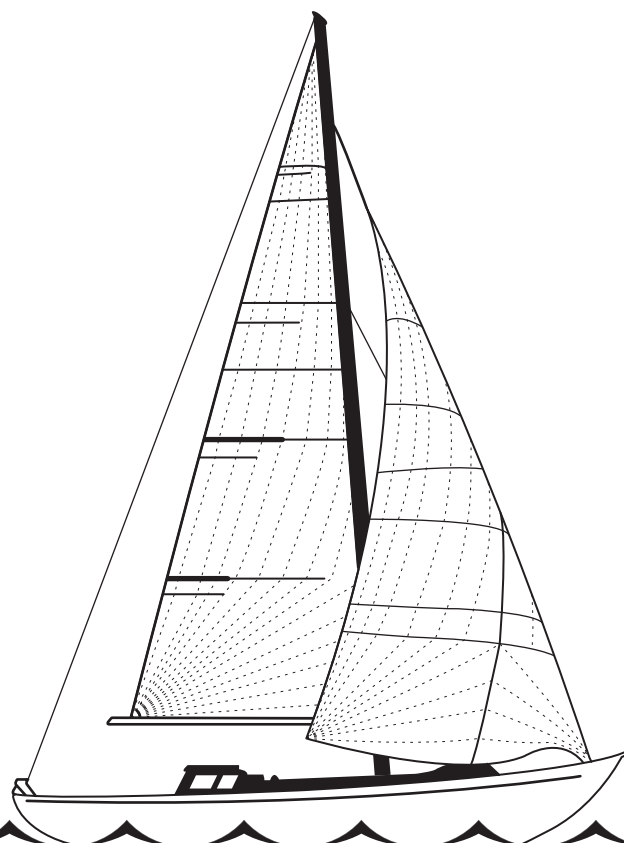
Please go to the Cairns Convention Centre administration which will operate from 08:00 – 17:30 each day.

• Mobile phones

As a courtesy to other delegates, please ensure all mobile telephones are turned off or are in silent mode during all sessions and social functions.

• Name Badge

Your name badge is your entry into the conference sessions, exhibition, morning/afternoon teas and social functions (along with a ticket). Please ensure you wear your name badge at all times and if misplaced, please see the staff at the registration desk as soon as possible.



GENERAL INFORMATION

• Non-Smoking Policy

Smoking is prohibited in all areas of the Centre other than the designated outdoor smoking area.

• Personal Insurance

Delegates shall be regarded as carrying their own risk for loss or injury to person or property in every aspect, including baggage during the conference. We strongly recommend that at the time of booking your travel and tours you take out a travel insurance policy of your choice. The policy should include the loss of deposit through cancellation, medical insurance, loss or damage to personal property, financial loss incurred through disruptions to accommodation or travel arrangements due to strikes or other industrial action. The organisers are in no way responsible for any claims concerning insurance.

• Special Needs

We endeavour to ensure delegates with special needs are catered for. Should you require particular assistance, please notify the registration desk.

• Weather

In July, the temperature in Cairns stays between the mid to high twenties (80s Fahrenheit) and the chance of rain is minimal. It is always good to take a light jacket if you are doing tours up the mountains as the mountain air can be a bit colder than in Cairns.

Useful Telephone Numbers •

Pullman Cairns International:
+61 7 4031 1300

Rydges Plaza Cairns:
+61 7 4046 0300

Novotel Cairns Oasis Resort:
+61 7 4080 1888

Park Regis City Quays:
+61 7 4042 6400

Ibis Styles Cairns:
+61 7 4051 5733

Hides Hotel Cairns:
+61 7 4051 1266

Gilligan's Backpacker Cairns
+61 7 4041 6566

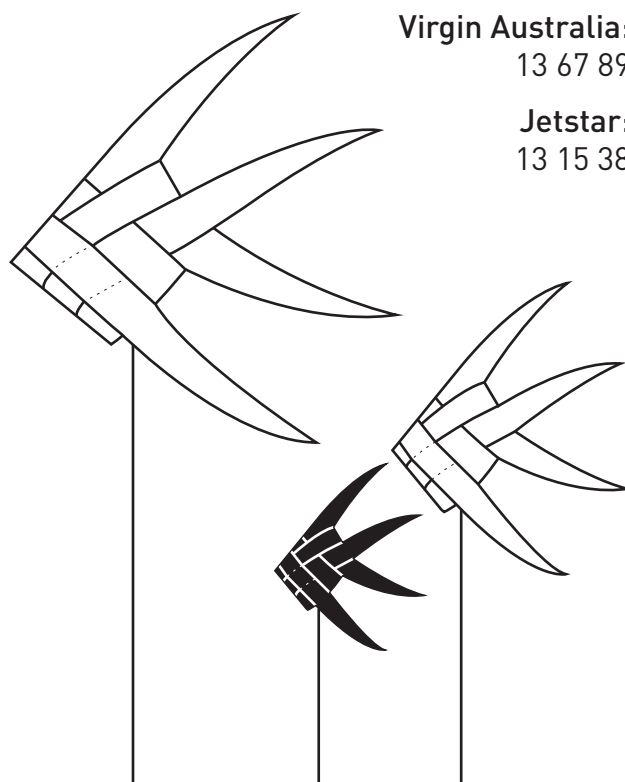
Cairns Taxis:
13 10 08

Sun Palm Transport (airport shuttle):
+61 7 4099 1191

Qantas:
13 13 13

Virgin Australia:
13 67 89

Jetstar:
13 15 38



SOCIAL PROGRAM



Welcome Reception

Time: 18:00 – 19:30

Date: Tuesday 25 July 2017

Venue: Outdoor Plaza, Cairns Convention Centre

Tickets: Included in full registration, \$50 for day registrations and additional tickets

Join us at the Outdoor Plaza to begin the conference with drinks and finger food. Network with fellow attendees and build the excitement towards the program. Highlights will include a close encounter with two iconic Australian animals and a didgeridoo performance.



Public Lecture

Time: 19:00 – 20:00

Date: Wednesday 26 July 2017

Venue: Hall A, Cairns Convention Centre

Free Access

Australia, the land of things that bite, sting and kill! Is it really that bad?

Associate Professor Jamie Seymour or the "Jelly Dude from Nemo land" has been researching and working with venomous and dangerous animals for over 20 yrs with his present interest being "Why do animals have venom?" Based in Cairns, in Northern Australia, an area that has an over abundance of venomous animals, he is uniquely placed to study the ecology and biology of Australia's venomous species.



Conference Dinner

Time: 19:00 – 22:00

Date: Monday 31 July 2017

Venue: Hall C & D, Cairns Convention Centre

Tickets: \$80 (standard), \$50 (student), \$50 (under 18)

Join us for the Conference Dinner on Monday evening. Hall C & D will be transformed into a comfortable space to eat, spend time with your colleagues and enjoy the evening.

SOCIAL PROGRAM



Weekend Tours

Take advantage of the weekend break in the middle of the conference program and reserve a place on one of the amazing tours offered through Destination Cairns Marketing to receive your special 10% discount. You can book online via:

www.cairnsconferences.com.au/events/icpeac2017 or at the tour desk during the conference.

As July and August are peak season in Cairns, it is highly recommended that you pre-book your tour to avoid disappointment.

Saturday Tours

Great Barrier Reef Adventure

Tickets:

\$208.80 (Adult), \$108.90 (Children: 4-14yrs),
\$526.50 (Family: 2Ad+2Ch)

The beauty of the Great Barrier Reef is yours to experience when you cruise from Cairns to our luxury 3 level pontoon on the Outer Reef.

Green Island Half Day:

Tickets:

\$83.70 (Adult), \$43.20 (Children: 4-14yrs),
\$210.60 (Family: 2Ad+2Ch)

Green Island is a beautiful 6000 year old coral cay located in the Great Barrier Reef Marine Park - a premier world heritage site and one of the Seven Natural Wonders of the World.

Sunday Tours

Kuranda Rail, Skyrail & Hartleys Crocodile Adventure:

Tickets:

\$175.50 (Adult), \$91.80 (Children: 4-14yrs),
\$474.30 (Family: 2Ad+2Ch)

An historical rail journey to Kuranda, enjoying breathtaking views across the cane fields of Cairns to the tropical rainforest of Kuranda.

Cape Tribulation & Daintree:

Tickets:

\$176.40 (Adult), \$111.60 (Children: 4-14yrs),
\$558 (Family: 2Ad+2Ch)

Enjoy a day exploring the rainforest and amazing landscapes of the Cape Tribulation wilderness area.

* All prices are in AUD\$
To book and/or find out more, please visit the tour desk during the conference or go online: www.cairnsconferences.com.au/events/icpeac2017

SOCIAL PROGRAM

Accompanying Persons Program

We look forward to welcoming accompanying persons to Cairns. The accompanying person registration includes entry to the Welcome Reception, morning and afternoon teas (with delegates at the conference venue), the exhibition and the public lecture. There will be a special Australian themed Accompanying Persons Welcome which is also included.

Tours on conference program days can be booked at an additional cost online via: www.cairnsconferences.com.au/events/icpeac2017 or at the tour desk during the conference.

Also it is highly recommended that you pre-book your tour to avoid disappointment.



Social Media

Join the online conversation through Twitter:

Use the hashtags:

#ICPEAC17 #exploreTNQ #thisisqueensland

Cultivate your networks through social media. Whether you are a presenter, delegate, sponsor or exhibitor, social media is a great way for you to share what is happening at the conference, comment and ask questions.

Also, feel free to share your great pictures while you are on the weekend tours enjoying what the Cairns region has to offer!

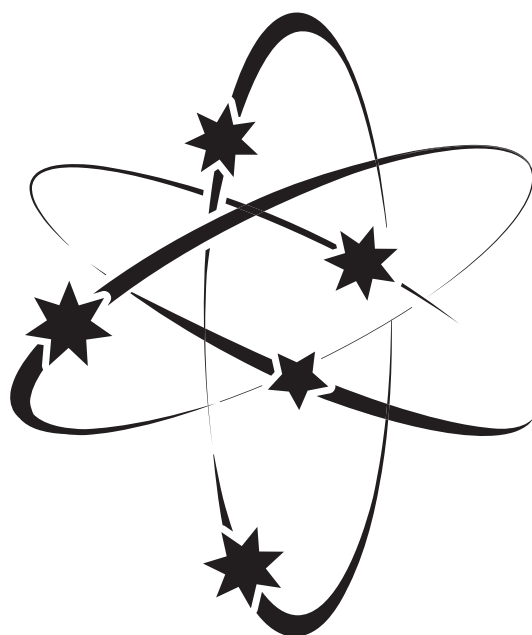
#ICPEAC17 #exploreTNQ #thisisqueensland

Presenters and Delegates:

- As a presenter, promote your session or poster through social media
- Share your opinions and ideas with your network. This might include a quote from a plenary session, a message from a presenter or a comment about a poster
- Broaden your network! Chat to others on social media about sessions you have attended
- Ask questions and find out what other people think

Sponsors and Exhibitors:

- Raise awareness of your sponsorship or exhibition booth
- Run your own promotion by linking photos, videos and website to your Twitter feed or Facebook page
- Encourage visitors to your booth by highlighting something special you have to offer



ICPEAC
2017

Cairns, Australia

XXX INTERNATIONAL CONFERENCE
ON PHOTONIC, ELECTRONIC
AND ATOMIC COLLISIONS

26 JULY - 1 AUGUST 2017 | QUEENSLAND, AUSTRALIA

CONFERENCE PROGRAM

Edited by:
Anatoli Kheifets,
Maarten Vos and Steve Gibson

Graphic design by:
Olya Kheifets

XXX ICPEAC LOCAL ORGANISING COMMITTEE

Chair: **Anatoli Kheifets** (Australian National University, Canberra)

Co-Chair: **Igor Bray** (Curtin University, Perth)

Members: **Steve Buckman** (Australian National University, Canberra)
Andrei Rode (Australian National University, Canberra)
Maarten Vos (Australian National University, Canberra)
Steven Gibson (Australian National University, Canberra)
Joshua Machacek (Australian National University, Canberra)
Sean Hodgman (Australian National University, Canberra)
Alexander Bray (Australian National University, Canberra)
Dmitry Fursa (Curtin University, Perth)
Alisher Kadyrov (Curtin University, Perth)
Robert Sang (Griffith University, Brisbane)
Christopher Chantler (University of Melbourne)
Feng Wang (Swinburne University, Melbourne)

TUESDAY, 25 JULY 2017

XXX ICPEAC WELCOME & REGISTRATION

13:00 - 19:00	Registration (Exhibition level, Cairns Convention Centre)
13:50 - 14:00	Welcome by Anatoli Kheifets (ICPEAC Chair, Australian National University, Canberra)
14:00 - 17:30	Tutorial Lectures (Room 1-2, Cairns Convention Centre)
14:00 - 15:00	Tutorial Lecture I Chair: Alicia Palacios (Universidad Autónoma de Madrid, Spain) Barry Schneider (National Institute of Science and Technology, USA) Topic: <i>45 Years of Computational Atomic and Molecular Physics: What Have We Learned</i>
15:00 - 16:00	Thomas Pfeifer (Max Planck Institute, Heidelberg, Germany) Topic: <i>Shaping atoms and molecules with strong laser fields</i>
16:00 - 16:30	Break
16:30 - 17:30	Tutorial Lecture II Chair: Alexei Grum-Grzhimailo (Moscow State University, Russia) Chris Greene (Purdue University, USA) Topic: <i>Rydberg states of atoms and exotic molecules</i>
18:00 - 19:30	Welcome Reception (Outdoor Plaza, Cairns Convention Centre)
18:00 - 21:00	ICPEAC Executive Committee meeting (Boardroom 1, Pullman Cairns International)

WEDNESDAY, 26 JULY 2017

08:45 - 09:00	XXX ICPEAC OPENING SESSION (Hall A)
09:00 - 10:00	Plenary Session (Hall A) Chair: Joachim Burgdörfer (Vienna Technical University, Austria), Reinhard Kienberger (Technical University Munich, Germany) PL: <i>Attosecond electron dynamics on surfaces and layered systems</i>
10:00 - 10:30	Morning tea
10:30 - 12:30	1A Parallel Lepton Session: Anti-matter (Hall A) Chair: Michael Bromley (University of Queensland, Australia)
10:30 - 11:00	David Cassidy (University College London, UK) PR: <i>Excited states of Positronium in electric fields</i>
11:00 - 11:30	Ilya Fabrikant (University of Nebraska-Lincoln, USA) PR: <i>Positronium collisions with atoms and molecules</i>
11:30 - 12:00	Yasuyuki Nagashima (Tokyo University of Science, Japan) PR: <i>Shape resonance of the positronium negative ion</i>
12:00 - 12:15	Dermot Green (Queen's University Belfast, UK) SR: <i>Calculations of positron cooling and annihilation in noble gases</i>
12:15 - 12:30	Stefan Eriksson (Swansea University, UK) SR: <i>Observation of the 1S - 2S transition in trapped antihydrogen</i>
10:30 - 12:30	1B Parallel Lepton Session: Atomic Collision (Room 1-2) Chair: John Tanis (University of Western Michigan, USA)
10:30 - 11:00	Ilkhom Abdurakhmanov (Curtin University, Australia) PR: <i>Convergent close-coupling calculations for heavy-particle collisions</i>
11:00 - 11:30	Takashi Mukaiyama (University of Potsdam, Germany) PR: <i>Collisional properties of ultracold ions with neutral atoms</i>
11:30 - 12:00	Yury Kozhedub (St. Petersburg State University, Russia) PR: <i>Pair creation in low-energy heavy ion-atom collisions</i>
12:00 - 12:15	Matthieu Génévriez (Université Catholique de Louvain, Belgium) SR: <i>Electron impact ionization of He(1s2s ³S) and He-(1s2s2p ⁴P)</i>
12:15 - 12:30	Chintan Shah (Max Planck Institute for Nuclear Physics, Germany) SR: <i>Laboratory measurements compellingly support a charge-exchange mechanism for the "Dark matter" ~ 3.5 keV X-ray line</i>

WEDNESDAY, 26 JULY 2017

12:30 - 14:00

Lunch break

14:00 - 16:00

2A Parallel Session: Photons Ultrafast (Hall A)

Chair: **Nora Berrah** (University of Connecticut, USA)

14:00 - 14:30

Christiane Koch (Universität Kassel, Germany)

PR: *Theory of photoelectron angular distributions: From understanding photoelectron circular dichroism to strong field coherent control*

14:30 - 15:00

Andr  Staudte (University of Ottawa, Canada)

PR: *Molecular Imaging with Intense Laser Pulses and Coincidence Spectroscopy*

15:00 - 15:30

Olga Smirnova (Max-Born Institute, Germany)

PR: *Looking inside chiral molecules on femtosecond time-scale*

15:30 - 16:00

Igor Litvinyuk (Griffith University, Australia)

PR: *Strong-field ionisation of hydrogen*

14:00 - 16:00

2B Parallel Session: Ultracold (Room 1-2)

Chair: **Tom Killian** (Rice University, TX, USA)

14:00 - 14:30

Richard Schmidt (Harvard University, USA)

PR: *Many-body physics with ultracold atoms*

14:30 - 15:00

Sebastian Will (Columbia University, USA)

PR: *Quantum Control of Ultracold Dipolar Molecules*

15:00 - 15:30

Jennifer Meyer (Universit t Innsbruck, Austria)

PR: *Quantum state-to-state scattering in ion-neutral collisions*

15:30 - 15:45

Joe Whalen (Rice University, TX, USA)

SR: *Lifetimes of ultralong-range strontium Rydberg molecules in a dense BEC*

15:45 - 16:00

Radek Plasil (Charles University, Czech Republic)

SR: *Reactions of O  with D2 at low temperatures 10 – 300 K*

16:00 - 18:00

Poster Session 1 (Hall B)

19:00 - 20:00

Public Lecture (Hall A)

Chair: **Anatoli Kheifets** (ICPEAC Chair, Australian National University, Canberra)

Jamie Seymour (James Cook University)

Australia, the land of things that bite, sting and kill! Is it really that bad?

THURSDAY, 27 JULY 2017

09:00 - 10:00	Plenary Session 2 (Hall A) Chair: Dominique Vernhet (University Pierre and Marie Curie, France) Henrik Cederquist (Stockholm University, Sweden), PL: <i>Heavy particle collisions: from single atomic targets to complex molecular clusters</i>
10:00 - 10:30	Morning Tea
10:30 - 12:30	3A Parallel Lepton Session: Photon Strong Field (Hall A) Chair: Anthony Starace (University of Nebraska, Lincoln, USA)
10:30 - 11:00	Katharina Doblhoff-Dier (Leiden University, Netherlands) PR: <i>Mechanisms of strong-field control in the fragmentation of small molecules</i>
11:00 - 11:30	Takeshi Sato (The University of Tokyo, Japan) PR: <i>Multielectron dynamics of atoms and molecules in strong laser fields</i>
11:30 - 12:00	Dimitris Charalambidis (University of Crete, Greece) PR: <i>Novel high harmonic generation schemes</i>
12:00 - 12:30	Jian Wu (East China Normal University, China) SR: <i>Photon energy deposition in strong-field ionization of molecules</i>
10:30 - 12:30	3B Parallel Lepton Session: Rings/Traps (Room 1-2) Chair: Thomas Stoelker (GSI Helmholtz Center, Germany)
10:30 - 11:00	Henrik B. Pedersen (Aarhus University, Denmark) PR: <i>Photofragmentation of ions and fragment storage in a compact storage ring</i>
11:00 - 11:30	Oldrich Novotný (Max Planck Institute for Nuclear Physics, Germany) PR: <i>Internally cold ions in the Cryogenic Storage Ring</i>
11:30 - 12:00	Yury Litvinov (GSI Helmholtz Center, Germany) PR: <i>Studies at the border between atomic and nuclear physics</i>
12:00 - 12:30	Bingsheng Tu (Université Catholique de Louvain, Belgium) PR: <i>Photorecombination studies at Shanghai EBIT</i>
12:30 - 14:00	Lunch break
12:45 - 13:15	ICPEAC General Committee meeting (Room 1-2)

THURSDAY, 27 JULY 2017

14:00 - 16:00

4A Parallel Lepton Session: Leptons Plasma (Hall A)

Chair: **Alfred Mueller** (Justus Liebig University Giessen, Germany)

14:00 - 14:30

Yuri Ralchenko (National Institute of Standards and Technology, USA)

PR: *Collisional-radiative modeling of hot plasmas*

14:30 - 15:00

Simon Preval (University of Strathclyde, UK)

PR: *The Tungsten Project: Electron-ion recombination rate coefficients for the isonuclear sequence of tungsten*

15:00 - 15:30

Zhimin Hu (China Academy of Engineering Physics, China)

PR: *Dielectronic Recombination in EBIT*

15:30 - 15:45

Zhongkui Huang (Chinese Academy of Sciences, China)

SR: *Dielectronic Recombination of Be-like 40Ar^{14+} at the CSRm*

15:45 - 16:00

Nobuyuki Nakamura (The University of Electro-Communications, Japan)

SR: *Extreme ultraviolet spectra of multiply charged tungsten ions*

14:00 - 16:00

4B Parallel Lepton Session: Ion/Molecule (Room 1-2)

Chair: **Emily Lamour** (University Pierre and Marie Curie, France)

14:00 - 14:30

Alicja Domaracka (CIMAP-CNRS, France)

PR: *Low-energy ion processing of carbonaceous molecular clusters leading to molecular growth phenomena*

14:30 - 15:00

Yang Wang (Universidad Autónoma de Madrid, Spain)

PR: *The relative stability of highly charged fullerenes produced in energetic collisions*

15:00 - 15:30

Ismanuel Rabadan Romero (Universidad Autónoma de Madrid, Spain)

PR: *Orientation effects in ion-molecule collisions*

15:30 - 15:45

David La Mantia (Western Michigan University, USA)

SR: *Radiative Double Electron Capture (RDEC) in $F^{9+} + \text{Ne}$, He Collisions*

15:45 - 16:00

Gustav Eklund (Stockholm University, Sweden)

SR: *Rotationally cold ($>99\%$ $J = 0$) OH^+ molecular ions in a cryogenic storage ring*

16:00 - 18:00

Poster Session 2 (Hall B)

FRIDAY, 28 JULY 2017

09:00 - 11:00	Poster Session 3 (Hall B)
11:00 - 12:00	Plenary Session 3 (Hall A) Chair: Roberto Rivarola (Universidad Nacional de Rosario, Argentina), Linda Young (Argonne National Laboratory/UChicago, USA) PL: <i>Harnessing ultra-intense x-rays for dynamic imaging</i>
12:00 - 12:30	IUPAP Prize Chair: Toshiyuki Azuma (RIKEN Tokyo, Japan)
12:30 - 14:00	Lunch break
14:00 - 15:30	5A Parallel Lepton Session: Orientation (Hall A) Chair: Klaus Bartschat (Drake University, USA)
14:00 - 14:30	Andrew Murray (University of Manchester, UK) PR: <i>Natural and Unnatural-Parity Contributions in Electron-Impact Ionization of Laser-Aligned Atoms</i>
14:30 - 15:00	Laurent Nahon (Synchrotron Soleil, France) PR: <i>Photoelectron circular dichroism in photoionization of gas phase chiral systems</i>
15:00 - 15:15	Nathan Clayburn (University of Nebraska, Lincoln, USA) SR: <i>Measurement of the Integrated Stokes Parameters for Zn 468 nm Florescence Excited by Polarized-Electron Impact</i>
15:15 - 15:30	Mai Yoshida (Tokyo Metropolitan University, Japan) SR: <i>Detection of recurrent fluorescence photons emitted from C_4^-</i>
14:00 - 15:30	5B Parallel Lepton Session: Heavy/Cold (Room 1-2) Chair: Robin Côté (University of Connecticut, USA)
14:00 - 14:30	Andrew Truscott (Australian National University, Australia) PR: <i>Highly correlated scattered atoms: – demonstrating ghost imaging with matter waves</i>
14:30 - 15:00	Johannes Deiglmayr (ETH Zurich, Switzerland) PR: <i>Rydberg macrodimers: micrometer-sized molecules bound by long-range van der Waals interactions</i>
15:00 - 15:30	Niels Kjaergaard (University of Otago, New Zealand) PR: <i>Quantum Scattering in a Collider for Ultracold Atoms</i>

FRIDAY, 28 JULY 2017

15:30 – 16:00

Afternoon tea

16:00 – 18:00

6A Parallel Session: Photons Ultrafast (Hall A)Chair: **Fernando Martin** (Universidad Autónoma de Madrid, Spain)

16:00 – 16:30

Hans Jakob Wörner (ETH Zürich, Switzerland)PR: *Attosecond electron dynamics in molecules and liquids*

16:30 – 17:00

Jesús González-Vázquez (Universidad Autónoma de Madrid, Spain)PR: *Mapping the dissociative ionization dynamics of molecular Nitrogen with attosecond resolution*

17:00 – 17:30

Kyung Taec Kim (Gwangju Institute of Science and Technology, Korea)PR: *Time-resolved spectroscopy of ultrafast autoionization of He*

17:30 – 18:00

Serguei Patchkovskii (Max-Born-Institut, Germany)PR: *Probing molecules with photoelectron rescattering and harmonics generation*

16:00 – 18:00

6B Parallel Session: Leptons/Imaging (Room 1-2)Chair: **Masahiko Takahashi** (Tohoku University, Japan)

16:00 – 16:30

Martin Centurion (University of Nebraska, USA)PR: *Ultrafast imaging of isolated molecules with electron pulses*

16:30 – 17:00

Masakazu Yamazaki (Tohoku University, Japan)PR: *Molecular orbital and atomic motion imaging using time-resolved electron scattering*

17:00 – 17:30

Gregory Boyle (James Cook University, Townsville, Australia)PR: *Electron and positron scattering and transport in simple liquids*

17:30 – 17:45

Dhananjay Nandi (Indian Institute of Science Education and Research Kolkata, India)SR: *Dissociative electron attachment to CO molecule probed by velocity slice imaging technique*

17:45 – 18:00

Miriam Weller (Goethe-Universität Frankfurt, Germany)SR: *Imaging the Temporal Evolution of Molecular Orbitals during Ultrafast Dissociation*

SATURDAY, 29 JULY 2017

SOCIAL PROGRAMME: GREAT ADVENTURES

Great Barrier Reef Adventure:

Ad: \$208.80 / Ch: \$108.90 (4-14yrs) / Family: \$526.50 (2Ad+2Ch)

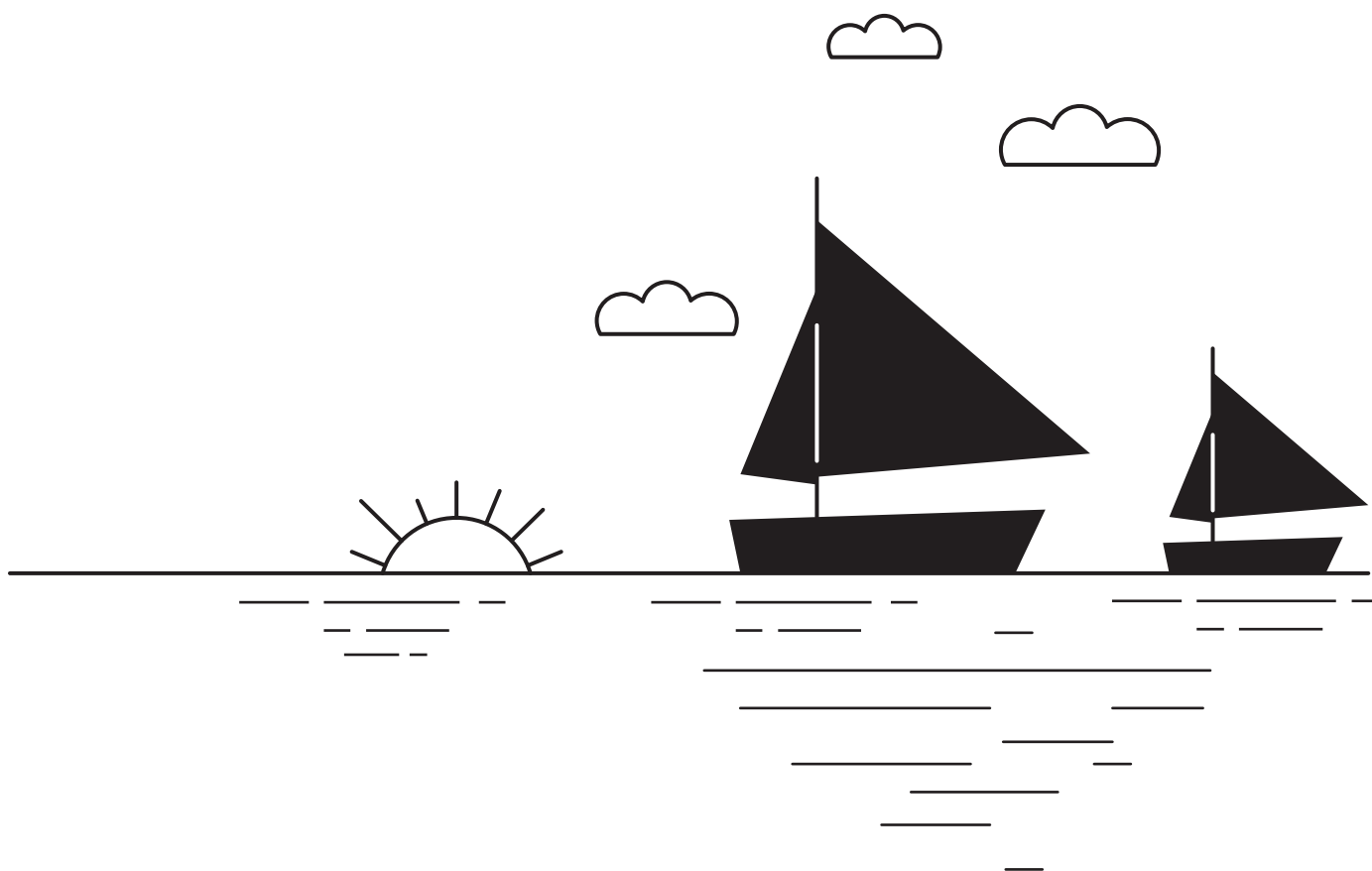
The beauty of the Great Barrier Reef is yours to experience when you cruise from Cairns to our luxury 3 level pontoon on the Outer Reef.

Green Island Half Day:

Ad: \$83.70 / Ch: \$43.20 (4-14yrs) / Family: \$210.60 (2Ad+2Ch)

Green Island is a beautiful 6000 year old coral cay located in the Great Barrier Reef Marine Park - a premier world heritage site and one of the Seven Natural Wonders of the World.

[Prices are in AUD.]



To book and/or find out more, please visit the tour desk during the conference or go online: www.cairnsconferences.com.au/events/icpeac2017

SUNDAY, 30 JULY 2017

SOCIAL PROGRAMME: VALUE DAY TOURS

Kuranda Rail, Skyrail & Hartleys Crocodile Adventure:

Ad: \$175.5 | Ch: \$91.80 (4-14yrs) | Family: \$474.30 (2Ad+2Ch)

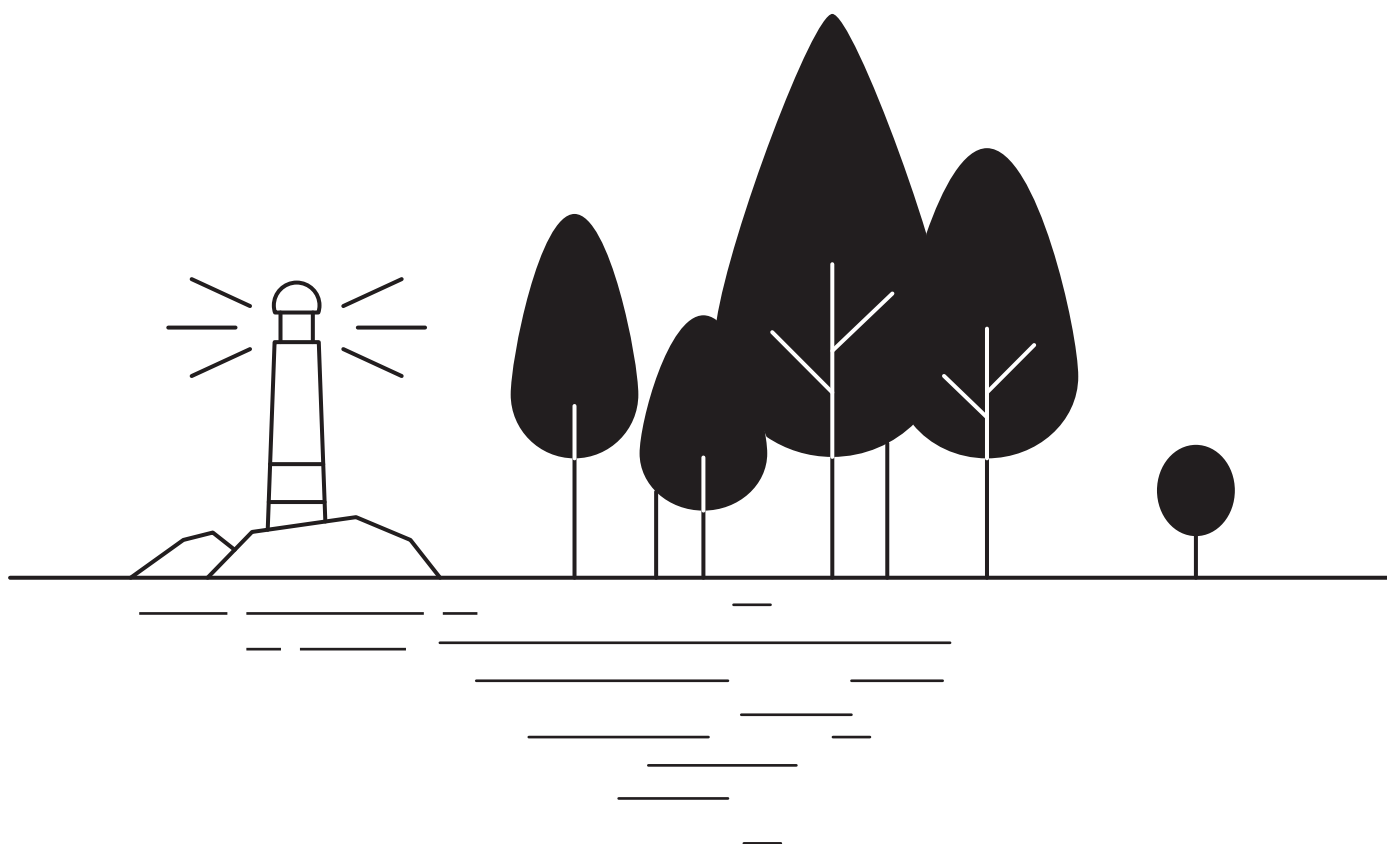
An historical rail journey to Kuranda, enjoying breathtaking views across the cane fields of Cairns to the tropical rainforest of Kuranda.

Cape Tribulation & Daintree:

Ad: \$176.40 | Ch: \$111.60 (4-14yrs) | Family: \$558 (2Ad+2Ch)

Enjoy a day exploring the rainforest and amazing landscapes of the Cape Tribulation wilderness area.

(Prices are in AUD.)



To book and/or find out more, please visit the tour desk during the conference or go online: www.cairnsconferences.com.au/events/icpeac2017

MONDAY, 31 JULY 2017

09:00 – 10:00

Plenary Session 4 (Hall A)

Chair: **Igor Bray** (Curtin University, Australia)

Clifford Surko (University of California, USA)

PL: *New Physics with Advanced Positron Traps and Beams*

10:00 – 10:30

Morning tea

10:30 – 12:30

7A Parallel Session: Photon FEL (Hall A)

Chair: **Maria Novella Piancastelli** (Uppsala University, Sweden)

10:30 – 11:00

Kiyonobu Nagaya (Kyoto University, Japan)

PR: *Ultrafast dynamics of atomic clusters probed by XFEL*

11:00 – 11:30

Kevin Prince (Elettra Sincrotrone Trieste, Italy)

PR: *Attosecond coherent control at FELs*

11:30 – 12:00

Tommaso Mazza (European XFEL Facility GmbH, Germany)

PR: *Dichroism and resonances in intense radiation fields*

12:00 – 12:15

Chuncheng Wang (Jilin University, China)

SR: *Footprints of electron correlation in strong field double ionization of Kr close to sequential ionization regime*

12:15 – 12:30

Fabian Holzmeier (Synchrotron Soleil, France)

SR: *Control of H_2 and D_2 dissociative ionization in the non-linear regime using EUV femtosecond pulses @FERMI*

10:30 – 12:30

7B Parallel Session: Clusters/Surfaces (Room 1-2)

Chair: **Xiaohong Cai** (Institute of Modern Physics (IMP) of the Chinese Academy of Sciences, China)

10:30 – 11:00

Maria Silvia Gravielle (Instituto de Astronomía y Física del Espacio, Argentina)

PR: *Fast interactions of atoms and laser pulses with crystal surfaces*

11:00 – 11:30

Maksim Kunitski (Goethe University Frankfurt, Germany)

PR: *Observation of the Efimov State of the Helium Trimer*

11:30 – 12:00

Naoki Watanabe (Hokkaido University, Japan)

PR: *H_2 ortho-para conversion on amorphous solid water*

12:00 – 12:15

Moemi Asamura (Nara Women's University, Japan)

SR: *MeV ion beam extraction into air with a glass capillary filled with He*

12:15 – 12:30

Daniel Rolles (Kansas State University, USA)

SR: *Studying Molecular Structure and Dynamics via Coulomb Explosion Imaging with X-rays and Ultrafast Laser Pulses*

MONDAY, 31 JULY 2017

12:30 – 14:00	Lunch break
14:00 – 16:00	8A Parallel Session: Photons Control (Hall A) Chair: Kiyoshi Ueda (Tohoku University, Japan)
14:00 – 14:30	Hugo Van Der Hart (Queen's University, Belfast, UK) PR: <i>Stimulating electron competition with XUV-initiated high harmonic generation</i>
14:30 – 15:00	Jan Marcus Dahlström (Stockholm University, Sweden) PR: <i>Precise attosecond pulse characterization using coherent bound wave packets</i>
15:00 – 15:30	Matthias Kling (Ludwig-Maximilians-Universität Munich, Germany) PR: <i>Strong Near-Field Induced Molecular Processes on Nanoparticles</i>
15:30 – 15:45	Fabian Lackner (Vienna University of Technology, Austria) SR: <i>Time-Dependent Two-Particle Reduced Density Matrix Theory: Application to High-Harmonic Generation</i>
15:45 – 16:00	Song Bin Zhang (Shaanxi Normal University, China) SR: <i>Nonlinear resonant Auger spectra and transient x-ray absorption spectra in CO using an x-ray pump-control scheme</i>
14:00 – 16:00	8B Parallel Session: Leptons (Room 1-2) Chair: Tim Gay (University of Nebraska, USA)
14:00 – 14:30	Alexander Dorn (Max Planck Institute for Nuclear Physics, Germany) PR: <i>Electron impact ionization of molecules and clusters</i>
14:30 – 15:00	Ioan F. Schneider (Université du Havre, France) PR: <i>Reactive collisions of electrons with molecular cations: multichannel fragmentation dynamics via super-excited states</i>
15:00 – 15:30	Fábris Kossoski (State University of Campinas, Brazil) PR: <i>Resonant anion states of radiosensitizers</i>
15:30 – 16:00	Gustavo Garcia (CSIC, Spain) PR: <i>Evaluated electron scattering cross sections from furfural molecules for modelling particle transport in the energy range 0-10000 eV</i>
16:00 – 18:00	Poster Session 4 (Hall B)
19:00 – 22:00	Conference Dinner (Hall C & D)

TUESDAY, 1 AUGUST 2017

09:00 – 11:00	Poster Session 5 (Hall B)
11:00 – 12:00	Plenary Session 5 (Hall A) Chair: Hossein Sadeghpour (Harvard University, USA) Tilman Pfau (Physikalisches Institut, Universität Stuttgart, Germany), PL: <i>Dipolar quantum gases and liquids</i>
12:00 – 12:30	Sheldon Datz & Other Prizes Chair: Emma Sokell (University College Dublin, Ireland)
12:30 – 14:00	Lunch break
12:30 – 13:00	Business Meeting (Hall A)
14:00 – 15:30	9A Parallel Session: Molecules (Hall A) Chair: Andreas Wolf (Max Planck Institute, Heidelberg, Germany)
14:00 – 14:30	Thomas Schlathöller (Zernike Institute for Advanced Materials, Netherlands) PR: <i>Ion and photon interactions with trapped biomolecular ions</i>
14:30 – 15:00	Li Chen-yu (University of Illinois, USA) PR: <i>Excitation, fragmentation and radiative decay of molecules studied with fast ion beams</i>
15:00 – 15:15	Roman Krems (University of British Columbia, Canada) SR: <i>Machine-learning the best potential surfaces for polyatomic molecules and the error bars for non-adiabatic atomic collisions</i>
15:15 – 15:30	Tomoyuki Endo (Institut National de la Recherche Scientifique, Canada) SR: <i>Tunneling ionization imaging of photoexcitation of NO by ultrafast laser pulses</i>
14:00 – 15:30	9B Parallel Session: Photons Weak Field (Room 1-2) Chair: Lorenzo Avaldi (Institute of Structure of Matter, Rome, Italy)
14:00 – 14:30	Paola Bolognesi (Institute of Structure of Matter, CNR, Italy) PR: <i>Basic mechanisms of photon/ion induced fragmentation of molecules of biological interest</i>
14:30 – 15:00	Oksana Travnikova (University Pierre and Marie Curie, Paris, France) PR: <i>Ultrafast dissociation induced by hard X-Rays</i>
15:00 – 15:30	Elena Gryzlova (Moscow State University, Russian Federation) PR: <i>Polychromatic resonant ionization of many-electron atoms</i>

TUESDAY, 1 AUGUST 2017

15:30 – 16:00

Afternoon tea

16:00 – 18:00

10A Parallel Session: Photons SF/Atto (Hall A)Chair: **Armin Scrinzi** (Ludwig Maximilians University, Munich, Germany)

16:00 – 16:30

Zenghu Chang (University of Central Florida, USA)PR: *Attosecond soft x-rays in the water window*

16:30 – 17:00

Jens Biegert (ICFO, Barcelona, Spain)PR: *Imaging molecular bond breaking with one electron*

17:00 – 17:30

Marcelo Ciappina (ELI-Beamlines, Czech Republic)PR: *Attosecond Physics gets Nano*

17:30 – 17:45

Alexander Blättermann (Max Planck Institute for Nuclear Physics, Germany)SR: *Observing the ultrafast buildup of a Fano resonance*

17:45 – 18:00

Alexander Bray (Australian National University, Australia)SR: *Attosecond Time Delay in Photoemission and Electron Scattering near Threshold*

16:00 – 18:00

10B Parallel Session: Leptons/Bio (Room 1-2)Chair: **Xiangjun Chen** (University of Science and Technology, Hefei, China)

16:00 – 16:30

Darryl Jones (CAPS, Flinders University, Australia)PR: *Inelastic electron scattering from biologically important molecules and radicals*

16:30 – 17:00

S V K Kumar (Tata Institute of Fundamental Research, India)PR: *Low Energy Electron interaction with DNA and Protein*

17:00 – 17:30

Małgorzata Smiatek-Telega (Gdansk University of Technology, Poland)PR: *Low energy electron interaction with molecules of biological interest*

17:30 – 17:45

Mateusz Zawadzki (J. Heyrovský Institute of Physical Chemistry Czech Republic)SR: *Energy Flow Between Pyrimidines and Water Triggered by Low Energy Electrons*

17:45 – 18:00

Benjamin Laws (Australian National University, Australia)SR: *NOO peroxy isomer discovered in the velocity-map imaged photoelectron spectrum of NO⁻*



ICPEAC
2017

Cairns, Australia

XXX INTERNATIONAL CONFERENCE
ON PHOTONIC, ELECTRONIC
AND ATOMIC COLLISIONS



speaker abstracts

TL - Tutorial lecture (55min + 5min discussion)
PL - Plenary lecture (55min + 5min discussion)
PR - Progress Report (25min + 5min discussion)
SR - Special Report (13min + 2min discussion)

45 Years of Computational Atomic and Molecular Physics: What Have We Learned

Barry I. Schneider^{*1}

^{*} Applied and Computational Mathematics Division, National Institute of Standards and Technology,
Gaithersburg, MD 20899
USA

Synopsis Atomic and molecular physics was an early beneficiary of the development of electronic computation. Luckily, most of the interactions between electrons and nuclei are well understood and it may appear that all that remains is to “turn the crank”. In retrospect, this was not quite so simple. These are complex many-body systems and in order to overcome the exponential scaling of these computations with the number of particles, clever algorithms and efficient codes needed to be developed. In this tutorial I describe a number of the important developments that have taken place over the past four decades and how they have impacted our qualitative and quantitative understanding of scattering processes and the interaction of radiation with matter.

From the very earliest days in the development of quantum mechanics, there was a great interest in applying the developing methods to atomic and molecular (A&M) structure and to the scattering of electrons from atoms and molecules. The quantum mechanical behavior of atoms and molecules was better understood than its nuclear counterpart and the results of the calculations could be directly compared to experiment. As time passed, the need for more efficient computational techniques in A&M physics become increasingly more critical as the complexity of the problems grew, especially for the accurate treatment of electron and atomic collisions and the interactions laser fields with atoms and molecules where

the continuous spectrum plays a critical role. A&M physicists are active today in developing new algorithms and large-scale computer codes to simulate these phenomena and increase understanding of these complex processes, enabling predictions that would have been impossible without computation. The role of high performance computing platforms have been critical to progress in A&M physics. Here, I will review the history of computational A&M physics from the late 1920's up to the present. The talk illustrates how new/clever algorithms have impacted the field and how these calculations have improved out understanding of the atomic and molecular many-body problem.

A Short History of Computational Atomic and Molecular Physics

- Late 1920's - 1950's
 1. Development of valence bond and Hartree-Fock methods. Applications to atomic structure using mechanical calculators.
 2. First numerical calculations on low energy electron scattering from atoms.
 3. Kohn and related variational methods are developed and applied to atoms and simple molecules.
- 1960's - 1980's
 1. Electron scattering and photoionization processes computed using the close-coupling method. Digital computers play a critical role in advancing the state-of-the-art as resonances are discovered for the first time from computation.
 2. Stabilization, complex scaling, complex coordinate, R-matrix, J-matrix, Kohn, complex Kohn, Schwinger and multichannel quantum defect methods are developed and applied.
 3. Accurate calculations of vibrational excitation and dissociation in simple diatomic molecules.
- 1990's - 2000
 1. Extensions/refinements of close-coupling, R-matrix and Complex Kohn approaches. Many applications are made to atoms and polyatomic molecules.
 2. First quantitative treatment of impact ionization of H.
- 2000 - Present
 1. Interest grows in the interaction of short, intense laser radiation with matter. Earlier computational developments in scattering theory are applied to these problems.

¹E-mail: bis@nist.gov

Shaping atoms and molecules with strong laser fields

Thomas Pfeifer

Max-Planck-Institut für Kernphysik, Saupfercheckweg 1, 69117 Heidelberg, Germany

Synopsis Employing spectroscopy and imaging in attosecond XUV and femtosecond x-ray light allows to observe atoms and molecules changing their shape in strong laser fields.

Atoms are commonly regarded as fundamental, well-defined and rigid quantum systems, even operated as clockworks in the most precise time-pieces ever build for applications in temporal and frequency metrology. However, as atoms and small molecules interact with intense electric fields, their charged constituents (electrons, nuclei) and their natural quantum dynamics are significantly bent out of shape. As a consequence, the intrinsic properties of atoms and molecules, their spectroscopic and spatial structure, can change dramatically.

High-frequency radiation such as extreme ultraviolet (XUV) and x-ray light is ideally suited to examine atoms and molecules as they change their natural structure and shape in strong laser fields. For attosecond spectroscopy, high harmonics generated by intense optical lasers are of great use, whereas for the imaging of tiny molecular sizes one can employ coherent femtosecond-pulsed x-ray light delivered by free-electron lasers (FELs).

In this tutorial, we will cover some recent developments in strong-field intra-atomic and intra-molecular physics on short time scales which may, at some point in the future, transform synthetic chemistry from the purely classical, population-based thermodynamic realm into the quantum-mechanical domain of phase- and amplitude controlled laser-driven reactions.

References

- [1] C. Ott, A. Kaldun, P. Raith, K. Meyer, M. Laux, J. Evers, C. H. Keitel, C. H. Greene, and T. Pfeifer. *Science* **340**, 716 (2013)
- [2] C. Ott, A. Kaldun, L. Argenti, P. Raith, K. Meyer, M. Laux, Y. Zhang, A. Blättermann, S. Hagstotz, T. Ding, R. Heck, J. Madronero, F. Martín, and T. Pfeifer. *Nature* **516**, 374 (2014)
- [3] A. Kaldun, C. Ott, A. Blättermann, M. Laux, K. Meyer, T. Ding, A. Fischer, and T. Pfeifer. *Phys. Rev. Lett.* **112**, 103001 (2014)
- [4] K. Meyer, Z. Liu, N. Müller, J.-M. Mewes, A. Dreuw, T. Buckup, M. Motzkus, and T. Pfeifer. *Proc. Natl. Acad. Sci. USA (PNAS)* **112**, 15613 (2015)
- [5] A. Kaldun, A. Blättermann, V. Stooß, S. Donsa, H. Wei, R. Pazourek, S. Nagele, C. Ott, C. D. Lin, J. Burgdörfer, and T. Pfeifer. *Science* **354**, 738 (2016)

E-mail: thomas.pfeifer@mpi-hd.mpg.de

Rydberg states of atoms and exotic molecules

Chris H. Greene^{*1}

^{*} Department of Physics and Astronomy, Purdue University, West Lafayette, Indiana 47907, USA

Synopsis This lecture will review some of the main theoretical ideas that have proven to be useful in describing the physics of Rydberg atoms and Rydberg molecules. The basics of multichannel quantum defect theory will be discussed from a practical point of view, and the description of molecular Rydberg states will also be summarized. This lecture will cover not only some of the basic theoretical ideas, but it will also address some of the phenomenology and motivations for exploring Rydberg systems.

Rydberg atoms and molecules have in recent years experienced intense theoretical and experimental activity, owing to their high quasi-degeneracy which results in a unique ease of manipulation by comparatively weak electric and/or magnetic fields and in dramatically stronger long-range interactions and reactivity compared to ground state species. And in fact tremendous headway has been made in their theoretical description, especially during the past 5 decades. During that period, a key generalization was developed beyond single channel Rydberg state properties, understood well since where a simple quantum defect parameter that is nearly energy-independent adequately describes each Rydberg series. This single channel quantum defect theory (QDT) is effective in describing the low angular momentum states of an alkali-metal atom consisting of a single electron moving in the field of a closed-shell ion core.

A first goal of this tutorial lecture is to summarize extensions that were pioneered by Seaton, Fano, Jungen, and others to develop a quantitative description of atomic and molecular Rydberg states, the theory known as multichannel quantum defect theory (MQDT). [1, 2] This level of theory is already vital for describing atoms in the second column of the periodic table, owing to the rich multiplicity of doubly-excited state perturbing levels in atoms such as calcium, strontium, and barium, as well as all atomic Rydberg electrons that move in the field of an open shell positive ion. And some of the most important applications of MQDT [2] have come in the context of conventional molecular Rydberg states where the nuclei remain at small internuclear distances, typically $R < 10$ bohr radii, but one or more electrons is highly excited.

A second key element of the theoretical toolkit that has enjoyed tremendous success in treating such

multichannel quantum states is the frame transformation theory, which has enabled the solution of extremely challenging problems in Rydberg atom or molecule physics [2] and beyond in other far-reaching contexts [3]. In the context of molecular physics, highly complex phenomena such as rovibrational level perturbations, autoionization or preionization, and predissociation in Rydberg molecules such as H_2 and H_3 have been handled in a unified manner by this theoretical technique. [2]

A third point of focus in this tutorial will be to discuss applications of these methods to predict and control new classes of quantum states, such as the ultra-long-range Rydberg molecules [4, 5] that have been receiving extensive recent attention in experiments as well as theoretical applications. The basic level of theory based on the Fermi pseudopotential and its extensions will be summarized as well as some of the peculiar diatomic and polyatomic molecules that can be formed at very large internuclear distances, such as trilobite and butterfly Rydberg molecules with enormous electric dipole moments.

References

- [1] C. H. Greene, M. Aymar, E. Luc-Koenig 1996 *Rev. Mod. Phys.* **68** 1015
- [2] M. Sommariva, F. Merkt, J. Z. Mezei, and Ch. Jungen 2016 *J. Chem. Phys.* **144** 084303
- [3] F. Robicheaux, P. Giannakeas, and C. H. Greene, *Phys. Rev. A* **92** 022711
- [4] C. H. Greene, A. S. Dickinson, and H. R. Sadeghpour 2000 *Phys. Rev. Lett.* **85** 2458
- [5] A. A. Khuskivadze, M. I. Chibisov, and I. I. Fabrikant 2002 *J. Phys. B* **66** 042709

¹E-mail: chgreene@purdue.edu

Attosecond electron dynamics on surfaces and layered systems

Reinhard Kienberger*

*Fakultät für Physik, E11, Technische Universität München, James Franck Straße, 85748 Garching

Synopsis The generation of single isolated attosecond pulses in the extreme ultraviolet (XUV) together with fully synchronized few-cycle infrared (IR) laser pulses allowed to trace electronic processes on the attosecond time-scales. The pump/probe technique was used to investigate electron dynamics on surfaces and layered systems with unprecedented resolution.

The attosecond streaking method [1] is the most established technique in attosecond science. Photoelectrons generated by laser based attosecond extreme ultraviolet pulses (XUV), are exposed to a dressing electric field from well synchronized laser pulses. The energy shift experienced by the photoelectrons by the dressing field is dependent on the delay between the XUV pulse and the dressing field and makes it possible to measure the respective delay in photoemission between electrons of different type (core electrons vs. conduction band electrons). The information gained in such experiments on tungsten [2] triggered many theoretical activities leading to different explanations on the physical reason of the delay. Attosecond streaking experiments have been performed on different solids [3], leading to different delays – also depending on the excitation photon energy.

A systematic investigation of photon-energy-dependent ($E_{\text{Ph}} = 95 \text{ eV} \dots 145 \text{ eV}$) delay times measured in tungsten at different crystal orientations giving insight into possible effects responsible for the delay is presented and will be discussed.

Further, we show measurements of time-resolved transport of different types of electrons through a defined number of adlayers on a bulk material on an attosecond timescale (Fig 1) [4]. While the linear behavior in delay between the different types of electrons can be explained by transport effects the delay of conduction band electrons is more complex and not fully understood.

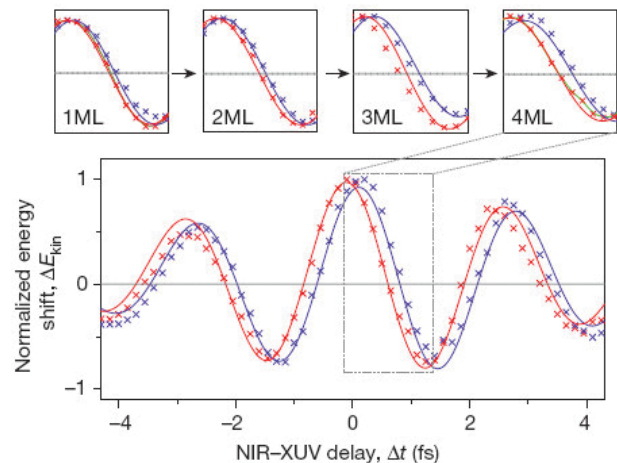


Figure 1. Delay of W 4f electron with respect to Mg electrons depending of the number of Mg adlayers (from [4]).

Recent experiments on the investigation of electron transport through sub-monolayer structures will be presented, too. By extrapolation to zero coverage of the surface and carefully take into account atomic delays one is able to extract for the first time not only relative delays in electron emission but the absolute time an electron needs to travel through matter.

References

- [1] R. Kienberger et al., Nature 427, 817 (2004).
- [2] A. Cavalieri et al., Nature 449, 1029 (2009).
- [3] S. Neppl et al., PRL 109 (8), 087401 (2012).
- [4] S. Neppl et al., Nature 517, 342 (2015).

E-mail: reinhard.kienberger@tum.de

Excited states of Positronium in electric fields

David. B. Cassidy¹,

Department of Physics and Astronomy, University College London, United Kingdom

Synopsis The effects of electric and magnetic fields on positronium (Ps) atoms prepared in excited states have been studied. For $n = 2$ states we have measured Stark and Zeeman mixing via their effects Ps decay rates. By exciting higher-lying (Rydberg) states we eliminate annihilation and are able to control Ps translational motion using inhomogeneous electric fields, owing to the large dipole moments of Rydberg atoms. Applications of these techniques will be discussed.

Exotic atoms play a unique role in atomic physics as they may have exaggerated or suppressed properties compared to their non-exotic counterparts. These are systems in which an electron or proton is replaced with a different particle of the same charge, so as to form an analogous bound-state. Thus, to produce exotic forms of hydrogen one can replace the electron with a negative muon, and create muonic hydrogen, or one can replace the proton with a positive anti-muon, making muonium. Alternatively one can replace a proton with a positron, making positronium. Positronium is the easiest such system to produce, primarily because positrons can be easily obtained from the decay of radio-isotopes, although the short lifetime against annihilation (142 ns) does lead to experimental complications. In recent years spectroscopy of muonic hydrogen has been used to accurately measure the size of the proton, with unexpected results [1]. On the other end of the scale, Ps has no proton, and as such could provide a "pure" measurement of the Rydberg constant. Ps is in general a good system to test bound state QED theory, and there is some interest in using it to probe possible antimatter-gravity effects.

I will discuss recent experiments carried out at UCL in which we prepare Ps atoms in excited states in electric and magnetic fields. This allows us to study mixed states for low n [2], and to produce long-lived [3] Rydberg-stark states [4]. The translational motion of the latter can be controlled using inhomogeneous electric fields [5], which opens the door for deceleration and focusing of long-lived Ps, which in turn can facilitate precision spectroscopy and gravity measurements. I will describe recent progress in this area, and give an overview of future plans. As an example, Fig. 1 shows results from experiments designed to produce metastable 2^3S_1 atoms by single photon excitation. Here ℓ -mixed states are prepared in an electric field, which is rapidly switched off after the laser pulse. This allows some atoms to evolve into long-lived 2^3S_1 states, which we plan to use to per-

form Ps interferometry experiments, and to study the Ps $n = 2$ fine structure via microwave spectroscopy.

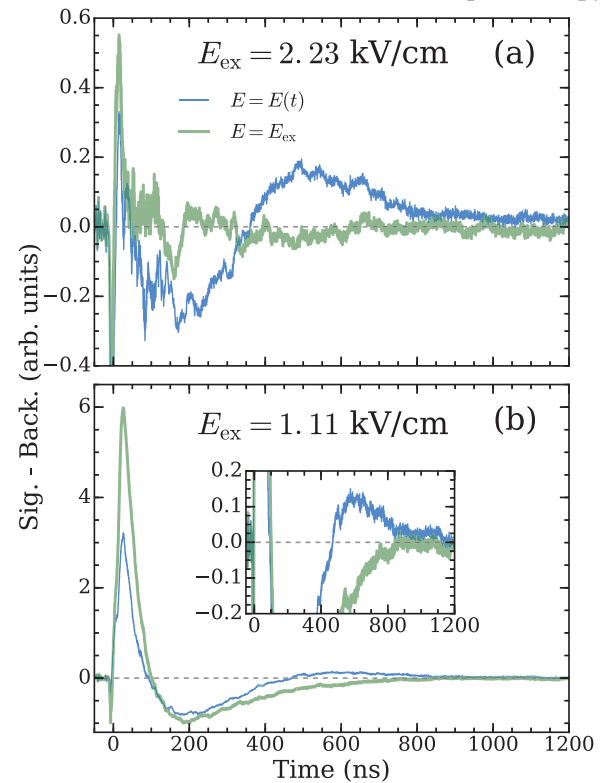


Figure 1. Production of 2^3S_1 Ps atoms by single photon excitation. The long lived atoms, indicated by a gamma signal at late times, are observed only if the excitation electric field is turned off after the laser excitation.

References

- [1] R. Pohl *et al.* 2013 *Ann. Rev. Nucl. Part. Sci.* **63** 175
- [2] A. M. Alonso *et al.* 2015 *Phys. Rev. Lett.* **115** 183401
- [3] A. Deller *et al.* 2016 *Phys. Rev. A.* **93** 062513
- [4] T. E. Wall *et al.* 2015 *Phys. Rev. Lett.* **114** 173001
- [5] A. Deller *et al.* 2016 *Phys. Rev. Lett.* **117** 073202

¹E-mail: d.cassidy@ucl.ac.uk

Positronium collisions with atoms and molecules

I. I. Fabrikant^{*1}, G. F. Gribakin[†], and R. S. Wilde[‡]

^{*} Department of Physics and Astronomy, University of Nebraska-Lincoln, Lincoln, NE 68588, USA

[†] School of Mathematics and Physics, Queen's University Belfast, Belfast BT7 1NN, UK

[‡] Department of Natural Sciences, Oregon Institute of Technology, Klamath Falls, OR 97601, USA

Synopsis Experimental data on positronium (Ps) collisions with atoms and molecules exhibit a striking similarity between electron and Ps scattering. By the use of various theoretical tools, including the impulse approximation and a pseudopotential method, it is possible to explain these similarities in the energy region above the Ps ionization threshold.

Recently observed similarities between positronium (Ps) scattering and electron scattering from several atoms and molecules [1] in the intermediate energy range were explained [2, 3] by the dominance of the electron exchange interaction with the target atom or molecule. An explicit proof of this equivalence was given within the framework of the impulse approximation [2], valid above the Ps ionization threshold. For lower collision energies a pseudopotential method [3] was developed. The most significant processes contributing to the total Ps cross section are elastic scattering and Ps break-up (ionization) whereas excitation of Ps plays insignificant role. For calculation of ionization cross sections we use a binary-encounter model whose results agree very well with results of the more sophisticated impulse approximation.

The described methods were successfully applied to the calculation of Ps scattering from heavy rare gas atoms, and gave results in good agreement with those of the beam experiments [1]. The same method was applied to Ps collisions with molecular hydrogen [4]. In general we observe the similarity between electron and Ps scattering cross sections at energies above the Ps ionization threshold when they are plotted as functions of the projectile velocity. However, below the threshold the two sets of cross sections are different because of the different nature of the long-range interaction between the projectile and the target, the polarization interaction in the case of electron collisions and the van der Waals interaction in the case of Ps collisions. In Fig. 1 we present the Ps-H₂ cross sections. The total cross sections are similar to *e*-H₂ cross section above the threshold velocity (0.5 a.u.), but differ significantly at lower velocities.

In the case of heavy rare-gas atoms the theoretical cross sections do not exhibit the Ramsauer-Townsend minimum [5]. This result is at odds with the recent beam experiment [6] on low-energy Ps-Ar and Ps-Xe

collisions which shows the cross sections decreasing towards lower velocities.

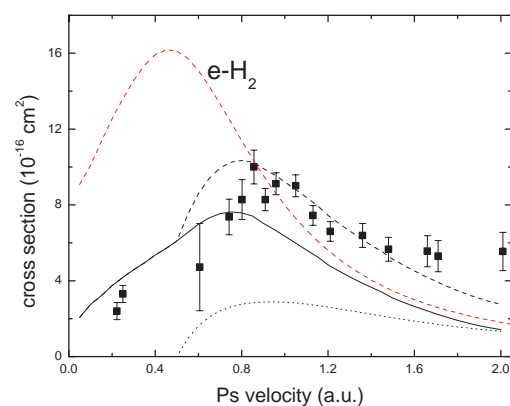


Figure 1. Ps-H₂ cross sections. Solid line: elastic cross section. Dotted line: Ps ionization cross section. Black dashed line: total cross section. Red dashed line: *e*-H₂ cross section. Error bars: measurements [7] for low velocities and [8] for $v = 0.6$ a.u. and above.

References

- [1] S. J. Brawley *et al.* 2010 *Science* **330** 789
- [2] I. I. Fabrikant and G. F. Gribakin 2014 *Phys. Rev. Lett.* **112** 243201
- [3] I. I. Fabrikant and G. F. Gribakin 2014 *Phys. Rev. A* **90** 052717
- [4] R. S. Wilde and I. I. Fabrikant 2015 *Phys. Rev. A* **92** 032708 (2015)
- [5] G. F. Gribakin *et al.* 2016 *J. Phys. B* **49** 064004
- [6] S. J. Brawley *et al.* 2015 *Phys. Rev. Lett.* **115** 223201
- [7] M. Skalsey *et al.* *Phys. Rev. A* **67**, 022504 (2003).
- [8] A. J. Garner, G. Laricchia, and A. Özen, *J. Phys. B* **29**, 5961 (1996).

¹E-mail: ifabrikant@unl.edu

Shape resonance of the positronium negative ion

Yasuyuki Nagashima^{* 1}, Koji Michishio^{*}, Tsuneto Kanai[†], Susumu Kuma[‡], Toshiyuki Azuma[‡], Ken Wada[‡], Izumi Mochizuki[‡], Toshio Hyodo[‡], Akira Yagishita[‡]

^{*} Department of Physics, Tokyo University of Science, 1-3 Kagurazaka, Shinjuku, Tokyo 162-8601, Japan

[†] Atomic, Molecular and Optical Physics Laboratory, RIKEN, 2-1 Hirosawa, Wako, Saitama 351-0198, Japan

[‡] Institute of Materials Structure Science, High Energy Accelerator Research Organization (KEK), 1-1, Oho, Tsukuba, Ibaraki 305-0801, Japan

Synopsis We have observed the shape resonance of positronium negative ions for the first time.

Positronium (Ps) is a hydrogenic atom composed of a positron and an electron. Another electron can bind to Ps weakly to form a positronium negative ion (Ps⁻) [1-3]. Although Ps⁻ is similar to H⁻, Ps⁻ consists of three particles flying around their center of mass while H⁻ consists of a massive proton and two light particles moving in the central field of the proton. Thus theoretical simplifications such as assumption of a heavy nucleus for H⁻ or the Born-Oppenheimer approximation for H₂ cannot be applied. In order to explore the nature of Ps⁻, many theorists have challenged to investigate this ion using their own techniques. For example, autoionization states and resonant photodetachment of Ps⁻ have been studied using the complex-rotational method and the hyperspherical close-coupling method, respectively [4-6]. Detailed resonant structures have also been calculated and a series of Feshbach resonances and a shape resonance near the Ps (n=2, 3 and 4) were reported [7]. However, experimental investigations on this ion have been scarce. In particular, its resonances have never been studied.

In the present work, the first observation of the shape resonance of Ps⁻ formed using an efficient formation technique developed recently has been performed [8]. A pulsed slow positron beam at the KEK-IMSS slow positron facility [9] was used to synchronize the Ps⁻ beam and a pulsed ultraviolet laser beam of sufficient pho-

ton density for the photodetachment of the short-lived Ps⁻ ions. The slow positrons impinged onto a Na coated tungsten surface to form Ps⁻ ions [3]. The formed ions were accelerated to a few keV and were irradiated with UV laser. The obtained neutral Ps atoms were detected by a micro-channel plate.

Peaks due to the shape resonance were clearly seen in the measured spectra. The resonance energy in the rest frame has been deduced to be 5.437(1) eV, which is consistent with theoretical calculations [5, 7, 10].

References

- [1] J.A. Wheeler, 1946 *Ann. N.Y. Acad. Sci.* **48** 219
- [2] A.P. Mills, Jr., 1981 *Phys. Rev. Lett.* **46** 717
- [3] Y. Nagashima, 2014 *Phys. Rep.* **545** 95
- [4] Y.K. Ho, 1979 *Phys. Rev. A* **19** 2347
- [5] J. Botero and C.H. Greene, 1986 *Phys. Rev. Lett.* **56** 1366
- [6] S.J. Ward, J.W. Humberston and M.R.C. McDowell, 1987 *J. Phys. B: At. Mol. Phys.* **20** 127
- [7] A. Igarashi, I. Shimamura and N. Toshima, 2000 *New J. Phys.* **2** 17
- [8] K. Michishio *et al.* 2016 *Nat. Commun.* **7** 11060
- [9] K. Wada *et al.* 1013 *J. Phys.: Conf. Ser.* **443** 012082
- [10] A.K. Bhatia and Y.K. Ho, 1990 *Phys. Rev. A* **42** 1119

¹ E-mail: ynaga@rs.kagu.tus.ac.jp

Calculations of positron cooling and annihilation in noble gases

D. G. Green¹, P. Mullan, M. Lee² and G. F. Gribakin³

School of Mathematics and Physics, Queen's University Belfast, Belfast BT7 1NN, Northern Ireland, United Kingdom

Synopsis Positron cooling in noble gases is studied via Monte Carlo simulation and by solving the Fokker-Planck equation, using high-quality scattering and annihilation cross sections calculated from many-body theory.

Observation of lifetime spectra for positrons annihilating in a gas was one of the first sources of information on positron interaction with atoms and molecules [1]. In particular, measurements of the normalised annihilation rate $Z_{\text{eff}}(t)$ during positron thermalization provided information on the energy dependence of the scattering cross sections and Z_{eff} .

Understanding the dynamics of positron cooling, including the fraction of positrons surviving to thermalization, is critical for accurate interpretation of such experiments. Incomplete thermalization was found to be responsible for the lack of consensus among the Z_{eff} data in Xe [2], while modelling of $Z_{\text{eff}}(t)$ [3] revealed deficiencies in the theoretical data for the heavier noble-gas atoms. Understanding of positron kinetics is also crucial for the development of efficient positron cooling in traps and accumulators [4], and for a cryogenically cooled, ultra-high-energy-resolution, trap-based positron beam [5].

Many-body theory calculations provide an accurate description of the whole body of data on low-energy positron scattering and annihilation rates on noble-gas atoms [6]. In this work we use our elastic scattering cross sections and Z_{eff} , parameterized by Padé approximants, to study positron cooling and annihilation in noble gases via Monte Carlo simulation and numerical solution of the Fokker-Planck equation. Both methods yield the positron probability density in momentum space $f(p, t)$, which allows us to calculate $Z_{\text{eff}}(t) = \int Z_{\text{eff}}(p) f(p, t) dp / \int f(p, t) dp$, and γ -spectra W (wing) parameters, and compare these with experiment, where available.

For room temperature gases, we find that significant fractions of the initial positrons annihilate before thermalizing, e.g., $\sim 80\%$ in He (see Fig. 1), rising to $> 99\%$ in Xe due to the larger mass of the atom, and that in Xe, the positron lifetime is significantly increased with admixtures of He. The use of accurate atomic data leads to a better agreement with measured $Z_{\text{eff}}(t)$, though we find discrepancies between measured shoulder widths of $Z_{\text{eff}}(t)$, which we

believe have suffered from incomplete knowledge of these fractions.

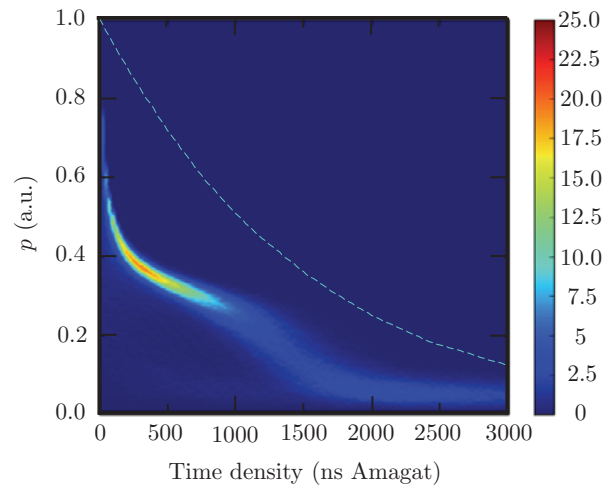


Figure 1. Momentum distribution $f(p, t)$ for positrons in helium at 293K, initially distributed uniformly in energy up to the Ps-formation threshold. The distribution is normalized as $\int f(p, t) dp = F(t)$, where $F(t)$ is the fraction of initial positrons surviving at time density t (shown as the dashed line).

References

- [1] Coleman P G *et al.* 1975 *J. Phys. B* **8** 1734; Coleman P G, Griffith T C and Heyland G R 1981 *ibid.* **14** 2509
- [2] Wright G L *et al.* 1985 *J. Phys. B* **18** 4327
- [3] Campeanu R 1982 *Can. J. Phys.* **60** 615
- [4] Al-Qaradawi I *et al.* 2000 *J. Phys. B* **33** 2725
- [5] Natsin M R, Danielson J R and Surko C M 2014 *J. Phys. B* **47** 225209; Natsin M R, Danielson J R and Surko C M 2016 *Appl. Phys. Lett.* **108** 024102
- [6] Green D G, Ludlow J A and Gribakin G F 2014 *Phys. Rev. A* **90**, 032712; Green D G and Gribakin G F 2015 *Phys. Rev. Lett.* **114** 093201
- [7] Boyle G J *et al.* 2014 *Phys. Rev. A* **89** 022712

¹E-mail: d.green@qub.ac.uk

²Current address: Department of Mathematical Sciences, University of Bath, Bath BA2 7AY, United Kingdom

³E-mail: g.gribakin@qub.ac.uk

Observation of the 1S - 2S transition in trapped antihydrogen

Stefan Eriksson* ¹ from the ALPHA-collaboration[†]

* Department of Physics, College of Science, Swansea University, Swansea SA2 8PP, UK

[†] CERN, CH-1211 Geneve 23, Switzerland

Synopsis The two-photon transition to the first excited state of antihydrogen has been observed in the ALPHA experiment at CERN. This first observations of the optical spectrum of neutral antimatter is the most precise measurement on an antiatom. Our result is consistent with CPT invariance to a relative precision of around 2×10^{-10} .

Antihydrogen offers a unique way to test matter/antimatter symmetry. Antihydrogen can reproducibly be synthesized and trapped in the laboratory for extended periods of time [1, 2] offering an opportunity to study the properties of antimatter with high precision. New techniques to study antihydrogen have emerged; the ALPHA-collaboration at CERN can now interrogate the bound state energy structure with resonant microwaves [3], determine the gravitational mass to inertial mass ratio [4] and measure charge neutrality [5,6]. Here, the first observation of the two-photon transition to the first excited state in antihydrogen is presented [7].

Antihydrogen is synthesized by mixing antiproton plasmas originating from the Antiproton Decelerator at CERN and positrons from a Surko-type accumulator. Mixing 90,000 antiprotons and 1.6 million positrons results in about 25,000 antihydrogen atoms per attempt. Atoms with kinetic energy less than the 0.5 K (in units of the Boltzmann constant) can be trapped in the superconducting magnetic minimum trap. In this work, about 14 anti-atoms were trapped per trial. Antihydrogen is detected by releasing the anti-atoms from the trap and collecting the annihilation byproducts on a silicon vertex detector. The topology of the events is used to distinguish antiproton annihilation from cosmic rays.

Whilst trapped, the anti-atoms are illuminated with 243 nm light from a frequency stabilized laser system. A cryogenic ultrahigh-vacuum enhancement cavity ensures sufficient power to both drive the two-photon transition and subsequently ionize the atom. The ionized atoms leave the trap. The atoms are exposed to light at the two possible hydrogenic resonance frequencies in trapped atoms (Figure 1) during 300 s each. Control experiments are performed with the laser detuned by 200 kHz (at 243 nm) off resonance and with no laser light present under otherwise identical conditions. In eleven runs of each type, 159 ± 13 antihydrogen detector counts were ob-

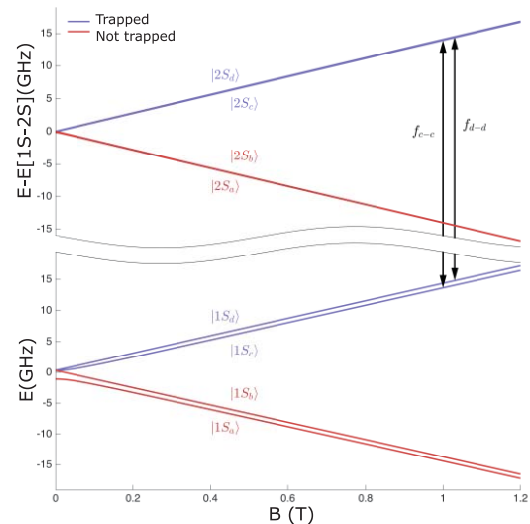


Figure 1 Energy levels of (anti)hydrogen in a magnetic field. The magnetic trap field minimum is about 1T. Possible two-photon transitions of trapped atoms are indicated by black arrows.

served off resonance, 67 ± 8.2 counts on resonance, i.e. $58\% \pm 6\%$ of the trapped atoms are removed by the resonant 1S-2S excitation. Counts during the hold time are in good agreement.

Assuming no asymmetries in the antihydrogen spectrum, together with a simulated spectrum which takes into account the motion of the atoms in the trap, the result can be interpreted as a test of CPT symmetry at a precision of 200 parts per trillion.

References

- [1] G. B. Andresen *et al.* 2010 *Nature* **468** 673
- [2] G. B. Andresen *et al.* 2011 *Nature Phys.* **7** 558
- [3] C. Amole *et al.* 2012 *Nature* **483** 439
- [4] A. E. Charman *et al.* *Nature Commun.* 2013 **4** 1785
- [5] C. Amole *et al.* 2014 *Nature Commun.* 2014 **5** 3955
- [6] M. Ahmadi *et al.* 2016 *Nature* **529** 373
- [7] M. Ahmadi *et al.* 2017 *Nature* **541** 506

¹ E-mail: s.j.eriksson@swansea.ac.uk

Convergent-close coupling calculations for heavy-particle collisions

I. B. Abdurakhmanov¹, A. S. Kadyrov, and I. Bray

Department of Physics, Astronomy and Medical Radiation Sciences, Curtin University,
GPO Box U1987, Perth, WA 6845, Australia

Synopsis We report on recent progress in applications of the convergent close-coupling approach to ion-atom collisions. This includes a development of a wave-packet continuum-discretisation approach to the description of the target structure and applications to antiproton and proton collisions with atomic targets.

Studies of collisions involving heavy projectiles are the quest driven not only by basic science but also by the relevance of such collisions to critically important industries, such as radiobiology and fusion energy. We have developed two distinct versions of the one- and two-centre convergent close-coupling (CCC) approaches to address this challenge. In one the relative motion of the heavy particles is treated fully quantum-mechanically (QM-CCC) [1, 2], the other classically (SC-CCC) [3, 4]. Depending on the properties of the collision system we tackle the problem using either one- or two-centre model. In the one-centre treatment the total scattering wave function is expanded in terms of only target pseudostates. This model is ideal for collisions where the likelihood of the projectile to form bound states with the constituents of the target system is negligibly small, e.g. for collisions with antiproton projectiles at sufficiently large energies. Two-centre treatment is applied to collisions where the projectile can capture the target electron. In this case two separate expansions utilising projectile and target states are used to form the scattering wave function. The two-centre CCC approach allows addressing the target electron loss in a way where we can exactly tell which part is due to ionisation and which is due to electron capture. In addition, it gives us an opportunity to test internal consistency of the CCC approach.

Successful implementation of the CCC approach relies on the accurate description of the target structure. Previously the CCC approach relied on the target continuum discretisation using the basis of orthogonal Laguerre pseudostates. The convergence and accuracy of cross sections were achieved by increasing the basis size. The increasing the basis size insured a denser discretization of continuum and a better representation of bound states. In this approach the pseudostates are produced with energies distributed only in a certain way which cannot be changed arbitrarily. Also, distributions of

pseudostates for different angular momenta are not aligned, which makes calculations of differential ionisation cross sections more complicated. Recently we have developed an alternative approach, where the continuous spectrum of the target is discretised using the wave packets (WP) constructed from the Coulomb wave functions. Unlike the Coulomb functions the generated wave packets are normalisable and applicable for scattering calculations. Due to the flexibility in choosing state energies, the target description based on the wave packets is ideal for differential ionisation studies. These wave packets have been incorporated into both one- and two-centre CCC approaches.

For antiproton-impact ionisation of hydrogen a comprehensive set of benchmark results from integrated to fully differential cross sections has been obtained [3]. Contrary to the results obtained using Laguerre pseudostates, the low-energy singly differential cross section has a maximum away from the zero emission energy. Calculations showed that only a fine discretisation of the low-energy continuum can reveal this feature.

Implementation of the wave packets to proton-hydrogen collisions produced accurate cross sections for all undergoing processes including ionisation and excitation of the target and electron capture to the projectile's bound and continuum states. In addition, this allowed to investigate various differential ionisation cross sections where the accurate calculations of the breakup amplitudes corresponding to direct ionisation and electron capture to the continuum is important.

References

- [1] I B Abdurakhmanov *et al.* 2016 *J. Phys. B* **49** 03LT01
- [2] I B Abdurakhmanov *et al.* 2016 *J. Phys. B* **49** 115203
- [3] I B Abdurakhmanov *et al.* 2016 *Phys Rev A* **94** 022703
- [4] S K Avazbaev *et al.* 2016 *Phys Rev A* **93** 022710

¹E-mail: Ilkhom.Abdurakhmanov@curtin.edu.au

Collisional properties of ultracold ions with neutral atoms

R. Saito^{*1}, S. Haze^{*}, M. Sasakawa^{*}, R. Nakai^{*}, M. Raoult[†], H. Da Silva Jr[†],

O. Dulieu[†], and T. Mukaiyama^{*2}

^{*} Institute for Laser Science, University of Electro-Communications, Tokyo, 182-8585, Japan

[†] Laboratoire Aimé Cotton, CNRS, Université Paris-Sud, ENS Cachan, Université Paris-Saclay, 91405 Orsay Cedex, France

Chemical properties of particles at low temperatures are expected to be quite different from those at high temperatures. At high temperatures, chemical reactions proceed by getting over the energy barrier (activation energy) separating the reactant state and the product state due to thermal fluctuations. However, at low temperatures, where the wave nature of a particle plays an important role in the chemical reaction, tunneling of the energy barrier affects both the reaction and the reaction rate. In such situations, the reaction rate may differ significantly from that predicted by classical mechanics. In addition, at extremely low temperatures, the quantum statistics of the particles may influence the chemical reaction, and either bosonic enhancement or suppression due to Fermi statistics may affect the chemical reaction rate.

To study quantum statistical feature in the chemical reactions, we investigate the collisional properties of ultracold atoms and ions. In our experiment, we create a mixture of fermionic ${}^6\text{Li}$ atoms and ${}^{40}\text{Ca}^+$ ions in the temperature range of mK [1]. In the ${}^6\text{Li}$ - ${}^{40}\text{Ca}^+$ combination, the threshold energy scale to enter the quantum scattering regime is on the order of $k_B \times 10 \mu\text{K}$, which is much higher than the values for the other atom-ion combinations that have been demonstrated so far. In the experiment, we have been able to observe the inelastic collisions and identified the collisions as charge-exchange collisions [2]. By observing the charge-exchange collisions at a single atom level by resolving single ions in the fluorescence images, we are able to quantitatively measure the charge-exchange collision rate as a function of collision energies. We measure the charge-exchange collision rate for ions in different energy levels and found that the ion in

the electronically ground state is robust against the ion loss due to the inelastic collisions while ions in metastable $D_{3/2}$ and $D_{5/2}$ states undergo charge exchange collisions much more efficiently. Within the energy range of our measurement, the charge-exchange cross section depends on $E^{-1/2}$ with E being the collision energy, which can be understood by the Langevin collision model. With the help of the theory calculation, we have identified the route of the charge-exchange process in the potential energy curves [3].

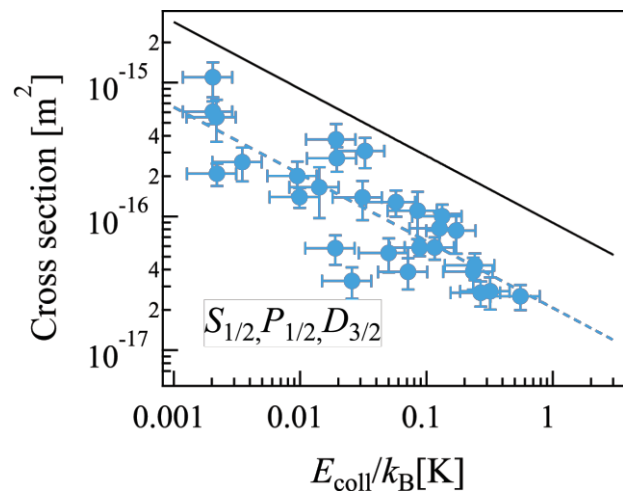


Figure 1. Charge-exchange collision cross sections as a function of the collision energy for the Ca^+ ions in the mixture of the $S_{1/2}$, $P_{1/2}$ and $D_{3/2}$ states,

References

- [1] S. Haze, S. Hata, M. Fujinaga, and T. Mukaiyama, Phys. Rev. A **87**, 052715 (2013).
- [2] S. Haze, R. Saito, M. Fujinaga, and T. Mukaiyama, Phys. Rev. A **91**, 032709 (2015).
- [3] R. Saito, S. Haze, M. Sasakawa, R. Nakai, M. Raoult, H. Da Silva Jr, O. Dulieu, and T. Mukaiyama, Phys. Rev. A, in press.

エラー! 参照元が見つかりませ

ん。 E-mail: r_saito@ils.uec.ac.jp

エラー! 参照元が見つかりませ

ん。 E-mail: muka@ils.uec.ac.jp

Pair creation in low-energy heavy ion-atom collisions

Y. S. Kozhedub^{*1}, A. I. Bondarev^{†*}, I. A. Maltsev^{*}, I. I. Tupitsyn^{*}, V. M. Shabaev^{*}, Th. Stöhlker^{‡§¶}

^{*} Department of Physics, St. Petersburg State University, 199034 St. Petersburg, Russia

[†] Center for Advanced Studies, Peter the Great St. Petersburg Polytechnic University, 195251 St. Petersburg, Russia

[‡] Helmholtz-Institut Jena, D-07743 Jena, Germany

[§] Institut für Optik und Quantenelektronik, Friedrich-Schiller-Universität, D-07743 Jena, Germany

[¶] GSI Helmholtzzentrum für Schwerionenforschung, D-64291 Darmstadt, Germany

Synopsis The probabilities and cross sections of electron-positron pair creation in low-energy heavy ion-atom collisions are evaluated. The calculations are performed beyond the one-center monopole approximation.

Heavy-ion collisions play a very important role in studying relativistic quantum dynamics of electrons in the presence of strong electromagnetic fields [1-3]. Moreover, if the total charge of the colliding nuclei is larger than the critical one, $Z_c = Z_1 + Z_2 > 173$, such collisions can provide a unique tool for tests of quantum electromagnetics at the supercritical fields [1]. At the future FAIR [2] and HAIF (see, e.g., Ref. [3]) facilities wide experimental investigations aimed at comprehensive study of various processes in low-energy heavy ion-atom collisions including ones with combined nuclear charges greater than the critical one are planned and theoretical investigations are urgently required.

Electron-positron pair creation processes due to spontaneous decay of the unstable vacuum state in the presence of supercritical fields is one of the most fundamental and attractive for investigation phenomenon. To date, nonperturbative calculations of the pair creation are mainly confined within the monopole approximation [4, 5], in which only the spherically symmetric part of the two-center potential is taken into account, and for bare nuclei collision systems. The present work is devoted to nonperturbative calculations beyond the one-center approximation and considers heavy ion-atom collisions, which are much more preferable for experimental study.

The method of calculations is based on an independent particle model, where the many-particle Hamiltonian is approximated by a sum of single-particle Hamiltonians, thus reducing the electronic many-particle problem to a set of single-particle equations for all electrons in the collision system, including negative-energy continuum ones. After solving this set of effective single-particle equations, the many-particle probabilities (including pair-creation probabilities) can be calculated [6, 7]. Solving the effective single-particle equations is based on the

coupled-channel approach with atomic-like Dirac-Fock and Dirac-Fock-Sturm orbitals, localized at the ions (atoms) [8]. This approach was successfully applied to calculations of relativistic quantum dynamics of electrons in low-energy heavy-ions collisions [8, 9].

In this work systematic calculations of the pair-creation probabilities and cross sections are performed for low-energy ion-atom collisions with different nuclear charge numbers. The role of the non-monopole effects is investigated. Special attention is paid to investigations of processes at the supercritical field, which occurs when the total charge of the colliding nuclei exceeds the critical value Z_c . The obtained results are compared with the previous calculations and the possibility of observation of the pair creation in low-energy collisions is discussed.

This work was supported by SPSU-DFG (Grant No. 11.65.41.2017) and RFBR-NSFC (Grant No. 17-52-53136).

References

- [1] W. Greiner *et al.* 1985 *Quantum Electrodynamics of Strong Fields*, Springer-Verlag, Berlin
- [2] <http://www.gsi.de/en/research/fair.htm>
- [3] J. C. Yang *et al.* 2013 *Nucl. Instrum. Methods Phys. Res. B* **317** 263
- [4] U. Müller *et al.* 1988 *Phys. Rev. A* **37** 1449
- [5] I. A. Maltsev *et al.* 2015 *Phys. Rev. A* **91** 032708
- [6] H. J. Lüdde and R. M. Dreizler 1985 *J. Phys. B* **18** 107
- [7] E. S. Fradkin *et al.* 1991 *Quantum Electrodynamics with Unstable Vacuum*, Springer-Verlag, Berlin
- [8] I. I. Tupitsyn *et al.* 2010 *Phys. Rev. A* **82** 042701; 2012 *Phys. Rev. A* **82** 032712
- [9] Y. S. Kozhedub *et al.* 2014 *Phys. Rev. A* **90** 042709

¹E-mail: y.kozhedub@spbu.ru

Electron impact ionization of $\text{He}(1s2s^3S)$ and $\text{He}^-(1s2s2p^4P)$

Matthieu G  n  vriez^{*1}, Jozo J. Jureta^{*}, Pierre Defrance^{*}, Xavier Urbain^{*}

^{*}Institute of Condensed Matter and Nanosciences, Universit   Catholique de Louvain, Louvain-la-Neuve, Belgium

Synopsis We present experimental cross section for electron impact single and double ionization of $\text{He}(1s2s^3S)$ and for ionization of $\text{He}^-(1s2s2p^4P)$. The experiment has required the development of a novel source producing a fast, intense beam of $\text{He}(1s2s^3S)$ with high purity, based upon the photodetachment of He^- . The results for single ionization of $\text{He}(1s2s^3S)$ solve a long-lasting discrepancy between theory and experiment, while the results for double ionization are the first determination of the cross section for these processes.

Helium is considered a benchmark for the study of electron correlation and, as such, has been the subject of much investigation on both theoretical and experimental grounds. In the case of single and double electron-impact ionization, good agreement has been reached for the ground states of He and He^+ . However, data for the first excited state $\text{He}(1s2s^3S)$ and for the helium negative ion He^- suffer either from major discrepancies between theory and experiment, or simply do not exist in the literature.

We have measured the absolute cross section for electron impact single and double ionization of $\text{He}(1s2s^3S)$, and double ionization of $\text{He}^-(1s2s2p^4P)$. To do so, we have designed a novel source of metastable helium atoms, based upon the production of a fast, intense beam of He^- and its subsequent photodetachment. It overcomes the fundamental limitation of other production techniques, plagued with the presence of non-negligible fractions of other excited states (1^3S , 1^3P), as it produces a beam of pure $\text{He}(1s2s^3S)$ with contamination limited to $\text{He}(1s^2)$ and as low as 5%. The flux of metastable atoms also keeps up with the highest fluxes achieved with other techniques. The cross section measurements are performed using the animated crossed beam technique of Defrance *et al.* [1].

The results for single ionization of $\text{He}(1s2s^3S)$, presented in Fig. 1, are in excellent agreement with the calculations of Fursa and Bray [2]. They also lie significantly lower than the only other experiment available for this energy range [3], thus solving a long-lasting discrepancy. Calculations using the frozen-core approximation (see, *e.g.*, [4]) deviate from the present results at higher energies, highlighting the importance of doubly excited states.

The results for double ionization of $\text{He}(1s2s^3S)$ and He^- represent the first determination of these cross sections. Surprisingly, the cross section for double ionization of $\text{He}(1s2s^3S)$ has roughly the same magnitude as that of $\text{He}(1s^2^1S)$, although the former lies 19.8 eV above the latter. The cross sec-

tion for double ionization of He^- is very high when compared to typical values, as may be expected from such a weakly bound system (77 meV), and does not match the universal formula of Rost and Pattard [5], thus hinting towards the importance of indirect double ionization mechanisms. Surely, there is room, and need, for theoretical input in order to understand the mechanisms underlying these intricate processes.

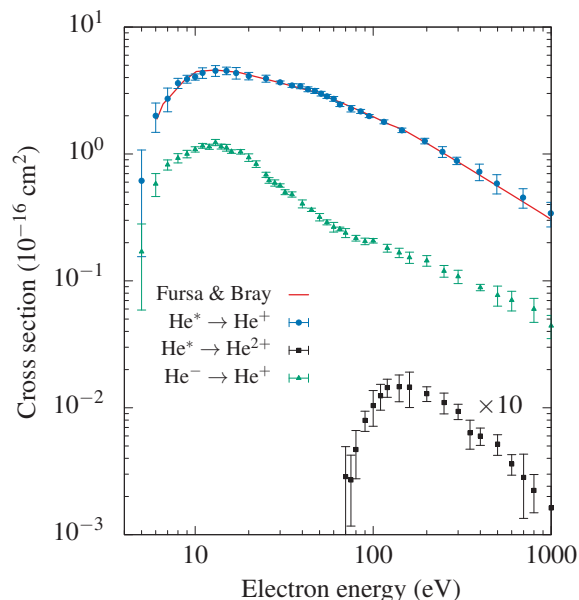


Figure 1. Cross section for electron impact single and double ionization of $\text{He}(1s2s^3S)$, and double ionization of He^- . The cross section for double ionization of $\text{He}(1s2s^3S)$ is multiplied by 10 for clarity.

References

- [1] P. Defrance *et al.* 1981 *J. Phys. B* **14** 103
- [2] D. V. Fursa and I. Bray 2003 *J. Phys. B* **36** 1663
- [3] A. J. Dixon *et al.* 1976 *J. Phys. B* **9** 2617
- [4] Y. Ralchenko *et al.* 2008 *At. Data Nucl. Data Tables* **94** 603
- [5] J. M. Rost and T. Pattard 1999 *J. Phys. B* **32** 603

¹E-mail: matthieu.genevriez@uclouvain.be

Laboratory measurements compellingly supports a charge-exchange mechanism for the "Dark matter" ~ 3.5 keV X-ray line

Chintan Shah*, Stepan Dobrodey*, Sven Bernitt^{*†}, René Steinbrügge*,
Liyi Gu[‡], Jelle Kaastra^{‡#}, and José R. Crespo López-Urrutia^{*}

^{*}Max-Planck-Institut für Kernphysik, Saupfercheckweg 1, 69117 Heidelberg, Germany

[†]Friedrich-Schiller-Universität Jena, Fürstengraben 1, 07743 Jena, Germany

[‡]SRON Netherlands Institute for Space Research, Utrecht, The Netherlands

[#]Leiden Observatory, Leiden University, 2300 RA Leiden, The Netherlands

Synopsis The reported observations of an unidentified X-ray line feature at ~ 3.5 keV from galaxy clusters have driven a lively discussion about its possible dark matter origin. Motivated by this, we have investigated the X-ray spectra of highly ionized bare sulfur ions following charge exchange with residual gas in the electron beam ion trap, as a source or a contributor to this X-ray line. The X-ray feature at about 3.5 keV shows up in the experiment, which could explain the the astrophysical observations and confirm the predictions of Gu *et al.*

A mysterious X-ray signal at 3.5 keV from nearby galaxies and galaxy clusters [1] recently sparked an incredible interest in the scientific community and given rise to a tide of publications attempting to explain the possible cause for this line. The origin of this line has been hypothesized as the result of decaying sterile neutrinos—potential dark matter particle candidate, presumably on the fact that this X-ray line is not available in the standard spectral databases and models for thermal plasmas. Cautiously, Gu *et al.* [2] have pointed out to an alternative explanation for this phenomenon: charge exchange between bare ions of sulfur and atomic hydrogen. Their model shows that X-rays should emitted at 3.5 keV by a set of S^{16+} transitions from $n \geq 9$ to the ground states, where n is the principle quantum number.

With this motivation, we tested the hypothesis of Gu in the laboratory by measuring K -shell X-ray spectra of highly ionized bare sulfur ions following charge exchange with gaseous molecules in an electron beam ion trap. We produced bare S^{16+} and H-like S^{15+} ions and let them capture electrons in collision with those molecules with the electron beam turned off while recording X-ray spectra. The 3.5 keV transition clearly shows up in the charge-exchange induced spectrum under broad range of conditions. The inferred X-ray energy, 3.47 ± 0.06 keV, is in full accord agreement with both the astrophysical observations and theoretical calculations, and confirms the novel scenario proposed by Gu [2, 3]. Taking the experimental uncertainties and inaccuracies of the astrophysical measure-

ments into account, we conclude that the charge exchange between bare sulfur and hydrogen atoms can outstandingly explain the mysterious signal at around 3.5 keV [3].

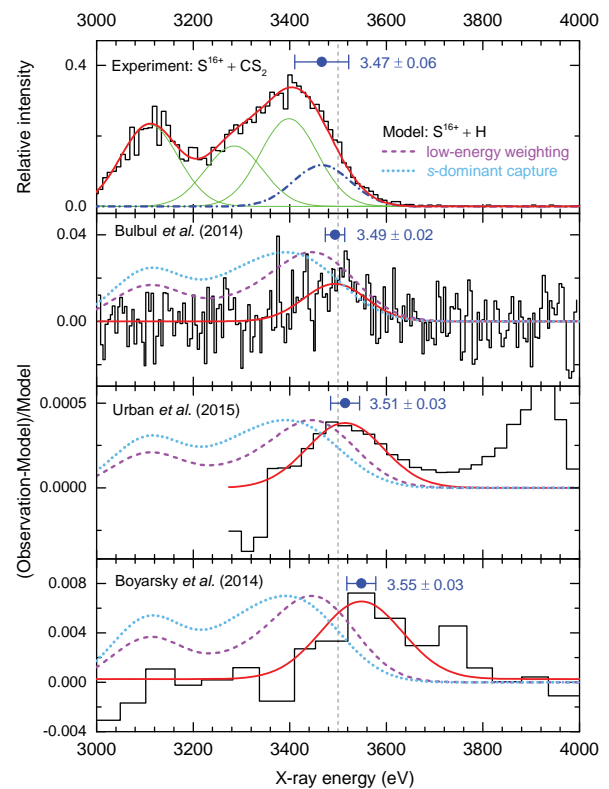


Figure 1. Charge-exchange-induced X-ray spectrum in comparison with recently reported astrophysical observations. The experimental data and observations are compared with the charge exchange model of Gu.

References

- [1] E. Bulbul *et al.* 2014 *Astrophys. J* **13** 789
- [2] L. Gu *et al.* 2015 *A & A* **L11** 584
- [3] C. Shah *et al.* 2016 *Astrophys. J* **833** 52

Theory of photoelectron angular distributions: From understanding photoelectron circular dichroism to strong field coherent control

Christiane P. Koch^{*1}

^{*} Theoretische Physik, Universität Kassel, Heinrich-Plett-Str. 40, 34132 Kassel, Germany

Synopsis Circular dichroism in the photoelectron angular distribution of chiral molecules is an intriguing effect, relying on electric dipole transitions only. A theoretical model to describe this effect in multi-photon ionization is developed. Moreover, coherent control of strong field ionization is shown to allow for asymmetric photoelectron emission from noble gas atoms.

Photoelectron spectra and photoelectron angular distributions obtained in photoionization reveal important information on electron dynamics in atoms and molecules. A striking effect is photoelectron circular dichroism which refers to the forward/backward asymmetry in the photoelectron angular distribution with respect to the propagation axis of circularly polarized light. It has recently been demonstrated in femtosecond multi-photon photoionization experiments with randomly oriented chiral molecules [1, 2]. I will show how to construct a theoretical framework combining perturbation theory for the light-matter interaction with ab initio calculations for the two-photon absorption and a single-center expansion of the photoelectron wavefunction. This model results in semi-quantitative agreement with the experimental data, explaining the latter in terms of the *d*-wave character of an intermediate state [3].

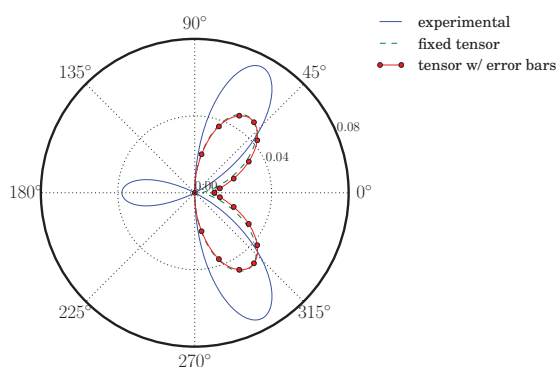


Figure 1. Photoelectron circular dichroism after 2+1 resonantly enhanced multiphoton ionization of camphor, comparing the experimental values obtained in Ref. [1] to calculations with a fixed two-photon absorption tensor and including error bars [3]

In the non-perturbative regime, tailoring the pulsed electric field in its amplitude, phase or polarization allows for the control of ultrafast dynamics. I will show that optimal control can be used to enhance desired features in the photoelectron spectra and angular distributions. The optimization target can ac-

count for specific desired properties in the photoelectron angular distribution alone, in the photoelectron spectrum, or in both. As an example, I show how to achieve directed electron emission for the photoionization of argon in the XUV regime [4]. In general, our method allows for determining the driving field that realizes a certain photoelectron spectrum. This may find application in extracting pulse information from measured spectra in experiments that have difficulty to characterize their pulses otherwise.

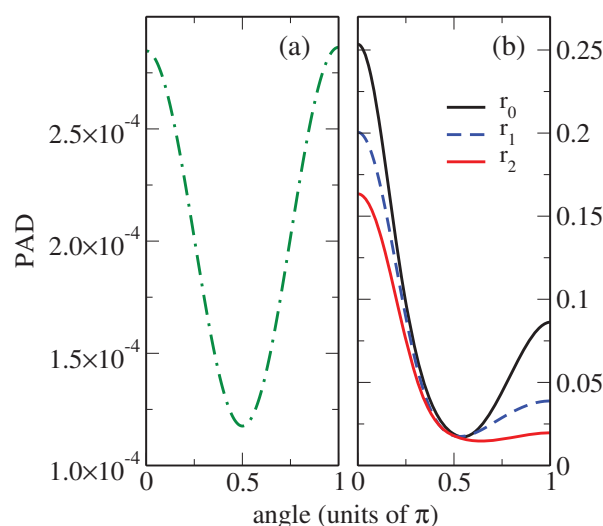


Figure 2. Compared to a symmetric photoelectron angular distribution obtained with a Gaussian pulse (a), shaped XUV pulses may result in asymmetric photoelectron emission (b), see Ref. [4] for details

References

- [1] C. Lux, M. Wollenhaupt, T. Bolze, Q. Liang, J. Köhler, C. Sarpe, and T. Baumert 2015 *Angew. Chem. Int. Ed.* **51** 5001
- [2] C. S. Lehmann, N. B. Ram, I. Powis, and M. H. M. Janssen 2013, *J. Chem. Phys.* **139**, 234307
- [3] R. E. Goetz, T. A. Isaev, B. Nikoobakht, R. Berger and C. P. Koch 2017 *J. Chem. Phys.* **146**, 024306
- [4] R. E. Goetz, A. Karamatskou, R. Santra, and C. P. Koch 2016 *Phys. Rev. A* **93**, 013413

¹E-mail: christiane.koch@uni-kassel.de

Molecular Imaging with Intense Laser Pulses and Coincidence Spectroscopy

A. Staudte* ¹

* Joint Attosecond Science Lab of the National Research Council of Canada and the University of Ottawa,
National Research Council, 100 Sussex Drive, Ottawa, Ontario, Canada K1A 0R6,
University of Ottawa, 75 Laurier Ave E, Ottawa, Ontario, Canada, K1N 6N5

Synopsis Several approaches to image molecular structure by recording the 3-dimensional momentum of photoelectrons in coincidence with the parent ion are discussed and corresponding experiments are presented.

During the last two decades, the imaging of orbitals from molecules has drawn significant interest. Advances in scanning tunneling microscopy (STM) have enabled the direct imaging of the electron density of complex molecules adsorbed on a surface [1]. On the other hand, the promise to time-resolve transient molecular orbitals, e.g., in chemical reactions, has stimulated vigorous efforts to reconstruct the orbital amplitude and phase from the high harmonic radiation emitted from molecules, irradiated by intense, infrared laser pulses [2]. However, the conceptual simplicity of STM can be combined with the time-resolution of femtosecond laser pulses, when the photoelectrons are imaged. For example, the angular dependence of the ionization current in the molecular frame has been shown to map out the electron density of the outer orbitals (e.g., [3-6]). Subsequently, using the same technique, time-dependent charge oscillations in Ne^+ were imaged in a pump-probe experiment [7].

Whereas the above yields a 1-dimensional observable of the charge density, it was demonstrated, that a 2-dimensional projection of the molecular orbital for a fixed molecular alignment can be obtained by imaging the momentum distribution of the photo-electron [8]. This opens the route to a tomographic reconstruction of the 3-dimensional shape of a molecular orbital.

More recently, the advance of mid-infrared laser pulses has allowed the application of established electron scattering concepts such as electron diffraction and holography. Laser induced electron diffraction has been successfully applied to resolve molecular bond lengths [8-11]. Strong field photoelectron holography, on the other hand, has been shown to reveal transient electronic structure [12,13].

In my talk I will review the progress made in molecular imaging at the Joint Attosecond Science Laboratory using Cold Target Recoil Ion Momentum Spectroscopy (COLTRIMS) [14].

References

- [1] J. Repp et al. Phys. Rev. Lett. 94, 026803 (2005).
- [2] J. Itatani et al. Nature 432, 867 (2004).
- [3] A.S. Alnaser et al. Phys. Rev. Lett. 93,183202 (2004).
- [4] D. Pavicic, et al. Phys. Rev. Lett. 98, 243001 (2007).
- [5] H. Akagi et al. Science 325, 1364 (2009).
- [6] L. Holmegaard et al. Nature Phys. 6, 428 (2010).
- [7] A. Fleischer et al. Phys. Rev. Lett. 107, 113003 (2011).
- [8] M. Meckel et al. Science 320, 1478 (2008).
- [9] C. Blaga et al. Nature 483, 194 (2012).
- [10] D. Comtois et al. Journ. Mod. Opt. 60, 1395 (2013).
- [11] M. Pullen et al. Nature Comm. 6, 7262 (2015).
- [12] M. Meckel et al. Nature Physics 10, 594 (2014).
- [13] M. Haertelt et al. PRL 116, 133001 (2016).
- [14] J. Ullrich, et al. Rep. Prog. Phys. 66, 1463 (2003).

¹ E-mail: andre.staudte@nrc.ca

Looking inside chiral molecules on femtosecond time-scale

Olga Smirnova^{*†1}, S. Beaulieu^{‡,§}, A. Comby[‡], D. Descamps[‡], B. Fabre[‡], G. A. Garcia[¶], R. Genaux[&], A. G. Harvey^{*}, F. Legare[§], Z. Mašin^{*}, L. Nahon[¶], A. F. Ordonez^{*}, S. Petit[‡], B. Pons[‡], Y. Mairesse[‡], V. Blanchet[‡],

^{*}Max-Born-Institute, Max-Born-Str. 2A, 12489 Berlin, Germany

[†]Technische Universität Berlin, Hardenbergstr. 36 A, 10623, Berlin, Germany,

[‡]Université de Bordeaux - CNRS - CEA, CELIA, UMR5107, F33405 Talence, France

[§]Institut National de la Recherche Scientifique, Varennes, Quebec, Canada

[¶]Synchrotron Soleil, l'Orme des Merisiers, BP48, St Aubin, 91192 Gif sur Yvette, France

[&]LIDYL, CEA, CNRS, Université Paris-Saclay, CEA Saclay, 91191 Gif-sur-Yvette France.

We describe a new technique of chiral recognition, based on the excitation of coherent helical motion of bound electrons in valence shells of a chiral molecule. Unlike the helix of light, traditionally used for chiral recognition in neutral molecules, the helical motion of the electrons has the right size to explore molecular chirality, leading to strong ultrafast chiral response. A purely quantum consequence of using such helical motion is the possibility to make a chiral object interact with itself, albeit in a different quantum state, allowing for a new and fundamentally quantum effect -- chiral self-recognition..

The most established technique of probing chiral interactions, the photoabsorption circular dichroism, relies on interacting with circularly polarized light. Distinguishing right-handed from left-handed molecules relies on the molecule sensing the chiral nature of the circular light. The helix of the light-wave is given by its wavelength. Hence, for optical fields, it exceeds the size of the molecule by several orders of magnitude. As a consequence, the related chiral effect – the photoabsorption circular dichroism – is very small. Formally, to feel the pitch of the lightwave, one needs to look beyond the dipole approximation, relying on the magnetic component of the laser field. Small value of the chiral signal makes ultrafast measurements of chiral dynamics very challenging.

In this work [1], we show that chiral response increases by several orders of magnitude as soon as the circularly polarized laser pulse incident on the molecule becomes sufficiently short. Sufficiently large coherent spectral bandwidth of such pulse coherently excites multiple electronic or vibronic states. We show that

the excited wavepacket dynamics leads to the helical motion of the bound electrons. The helix formed by this motion not only has the right size to explore molecular chirality, but it is also inherently ultrafast, leading to strong ultrafast chiral response. What's more, this excitation forms macroscopic chiral density and macroscopic chiral dipole in randomly oriented medium of chiral molecules.

We also show that, surprisingly, the dynamical chirality excited by the ultrafast pump pulse can be probed without the help of further chiral interactions, using linearly polarized laser pulse.

We develop detailed theory of the effect and show how coherent population of several bound states leads to chiral self-recognition: the possibility to make a chiral object interact with itself, albeit in a different quantum state.

References

- [1] S. Beaulieu, et al. "Photoexcitation Circular Dichroism in Chiral Molecules." arXiv:1612.08764 (2016).

¹ E-mail: Olga.Smirnova@mbi-berlin.de

Strong-field ionization of hydrogen

Igor V. Litvinyuk* ¹

* Australian Attosecond Science Facility & Centre for Quantum Dynamics, Griffith University, Nathan, Queensland 4111, Australia

Synopsis We present a series of experiments on strong-field ionization of atomic and molecular hydrogen. We compare atomic hydrogen results with “exact” numerical simulations to obtain precise calibration of laser intensity and absolute CEP and to interpret “attoclock” experiments. For molecular hydrogen we demonstrate failure of the frozen-nuclei approximation by measuring much higher ionization rates for the light isotope.

In strong-field physics, a quantitative comparison of theoretical predictions with results of experimental measurements – necessary to validate any theory – often remains problematic due to difficulties with obtaining precise and accurate results, both experimental and theoretical. One approach is to compare careful experiments with numerical *ab initio* modeling performed on atomic hydrogen, the only target where such modeling is quantitatively exact. Here we present a set of experiments performed on atomic hydrogen interacting with intense few-cycle laser pulses. We measure both ionization yields and photoelectron spectra as a function of intensity and carrier-envelope phase (CEP). By comparing our results for H with accurate TDSE calculations and also with experiments and approximate calculations for noble gas atoms we achieve (i) a transferable intensity calibration standard with 1-2% accuracy [1]; and (ii) an absolute measurement of CEP for few-cycle pulses.

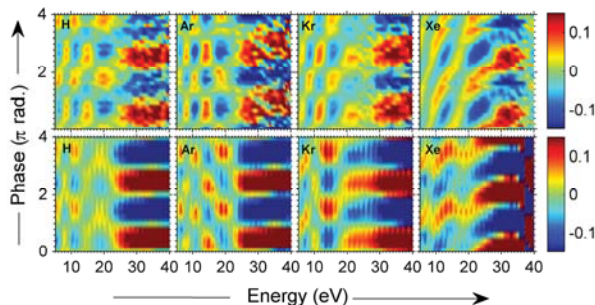


Figure 1. CEP maps for different atomic species at $2.5 \times 14 \text{ W/cm}^2$. (Top panel, left to right) CEP resolved experimental results for H, Ar, Kr and Xe. (Bottom panel, left to right) Theoretical simulations, in case of H, exact TDSE simulations are used whereas for Ar, Kr and Xe theoretical simulations are based on SAE approximation.

We also performed the attosecond angular streaking (« attoclock ») experiments on atomic hydrogen. In those experiments we measured 3D momentum spectra of electrons ionised from H by few-cycle elliptically polarized pulses in a range of intensities from 1.6×10^{14} to 4×10^{14}

W/cm^2 . Comparing our experimental results with precise *ab initio* theoretical modeling (numerical TDSE solutions) we observe excellent agreement between the theory and experiment. Based on that comparison, we conclude that our results are consistent with instantaneous (zero delay time) electron tunneling through the potential barrier.

For molecular targets accurate *ab initio* calculations are not yet feasible – modeling always involves one or several approximations. In this case, to validate theoretical approximations one may compare measurements performed on different isotopes, i.e. light and heavy hydrogen, under exactly the same conditions. Here we present one example of experimental measurement of isotope effects observed in light and heavy hydrogen molecules. We measured single ionization yields for H_2 and D_2 for a number of different intensities. It has been recently predicted theoretically by Tolstikhin, Worner and Morishita [2] that tunneling ionization rate for neutral hydrogen molecules should exhibit a significant isotope effect, which becomes more pronounced at lower intensities. We performed the measurements using circularly polarized pulses and coincident REMI detection of protons, deuterons and electrons [3]. We found excellent agreement with predictions of Tolstikhin et al. with hydrogen more likely to be ionized (up to 1.7 times more likely at the lowest intensity) than deuterium. This observation constitutes a failure of the frozen-nuclei approximation, which predicts the same ionization yield for both isotopes.

References

- [1] W.C. Wallace *et al.*, Phys. Rev. Lett. **117**, 083003 (2016).
- [1] O.Tolstikhin, H.-J. Worner, T. Morishita, Phys. Rev. A **87**, 041401(R) (2014).
- [3] X. Wang *et al.*, Phys. Rev. Lett. **117**, 053001 (2016).

¹ E-mail: i.litvinyuk@griffith.edu.au

Many-body physics with ultracold atoms

Richard Schmidt^{*,† 1}

^{*} Department of Physics, Harvard University, Cambridge MA 02138, USA

[†] ITAMP, Harvard-Smithsonian Center for Astrophysics, Cambridge MA 02138, USA

Synopsis In this talk I will review recent experimental and theoretical progress on studying the many-body physics of polarons in ultracold atomic systems. In particular, I will discuss how ultracold atomic systems allow not only for the study of the real-time dynamics of polaron formation, but also provide a means to realize novel regimes of polaron physics beyond paradigm models studied in traditional condensed matter physics.

Understanding the role of interactions between an impurity and its environment is a fundamental problem in quantum many-body physics. A central concept for the description of such systems is the formation of quasiparticle excitations called polarons. These describe impurities as being dressed by many-body excitations in the medium which changes not only the properties of the impurity, but which can also have a profound influence on the impurity's environment.

Depending on the character of the environment and the form of interactions, different types of polarons are created. For instance, the immersion of an impurity into a Fermi gas leads to the formation of Fermi polarons. Such polarons are at the center of the first part of the talk, where I discuss the dynamical response of heavy quantum impurities immersed in a Fermi gas at zero and finite temperature [1]. I review recent experimental approaches taken to study and observe Fermi polarons [2] and highlight their universal connection. By investigating both the frequency and time domain, interaction regimes are identified which are characterized by distinct many-body dynamics. From our theoretical study a picture emerges in which the impurity dynamics is universal on essentially all time scales, and where the short-time few-body response is tied to the long-time dynamics of the Anderson orthogonality catastrophe by Tan relations. Using an analytical description we calculate the impurity-induced thermal decoherence rate of the fermionic system and prove that the fastest long-time decoherence rate is universally given by $\gamma = \pi k_B T/4$ for a large class of models describing Fermi polarons. Our results are in excellent agreement with recent experiments [3] and show new paths to experimentally study impurity physics with ultracold atomic systems.

In the second part of the talk I will review recent progress on the theoretical description of

impurities interacting with bosonic quantum gases. Here I will emphasize the relation between various polarons models such as strong coupling Bose polarons, as created by the coupling of impurities to Bose-Einstein condensates by Feshbach resonances [4,5,6], Rydberg polarons created by Rydberg excitations in a Bose gas [7], and angulons, which describe quantum rotors coupled to a many-body environment [8,9]. Each of these examples highlights novel mechanisms of polaron formation that go beyond paradigms of traditional condensed matter physics and allow for studying novel regimes of many-body polaron physics with ultracold atoms.

References

- [1] Schmidt *et al.* 2017 *in prep.*
- [2] Cetina *et al.* 2016 *Science* **354** 96
- [3] Cetina *et al.* 2015 *Phys. Rev. Lett.* **115** 135302
- [4] Schmidt *et al.* 2013 *Phys. Rev. A* **88** 053632
- [5] Hu *et al.* 2016 *Phys. Rev. Lett.* **117** 055301
- [6] Jörgensen *et al.* 2015 *Phys. Rev. Lett.* **117** 055302
- [7] Schmidt *et al.* 2016 *Phys. Rev. Lett.* **116** 105302
- [8] Schmidt *et al.* 2015 *Phys. Rev. Lett.* **114** 203001
- [9] Schmidt *et al.* 2016 *Phys. Rev. X* **6** 011012

^{† 1} E-mail: richard.schmidt@cfa.harvard.edu

Quantum Control of Ultracold Dipolar Molecules

Sebastian Will¹

Columbia University, New York, NY 10027, USA
Massachusetts Institute of Technology, Cambridge, MA 02139, USA

Synopsis Dipolar molecules are expected to open new avenues for many-body quantum physics, quantum chemistry, and quantum information. Therefore, quantum gases of dipolar molecules are attracting increased interest - both in theory and experiment. At MIT, we have pioneered the creation of ultracold, strongly dipolar NaK molecules. This talk will summarize our recent results and give an outlook on the next steps on the experimental agenda.

Ultracold molecules open up new routes for precision measurements, quantum information processing and many-body quantum physics. In particular, dipolar molecules with long-range interactions promise the creation of novel states of matter, such as topological superfluids and quantum crystals. Dipolar molecules can be efficiently assembled from ultracold atoms. Using this approach we created the first near-degenerate gases of strongly dipolar NaK molecules [1, 2]. At temperatures as low as few hundred nanokelvin, we prepare spin-polarized ensembles, in which each molecule occupies the rovibrational and hyperfine ground state.

I will discuss our advances on coherent quantum control in ultracold NaK. Starting from the absolute ground state, we demonstrate coherent microwave coupling into higher rotational and hyperfine states [3]. This type of coherent coupling enables direct control over long-range dipolar interactions between the molecules. Furthermore, we use two-photon microwave coupling to create superposition states between the two lowest hyperfine states of

NaK. This molecular qubit displays coherence times on the scale of one second, enabling Ramsey spectroscopy with Hertz-level resolution [4] - suggesting new possibilities for precision metrology and quantum information.

References

- [1] J. W. Park, S. A. Will, and M. W. Zwierlein "Ultracold Dipolar Gas of Fermionic $^{23}\text{Na}^{40}\text{K}$ Molecules in Their Absolute Ground State" *Phys. Rev. Lett.* **114** 205302 (2015)
- [2] J. W. Park, S. A. Will, and M. W. Zwierlein "Two-Photon Pathway to Ultracold Ground State Molecules of $^{23}\text{Na}^{40}\text{K}$ " *New J. Phys.* **17** 075016 (2015)
- [3] S. A. Will, J. W. Park, Z. Z. Yan, H. Loh, and M. W. Zwierlein "Coherent Microwave Control of Ultracold $^{23}\text{Na}^{40}\text{K}$ Molecules" *Phys. Rev. Lett.* **116** 225306 (2016)
- [4] J. W. Park, Z. Z. Yan, H. Loh, S. A. Will, and M. W. Zwierlein "Second-Scale Nuclear Spin Coherence Time of Trapped Ultracold $^{23}\text{Na}^{40}\text{K}$ Molecules" [arXiv:1606.04184](https://arxiv.org/abs/1606.04184) (2016)

¹E-mail: sebastian.will@columbia.edu

Quantum state-to-state scattering in ion-neutral collisions

Jennifer Meyer^{*1}, Daniel Hauser^{*}, Tim Michaelsen^{*}, Björn Bastian^{*}, Steffen Spieler^{*}, Olga Lakhmanskaya^{*}, Eric S. Endres^{*}, Fabio Carelli^{*}, Seunghyun Lee^{*}, Sunil S. Kumar^{*}, Francesco Gianturco^{*}, Roland Wester^{*2}

^{*} Institute for Ion Physics and Applied Physics, Universität Innsbruck, Technikerstr. 25, 6020 Innsbruck, Austria

Synopsis Quantum state specific inelastic as well as reactive ion-neutral scattering experiments will be presented. Non-resonant photodetachment is employed to investigate the state-to-state inelastic collisions of OH^- ions with helium at low temperatures in a cryogenic radiofrequency trap. Absolute rate coefficients are measured for the $J = 1 \rightarrow 0$ and compared with quantum scattering calculations. Crossed beam reactive scattering experiments of molecular hydrogen, prepared in a molecular beam, with Ar^+ show a vibrational state specific reactivity depending on the spin-orbit state of Ar^+ . Differential scattering cross sections of the charge transfer reaction will be presented. H_2^+ in $v = 2$ product ions are formed predominantly through a near resonant process.

Quantum state control of ion molecule scattering experiments aims at the understanding of the intrinsic dynamics of a collision. The goal is full state to state control of the target collision in experiments, including the involved vibrational, rotational and hyperfine structure levels, and to provide benchmark experimental data for high level *ab initio* scattering theory.

The preparation of a quantum state selected sample requires the understanding of the elementary process involved, e.g. rotationally inelastic collisions at low temperatures. In this talk, I will present our investigations of cold OH^- ions colliding with helium [1] using a cryogenic radiofrequency multipole trap [2, 3]. Rotational state analysis by non-resonant photodetachment spectroscopy [4] was employed to measure the inelastic scattering rate coefficient for the $J = 1$ to $J = 0$ rotational quenching in $\text{OH}^- + \text{He}$ collisions [1]. The measurements are compared with *ab initio* quantum scattering calculations. Furthermore, energy transfer from the hydrogen $J = 1$ rotation to OH^- was observed.

The reactions of argon cations Ar^+ with molecular hydrogen have been investigated by crossed beam velocity map imaging [5]. The two spin orbit states of the Ar^+ exhibit a distinct influence on the reactivity towards molecular hydrogen H_2 and its isotopologue deuterium D_2 [6]. The formed H_2^+ product ions are predominantly scattered in forward direction and show a strong preference for a specific vibrational states of the H_2^+ , i.e. ($v = 2$). This agrees with former experiments and theoretical results [7, 8]. A near energetic degeneracy of the spin orbit excited argon $\text{P}_{1/2}$ state to the formation of H_2^+ ($v = 2$) leads to an enhancement of this state-to-state channel compared to the population of H_2^+ ($v = 0, 1, 3$) levels which are energetically accessible. From the product internal

energy distributions the rotational excitation of H_2^+ is inferred.

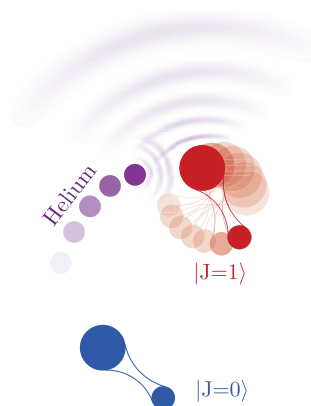


Figure 1. Schematic view of inelastic collisions between OH^- and helium [1]

Future work will address the reaction of the Fe^+ ion with molecular hydrogen investigating the catalytic properties and the influence of the electronic state of Fe^+ on the dynamics of elementary reactions.

References

- [1] D. Hauser, S. Lee, F. Carelli, S. Spieler, O. Lakhmanskaya, E. S. Endres, S. S. Kumar, F. Gianturco, R. Wester 2015 *Nature Phys.* **11** 467
- [2] D. Gerlich 1995 *Phys. Scr.* **T59** 256
- [3] R. Wester 2009 *J. Phys. B* **42** 154001
- [4] R. Otto, A. von Zastrow, T. Best, R. Wester 2013 *Phys. Chem. Chem. Phys.* **15** 612
- [5] R. Wester 2014 *Phys. Chem. Chem. Phys.* **16** 396
- [6] K. Tanaka, T. Kato, I. Koyano 1981 *J. Chem. Phys.* **75** 4941
- [7] P. M. Hierl, V. Pacák, Z. Herman 1977 *J. Chem. Phys.* **67** 2678
- [8] M. Baer, C.-L. Liao, R. Xu, D. Flesch, S. Nourbakhsh, C. Y. Ng, D. Neuhauser 1990 *J. Chem. Phys.* **93** 4845

¹E-mail: jennifer.meyer@uibk.ac.at

²E-mail: roland.wester@uibk.ac.at

Lifetimes of ultralong-range Strontium Rydberg molecules in a dense BEC

F. Camargo*, J. D. Whalen*, R. Ding*, T. C. Killian*, F. B. Dunning*¹, J. Pérez-Ríos[†], S. Yoshida[‡], and J. Burgdörfer[‡]

* Department of Physics & Astronomy, Rice University, Houston, Texas, USA

[†] Department of Physics & Astronomy, Purdue University, West Lafayette, Indiana, USA

[‡] Institute for Theoretical Physics, Vienna University of Technology, Vienna, Austria, EU

Synopsis The lifetimes and decay channels of ultralong-range strontium Rydberg molecules that contain tens to hundreds of ground-state atoms within the electron orbit are examined by monitoring the time evolution of the Rydberg population using field ionization.

Ultralong-range Rydberg molecules excited in a BEC can be used to explore collective phenomena in quantum degenerate gases such as the creation of polarons[1]. Their use as a probe, however, requires that their lifetimes be sufficient to allow interactions to produce measurable effects. Here we examine the lifetimes of strontium Rydberg molecules in a BEC and the reactions responsible for their destruction.

⁸⁴Sr atoms cooled in a magneto-optical trap are loaded into an optical dipole trap where they are subject to evaporative cooling to create a BEC with a peak density of $\sim 4 \times 10^{14} \text{ cm}^{-3}$. Two-photon excitation is used to create Rydberg molecules with values of principal quantum number n in the range $49 \leq n \leq 72$. A typical excitation spectrum is included in Fig. 1, expressed as a function of detuning from the atomic line. The sharp peak at zero detuning results from excitation of thermal non-condensed atoms present in the trap, the broad feature extending to the red results from molecular excitation, the larger the detuning the larger the number of atoms present in the molecule. The evolution of the Rydberg population is monitored by field ionization. Analysis of the data indicates that the destruction of Rydberg molecules results from the same processes as identified in earlier studies with rubidium[2], namely associative ionization, leading to formation of Sr_2^+ molecules, and L -changing reactions.

Figure 1 shows the time evolution of the total Rydberg population. The initial rapid decrease in the Rydberg population results from associative ionization. The slower rate of loss

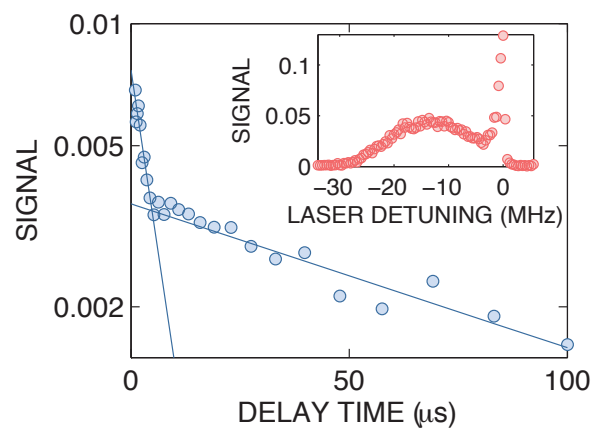


Figure 1. Time evolution of the Rydberg population following excitation of $n=60$ Rydberg molecules at a detuning of -21.6 MHz in a BEC. The inset shows the $n=60$ excitation spectrum.

seen at later times results from the decay of L -changed Rydberg atoms. The measured molecular lifetimes, $\sim 3\text{-}10 \text{ } \mu\text{s}$, limit the timescales over which studies involving Rydberg molecules in cold, dense gases can be undertaken, and reduce the coherence time in such measurements.

Research supported by the AFOSR, the NSF, the Robert A. Welch Foundation, and the FWF (Austria)

References

- [1] F. Camargo et al. to be published
- [2] M. Schlagmüller et al. 2016 *Phys. Rev. X* **6**, 031020

E-mail: fbd@rice.edu

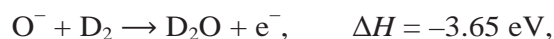
Reactions of O^- with D_2 at low temperatures 10 – 300 K

Radek Plašil^{*1}, Thuy Dung Tran^{*}, Štěpán Roučka^{*}, Pavol Jusko^{*}, Dmytro Mulin^{*}, Illia Zymak^{*}, Petr Dohnal^{*}, and Juraj Glosík^{*¶}

^{*} Department of Surface and Plasma Science, Faculty of Mathematics and Physics, Charles University in Prague, 180 00 Prague, Czech Republic

Synopsis The reaction of O^- anions with molecular deuterium D_2 has been studied experimentally using a cryogenic 22-pole radiofrequency ion trap. There were observed two reaction channels. In the associative detachment D_2O is formed and for atom transfer formation $OD^- + D$ was observed. The rate coefficients of the reactions have been determined at temperatures ranging from 10 K to 300 K.

The reaction of O^- with D_2 has two exothermic channels corresponding to associative detachment and deuterium atom transfer



Energetically possible are also reactions leading to the formation of metastable D_2O^- anion in three body or radiative association. However these processes have not been detected experimentally. Studies of gas-phase processes involving water and especially those leading to isotopic fractionation [1] is essential for understanding of the water formation in the Universe.

The reactions were studied using a 22-pole radiofrequency ion trap. It was mounted on a cryo-cooler in an ultra-high vacuum system. The measuring procedure was based on iterative filling of the trap with a well-defined number of primary ions O^- where they react with molecular deuterium. The content of the trap were analyzed after chosen times using a quadrupole mass spectrometer and a micro-channel plate detector. Further detail may be found in [2] and references therein.

We studied previously analogous reactions involving O^- and H_2 . At first we measured electron energy spectrum originating from associative detachment [3] at 300 K. Later on we studied both reactions using the 22-pole ion trap [4].

Very interesting dependence on temperature is shown on Figure 1. Up to now the associative detachment has been measured mostly at temperatures higher than 300 K and the observed reaction rate coefficient was about $\frac{1}{3}$ of the Langevin rate. It is explained by the fact that trajectories on only one of three electronic surfaces of the collision system can lead directly to autodetachment.

At lower temperatures we observed unexpectedly high value of the associative detachment rate coefficient. Theoretical model in our paper [4] for the reaction $O^- + H_2$ explained this behavior by rearrangement of the collisional system in a shallow local minimum. The increase of the reaction rate coefficient at low temperatures is in qualitative agreement with the theoretical predictions. The presented data will be compared with classical trajectory simulation model. An isotopic effect will be evaluated.

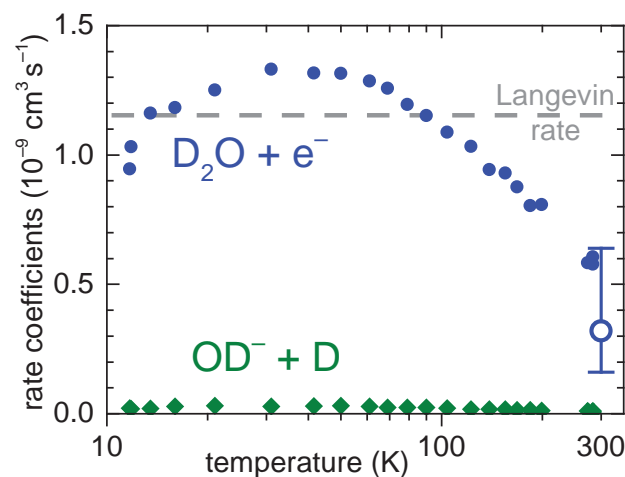


Figure 1. Measured temperature dependencies of the reaction rate coefficients for both channels of $O^- + D_2$ reaction. The open circle indicates results of our previous experiment [4].

We thank the TU Chemnitz, the DFG and prof. D. Gerlich for lending us the apparatus. Supported by GACR 15-15077S and GACR 17-18067S.

References

- [1] L. I. Cleaves *et al.* 2014 *Science* **345** 1590
- [2] D. Gerlich and G. Borodi 2009 *Faraday Discussions* **142** 57
- [3] P. Jusko *et al.* 2013 *Int. J. Mass Spectr.* **352** 19
- [4] P. Jusko *et al.* 2015 *J. Chem. Phys.* **142** 014304

¹ E-mail: Radek.Plasil@mff.cuni.cz

Heavy particle collisions: from single atomic targets to complex molecular clusters

Henrik Cederquist* ¹

* Department of Physics, Stockholm University, AlbaNova University center, S 106 91, Stockholm, Sweden.

Synopsis Charge-, energy- and mass-transfer reactions in collisions between ions, atoms, or other heavy systems and different types of targets (atoms, molecules, clusters etcetera) will be discussed. When applicable, the mechanisms behind the reactions will be compared to the corresponding ones due to photon- and lepton interactions.

The different types of reactions that may occur when ions, atoms, or other types of heavy particles collide with different types of targets such as single isolated atoms or molecules, biomolecular ions, clusters of atoms or molecules, or molecules in solutions will be discussed. The mechanisms behind the phenomena that then occur will also be discussed and, when useful, compared to those caused by interactions with photons or electrons. Key experimental and theoretical results contributing to the understanding of various charge-transfer and excitation processes, molecular- and cluster fragmentation processes, and of molecular growth processes will be reviewed and highlighted. We will mainly discuss results for collision energies from the few eV to the hundreds of keV range, but results for the important sub-eV and MeV regimes may also be touched upon.

It is indeed important to understand the mechanisms behind charge- and energy transfer reactions and of heavy particle rearrangement processes (chemical reactions) as such processes are important in many different types of environments ranging from the cold interstellar medium, to stellar atmospheres, processes in planetary atmospheres including that of Earth, biomolecular radiation damage processes etcetera. In the latter case it is also particularly interesting to study how a solvent environment influences the type of processes that occur.

For the studies and fields mentioned above it would in most cases be extremely useful if one could prepare the systems in single quantum states before they are brought to interact. For complex systems containing many atoms this is extremely difficult but can be achieved for atomic and small molecular systems using traps or storage rings. In several different laboratories, new instruments are now being prepared for experiments on simple and complex atomic

or molecular systems in single quantum states, or in narrow ranges of quantum states, for refined studies of their interactions with ions, neutrals, electron, and photons. These new intriguing possibilities will be briefly touched upon in the talk.

¹ E-mail: cederq@fysik.su.se

Mechanisms of strong-field control in the fragmentation of small molecules

K. Doblhoff-Dier^{*1}, M. Kitzler[†], S. Gräfe[‡]

^{*} Leiden Institute of Chemistry, Leiden University, NL-2333 CC Leiden, Netherlands

[†] Photonics Institute, Vienna University of Technology, A-1040 Vienna, Austria

[‡] Institute for Physical Chemistry and Abbe Center of Photonics, Friedrich-Schiller University, D-07743 Jena, Germany

Synopsis Ultra-strong, few femtosecond laser fields trigger a multitude of dynamical effects in molecules. We address the question of whether and how the electronic and nuclear response to such fields can be used to guide and control molecular reactions. Via a combination of quantum and semi-classical calculations we shed light on the processes underlying strong-field fragmentation of C_2H_2 and explain the reaction control via carrier-envelope phase and alignment observed in experiments.

Steering molecular reactions is a long standing goal in chemistry and physics. With the advent of strong ($\sim 10^{14} \text{ W/cm}^2$) and ultra-short ($< 5 \text{ fs}$) infrared pulses, the question arose whether these strong fs-pulses can be used to steer molecular motion. — An interesting question since the timescales accessible to such pulses is too short to directly steer the nuclear dynamics. The first experimental realization of strong-field reaction control in polyatomic molecules was the proof of reaction control in acetylene, C_2H_2 , to the product channels $C_2H^+ + H^+$, $CH^+ + CH^+$ and $CH_2^+ + C^+$ as well as the ionic products $C_2H_2^+$ and $C_2H_2^{2+}$ in dependence of the carrier-envelope phase (CEP) and the alignment of laser polarization axis with respect to the molecular axis[1, 2].

Our theoretical investigations show that two fundamentally different processes are responsible for the reaction control in these cases: The reaction control via the CEP is governed by the intimate interplay of the electrons' recollisional energy in dependence of the carrier-envelope phase and the accessibility of dissociative states[1]. This could be shown by quantum chemical analysis of the relevant potential energy surfaces, followed by wavepacket simulations and semi-classical simulations of the recolliding electron's motion.

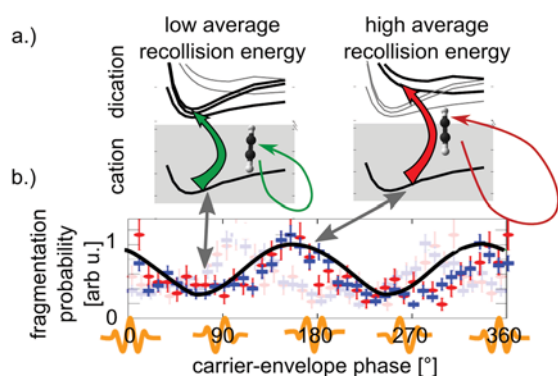


Figure 1. Reaction control via the CEP: a.) recollision model, b.) comparison with experiment [1]

The control of the nuclear dynamics occurring on the femtosecond timescale is thus promoted by the sub-fs control of the electronic dynamics.

In the case of reaction control via the alignment of the molecule relative to laser polarization axis, sub-fs timescales are less important: In this case, the mechanism relies on sequential double ionization and the angle dependence of tunneling-ionization from different (Dyson-)orbitals. With the aid of time-dependent density functional theory and semi-classical tunneling models, we could qualitatively and quantitatively reproduce the alignment dependence for most of the experimentally observed reaction channels[1, 3]. For some reaction channels, recollisional ionization becomes important. This was shown by comparison of experimental and theoretical calculations for linear and circularly polarized light.

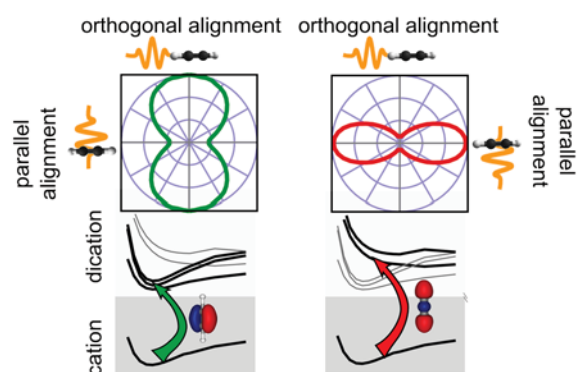


Figure 1. Reaction control via the alignment: ionization to different states corresponds to different Dyson orbitals showing distinct alignment dependent ionization probabilities[2, 3].

References

- [1] X. Xie, K. Doblhoff-Dier *et al.* 2012 *Phys. Rev. Lett.* **109** 243001
- [2] X. Xie, K. Doblhoff-Dier *et al.* 2014 *Phys. Rev. Lett.* **112** 163003
- [3] K. Doblhoff-Dier *et al.* 2016 *Phys. Rev. A* **94** 013405

¹ E-mail: k.doblhoff-dier@umail.leidenuniv.nl

Multielectron dynamics of atoms and molecules in strong laser fields

Takeshi Sato^{*†1}

^{*} Photon Science Center, School of Engineering, The University of Tokyo, Tokyo 113-8656, Japan

[†] Department of Nuclear Engineering and Management, School of Engineering, The University of Tokyo, Tokyo 113-8656, Japan

Synopsis We have developed *ab initio* time-dependent many-electron theories with complete-active-space (TD-CASSCF) and occupation-restricted multiple-active-space (TD-ORMAS) models, which enables accurate description of multielectron dynamics of atoms and molecules in strong laser fields.

An important goal of high-field and ultrafast physics is the direct measurement and control of electron dynamics in atoms and molecules. To theoretically investigate multielectron dynamics in intense laser fields, the multiconfiguration time-dependent Hartree-Fock (MCTDHF) method has been developed [1, 2], in which the wavefunction is given by the superposition of Slater determinants constructed with timely varying orbitals. Though powerful, the MCTDHF method suffers from the exponential increase of the computational cost against the number of electrons.

To circumvent this difficulty, we have proposed the TD-CASSCF method [3], which classifies the occupied orbitals into *frozen core* (doubly occupied and fixed in time), *dynamical core* (doubly occupied but time dependent) and *active* (fully correlated and time dependent) orbitals. See Fig. 1. We have also developed the TD-ORMAS method [4], which further subdivides the active orbitals into an arbitrary number of subgroups, and poses the *occupation restriction* in each subgroup.

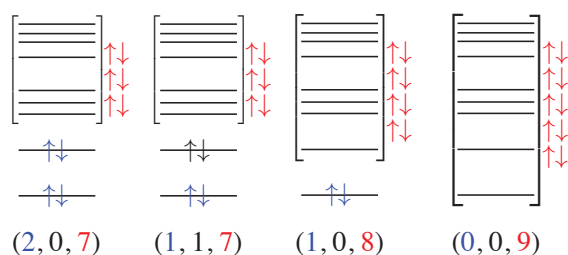


Figure 1. Illustration of the TD-CASSCF concept for a ten-electron system with nine occupied orbitals. The up and down arrows represent electrons decomposed into FC electrons (blue), DC electrons (black), and active electrons (red). The horizontal lines represent occupied orbitals, classified into doubly occupied FC and DC orbitals and active orbitals (bracketed).

These methods, implemented for atoms [5] and molecules [6] employing state-of-the-art numerical techniques, enable a compact yet accurate description of multielectron dynamics in intense laser fields. In this progress report, we briefly describe the theoretical background and three-dimensional implementation of TD-CASSCF and TD-ORMAS methods, and discuss their applications (see Fig. 2, e.g.) to intense-field driven multielectron dynamics of atoms and molecules.

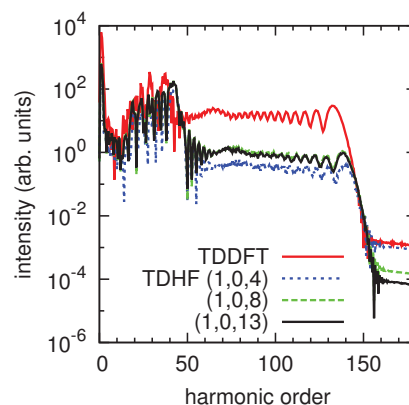


Figure 2. High harmonic generation spectrum of Ne exposed to a near-infrared laser pulse with a wavelength of 800 nm and an intensity of 1×10^{15} W/cm², computed with TDDFT, TDHF, and TD-CASSCF methods with various active spaces.

References

- [1] J. Caillat *et al* 2005 *Phys. Rev. A* **71** 012712
- [2] T. Kato and H. Kono 2004 *Chem. Phys. Lett.* **392** 533
- [3] T. Sato and K. L. Ishikawa 2013 *Phys. Rev. A* **88** 023402
- [4] T. Sato and K. L. Ishikawa 2015 *Phys. Rev. A* **91** 023417
- [5] T. Sato *et al* 2016 *Phys. Rev. A* **94** 023405
- [6] R. Sawada, T. Sato and K. L. Ishikawa 2016 *Phys. Rev. A* **93** 023434

¹E-mail: sato@atto.t.u-tokyo.ac.jp

Novel high harmonic generation schemes

Dimitris Charalambidis^{*,†,‡}

^{*}FORTH-IESL, PO Box 1527, GR711 10 Heraklion, Crete, Greece

[†]Department of Physics, Univ.of Crete, PO Box 2208, GR71003 Heraklion, Greece

[‡]ELI-ALPS, ELI-Hu Kft., Dugonics ter 13, H-6720 Szeged Hungary

High order harmonic generation (HHG) sources based on the interaction of fs laser pulses with gas or solid targets, acting as non-linear media, have undergone enormous progress in the last 25 years. This evolution that resulted new science, novel technologies and rather robust operation of attosecond beam-lines, encounters still lots of challenges. Ongoing developments target advanced operational parameters such as high photon fluxes, high photon energies, high repetition rates, controllable polarization and advanced diagnostics.

A substantial increase of the source throughput can be achieved by properly scaling the source geometry and emitting medium density [1]. In this framework advanced schemes for intense harmonic generation have opened up the era of XUV non-linear optics, achieving amongst others spatially resolved two-XUV-photon ionization [2], XUV-pump-XUV-probe studies of 1fs scale dynamics in atomic [3] and molecular systems [4] using broad band XUV continua [5] or harmonic combs [6] in the spectral region ~10-25eV. Two XUV-photon atomic double ionization has been recently demonstrated at higher photon energies (20-50 eV) in Neon [7] and He at central photon energy ~90eV [8]. The plasma vacuum interface, holds the promise of substantially increasing the number of photons carried away even in single attosecond bursts [9]. Phase locking of laser surface plasma harmonics leading to sub-fs localization and the highest XUV pulse energies have been already demonstrated in this area [10].

Recent developments have reached control of the ellipticity of the HHG by circularly polarized IR pulses in laser aligned molecules [11]. Although photon fluxes are here

substantially reduced, increased repetition rates of upcoming laser systems, hold promise for enough statistics when using circularly polarized attosecond pulses for e.g. magnetic circular dichroism or chirality studies.

Finally novel mid-IR lasers bring sound advantages in HHG due to i) the λ^{-1} scaling of the group velocity dispersion and the subsequent $\lambda^{-1/2}$ scaling of the attosecond pulse duration and ii) the λ^2 scaling of the ponderomotive potential, shifting the cut-off energy of the gas harmonic spectrum to the water window region and beyond.

One of the key factors in the improvement of the attosecond sources is the advancement of the driving laser sources. Indeed, innovative laser systems driving beyond the state of the art attosecond sources are currently developed for the European User Research Infrastructure “Extreme Light Infrastructure- Attosecond Light Pulsed Source (ELI-ALPS)”.

In this talk I will report on some of the above achievements and highlight future prospects of ELI-ALPS.

References

- [1] C. M. Heyl *et al.* 2016 *Optica* **3**, 75
- [2] N. Tsatrafyllis *et al.* 2016 *Sci. Rep.* **6**, 21556
- [3] P. Tzallas *et al.* 2011 *Nature Physics* **7**, 781
- [4] P. A. Carpegiani *et al.* 2014 *Phys. Rev.* **A89**, 023420
- [5] P. Tzallas *et al.* *Nature Physics* **3**, 846 (2007)
- [6] Y. Nabekawa *et al.* 2016 *Nature Comm.* DOI: 10.1038/ncomms12835
- [7] B. Manschwetus *et al.* 2016 *Phys. Rev* **A93**, 061402(R)
- [8] B. Bergues *et al.* (in preparation)
- [9] G. D. Tsakiris *et al.* 2006 *New J. Phys.*, **8**, 19
- [10] Y. Nimura *et al.* 2009 *Nature Physics* **5**, 124
- [11] E. Skatzakis *et al.* 2016 *Sci. Rep.* **6**, 39295

¹E-mail: chara@iesl.forth.gr

²E-mail: Charalambidis.Dimitris@eli-alps.hu

Photon energy deposition in strong-field ionization of molecules

Wenbin Zhang, Peifen Lu, Xiaochun Gong, Qiyong Song, Qinying Ji, Kang Lin, Junyang Ma, Hui Li, Heping Zeng, and Jian Wu¹

State Key Laboratory of Precision Spectroscopy, East China Normal University, Shanghai 200062, China

Synopsis We experimentally demonstrate the electron-nuclear sharing of the absorbed energy of multiple photons in strong-field ionization of molecules.

Atoms and molecules may coherently absorb multiple photons beyond the minimal number required for ionization driven by a strong laser fields, leading to discrete peaks in the photoelectron spectrum spaced by the photon energy, i.e. above threshold ionization (ATI) as firstly observed by P. Agostini *et al* in 1979 [1]. The primary phase of the light-molecule interaction is the photon energy absorption and deposition. As compared to atoms where the electron keeps most of the absorbed photon energy, the additional vibrational and rotational nuclear motions of molecules also serve as energy reservoir. The photon energy deposits into the nuclei governs the succeeding dynamics and thus the fate of the molecules.

Until recently the electron-nuclear sharing of the absorbed photon energy in strong-field multiphoton single ionization of molecules was revealed for the simplest one or two-electron systems of H_2^+ [2,3] and H_2 [4]. On the other hand, the recent experiments show negligible photon energy sharing between the emitted electrons and nuclei in multiphoton above threshold double ionization of a polyatomic hydrocarbon molecule [5]. Does the electron-nuclear sharing of the absorbed photon energy in multiphoton ionization of molecules merely exist in the simplest one- or two-electron systems? Which rules govern the electron-nuclear sharing of the photon energy?

Here, we demonstrate the first experimental observation of the electron-nuclear sharing of the absorbed photon energy in strong-field above-threshold dissociative single ionization of multielectron molecules. Vibrational and orbital resolved electron-nuclear sharing of the absorbed photon energy is identified for the

carbon monoxide molecule. The photon energy sharing between the electron and nuclei is governed by the population of numerous vibrational states of the molecular cation in the ionization process, which are altered by the orbitals from which the electron is removed and the potential energy surfaces of the cation state on which the nuclei dissociate.

We further report the experimental observation of photon energy sharing among two electrons and two ions ejected from a doubly ionized molecule [7]. Although two electrons are successively released one after the other, bridged by the nuclear motion via their interaction, photon energy sharing among four particles is observed as multiple energy conservation lines in their joint energy spectrum. For sequential double ionization of H_2 , the electron-nuclear joint energy spectrum allows us to identify three pathways towards the charge-resonance enhanced ionization of the stretching H_2^+ in strong laser fields. By counting the photon number absorbed by the molecule, we trace the accessibility, enhancement and suppression of various pathways. The correlated electron-nuclear motion provides profound insights of the complicated strong-field dynamics of molecules.

References

- [1] P. Agostini *et al.* 1979 Phys. Rev. Lett. [42, 1127](#)
- [2] C. Madsen *et al.* 2012 Phys. Rev. Lett. [109, 163003](#)
- [3] K. Liu *et al.* 2014 Phys. Rev. A [89, 053423](#)
- [4] J. Wu *et al.* 2013 Phys. Rev. Lett. [111, 023002](#) (2013).
- [5] X. Gong *et al.* 2015 Phys. Rev. Lett. [114, 163001](#)
- [6] W. Zhang *et al.* 2016 Phys. Rev. Lett. [117, 103002](#)
- [7] P. Lu *et al.*, submitted for publication (2016).

¹ E-mail: jwu@phy.ecnu.edu.cn

Photofragmentation of ions and fragment storage in a compact storage ring

Henrik B. Pedersen^{*1}, Annette Svendsen^{*} Hjalte V. Kiefer^{*} Ricky Teiwes^{*} Lars H. Andersen^{*2},

^{*} Department of Physics and Astronomy, Aarhus University, 8000 Aarhus C, Denmark

Synopsis We report on the development of a novel electrostatic storage ring for studies of photofragmentation processes of molecular ions. We demonstrate how the ring can simultaneously be exploited as an electrostatic analyzer and as a time-of-flight spectrometer to analyze dynamics of photon-induced processes.

During the last decades, the application of electrostatic storage devices, i.e. systems that enable the trapping of fast moving ion beams by means of electrostatic fields only, have proven extremely valuable for studies of atomic and molecular ions. In an electrostatic ion trap, the conditions for ion storage is only determined by the energy-to-charge ratio of the ions. Intense development of electrostatic storage devices has occurred, for instance with respect to cryogenic devices and with respect to characterizing spontaneous or induced reactions of the stored ions.

At Aarhus University, we have recently constructed a compact electrostatic storage ring SAPHIRA (Storage ring in Aarhus for PHoton-Ion Reaction Analysis) [1] dedicated to the study of photon-induced processes in molecular ions. A schematic layout of the SAPHIRA ring is displayed in Fig. 1.

In SAPHIRA, ions are confined by four identical electrostatic corner modules that both provide ion beam focusing and deflection by 90 degrees. The modules are placed in a square geometry with a side length of 1.00 m to form a closed structure. To inject or extract ions, the potentials on the deflection electrodes in the corners can be rapidly switched between two high voltage levels.

As also illustrated in Fig. 1, the stored ions can be laser-irradiated both in crossed and merged beams interaction geometries. In both cases the ion-photon interaction takes place inside an electrode system that allows the interaction region to be biased to a well-defined potential.

The potential on the electrodes surrounding the interaction region is switchable between ground and a high voltage level allowing for instance for acceleration of ions present inside the region during switching, and hence effectively altering the trapping con-

ditions for these ions [2].

With this technique, it is in fact possible to trap fragment ions while rejecting parent ions from SAPHIRA, i.e. in effect using the ring as an electrostatic mass analyzer. Moreover, the long flight path in the ring also allows to analyze properties of the fragment ions (kinetic energy release and angular distribution), essentially using the ring as a time-of-flight spectrometer.

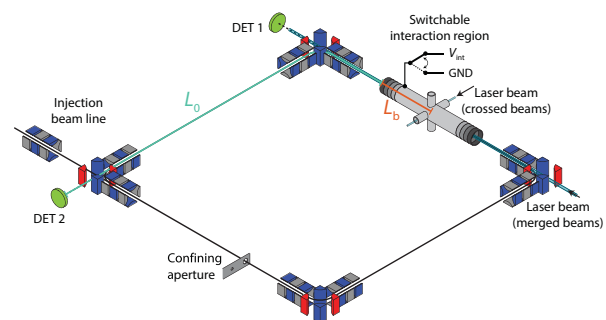


Figure 1. Schematic layout of the electrostatic storage ring SAPHIRA, showing the four compact corners used to confine a fast moving ion beam, and the switchable interaction region that enables the analysis of photofragment ions produced in crossed or merged beams experimental configurations. Fragment detectors are located outside of the ring.

References

- [1] H. B. Pedersen, A. Svendsen, L. S. Harbo, H. V. Kiefer, H. Kjeldsen, L. Lammich, Y. Toker, and L. H. Andersen, 2015 *Rev. Sci. Instrum.* **86** 063107
- [2] A. Svendsen, R. Teiwes, H. V. Kiefer, L. H. Andersen, and H. B. Pedersen, 2016 *Rev. Sci. Instrum.* **87** 013111

¹E-mail: hbjp@phys.au.dk

²E-mail: lha@phys.au.dk

Internally cold ions in the Cryogenic Storage Ring

Oldřich Novotný^{*1} for the CSR team

^{*} Max Planck Institute for Nuclear Physics, Heidelberg, Germany

Synopsis We present first results from experiments on internally cold ions using the recently commissioned Cryogenic Storage Ring.

In last decades heavy ion storage rings have proven to be unique tools for investigating properties and reaction dynamics of atomic and molecular ions, in particular low-energy electron-ion collisions in merged beams [1]. The two most prominent advantages are 1) the long storage of the ions allowing relaxation of the the internal ion states to the equilibrium with the black body radiation of the wall and 2) the ion beam phase-space cooling using an electron beam which prepares the ion beam target for experiments at high collision-energy resolution.

The black body radiation in the existing storage rings operated at room temperatures (300 K) became a limiting factor for these experiments. Even for small molecules, many rotational levels contributed to the reactions which compromised the comparison with theoretical calculations. Moreover, many low-temperature ion reactions are relevant for astrochemical models of the cold interstellar medium where the internal ion excitation drops down to ~ 10 K. This leaves ambiguities for data from 300 K storage rings, where many rotational states remain populated.

To resolve these limitations we have built the electrostatic Cryogenic Storage Ring (CSR) at the Max Planck Institute for Nuclear Physics, Heidelberg, Germany [2]. The ring is designed to store ion beams at energies up to 300 keV per unit charge, independently of ion mass. Cryogenic cooling of the whole beamline chamber leads to a low radiation field. Additionally, at 6K wall temperature reached, the cryo-pumping on the walls results in low residual gas densities ($< 140 \text{ cm}^{-3}$) and ion beam storage times of several hours.

The four straight sections of CSR house experimental setups (Figure 1). In the electron cooler the ion beam is merged with a cold photocathode-produced electron beam. With the electron energy spread of $\sim 1 \text{ meV}$ electron cooling of ions up to 160 u per unit charge is foreseen. The electron beam acts also as a target for experiments such as dissociative recombination of molecular ions and dielectronic recombination of highly charged atomic ions. From the corresponding counting and 3D-imaging detec-

tors operated in the cryogenic environment we derive not only cross section but also the fragmentation dynamics and internal excitations of reactants and products. Another ion collision target is a laser beam oriented at crossed or grazing-angle geometry, accessing processes like photodissociation, photodetachment, etc. In a separate section, a beam of neutral atoms is merged with the stored molecular beam to probe ion-neutral collisions at low relative collision energies. A large variety of ion beams to be stored can be produced from specialized ion sources.

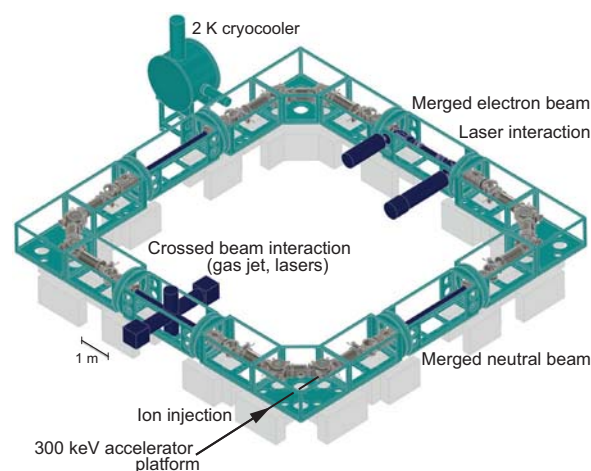


Figure 1. Overview of the CSR showing the cryostat structure and the main experimental sections.

In the talk results from the first CSR experimental campaigns will be presented. We demonstrate functionality of the storage ring and some of the experimental tools, and present first physics results on investigating molecular and cluster ions. Special emphasis will be given to the internal ion cooling for positive and negative molecular ions [3]. Future upgrades will be discussed as well.

References

- [1] R. Thomas *et al.* 2008 *Mass Spec. Rev.* **27** 485
- [2] R. von Hahn *et al.* 2016 *Rev. Sci. Instr.* **87** 063115
- [3] A. O'Connor *et al.* 2016 *Phys. Rev. Lett.* **116** 113002

¹E-mail: oldrich.novotny@mpi-hd.mpg.de

Studies at the border between atomic and nuclear physics

Yuri A. Litvinov^{*1} for the ESR/CRYRING^{*} and CSRe[†] Collaborations

^{*}GSI Helmholtzzentrum für Schwerionenforschung, 64291 Darmstadt, Germany

[†]Institute of Modern Physics, Chinese Academy of Sciences, Lanzhou 730000, China

Synopsis High atomic charge states can significantly influence nuclear decay rates. Recent experiments with stored exotic nuclei that have been performed at the ESR storage ring are discussed. A particular emphasis is given to two-body beta decays, namely bound-state beta decay and orbital electron capture.

The question on whether nuclear lifetimes are fundamental constants or can be modified by external manipulations was asked at the beginning of nuclear physics [1]. At present, the largest variations of nuclear decay rates were observed in highly charged ions (HCI) [2,3].

An obvious example is the electron capture (EC) decay probability, which depends strongly on the number of bound electrons [4,5]. One of straightforward motivations for studying β -decay of HCIs is that stellar nucleosynthesis proceeds at high temperatures, where the involved atoms are highly ionized. Furthermore, HCIs offer the possibility to perform basic investigations of β -decay under clean conditions: The decaying nuclei having, e.g., only a single bound electron, represent themselves well-defined quantum-mechanical systems, in which all interactions with other electrons are excluded, and thus corrections due to shake-off effects, electron screening etc. can be studied.

Largest modifications of nuclear half-lives with respect to neutral atoms were observed in β -decay of fully ionized nuclei. Presently, the ion-storage ring ESR at GSI in Darmstadt is the only tool in the world where radioactive decays of HCIs are routinely studied [6]. Here, the radionuclides produced at high kinetic energies as HCIs and purified from unwanted contaminants are stored in the cooler-storage ring ESR. Due to the ultra-high vacuum of about 10^{-10} mbar, the high atomic charge states of the ions can be preserved for extensive periods of time (minutes, hours). The decay characteristics of electron cooled stored HCIs can accurately be measured by employing the highly sensitive non-destructive time-resolved Schottky spectrometry technique [7,8].

Recent experiments with stored exotic nuclei that have been performed at the ESR will be discussed in this contribution. A particular emphasis will be given to two-body beta decays, namely bound-state beta decay and orbital electron capture.

At GSI, investigations of exotic radioactive decay modes like Nuclear Excitation by Electron Capture [9] or Bound Electron-Positron Pair Creation [10] are proposed for the ESR and the newly installed low-energy CRYRING [9].

As an outlook, the perspectives of future experiments with HCIs at existing storage ring facilities (ESR/CRYRING at GSI, Darmstadt, CSRe at IMP, Lanzhou, and R3 at RIKEN, Wako) as well as at the planned facilities (FAIR in Darmstadt and HIAF in Huizhou [11]) will be outlined.

References

- [1] E. Rutherford and F. Soddy 1902 *J. Chem. Soc. Trans.* **81** 837
- [2] Y. Litvinov and F. Bosch 2011 *Rep. Prog. Phys.* **74** 016301
- [3] F. Bosch, *et al.* 2013 *Prog. Part. Nucl. Phys.* **73** 84
- [4] Y. Litvinov, *et al.* 2007 *Phys. Rev. Lett.* **99** 262501
- [5] N. Winckler, *et al.* 2009 *Phys. Lett. B* **679** 36
- [6] Y. Litvinov, *et al.* 2013 *Nucl. Instr. Meth. B* **317** 603
- [7] F. Nolden, *et al.* 2011 *Nucl. Instr. Meth. A* **659** 69
- [8] P. Kienle, *et al.*, 2013 *Phys. Lett. B* **726** 638
- [9] M. Lestinsky, *et al.* 2016 *Eur. Phys. J. Special Topics* **225** 797
- [10] F. Bosch, *et al.* 2016 *EPJ Web of Conferences* **123** 04003
- [11] Y. Zhang, *et al.* 2016 *Phys. Scripta* **91** 073002

¹ E-mail: Y.Litvinov@gsi.de

Photorecombination studies at Shanghai EBIT

B. Tu, J. Xiao, K. Yao, Y. Shen, Y. Yang, D. Lu, Y. Q. Fu, B. Wei, C. Zheng, L. Y. Huang, R. Hutton, and Y. Zou¹

Shanghai EBIT Laboratory, Institute of Modern Physics, Fudan University, and the Key Laboratory of Applied Ion Beam Physics, Chinese Ministry of Education, China

Synopsis This work reported both experimental and theoretical study on photorecombination processes, including resonance levels, resonance strengths, radiative decay and interference effect, for highly charged ions at Shanghai EBIT.

Recombination processes between free electrons and ions are classified as photorecombination (PR) proceeding with photon emissions via two main pathways.

Dielectronic recombination (DR) used to be considered a resonant two-step process. In the first step a free electron is captured by an ion; at the same time a bound electron is promoted to form a multiply excited intermediate state sitting above the autoionization threshold. The second step is stabilization, in which one or more photons are emitted so as to reduce the ion energy to below its ionization limit. DR is an important process in hot plasma physics as well as in atomic structure and collision theory. It significantly affects the plasma temperature, the charge state distribution, and the ion level population. The radiative processes in DR cause unresolvable satellites, which may disturb line shape, line intensity, and line width, while the resolved satellite lines are often used for electron temperature diagnostics. Furthermore, DR of highly charged ions contributes significantly to radiation energy loss in fusion plasmas, and thus leading to the severe problem on the flameout of fusion.

There is another process called radiative recombination (RR), in which a free electron is captured by an ion and the excess energy is released by emitting a photon directly. If DR and RR have identical initial states, final states, and photon emissions, it is then impossible to distinguish through which process the recombination took place, and interference would occur. As a consequence, asymmetric resonant line profile called Fano line profile appears. Much work has been done to study PR processes, but only a very few studies have observed DR-RR interference [1-4] due to the fact that most studies were for the cases where RR was much weaker than DR and the interference was negligible.

In this work, we reported the recent study on PR processes for highly charged Ar, Xe and W ions through both experiment and calculation [3-7]. The measurement was performed on Shanghai electron beam ion trap by employing a fast electron beam-energy scanning technique. During the experiment, Ar, Xe or W was continuously injected into the EBIT by a gas injection system, and the electron beam energy was fast scanned through the resonant energy region, while the x-ray photons were detected by a HPGe detector. A fully relativistic configuration interaction method implemented in the flexible atomic code was employed to calculate DR process and also RR cross section.

The interference effect between DR and RR were studied in experiment. The dual Fano and Lorentzian line profile properties in an autoionizing state was demonstrated via selecting the DR resonances which go through an intermediate state with decay channels to both the final states with no excited electrons and the final states with more than two excited electrons. The DR resonance strengths were also determined in our work. Our experimental results show good agreements with the calculations within the uncertainty of about 10%. The comparison between two experimental results (analysis with or without the consideration of interference effect) indicates that the interference effect between DR and RR is revealed to be necessary to determine the resonance strength for highly charged heavy ions.

References

- [1] D. A. Knapp *et al.*, Phys. Rev. Lett. **74**, 54 (1995)
- [2] A. J. G. Martínez *et al.*, Phys. Rev. Lett. **94**, 203201 (2005)
- [3] B. Tu, *et al.*, Phys. Rev. A **91**, 060502(R) (2015)
- [4] B. Tu, *et al.*, Phys. Rev. A **93**, 032707 (2016)
- [5] K. Yao *et al.*, Phys. Rev. A. **81**, 022714 (2010)
- [6] B. Tu, *et al.*, Phys. Plasmas **23**, 053301 (2016)
- [7] G. Xiong *et al.*, In preparation

E-mail: zouym@fudan.edu.cn

Collisional-radiative modeling of hot plasmas

Yuri Ralchenko¹

National Institute of Standards and Technology, Gaithersburg MD 20899-8422, USA

Synopsis For plasmas far from local thermodynamic equilibrium, collisional-radiative (CR) models offer a robust and well-tested approach to analyze their emission and to infer their properties. CR simulations are known to be instrumental for spectroscopic diagnostics of astrophysical plasmas, magnetic fusion devices, laser-produced plasmas, and other environments. I will present an overview of recent developments in CR modeling with an emphasis on hot plasmas of highly-charged ions.

For most terrestrial and astrophysical plasmas, their emission remains the primary source of information on their properties. An accurately measured and carefully analyzed spectrum can reveal detailed data on electron and atom (ion) densities, particle temperatures, electric and/or magnetic fields, turbulent motions, velocity fields, and other parameters. While some of plasma characteristics can generally be inferred from qualitative considerations, it is nowadays customary to build comprehensive spectroscopic diagnostics of various plasmas upon extensive collisional-radiative (CR) models [1]. Such models now routinely include tens of thousands of atomic states with millions of collisional and radiative transitions thereby providing a very detailed theoretical grounds for comparisons with the measured spectra.

In this talk we will present an overview of recent developments in CR modeling of hot plasmas with temperatures of hundreds and thousands of electronvolts. Since accurate atomic data is of highest importance for CR simulations, the available tools for data generation as well as the general requirements for data quality will be addressed. Among the topics to be discussed are the spectroscopic modeling of non-Maxwellian plasmas of multiply-charged heavy atoms in electron beam ion traps (see Fig. 1) including studies of inner-shell dielectronic resonances, kinetic analysis of motional Stark effect for neutral beams in magnetic fusion research [2, 3], Monte Carlo CR modeling of multi-electron charge exchange [4], and diagnostics of about 50-times ionized high-Z atoms in laser-produced plasmas. We will also describe the ongoing efforts to develop the-

oretical techniques for benchmarking CR models and codes [5].

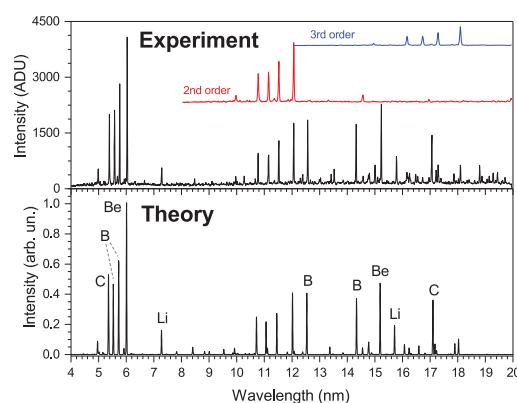


Figure 1. Comparison of the measured (top) and simulated (bottom) extreme-ultraviolet spectra from Y^{31+} – Y^{36+} in an electron beam ion trap. Electron beam energy is 5.15 keV.

References

- [1] Yu. Ralchenko (ed) 2016 *Modern Methods in Collisional-Radiative Modeling of Plasmas* (Springer)
- [2] O. Marchuk et al 2010 *J. Phys. B* **43** 011002
- [3] I. Bespamyatnov et al 2013 *Nucl. Fus.* **53** 123010
- [4] J.R. Machacek et al 2015 *Astrophys. J.* **809** 75
- [5] Yu. Ralchenko, *Validation and Verification of Collisional-Radiative Models*, in Ref. [1].

¹E-mail: yuri.ralchenko@nist.gov

The Tungsten Project: Electron-ion recombination rate coefficients for the isonuclear sequence of tungsten

S. P. Preval^{*1}, N. R. Badnell^{*2}, M. G. O'Mullane^{*3}

^{*} Department of Physics, University of Strathclyde, Glasgow, G4 0NG, United Kingdom

Synopsis Modelling the effect of tungsten impurities in hot magnetic fusion plasmas is essential for informing the future operation of the upcoming experimental fusion reactor, ITER, as well as other reactors that use tungsten components. Calculating the necessary atomic data, as well as the models presents their own unique computational challenges. For this progress report, I will discuss *The Tungsten Project*, which was a three-year endeavour to calculate partial final-state resolved dielectronic recombination rate coefficients for the isonuclear sequence of tungsten. I will then present preliminary results from collisional-radiative models including this new data, and what has been learned from this project.

The upcoming experimental fusion reactor, ITER, will produce its first plasma in 2025, with a projected deuterium-tritium plasma ignition in 2035. The reactor has been designed to output ten times more energy than it consumes. It will also dwarf the current largest tokamak reactor, JET, by a factor 10 in terms of plasma volume. Tungsten has been chosen as the primary material with which to construct the divertor in ITER due to its ability to withstand high power loads. Being a plasma-facing component, tungsten impurities will sputter into the main plasma, leading to cooling and potentially quenching. Detailed models of the tokamak plasma are required to understand the effects of tungsten impurities on the core plasma, as well as to inform future reactor operation.

The high electron temperature ($> 25\text{keV}$) and densities ($10^{18}\text{--}10^{21}\text{m}^{-3}$) present in magnetically confined fusion plasmas necessitates a collisional-radiative (CR) approach to modelling. Such models underpin the Atomic Data and Analysis Structure (ADAS). ADAS is a database and a set of interlinked codes for modelling the radiating properties of plasmas and is organized as a consortium, of mainly magnetic fusion laboratories, and universities.

Dielectronic recombination (DR) is the dominant mode of recombination in hot, dense plasmas such as those found in tokamaks. CR models of tokamak plasmas require partial final-state resolved DR rate coefficients for the element considered. While isonuclear datasets do exist, they are highly uncertain. This can be seen in Putterich et al [2], where the authors had to modify average ion data from Post et al. [1] in order to improve agreement with observed spectral emissions in ASDEX plasmas. To improve the baseline data for CR modelling, we recently completed a series of level, term, and configuration-resolved

calculations informally titled *The Tungsten Project* [3, 4] using the distorted wave code AUTOSTRUCTURE [5].

Calculation of the atomic data required presented its own unique challenges. For example, 4f-shell ions (in particular, half-filled) have tens of thousands of levels making the calculation intractable. Furthermore, the large number of levels leads to enhancement of the DR rate coefficient at low energy due to mixing, meaning that even treating the problem in term resolution only is not sufficient. With regards to CR modelling, the main challenge relates to the logistics and handling of the atomic data by the modelling programme. Each ionization state will have hundreds of partial DR rate coefficients, necessitating the use of bundling techniques to make the problem tractable.

In this talk I will give a brief overview of the ITER experiment and its aims. Next, I will discuss *The Tungsten Project*, with emphasis on calculational methods. Finally, I will present preliminary CR model calculations for ITER-like plasmas. I will conclude by considering the implications for future tokamak operation, and plans for the future.

References

- [1] Post D et al, 1977, *At. Data Nucl. Data Tables*, **20**, 397
- [2] Pütterich T et al, 2008, *Plasma Phys. Control. Fusion*, **50**, 8
- [3] Preval S P, Badnell N R, O'Mullane M G, 2016, *Phys. Rev. A*, **93**, 042703
- [4] Preval S P, Badnell N R, O'Mullane M G, 2017, *Submitted to J. Phys. B*
- [5] Badnell N R, 2011, *Comput. Phys. Commun.*, **182**, 1528

¹E-mail: simon.preval@strath.ac.uk

²E-mail: badnell@phys.strath.ac.uk

³E-mail: martin.omullane@strath.ac.uk

Dielectronic Recombination in EBIT

Zhimin Hu,^{*,1} Gang Xiong,^{*} Jiamin Yang,^{*} Stanislav Tashenov,[†] Chintan Shah,[†] Holger Joerg,[†]
Nobuyuki Nakamura,[‡] José R. Crespo López-Urrutia,[§] Jiyan Zhang,^{*} and Baohan Zhang^{*}

^{*}Laser Fusion Research Center, China Academy of Engineering Physics, Mianyang 621900, China

[†]Physics Institute, Heidelberg University, 69120 Heidelberg, Germany

[‡]Institute for Laser Science, University of Electro-Communications, Tokyo 182-8585, Japan

[§]Max-Planck-Institut für Kernphysik, Heidelberg, 69117 Heidelberg, Germany

Synopsis The resonance strength and x-ray asymmetry measurements of DR show the significant Breit interaction contribution to electron-electron interaction, and the Compton polarimetry gives a higher sensitivity to this intrinsically relativistic effect. Those works allow one to access the QED corrections of the generalized Breit interaction.

The quantum electrodynamics (QED) effects are of importance for fundamental science, in particular, for atomic physics. QED effects have been tested by the precise measurement of transition energy of few-electron heavy ions. However, the QED effects on the atomic collisions have never been done in experiments. The lowest order QED effect in the electron collision can be described through so-called generalized Breit interaction, it can be derived rigorously within the framework of quantum electrodynamics (QED) as the retardation in the exchange of a virtual photon between the electrons. When the frequency of the virtual photon approaches zero, the simplified version of the Breit interaction can be obtained, which is also can be derived in the classical electrodynamics frame.

The importance of the Breit interaction has been confirmed in the electron-ion collisions, such as impact ionization, dielectronic recombination (DR), and impact excitation. Nevertheless, all of the experiments mentioned previously can be reproduced by the simplified Breit interaction theory. Aiming to test the QED effect, generalized Breit interaction effect, we have already done the anisotropy and polarization measurements of the DR x ray lines. The do-

minance of the Breit interaction has been demonstrated in the anisotropy measurements, and polarization measurements show the significant contribution of the Breit interaction. Most importantly, Compton polarimetry, which gives a higher sensitivity to the intrinsically relativistic Breit interaction effect, has been used in the electron ion beam trap (EBIT) experiments, and this technique is a promising approach to allow one to access the QED corrections of the generalized Breit interaction.

In this talk, we present the measurements of anisotropy ^[1, 2], resonance strength ^[3, 4, 5] and linear polarization ^[6, 7, 8] of DR x-ray lines in EBIT.

References

- [1] Z. Hu *et al.* 2012 *Phys. Rev. Lett.* **108** 073002
- [2] Z. Hu *et al.* 2014 *Phys. Rev. A* **90**, 062702
- [3] Z. Hu *et al.* 2013 *Phys. Rev. A* **87**, 052706
- [4] G. Xiong *et al.* 2013 *Phys. Rev. A* **88**, 042704
- [5] N. Nakamura *et al.* 2008 *Phys. Rev. Lett.* **100**, 073203
- [6] H. Joerg *et al.* 2015 *Phys. Rev. A* **91**, 042705
- [7] C. Shah *et al.* 2015 *Phys. Rev. A* **92**, 042702
- [8] C. Shah *et al.* 2016 *Phys. Rev. E* **93**, 061201(R)

¹E-mail: zhimin.hu@caep.cn

Dielectronic Recombination of Be-like $^{40}\text{Ar}^{14+}$ at the CSRm

Z. K. Huang^{*, †}, W. Q. Wen[†], X. Xu[‡], T. H. Xu[¶], H. B. Wang^{*, †}, L.J. Dou^{*}, S. X. Wang[‡], K. Nadir^{*, †}, L. F. Zhu[‡], W.Q. Xu[§], K. Yao[¶], Y. Yang[¶], X. L. Zhu^{*, †}, L. J. Mao[†], J. Li[†], X. M. Ma[†], Y. J. Yuan[†], J. C. Yang[†] and X. Ma^{† 1}

^{*} Institute of Modern Physics, Chinese Academy of Sciences, 730000, Lanzhou, China

[†] University of Chinese Academy of Sciences, 100049, Beijing, China

[‡] Hefei National Laboratory for Physical Sciences at Microscale, Department of Modern Physics, University of Science and Technology of China, 230026, Hefei, China

[§] Department of Mathematics and Physics, Bengbu University, 233000, Bengbu, China

[¶] Institute of Modern Physics, Fudan University, 200433, Shanghai, China

Synopsis Absolute recombination rate coefficients of Be-like Ar^{14+} have been measured by employing the electron-ion merged-beams method at the cooler storage ring CSRm. All the resonances associated with dielectronic ($2s^2 \rightarrow 2s2p$) and trielectronic ($2s^2 \rightarrow 2p^2$) $\Delta N = 0$ recombination within the energy range of 0- 60 eV were studied.

Based on the successful DR measurement of Li-like $^{36}\text{Ar}^{15+}$ at the cooler storage ring CSRm [1], total recombination rate coefficients of Be-like $^{40}\text{Ar}^{14+}$ has also been experimentally studied. Figure. 1 shows measured spectrum covering the relative energy between electron and ion from 0 to 60 eV in the center-of-mass frame. The resonant capture, involving the core excitation of an electron, is called dielectronic recombination. If the resonant recombination via a triply excited states, the core excitation involves two electrons, it is termed trielectronic recombination (TR), which was first observed in the of Be-like Cl^{13+} by Schnell et al [2]. Both DR and TR processes lead to series of peaks in the measured recombination spectrum, which have been identified by extending downward in energy from their series limits with the Rydberg formula.

For a better understanding of the measured spectrum, a theoretical calculation using the atomic-structure code AUTOSTRUCTURE [3] is in progress by the group of N. R. Badnell. We will present the details of the experimental results and the comparison between experimental data and the calculation results in this conference.

This work is partly supported by the National Natural Science Foundation of China through No. 11320101003 and No. 91336102, and Youth Innovation Promotion Association CAS.

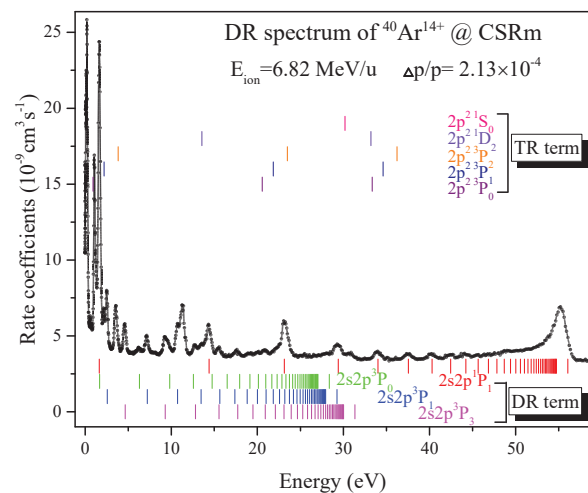


Figure 1. Measured recombination spectrum of Be-like $^{40}\text{Ar}^{14+}$ versus the relative energy between electron and the ion in the center-of-mass frame. Resonance positions based on the Rydberg formula are indicated by vertical short bar involving the spectrum for both dielectronic ($2s^2 \rightarrow 2s2p$) and trielectronic ($2s^2 \rightarrow 2p^2$) $\Delta N = 0$ recombination in different colors.

References

- [1] Z. K. Huang *et al.*, Physica Scripta **T166**, 014023 (2015).
- [2] M. Schnell *et al.*, Phy. Rev. Lett. **91**, 043001 (2003).
- [3] N. R. Badnell, Journal of Physics B: Atomic and Molecular Physics **19**, 3827 (1986).

Extreme ultraviolet spectra of multiply charged tungsten ions

Momoe Mita*, Hiroyuki A. Sakaue†, Daiji Kato†‡, Izumi Murakami†‡, and Nobuyuki Nakamura*¹

* Institute for Laser Science, The University of Electro-Communications, Tokyo 182-8585, Japan

† National Institute for Fusion Science, Gifu 509-5292, Japan

‡ Department of Fusion Science, SOKENDAI, Gifu 509-5292, Japan

Synopsis We present extreme ultraviolet spectra of multiply charged tungsten ions observed with an electron beam ion trap. The observed spectra are compared with theoretical spectra obtained with a collisional radiative model.

Tungsten is the main plasma-facing material in the future experimental fusion reactor ITER, and thus is considered to be the main impurity ions in the ITER plasma. In order to suppress the radiation loss caused by the emission from the impurity tungsten ions, it is important to understand the influx and the charge evolution of tungsten ions in the plasma through spectroscopic diagnostics. There is thus a strong demand for spectroscopic data of tungsten ions. In particular, it has been recently pointed out that the diagnostics and control of the edge plasma are extremely important for the steady state operation of high-temperature plasmas. Thus the atomic data of relatively low charged tungsten ions are of growing significance to the ITER plasma diagnostics [1]. In this study, we present extreme ultraviolet (EUV) spectra of multiply charged tungsten ions observed with an electron beam ion trap, and comparisons with collisional radiative (CR) model calculations.

Multiply charged tungsten ions were produced with a compact electron beam ion trap (EBIT) [2]. Tungsten was introduced into the trap through a gas injector as a vapor of $W(CO)_6$. Emission in the EUV range was observed with a grazing-incidence flat-field spectrometer [3] consisting of a 1200 g/mm concave grating (Hitachi 001-0660) and a Peltier-cooled back-illuminated CCD (Roper PIXIS-XO: 400B).

Figure 1 shows a typical example of the observed spectra. The electron energies shown in the figure are simply determined from the potential difference V_{dif} between the cathode (electron gun) and the middle electrode of the ion trap as eV_{dif} . Thus it should be noted that the actual electron energy (interaction energy between the beam electron and the trapped ions) can be different from the eV_{dif} value due to several reasons, such as the space charge of the electron beam and the trapped ions. Based on the electron energy dependence and the comparison with the previous observation with the Livermore EBIT [1], the observed lines have been assigned to W^{6+} to W^{8+} as

shown in the figure.

We have made CR model calculations [5] for analyzing the observed spectra. Atomic data used in the model were mainly calculated with the HULLAC atomic code [4]. Comparisons between the experimental and model spectra will be given at the conference.

This work was supported by JSPS KAKENHI Grant Number JP16H04623.

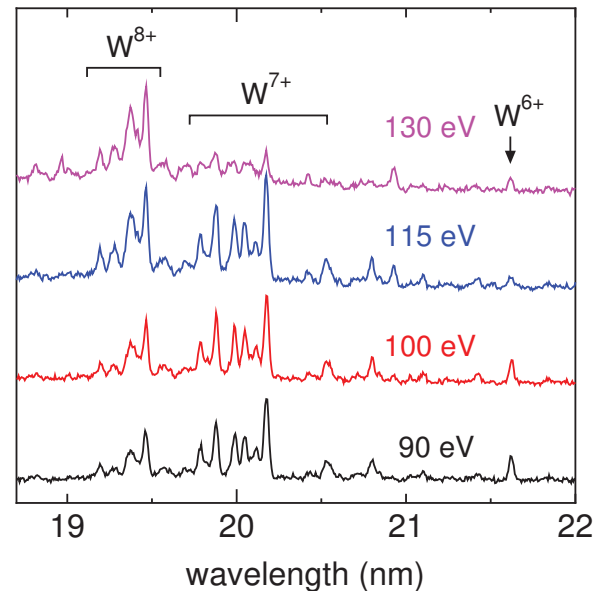


Figure 1. EUV spectra of tungsten ions observed with a compact EBIT at electron energies of 90 to 130 eV.

References

- [1] J. Clementson *et al.* 2015 *Atoms* **3** 407
- [2] N. Nakamura *et al.* 2008 *Rev. Sci. Instrum.* **79** 063104
- [3] H. Ohashi *et al.* 2011 *Rev. Sci. Instrum.* **82** 083103
- [4] A. Bar-Shalom *et al.* 2001 *J. Quant. Spectrosc. Radiat. Transfer* **71** 169
- [5] H. A. Sakaue *et al.* 2015 *Phys. Rev. A* **92** 012504

¹E-mail: n_nakamu@ils.uec.ac.jp

Low-energy ion processing of carbonaceous molecular clusters leading to molecular growth phenomena

Alicja Domaracka^{*1}, Rudy Delaunay^{*}, Michael Gatchell[†], Arkadiusz Mika^{*}, Lamri Adoui^{*}, Henning T. Schmidt[†], Henning Zettergren[†], Henrik Cederquist[†], Patrick Rousseau^{*}, and Bernd A. Huber^{*}

^{*} Normandie Univ, ENSICAEN, UNICAEN, CEA, CNRS, CIMAP, 14000 Caen, France

[†] Department of Physics, Stockholm University, AlbaNova University center, SE-103 91, Sweden

Synopsis To better understand the physical and chemical evolution of the atmospheres of planets/moons and the particle distribution in the interstellar medium it is essential to study energetic processing of carbon containing complex molecular systems. In the present work, we will illustrate low-energy ion-induced reactivity in clusters of small hydrocarbon, fullerene and PAH molecules. The mechanisms of molecular growth will be discussed.

In space, the sizes of carbonaceous particles cover a very large range: from small hydrocarbons, via large molecules (e.g. polycyclic aromatic hydrocarbons - PAHs and fullerenes) and nanometer-sized clusters up to micrometer-sized grains. Energetic processing of such systems in different astrophysical environments (e.g. interstellar medium, planetary atmospheres) by energetic photons or via supernova shocks, cosmic rays and solar wind ions strongly influences the complex chemistry of the Universe. On the one hand, destruction (fragmentation) of large dust grains can lead to a reduction in size forming smaller particles like PAHs/fullerenes (*top-down processes*). On the other hand, the interaction with carbonaceous molecules and clusters can contribute to the formation of larger PAH structures and nanoparticles (*bottom-up processes*).

In this talk, we will give an overview of results on ion-induced fragmentation and ion-induced molecular growth processes of carbon containing clusters colliding with slow ions. The experiments were performed in the ARIBE facility (GANIL, Caen, France) by means of time of flight spectrometry. Parallel theoretical calculations (classical molecular dynamic simulations and DFT calculations) were performed in order to guide the interpretations of the experimental results.

For example in the case of pyrene clusters a large distribution of new molecular species has been observed, much larger than the initial mass of pyrene molecules [1]. The projectile ions are scattered on the nuclei of the molecules and produce reactive molecular species by knockout processes on femtosecond timescales. These species react with other molecules in the cluster and intra-cluster growth processes drive the formation of a wide range of new, larger, molecules [1, 2].

In the second part of the talk, we will present recent results concerning molecular growth processes in clusters of butadiene (small hydrocarbon molecules). In this case, we have observed formation of “magic structures” of new species, which are more stable than similar sized products (see Figure 1). This higher stability is explained by the formation of cyclic structures, the energies of which are found to be lower than those of the linear isomers in almost all cases.

Acknowledgment: Research was conducted in the framework of the CNRS-International Associated Laboratory (LIA) DYNAMO and the XLIC COST action CM1204.

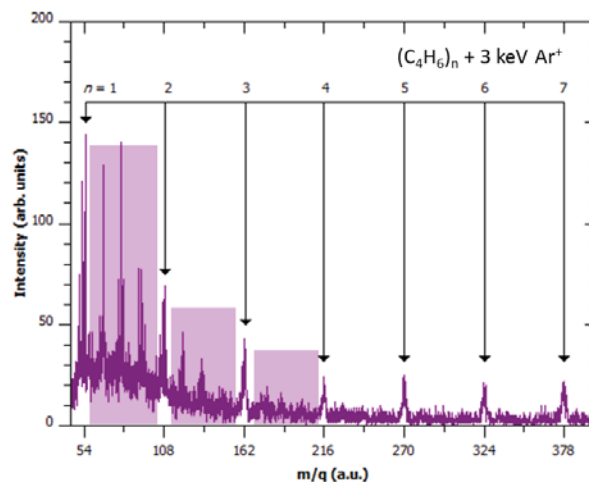


Figure 1. Mass spectrum of cationic products obtained after interaction of 3 keV Ar^+ ions with neutral 1,3-butadiene clusters. Arrows indicate positions of singly charged butadiene clusters $(\text{C}_4\text{H}_6)^+_n$ with $n=1-7$ and colored boxes indicate new covalently bound molecular species formed by ion collisions.

References

- [1] R. Delaunay *et al.* 2015 *J. Phys. Chem. Lett.* **6** 1536-1542
- [2] H. Zettergren *et al.* 2013 *Phys. Rev. Lett.* **110** 185501

¹ E-mail: domaracka@ganil.fr

The relative stability of highly charged fullerenes produced in energetic collisions

Yang Wang^{*†1}, Sergio Díaz-Tendero^{*†‡}, Manuel Alcamí^{*†§}, Fernando Martín^{*‡§}

^{*} Departamento de Química, Módulo 13, Universidad Autónoma de Madrid, 28049 Madrid, Spain

[†] Institute for Advanced Research in Chemical Sciences (IAdChem), Universidad Autónoma de Madrid, 28049 Madrid, Spain

[‡] Condensed Matter Physics Center (IFIMAC), Universidad Autónoma de Madrid, 28049 Madrid, Spain

[§] Instituto Madrileño de Estudios Avanzados en Nanociencia (IMDEA-Nanociencia), Cantoblanco, 28049 Madrid, Spain

Synopsis A simple and unified model has been proposed to fully understand the stability of both positively and negatively charged fullerenes produced in energetic collisions. Based on the concepts of cage connectivity and frontier π orbitals, the model requires only the knowledge of fullerene topology, and permits a rapid prediction of stable structures among a huge number of possibilities.

Multiply charged fullerenes have attracted increasing attention in recent years [1], stimulated by the birth of a new generation of high-energy collision experiments using different kinds of energetic projectiles. Cationic C_{60}^{q+} and C_{70}^{q+} with charges up to 9+ and 6+, respectively, have been produced in collisions of fullerenes with fast, highly charged ions, electrons, and intense laser pulses [1]. Upon collisional excitation, highly charged fullerenes can undergo further fragmentation by emitting one or several carbon fragments, giving rise to a large variety of charged species in mass spectra, which may cover the whole range of cage sizes, starting from the smallest C_{20}^{q+} up to the C_{60}^{q+} and C_{70}^{q+} parents. Sometimes, larger-sized fullerene ions are also formed from coalescence reactions between the highly reactive carbon fragments [2, 3]. Meanwhile, negatively charged fullerenes have also been generated in experiments performed in storage rings and studied by photoelectron spectroscopies. Interestingly, anionic fullerenes commonly exist in the form of intercalated or endohedral complex with metals, which have promising applications in material science and biomedicine.

Despite their abundant existence in nature and their ever-growing importance in chemistry and astrophysics, little progress had been made to understand the relative stability of charged fullerenes, especially for the long-ignored fullerene cations. As shown in earlier work, the experimentally observed isomeric forms of charged fullerenes are often very different from neutral species, for which simple intuitive rules work properly. In the realm of charged fullerenes, however, those well-established stability rules are no longer valid for many structures pro-

duced in experiments [1, 4, 5, 6]. Which are then the underlying principles that govern the stability of charged fullerenes? The answer to this question is not only of fundamental importance, but also practically useful to predict experimentally producible structures, which would be a needle in a haystack task due to the enormous number (tens of thousands or even millions) of possible isomers.

In this presentation, we report a simple and unified theoretical model that allows us to fully understand the stability of both positively and negatively charged fullerenes [5]. Based on the concepts of cage connectivity and frontier π orbitals, the model requires solely the knowledge of fullerene topology, with need for neither geometry optimizations nor iterative electronic structure calculations. Hence, this generalized method makes it possible to rapidly predict stable structures of fullerenes with different cage sizes and in different charge states, without resorting to elaborate quantum chemistry calculations. The model has recently been extended to more complex systems with a stunning success [7].

References

- [1] Y. Wang *et al.* 2010 *Handbook of Nanophysics: Clusters and Fullerenes*, CRC Press, Vol. 2, Chapter 25
- [2] H. Zettergren *et al.* 2013 *Phys. Rev. Lett.* **110** 185501
- [3] Y. Wang *et al.* 2014 *Phys. Rev. A.* **89** 062708
- [4] Y. Wang *et al.* 2009 *Phys. Rev. A.* **80** 033201
- [5] Y. Wang *et al.* 2015 *Nat. Chem.* **7** 927
- [6] Y. Wang *et al.* 2016 *J. Am. Chem. Soc.* **138** 1551
- [7] Y. Wang *et al.* 2017 *J. Am. Chem. Soc.* **139** 1609

¹E-mail: yang.wang@uam.es

Orientation effects in ion-molecule collisions

I. Rabadán¹, L. Méndez, Clara Illescas, L. F. Errea

Departamento de Química, Universidad Autónoma de Madrid, 28049 Madrid, Spain

Synopsis The effect of the anisotropy of the target is studied in Ion-molecule collisions at energies above 0.1 keV/u. Orientation-dependent charge-exchange cross sections are obtained using the eikonal approximation to describe the projectile trajectory, while the sudden approximation is employed to describe the nuclear degrees of freedom of the target.

The theoretical treatment of ion-molecule collisions at energies above 0.1 keV/u have usually been carried out using extensively tested ion-atom collision methods [1] and codes, in which the target is assumed to have spherical symmetry. However, molecules are objects that can show a pronounced anisotropy in the electron density (and electronic wavefunctions) that could influence the cross sections. In this work, we calculate orientation-dependent cross-sections using several methods that take into account the anisotropy of the target and discuss how isotropic methods (that greatly simplify calculations) can be used to obtain cross sections in agreement with the orientation-averaged ones.

As in ion-atom collisions, at the energy range mentioned above, semiclassical methods are adept to treat the collisional system combining a classical trajectory for the projectile and a quantal description of the electrons. Also, at sufficiently high energies, the simple Franck-Condon approximation can be employed to freeze the internal nuclear degrees of freedom of the target. In that context, cross-sections are functions of the projectile energy and the relative orientation between projectile trajectory and molecular axis.

In this work, we will discuss several methods to calculate orientation-dependent cross sections. In particular, we address the collisions of H^+ with BeH, a system of interest in ITER, where beryllium is planned to be one of the first-wall facing materials.

Following [2, 3], our first approach relies on the calculation of high-quality configuration interaction (CI) electronic wavefunctions. Three-center CI wavefunctions exhibit conical intersections that require diabaticization so the dynamical couplings between them do not diverge. Electronic energies and dynamical couplings are calculated for a number of geometries as a function of \mathbf{R} , the Jacobi coordinate connecting the projectile with the center of mass of the target (BeH), while keeping fixed the \mathbf{r} , target nuclear vector, and θ , the angle between \mathbf{R} and \mathbf{r} (see scheme in Fig. 1). Cross sections are obtained using the R -dependent electronic energies and couplings, for fixed θ and r , using the usual ion-atom

methods, provided that one allows for simultaneous radial and rotational couplings between electronic states, in contrast to ion-atom collisions. The results of this method are illustrated in figure 1. The relation between these θ -dependent cross sections with orientation-averaged ones will be discussed in a similar way as in [4] for $H^+ + H_2$ collisions.

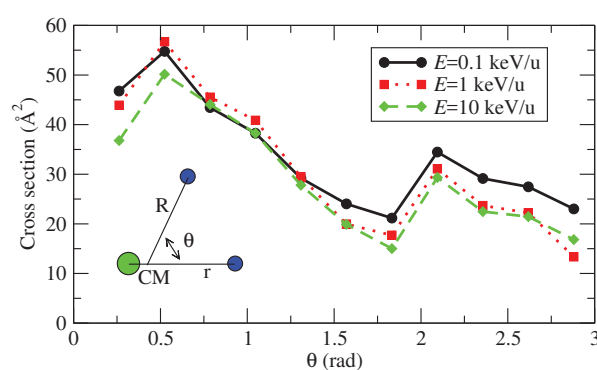


Figure 1. Charge-exchange cross section in proton-BeH collisions as a function of θ for three collisional energies.

In a second approach, we calculate one-electron wavefunctions using asymptotically-frozen molecular orbitals, see [5], for example. The simplicity of this formalism, that avoids the presence of conical intersections, makes feasible the calculation of transition probabilities along projectile trajectories, but requires the use of an independent particle model interpretation to obtain the final cross sections.

This work is partially supported by the project ENE2014-52432-R of Ministerio de Economía y Competitividad (Spain).

References

- [1] Bransden and McDowell 1992 *Charge Exchange and the Theory of Ion-Atom Collisions* Oxford, Clarendon
- [2] Rozsályi *et al.* 2012 *Phys. Rev. A* **85** 042701
- [3] Bene *et al.* 2011 *Int. J. Quant. Chem.* **111** 487
- [4] Errea *et al.* 2002 *Int. J. Mol. Sci.* **3** 142
- [5] Ravazzani *et al.* 2012 *Journal of Physics: Conference Series* **373** 012007

¹E-mail: ismanuel.rabadan@uam.es

Radiative Double Electron Capture (RDEC) in $F^{9+} + He, Ne$ Collisions

D. S. La Mantia¹, P. N. S. Kumara*, A. Kayani*, A. Simon[†], J. A. Tanis*

* Department of Physics, Western Michigan University, Kalamazoo, MI 49008-5252 USA

[†] Department of Physics, University of Notre Dame, Notre Dame, IN 46556-5670 USA

Synopsis Preliminary cross sections for RDEC, as well as total single and double electron capture, were measured for 40 MeV $F^{9+} + He$ and Ne targets. Emitted x rays and charge-changed particles were measured using coincidence techniques.

Radiative electron capture (REC) is a one-step process by which a target electron is captured to a projectile with the emission of an x ray and can be considered the time-inverse of photoionization. Double photoionization and the effect of electron correlation can be investigated through the process of radiative double electron capture (RDEC), in which two electrons are captured with the simultaneous emission of a single photon. Preliminary RDEC cross sections, as well as those for total single and double electron capture, for $F^{9+} + He$ and Ne were measured.

This work was performed using the tandem Van de Graaff accelerator at Western Michigan University. A 40 MeV beam of fully-stripped fluorine ions was collided with helium (40μ) and neon (25μ) targets inside a differentially pumped cell. A Si(Li) x-ray detector was positioned at 90° to the beamline on the gas cell. The ion beam was charge state analyzed using a dipole magnet and detected using silicon surface-barrier particle detectors. The x-ray and particle detector data were collected using an event-mode data acquisition system to assign the measured x rays to the corresponding charge-changed particles.

Previous RDEC experiments using high Z, high energy projectiles on gas targets [1][2] were performed and did not find evidence for the process. Theoretical predictions [3] suggest mid-Z projectiles in low energy collisions will give larger RDEC cross sections. Successful observations of RDEC were performed at WMU using bare oxygen [4] and fluorine [5] projectiles incident on thin carbon foil targets.

The events that can result in RDEC are the capture of two electrons to the projectile K shell ($1s^2$) or the capture of one electron to the K and L shells ($1s^1 2s^1$). X rays coincident with single (Q-1) and double (Q-2) electron capture for $F^{9+} + Ne$ (25μ) can be seen in Fig. 1. In the Q-1 spectrum, beyond the characteristic x rays for F, REC dominates. In the Q-2 spectrum the counts at the high energy end of the REC region can be due to RDEC from target KK \rightarrow projectile KL transitions, with the higher energy counts being due to target KK \rightarrow projectile KK transitions.

Preliminary analysis gives $\sigma_{RDEC}^{Ne} \sim 110$ mb

¹E-mail: david.s.lamantia@wmich.edu

(10^{-27} cm^2), which is in reasonable agreement with the theory of Mistonova and Andreev [6]. For He a single event was seen in the RDEC region, corresponding to $\sigma_{RDEC}^{He} \sim 3$ mb. At least an additional two months of continuous beam time is needed to obtain reliable statistics for each target.

*Supported in part by NSF Grant No. PHY-1401429.

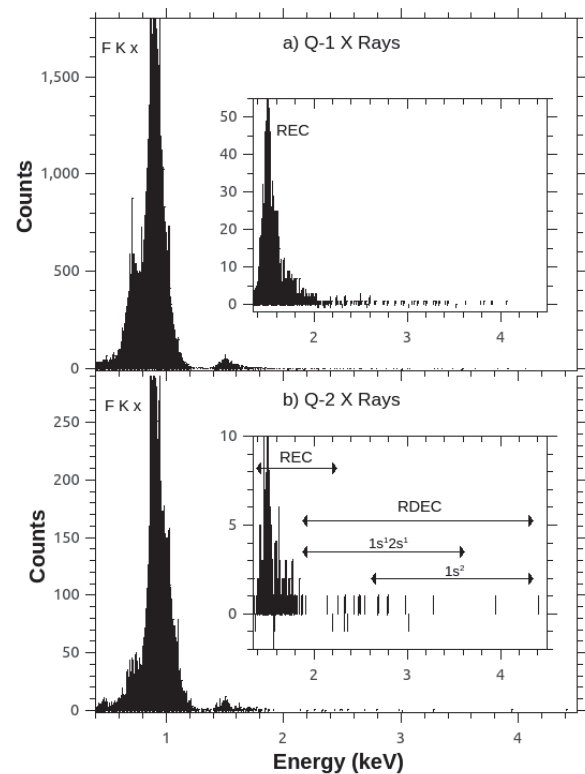


Figure 1. Spectra for x rays coincident with (a) single and (b) double capture for 40 MeV $F^{9+} + Ne$ collisions.

References

- [1] Bednarz *et al.* 2003 NIM B **205** 573-576
- [2] Winters *et al.* 2013 Phys. Scr. **T156** 014048
- [3] Nefiodov *et al.* 2005 PLA **346** 158
- [4] Simon *et al.* 2010 PRL **104** 123001
- [5] Elkafrawy *et al.* 2016 PRA **94** 042705
- [6] Mistonova and Andreev *et al.* 2013 PRA **87** 034702

Rotationally cold ($>99\%$ $J = 0$) OH^- molecular ions in a cryogenic storage ring

Henning T. Schmidt¹, Gustav Eklund*, Kiattichart Chartkunchand*, Emma K. Anderson*, Magdalena Kaminska^{*†}, Nathalie de Ruette*, Michael Gatchell*, Henning Zettergren*, Sven Mannervik*, Richard D. Thomas*, and Henrik Cederquist*

* Stockholm University, Department of Physics, Stockholm 10691, Sweden

† Institute of Physics, Jan Kochanowski University, Kielce 25-369, Poland

Synopsis We store beams of 10 keV OH^- ions in an electrostatic storage ring at a temperature of 13 K and a residual-gas density of the order of only 10^4 molecules per cm^3 . We monitor the rotational-level distribution of the stored ions as a function of time after injection by a laser-photodetachment technique. We find that the ions come close to thermal equilibrium with the surroundings after ten minutes of storage. Furthermore, by selectively depleting rotationally excited molecular ions, we form a $>99\%$ pure $J = 0$ beam with a storage lifetime in excess of six minutes.

When an ensemble of molecular ions only interacts with a black-body radiation field, characterized by a temperature T , thermal equilibrium at this temperature will be reached eventually. In such an idealized situation, the population of quantum levels will be given by the relevant Boltzmann factors. In a real environment the challenge is to approach this situation by minimizing any other possible sources of excitation. For ions stored with keV kinetic energies in a storage ring, the particular challenges are to maintain a very high vacuum to avoid excitations in collisions and to eliminate all sources of external radiation from warmer regions. We present an experiment in the cryogenic electrostatic ion-storage ring, DESIREE [1, 2], where we have stored OH^- ions at 10 keV with 10 minute $1/e$ lifetime and probed the distribution over rotational levels by investigating the effective cross section for photodetachment in the threshold region as a function of storage time. We find that after about ten minutes of storage the rotational distribution is well characterized by a thermal distribution with a temperature close to that of the surroundings [3].

We have adopted the method from Ref. [4] where OH^- was stored and cooled by buffer gas collisions in a radio-frequency trap and the rotational temperature probed by means of laser photo-detachment. Recently a similar technique based on laser *photodissociation* was applied to study the rotational distribution of CH^+ ions stored in the cryogenic storage ring CSR in Heidelberg [5].

In the present work, we did not only reach lower degree of excitation than in other similar studies. We, further, applied a second (cw) laser beam to actively remove rotationally excited molecular ions. With the depletion laser on we reached a situation where more than 99 % of the stored ions were in the $J = 0$, OH^-

ground state. In fig. 1 we show measured $J \geq 1$ fractional populations as function of time after injection in the storage ring. For this data set, the depletion laser was switched on at $t = 110$ s and switched off at $t = 380$ s. In the time interval $250 \text{ s} < t < 380 \text{ s}$ we clearly see that the fraction of rotationally excited OH^- ions is less than 1%. The increase in $J \geq 1$ population when the depletion laser is switched off is due to 'heating up' by the 13 K Planck radiation!

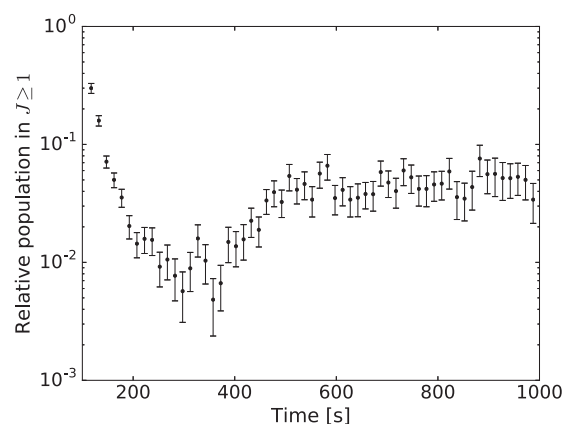


Figure 1. Measurement of the $J \geq 1$ fraction as functions of time with a merged cw-depletion laser detaching ions with $J \geq 1$ applied for the first 400 seconds.

References

- [1] R. D. Thomas *et al.* 2011 *Rev. Sci. Instrum.* **82** 065112
- [2] H. T. Schmidt *et al.* 2013 *Rev. Sci. Instrum.* **84** 055115
- [3] H. T. Schmidt *et al.* [manuscript in preparation](#).
- [4] R. Otto *et al.* 2013 *Phys. Chem. Chem. Phys.* **15** 612
- [5] A. P. O'Connor *et al.* 2016 *Phys. Rev. Lett.* **116** 113002

¹E-mail: schmidt@fysik.su.se

Harnessing ultra-intense x-rays for dynamic imaging

Linda Young^{*† 1}

^{*}Argonne National Laboratory, Argonne, IL, 60439 USA

[†]Department of Physics and James Franck Institute, The University of Chicago, Chicago, IL, 60637 USA

Synopsis X-ray free electron lasers have ushered in the era of nonlinear x-ray interactions with matter and the dream of 3D dynamical imaging at atomic spatial and temporal resolution. I will review the evolution of our understanding of the complex interactions that underpin this dream and the prospects emerging with next generation x-ray lasers.

In April 2009 the world's first hard x-ray free electron laser (XFEL) was born [1]. This seminal achievement of accelerator and optical physics provides roughly a billion-fold increase in peak intensity for engineered sources of radiation at Ångstrom wavelengths, and, produces focused intensities of 10^{20} W/cm². Early simulations using ultrafast and ultra-intense x-ray pulses suggested the feasibility of single molecule imaging via the “diffract-before-destroy” method [2] and largely inspired the construction of XFELs. While this method has successfully been employed for nanocrystalline biological samples [3], the original goal of 3D imaging of complex non-periodic objects at atomic resolution remains elusive [4].

Underpinning atomistic imaging applications is an understanding of the fundamental interactions of x-ray radiation with matter in the new nonlinear regime *provided* by XFELs and *required* for “diffract-before-destroy”. Nonlinear x-ray absorption, radiative and non-radiative decay, Coulomb explosion, and stimulated emission all occur on similar femtosecond timescales. Our strategy to a comprehensive understanding was first to establish far-off-resonance photon absorption mechanisms in simple atomic systems [5,6] and next to explore resonant excitation phenomena such as Rabi flopping [7]. These initial x-ray studies established sequential single photon absorption as the dominant mechanism (see Figure 1), with non-sequential processes playing only a minor role, in stark contrast to optical studies. They also revealed the difficulties associated with attempting inner-shell quantum control using the standard self-amplified spontaneous emission (SASE) pulses from XFELs.

In this lecture, I will review how our understanding of the response of atoms, molecules and clusters to ultra-intense x-rays has evolved into predictive modeling for more complex systems, see e.g. [8,9,10], and provide some perspective on opportunities arising from the next generation of XFELs that promise yet higher intensity, stability and multi-pulse control.

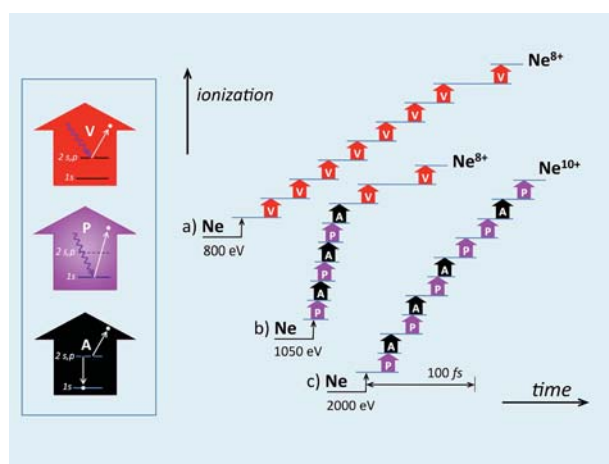


Figure 1. Sequential single photon absorption dominates interactions in an XFEL pulse [5].

References

- [1] P. Emma *et al.* 2010 *Nature Photon.* **4** 641
- [2] R. Neutze *et al.* 2000 *Nature* **406** 752
- [3] H. N. Chapman *et al.* 2011 *Nature* **470** 73
- [4] T. Ekeberg *et al.* 2015 *Phys Rev Lett* **114** 098102
- [5] L. Young *et al.* 2010 *Nature* **466** 56
- [6] G. Doumy *et al.* 2011 *Phys Rev Lett* **106** 083002
- [7] E. P. Kanter *et al.* 2011 *Phys Rev Lett* **107** 233001
- [8] R. Santra and L. Young 2015 *Synchrotron Light Sources and Free-Electron Lasers* (Ed. E. Jaeschke *et al.*, Springer 2015) p 1-24
- [9] P. J. Ho *et al.* 2014 *Phys Rev Lett* **113** 253001
- [10] P. J. Ho *et al.* 2016 *Phys Rev A* **94** 063823

¹E-mail: young@anl.gov

Natural and Unnatural-Parity Contributions in Electron-Impact Ionization of Laser-Aligned Atoms

Andrew Murray^{*1}, James Colgan[‡], Don Madison[†], Matthew Harvey^{*}, Ahmad Sakaamini^{*}, James Pursehouse^{*} and Kate Nixon[^]

^{*} Photon Science Institute, School of Physics & Astronomy, University of Manchester, Manchester M13 9PL, UK.

[‡] Los Alamos Labs, Los Alamos, New Mexico, NM 87545, USA.

[†] Department of Physics, Missouri Science & Technology, Missouri, Rolla, MO 65409, USA.

[^] School of Biology, Chemistry and Forensic Science, University of Wolverhampton, Wolverhampton WV11LY, UK

Synopsis. Experimental and theoretical results are presented for (e,2e) ionization cross sections from laser-aligned atoms. Both natural and unnatural parity contributions are found to be required to emulate the data.

In this talk experimental and theoretical results are presented for (e,2e) ionization measurements from laser-excited and aligned atoms. The experimental data are produced in Manchester, whereas theoretical work is from the groups of Don Madison in Missouri, and James Colgan at Los Alamos Labs in the USA.

The motivation for these studies arises since time-independent distorted wave (DWBA, 3DW) models predict zero flux for atoms aligned orthogonal to the scattering plane (see fig 1,2), in disagreement with the data. By contrast, time-dependent close coupling (TDCC) models predict a *non-zero* cross-section under these conditions, and find it is the *unnatural parity* contributions to the cross section that produce this flux [1-4]. An unnatural parity state has parity $(-1)^{L+1}$, compared to a natural parity state that has parity $(-1)^L$.

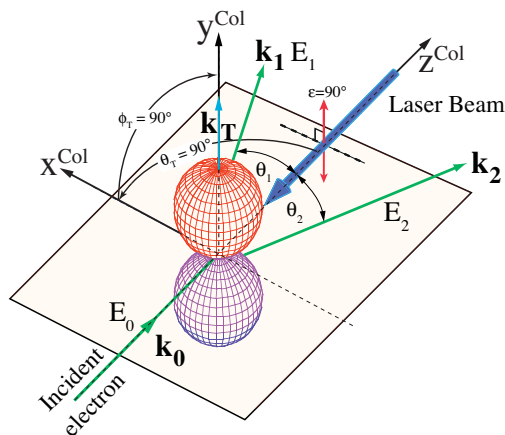


Figure 1. Ionization from atoms aligned orthogonal to the scattering plane using radiation linearly polarized at $\epsilon = 90^\circ$. DW theories predict the cross section to be zero in this configuration, whereas the TDCC model predicts a finite cross section.

It is important here for the laser-excited P-state to be fully aligned ($L=1$, $m_L=0$), with minimum contribution from orientation of the target

($L=1$, $m_L = \pm 1$). For this reason alkali-earth atoms are chosen since they have no hyperfine structure, and so can be aligned to better than 99% accuracy. Mg, Ca and Sr are to be used, so the effects of mass can also be determined.

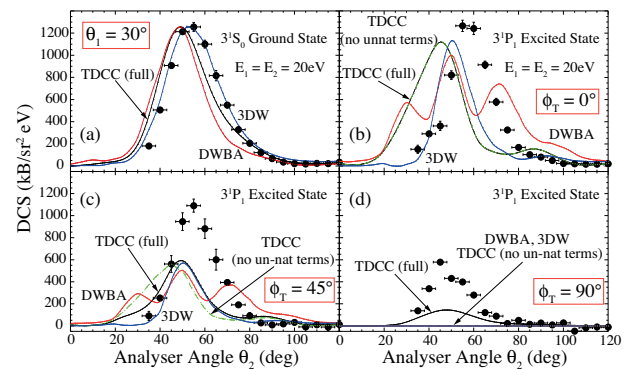


Figure 2. Comparison of experiment and theory for Mg, in the 3^1S_0 ground state and 3^1P_1 excited state at different angles ϕ_T to the plane. The data are normalized to the TDCC calculation for the 3^1S_0 state. The TDCC calculations are shown both with and without unnatural parity contributions.

The atoms are aligned using continuous wave radiation from a suite of lasers in Manchester. The cross-sections will be determined both for the incident electron in the scattering plane (as in fig. 1), and for out-of-plane geometries. The laser radiation will be injected into the interaction region through angles determined by theory, so that the cross-section sensitivity to different parity contributions can be explored.

The progress of this joint study will be presented, together with results from new experiments and theory.

References

- [1] KL Nixon *et al.* 2011 *Phys Rev Lett* **106** 123201
- [2] KL Nixon *et al.* 2014 *Phys Rev Lett* **112** 023202
- [3] S Amami *et al.* 2014 *Phys Rev A* **90** 062707
- [4] G Armstrong *et al.* 2015 *Phys Rev A* **92** 032706

¹ E-mail: Andrew.Murray@manchester.ac.uk

Photoelectron circular dichroism in photoionization of gas phase chiral systems

Laurent Nahon¹

Synchrotron SOLEIL, l'Orme des Merisiers, St Aubin BP 48, Gif sur Yvette Cedex, France

Synopsis. Photoelectron Circular Dichroism observed upon photoionization of randomly-oriented pure enantiomers is an intense orbital-specific chiroptical effect very sensitive to static and dynamic molecular structures.

Chiral molecules exist as two enantiomers, which cannot be superimposed but are mirror images of each other. They reveal their chiral nature when interacting with another chiral object such as Circularly Polarized Light (CPL) leading to enantio-specific photon/matter interactions such as the well-known circular dichroism (CD) in absorption.

Since 15 years, a new type of CD has been the subject of a large array of both theoretical and experimental studies: Photoelectron Circular Dichroism (PECD) in the angular distribution of photoelectrons produced by CPL-ionization of pure enantiomers in the gas phase observed as a very intense (up to 35 %) forward/backward asymmetry with respect to the photon axis and which reveals the chirality of the molecule (See Figure 1).

PECD happens to be an orbital-specific, photon energy dependent effect and is a very subtle probe of the molecular potential being very sensitive to static molecular structures such as conformers, chemical substitution, clusters, as well as to vibrational motion, much more so than other observables in photoionization such as the cross section or the β asymmetry parameter (for a recent review see [1]). Therefore PECD studies have both a fundamental interest as well and analytical interest, especially since chiral species are ubiquitous in the biosphere, food and medical industry. This last aspect is probably the driving force for the recent extension of PECD studies by the laser community, in the UV via REMPI schemes [2,3].

After a large introduction to chirality and the PECD process itself, several recent results on one-photon VUV PECD will be presented, including:

- Sensitivity to chemical substitutions [4], isomerism [5] and conformation [6]
- Case of a floppy biomolecule such as amino acids alanine and proline with a conformer analysis [7] and possible consequences for the origin of life's homochirality [8]
- Effect of clustering on mass-selected [9] and size-selected chiral clusters

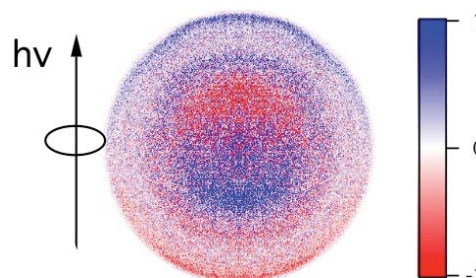


Figure 1. Raw difference (left-CPL – right CPL) electron image obtained at 17 eV on S-TFMOX, for which several orbital can be ionized. The forward/backward asymmetry (here of up to 20 %) is clearly visible as well as its orbital-specificity (adapted from Ref. [4])

Future trends for PECD studies will be given regarding the case of more complex/structured chiral systems as well as opportunities for time-resolved PECD opened by the recent first performance of PECD with fs HHG pulses [10] and REMPI time-resolved PECD [11].

References

- [1] L. Nahon *et al.* 2015 *J. Elec. Spec. Rel. Phen.* **204**, 322
- [2] C. Lux *et al.* 2012 *Angew. Chem.-Int. Edit.* **51**, 5001
- [3] C. S. Lehmann 2013 *J Chem Phys* **139**, 234307
- [4] G. A. Garcia *et al.* 2014 *Phys Chem Chem Phys* **16**, 16214
- [5] L. Nahon *et al.* 2016 *Phys Chem Chem Phys* **18**, 12696
- [6] S. Daly *et al* 2016 *Angew. Chem. Int. Ed. Engl.* **55**, 11054
- [7] M. Tia *et al* 2014 *J. Phys. Chem. A* **118**, 2765
- [8] M. Tia *et al* 2013 *J. Phys. Chem. Lett.* **4**, 2698
- [9] I. Powis *et al* 2014 *Phys Chem Chem Phys* **16**, 467
- [10] A. Ferré *et al.* 2015 *Nature Photonics* **9**, 93
- [11] A. Comby *et al.* 2016 *J. Phys. Chem. Lett* **7**, 4514

¹ E-mail: nahon@synchrotron-soleil.fr

Measurement of the Integrated Stokes Parameters for Zn 468 nm Florescence Excited by Polarized-Electron Impact

N. B. Clayburn¹ and T. J. Gay²

Jorgensen Hall, University of Nebraska, Lincoln, NE 68588-0299, USA

Synopsis These measurements resolve a standing inconsistency between experiment and state-of-the-art theory for Zn atom excitation by spin-polarized electrons. Our results are consistent with theory but not previous experiments.

We have measured the integrated Stokes parameters P_1 , P_2 , and P_3 (shown schematically in Fig. 1) of Zn ($4^3P_0 - 5^3S_1$) 468 nm florescence resulting from transversely-spin-polarized electron impact excitation of the Zn ($4s5s$) 5^3S_1 state. This work was motivated by similar studies reported several years ago by Pravica *et al.*[1], in which they measured non-zero values of the integrated Stokes parameter P_2 between the threshold for the ($4s5s$) 5^3S_1 excitation and the first cascading ($4s5p$) 5^3P_1 threshold.

In our experiment, the electrons scattered in the excitation process are not measured (hence the designation of the Stokes parameters as “integrated”), and the fluorescence is observed in the direction of the initial electron spin polarization. For this geometry (Fig. 1), Bartschat and Blum [2] have shown that P_2 must be identically zero, based on the symmetry properties of the $9j$ symbol used in the algebra required to describe the dipole fluorescence, and the assumption that the L and S angular momenta of the total wavefunction (atom plus incident electron) are factorizable throughout the scattering process. This assumption is invalid if (a) the excited state producing the fluorescence is not well LS -coupled or (b) the spin of the continuum electron precesses during the collision under the influence of a motional magnetic field, i.e., the electron undergoes Mott scattering. Since both possibilities are ruled out by state-of-the-art theory [3,4], which predicts P_2 values of order 10^{-4} , the results of reference [1], which are as large as 10^{-1} , are remarkable.

We used a standard GaAs polarized electron source to produce beams of electrons with a polarization of 0.25(1) and an energy width of *ca.* 400 meV. The atomic Zn target was produced by a Zn oven and a heated effusive channel that directed an atomic beam at right angles to both the fluorescence observation direction and the electron beam axis.

We observe optical excitation functions in agreement with those of Kontrosh *et al.* [5]. In the cascade-free range of excitation between 6.7 eV and 7.6 eV, we have measured P_2 at 7.0 eV and 7.3 eV and find its values in this range to be consistent with zero and inconsistent with those measured in [1].

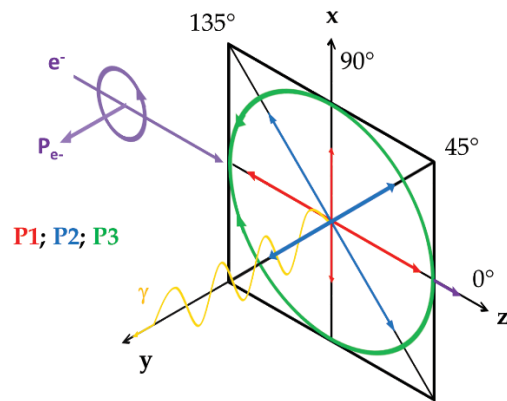


Figure 1. Geometry of integrated Stokes parameter measurements when transversely-polarized electrons, incident along \hat{z} , excite atoms, and the subsequent fluorescence is observed in the \hat{y} direction.

Work supported by the USA NSF Award PHY-1505794.

References

- [1] L. Pravica *et al* 2011 Phys. Rev. A **83** 040701
- [2] K. Bartschat and K. Blum 1982 Z. Phys. A **304** 85
- [3] C. J. Bostock *et al* 2013 Comments Phys. Rev. A **87** 016701
- [4] K. Bartschat and O. Zatsarinny 2013 Comments Phys. Rev. A **87** 016702
- [5] E. É. Kontrosh *et al* 2001 Opt. Spectrosc. **90** 339

¹ E-mail: nathan.clayburn@huskers.unl.edu

² E-mail: tgay1@unl.edu

Detection of recurrent fluorescence photons emitted from C_4^-

Mai Yoshida^{* 1}, Takeshi Furukawa^{* 2}, Jun Matsumoto[†], Hajime Tanuma^{*}, Toshiyuki Azuma^{‡*}, Haruo Shiromaru[†], and Klavs Hansen^{§¶}

^{*}Department of Physics, Tokyo Metropolitan University, Hachioji, Tokyo 192-0397, Japan

[†]Department of Chemistry, Tokyo Metropolitan University, Hachioji, Tokyo 192-0397, Japan

[‡]AMO Physics Laboratory, RIKEN, 2-1 Hirosawa, Wako, Saitama 351-0198, Japan

[§]Department of Physics, University of Gothenburg 41296 Gothenburg, Sweden

[¶]Tianjin International Center of Nanoparticles and Nanosystems, Tianjin University, China

Synopsis We detected recurrent fluorescence (RF) in the region of visible light emitted from small carbon cluster anions C_4^- and C_6^- stored in an electrostatic ion storage ring. The observed RF decay profile for C_4^- is consistent to our simulation under the assignment that the RF is associated with the $C^2\Pi_g-X^2\Pi_u$ transition. In addition, observation of the RF at two different wavelengths suggests that the RF band is rather broad.

Cooling dynamics of isolated molecules plays an important role in molecular physics, photochemistry and molecular evolution in universe. The major cooling process of isolated molecules has been considered to be infrared radiation associated with vibrational transition. It is usually slow and of the order of ms or longer in the time scale.

For the last few years, a much faster pathway of radiative cooling associated with electronic transition has been confirmed experimentally for some isolated molecules, for example, chain-form small carbon cluster anions C_4^- and C_6^- [1,2] and polycyclic hydrocarbon (PAH) cations [3]. It is the visible-photon emission process via the electronic transitions after inverse internal conversion, converting the vibrational energy to the electronic energy. This process is referred to as recurrent fluorescence (RF) or Poincaré fluorescence. At first, the RF process has been studied not by detecting the emitted photon, but by observing the statistical delayed detachment or dissociation process of the molecular ions, which provides the information on the evolution of the internal energy and the cooling rate: the unusually fast cooling is a signature of the RF [1-3].

Recently we have succeeded in direct measurements of the RF photons from the C_6^- stored in an ion storage ring [4]. We observed energy-resolved photons by employing a photomultiplier tube combined with a bandpass filter-I (CWL: 607 nm ($h\nu = 2.04$ eV), FWHM: 35nm) suitable for 2.04eV photons corresponding to the $C^2\Pi_g-X^2\Pi_u$ electronic transition of C_6^- .

In this report, we show new results of the RF photons from C_4^- . Hot anions produced in the

ion source, from C_2^- to C_6^- , were simultaneously stored in the ring. The time profile of the photon intensities detected by the photomultiplier tube, i.e., the synchronized periodic structure to the ion revolution, contributed to exclude uncorrelated background signals.

As is the case for the C_6^- anions, we detected the significant number of the 2.72 eV RF photons associated with the $C^2\Pi_u-X^2\Pi_g$ electronic transition of C_4^- anions by using a bandpass filter-II (CWL: 460 nm ($h\nu = 2.69$ eV), FWHM: 7 nm), and confirmed that the decay profile of the fluorescence is consistent with the simulated evolution of the level population based on the detailed balance theory. However, to our surprise, we found that the substantial amount of the RF photons for the C_4^- anions are detected with a bandpass filter-I.

The obtained experimental evidence is so far limited, however, this observation suggests that the RF band may be equipped with a non-negligible tail component to the longer wavelength side. This behavior is expected to be a crucial clue to clarify vibrational structures both on the high- and low-energy sides of the band origin of the RF spectrum, and they may imply transitions from the initial vibronic state to other states accompanying the vibrational excitation or deexcitation for several modes [4]

References

- [1] G. Ito *et al.* 2014 *PRL* **112** 183001; N. Kono *et al.* 2015 *PCCP* **17** 24732
- [2] V. Chandrasekaran *et al.* 2014 *JPCL* **5** 4078
- [3] S. Martin *et al.* 2013 *PRL* **110** 063003; S. Martin *et al.* 2015 *PRA* **92** 053425
- [4] Y. Ebara *et al.* 2016 *PRL* **117** 133004

¹ E-mail: yoshida-mai3@tmu.ac.jp

² E-mail: takeshi@tmu.ac.jp

Highly correlated scattered atoms – demonstrating ghost imaging with matter waves

R. I. Khakimov, B. M. Henson, D. K. Shin, S. S. Hodgman, R. G. K. G. H. Baldwin & A. G. Truscott^{1*}

Research School of Physics, Australian National University, Canberra ACT 2601, Australia

Synopsis Bose condensed ensembles of He* atoms are scattered off each other in the low energy s-wave scattering regime. Densities are sufficiently low that the collisions are almost entirely 2-body and hence conservation of energy and momentum dictate that the scattered atoms lie on a spherical shell (or halo). More importantly, the scattered constituents are highly correlated in both position and momentum – with correlated pairs of atoms lying on opposite sides of the collision sphere. Here we use these correlated atoms to demonstrate ghost imaging with matter waves for the first time.

Ghost imaging is a counter-intuitive phenomenon that enables the image of a mask to be reconstructed using the spatio-temporal properties of a beam of particles with which it never interacts. Typically, two beams of correlated photons are used: one passes through the mask to a bucket (single-pixel) detector while the spatial profile of the other is measured by a high-resolution (multi-pixel) detector. Here we report the realization of ghost imaging using massive particles.

As well as demonstrating complementarity for this phenomenon using matter waves, realizing ghost imaging with atoms is a potential precursor to experiments that test fundamental concepts in quantum mechanics with massive particles, such as ghost interference, Einstein–Podolsky–Rosen entanglement and Bell’s inequalities.

The experiments start with a BEC of helium atoms in the metastable (2^3S_1) state. This state enables single-atom detection with high efficiency because of the large internal energy of the atoms. To produce an s-wave halo, we collide atoms in the BEC via a two-photon Raman transition. This introduces a relative momentum difference between atoms in the different diffraction orders, which collide thus generating a series of s-wave scattering halos via binary collisions.

Ghost imaging is demonstrated by placing a thin metal mask 10 mm above the detector, which covers a portion of the detector’s surface such that only a fraction of the s-wave halo (containing at most one atom from each correlated pair) passes through the mask. The rest of the atoms are detected directly, without any interaction with the object, as shown in Fig. 1a.

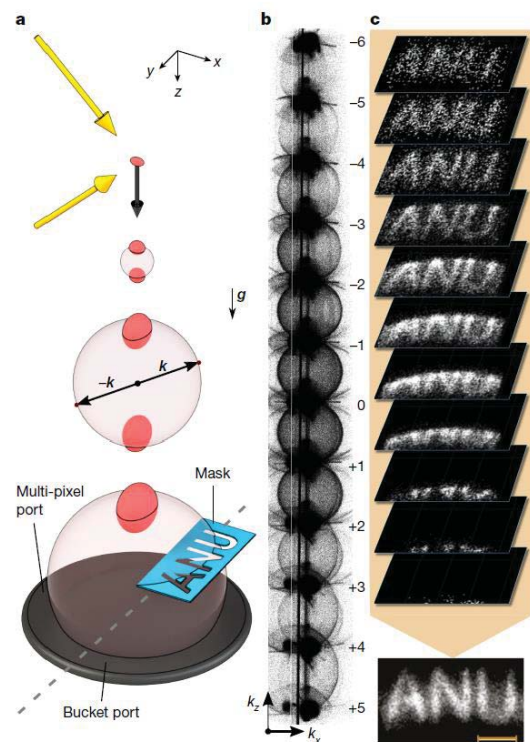


Figure 1. Schematic of the experiment and the resulting ghost image.

The ghost image is then reconstructed using coincidence-counting between atoms in the multi-pixel port and the bucket port. Combining the independent images from halos in the different diffraction orders results in the ghost image shown at the bottom of Fig. 1c.

References

- [1] R.I. Khakimov *et al.* 2016 Nature. [540](#) 100

E-mail: andrew.truscott@anu.edu.au

Rydberg macrodimers: micrometer-sized molecules bound by long-range van der Waals interactions

Johannes Deiglmayr¹, Heiner Saßmannshausen, Michael Peper, Frédéric Merkt

ETH Zurich, Laboratory of Physical Chemistry, Vladimir-Prelog-Weg 2, CH-8057 Zurich

Synopsis We report on the experimental characterization of Rydberg molecules bound by the long-range van der Waals interactions between two atoms in Rydberg states, so called “macrodimers”. The first observation of clear spectral signatures of macrodimers validates the accuracy of our recently developed theoretical model to describe strongly interacting Rydberg atoms. The validity of the Born-Oppenheimer approximation for these exotic molecular states will be discussed.

The strong polarizability of atoms in highly excited states, so called Rydberg states, leads to strong and long-ranging interactions between such atoms. Interacting pairs of Rydberg atoms represent a very exotic molecular system, characterized by high internal excitation, high density of electronic states, inter-nuclear separations exceeding one micrometer, and lifetimes beyond tens of microseconds.

We have recently developed a computational model to describe the interaction between Rydberg atoms using a multipole expansion of the interaction potential [1]. For strongly interacting Rydberg atoms, terms beyond the dipole-dipole interaction [2] and the convergence of the calculations with the size of the basis set and the truncation of the multipole series are of particular importance. The accurate modelling of the potential-energy curves allowed us to predict the binding energies of vibrationally-bound states of two interacting Rydberg atoms, so called “macrodimers”, correlated to $np(n+1)s$ Rydberg-atom pairs. The existence of such states was first predicted in 2002 by Boisseau and coworkers [3].

Experimentally, these exotic molecular states are formed by photoassociation of laser-cooled Cs atoms using a sequential two-photon excitation scheme with a spectral resolution of 1-2 MHz. Before photoassociation, the atoms are transferred from a compressed magneto-optical trap into a far-off-resonant crossed optical dipole trap, where about 10^5 atoms are trapped at a density of $1 \cdot 10^{12} \text{ cm}^{-3}$ and a temperature of $40 \mu\text{K}$. Exposing the atoms to sequential pulses of visible and ultra-violet laser light at precisely controlled frequencies leads to the formation of doubly-excited Rydberg-atom macrodimers. We report on the observation of macrodimers close to the $43p_{3/2}44s_{1/2}$ and $44p_{3/2}45s_{1/2}$ pair-state asymptotes and a characterization of their lifetime [4]. I will discuss the validity of the Born-Oppenheimer approximation for these states and the importance of radiative and non-adiabatic couplings.

¹E-mail: jdeiglma@ethz.ch

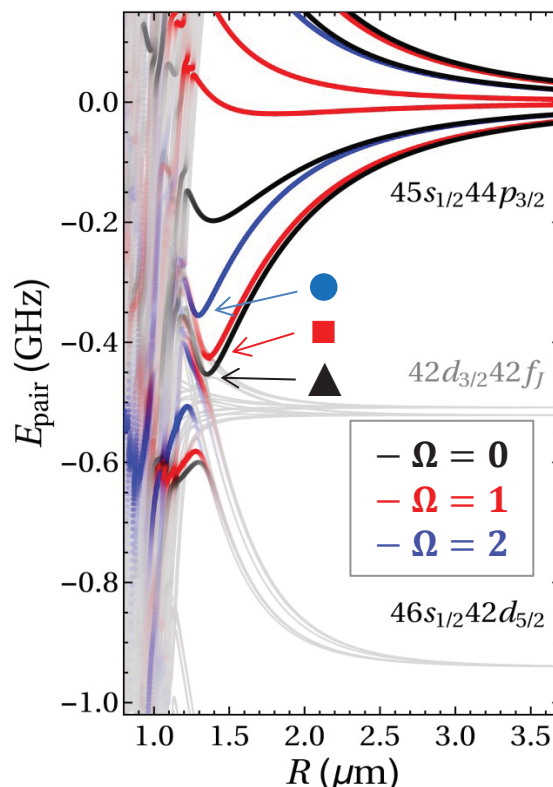


Figure 1. Potential-energy functions of two Cs Rydberg atoms in the vicinity of the $44p_{3/2}45s_{1/2}$ dissociation asymptote. The colour shading indicates the $44p_{3/2}45s_{1/2}$ character of the interacting Rydberg-atom-pair states, with 1% denoted by full colour. Black, red, and blue potentials functions correspond to molecular states with symmetry $\Omega = 0$, $\Omega = 1$, and $\Omega = 2$. Experimentally-observed macrodimer states are marked by symbols.

References

- [1] J. Deiglmayr 2016, *Phys. Scr.* **91** 104007
- [2] J. Deiglmayr *et al.* 2014, *Phys. Rev. Lett.* **113** 193001
- [3] C. Boisseau, I. Simbotin, and R. Côté, *Phys. Rev. Lett.* **88**, 133004
- [4] H. Saßmannshausen and J. Deiglmayr 2016, *Phys. Rev. Lett.* **117** 83401

Quantum Scattering in a Collider for Ultracold Atoms

Niels Kjærgaard¹, Matthew Chilcott, Craig Chisholm, Amita B. Deb, Milena Horvath, Bianca J. Sawyer, and Ryan Thomas

Department of Physics, QSO—Centre for Quantum Science, and Dodd-Walls Centre for Photonic and Quantum Technologies, University of Otago, Dunedin, New Zealand

Synopsis Paradigms from quantum scattering theory include shape and Feshbach resonances, and the collisions between indistinguishable bosons and fermions. This Progress Report will give an overview these effects elucidated in a miniaturized collider for ultracold atoms. In particular we will describe our recent work on multiple scattering dynamics through indistinguishable fermions at a shape resonance and our study of above-threshold behaviour for magnetic Feshbach resonances.

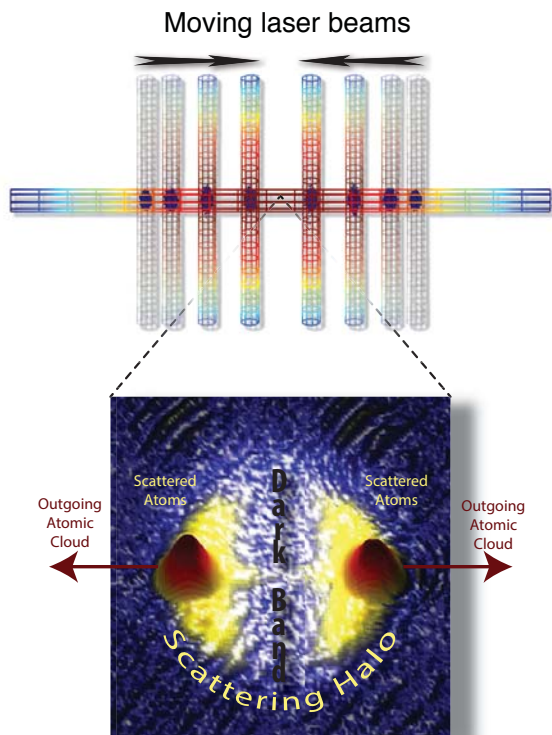


Figure 1. Illustration of the optical collider scheme and an annotated experimental absorption image showing the p-wave collisional halo resulting from indistinguishable fermionic ^{40}K atoms.

The scattering experiment arguably constitutes one of the most important methods for studying quantum mechanical systems. The advent of techniques to trap and cool atomic gases to the nanokelvin regime has opened the possibility of capturing phenomena of quantum scattering in their purest form. In a first generation of experiments, we employed magnetic fields to confine and accelerate pairs of ultracold clouds to collide at very low energies in the order of a few microelectronvolts [1]. As an example, the interference of a few (two or three) partial waves was directly imaged in the vicinity of an $\ell = 2$ shape resonance for ^{87}Rb . Furthermore, this was carried out for both distinguishable [3] and indistinguishable [2] (bosonic) collisional partners,

providing a beautiful illustration of the crucial role played by symmetrization in the latter case.

In a second generation of experiments, we have implemented a laser based collider [4] by means of steerable optical tweezers [5] which - unlike the magnetic collider - can handle atoms irrespective of their internal quantum state. Figure 1 illustrates the principle of the optical scheme along with data from a collision experiment on indistinguishable fermionic ^{40}K atoms. In the halo ensuing the collision between the two clouds, a dark band orthogonal to the collision axis can be seen. This results from the fact that indistinguishable fermions by anti-symmetry cannot scatter into 90 degree angles. However, multiple scattering can lead to a deviation to this rule and by using a pristine fermionic p-wave system we have used the characteristics of such deviations to classify the underlying multi-scattering dynamics [6].

Using our versatile optical collider we have recently studied magnetically tunable Feshbach resonances and traced out their positions in a parameter space spanned by both collision energy and magnetic field. This provides a unique way of investigating threshold scattering physics for inter-state as well as inter-species collision partners.

References

- [1] Kjærgaard N, Mellish A S and Wilson A C 2004 *New J. Phys.* **6** 146
- [2] Thomas N R, Kjærgaard N, Julienne P S and Wilson A C 2004 *Phys. Rev. Lett.* **93** 173201
- [3] Mellish A S, Kjærgaard N, Julienne P S and Wilson A C 2007 *Phys. Rev. A* **75** 020701(R)
- [4] Rakonjac A, Deb A B, Hoinka S, Hudson D, Sawyer B J and Kjærgaard N 2012 *Opt. Lett.* **37** 1085–1085
- [5] Roberts K O, McKellar T, Fekete J, Rakonjac A, Deb A B and Kjærgaard N 2014 *Opt. Lett.* **39** 2012–2015
- [6] Thomas R, Roberts K O, Tiesinga E, Wade A C J, Blakie P B, Deb A B and Kjærgaard N 2016 *Nat. Commun.* **7** 12069

¹E-mail: nk@otago.ac.nz

Attosecond electron dynamics in molecules and liquids

Hans Jakob Wörner

Laboratory of Physical Chemistry, ETH Zürich, Switzerland

Experimental and theoretical work on the measurement and interpretation of attosecond photoionization delays of molecules will be presented. Such delays are shown to reveal the transient trapping of outgoing photoelectrons in shape resonances. Extending attosecond science to the liquid phase, measurements of photoemission delays between liquid and gaseous water will be shown. These delays are shown to reflect the effect of solvation on the electronic structure of water molecules and elastic scattering delays of electrons with liquid water. Finally, the first realization of X-ray absorption spectroscopy with a water-window high-harmonic source will be presented.

Photoionization and electron transport in the condensed phase are phenomena that entirely take place on the attosecond time scale. I will present our recent experimental and theoretical work investigating photoionization dynamics of molecules [1, 2]. We have measured relative photoionization delays between the two outermost valence shells of two polyatomic molecules, H_2O and N_2O . Whereas the measured delays are all below 50 as in the case of H_2O , delays reach up to 160 as in the case of N_2O [1]. These large delays are shown to originate from the transient trapping of the photoelectron in shape resonances that have calculated lifetimes on the order of 100 as [2].

We have moreover extended attosecond science from gases to liquids by coupling an attosecond beamline with a liquid microjet [3]. This advance has enabled us to perform the first attosecond time-resolved measurements on liquids. We have studied the relative photoemission delays between the highest-occupied molecular orbitals of gas-phase and liquid-phase water molecules. The measured energy-dependent delays range from 30 to 70 as. Our analysis shows that these delays reflect the effects of solvation on the water molecules and the signatures of elastic scattering delays during electron transport. Finally, I will report on our very recent realization of the first time-resolved X-ray absorption experiment with a water-window high-harmonic source [4], which brings attosecond transient absorption experiments on solvated molecules within reach.

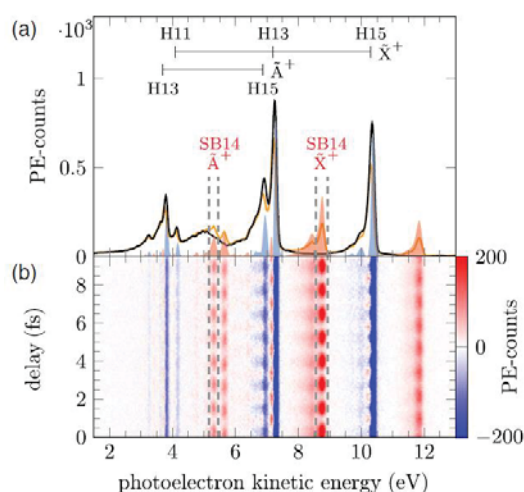


Fig. 1: (a) Photoelectron spectrum of N_2O generated by an attosecond pulse train transmitted through a Sn filter (black line) and in the presence of the dressing IR field (orange line). Difference spectra, obtained by subtracting XUV only from XUV + IR photoelectron spectra and vice versa, are shown in red and blue, respectively. (b) Difference spectrum as a function of the IR-XUV delay.

REFERENCES

- [1] M. Huppert, I. Jordan, D. Baykusheva, A. von Conta, and H. J. Wörner, *Phys. Rev. Lett.* **117**, 093001 (2016)
- [2] D. Baykusheva and H. J. Wörner, *J. Chem. Phys.*, accepted (2017)
- [3] I. Jordan, M. Huppert, M. A. Brown, J. A. van Bokhoven, H. J. Wörner, *Rev. Sci. Instrum.* **86**, 123905 (2015)
- [4] Yoann Pertot, Cédric Schmidt, Mary Matthews, Adrien Chauvet, Martin Huppert, Aaron von Conta, Andres Tehlar, Denitsa Baykusheva, Jean-Pierre Wolf, Hans Jakob Wörner, *Science* **355**, 264 (2017).

Mapping the dissociative ionization dynamics of molecular Nitrogen with attosecond resolution

J. González-Vázquez^{*1}, A. Trabattoni[§], M. Klinker^{*}, C. Liu^{**}, G. Sansone[§], R. Linguerri^{††}, M. Hochlaf^{††}, J. Klei^{§§}, M. J. J. Vrakking^{§§}, F. Martin^{*†‡}, M. Nisoli^{§¶}, F. Calegari[¶]

^{*} Departamento de Química, Universidad Autónoma de Madrid

28049 Madrid, Spain [§] Dipartimento di Fisica, Politecnico di Milano, Piazza Leonardo da Vinci 32, I-20133 Milano ^{**} State Key Laboratory of High Field Laser Physics, Shanghai Institute of Optics and Fine Mechanics, Chinese Academy of Sciences, Shanghai 201800, China ^{††} Université Paris-Est, Laboratoire Modélisation et Simulation Multi Echelle, MSME UMR 8208 CNRS, 5 bd Descartes, 77454 Marne-La-Vallée, France ^{§§} Max-Born-Institut, Max Born Strasse 2A, D-12489 Berlin, Germany [†] Instituto Madrileño de Estudios Avanzados en Nanociencia (IMDEA-Nanociencia) 28049 Madrid, Spain [‡] Condensed Matter Physics Center (IFIMAC), Universidad Autónoma de Madrid 28049 Madrid, Spain [¶] Institute for Photonics and Nanotechnologies, IFN-CNR, Piazza Leonardo da Vinci 32, I-20133 Milano, Italy

Synopsis Upon one photon ionization using attosecond lasers, N₂ shows an interference pattern when probing it with IR laser pulses. This pattern contains information of the potential of the ionic molecule and can be used to characterize the electronic dissociative electronic states.

N₂ is the most abundant molecule in the Earth's atmosphere and as such of integral importance to processes induced by solar radiation, in particular its dissociation induced by solar XUV light in the upper atmosphere. We present the experimental and theoretical investigation of the ionization and dissociation dynamics of N₂ induced by XUV radiation [1]. Isolated attosecond pulses [2] (energy range: 16- 50 eV, duration: 300 as) were used to ionize N₂ molecules, through a single photon transition. After a variable delay, NIR/VIS CEP controlled pulses (peak intensity: 8×10^{12} W/cm²) were used to probe the subsequent dissociation dynamics. The angularly resolved momentum distribution of the produced N⁺ fragments was measured as a function of the pump-probe delay using a velocity map imaging (VMI) spectrometer. We observed a depletion of a quasi-bound state of N₂⁺, 8 fs after zero time delay, together with a sub-cycle modulation of the N⁺ yield. To understand the origin of the dynamics a model was developed. The ionization process was simulated assuming an instantaneous transition from the electronic ground state of N₂ to a set of electronic levels of the N₂⁺ ion, obtained using *ab initio* multiconfigurational methodology. The relative initial populations of said set of ionic PECs were approximated using Dyson orbitals in first order perturbation theory [3, 4] and mod-

elling the leaving electron by a Coulomb wave. The dissociating ion subjected to the IR pulse was modelled by solving the TDSE using Split Operator and Fast Fourier [5] techniques. Careful investigation of the data produced by the aforementioned techniques yielded the F²Σ_g, 3²Σ_g, C²Σ_u and 5²Σ_u states of N₂⁺ as being capable of describing most features observed experimentally; most importantly a two photon transition from F²Σ_g to 3²Σ_g via 5²Σ_u was found to be responsible for the sub-femtosecond dynamics observed experimentally.

References

- [1] A. Trabattoni, M. Klinker, J. González-Vázquez, C. Liu, G. Sansone, R. Linguerri, M. Hochlaf, J. Klei, M. J. J. Vrakking, F. Martin, M. Nisoli and F. Calegari 2016 *Phys. Rev. X* **5** 041053.
- [2] M. Nisoli and G. Sansone 2016 *Progress in Quantum Electronics* **33** 17.
- [3] C. M. Oana and A. I. Krylov 2007 *J. Chem. Phys.* **127** 234106.
- [4] M. Spanner, S. Patchkovskii, C. Zhou, S. Matsika, M. Kotur, and T. C. Weinacht 2012 *Phys. Rev. A* **86** 053406.
- [5] R. Kosloff 1994 *Annu. Rev. Phys. Chem.* **45** 145.

¹E-mail: jesus.gonzalezv@uam.es

Time-resolved spectroscopy of ultrafast autoionization of He

Kyung Taec Kim^{*,†1}, Dong Hyuk Ko[‡], and Chang Hee Nam^{*,†}

^{*}Center for Relativistic Laser Science, Institute for Basic Science, Gwangju, Korea

[†]Department of Physics and Photon Science, Gwangju Institute of Science and Technology, Korea

[‡]Joint Attosecond Laboratory, Univ. of Ottawa and National Research Council, Ottawa, Canada

Synopsis Ultrafast electron dynamics of an autoionization process in He is studied by applying a phase retrieval algorithm to photoelectron spectra obtained by attosecond pulse trains and femtosecond laser pulses. The reconstructed temporal profile of the electron wave packet shows the decay profile of the autoionization state.

Ultrafast electron dynamics has been investigated using high harmonic attosecond pulses and femtosecond laser pulses. Pump-probe measurement enabled ultrafast processes to be time-resolved [1]. The coherent property of high harmonic radiations also allowed the interferometric measurement, in which the instantaneous ionization dynamics could be probed by measuring the interference of electron wave packets ionized through different paths [2]. In this work we measured autoionized electrons from the 2s2p state of He by introducing a time-delayed femtosecond laser pulse after excitation of He by an attosecond harmonic pulse. The decay profile of the autoionization process was reconstructed by applying the phase retrieval algorithm on photoelectron measured using the attosecond pulse train and the femtosecond laser pulses.

The autoionization process of the 2s2p doubly excited state in He was measured by applying pump-probe measurement with high harmonic pulses and femtosecond laser pulses. Autoionization is an example of fast multi-electron interacting processes in atoms or molecules. It is initiated by an incident X-ray pulse when atoms or molecules are pumped to a doubly excited state above an ionization threshold. After a short while, one electron is spontaneously liberated from the doubly excited state, whereas the other returns to the ground state. The relaxation time of the 2s2p doubly excited state is in the femtosecond scale. Since there are two ionization paths in the autoionization process, a large resonant peak is observed at the energy of the doubly excited state in the photoelectron spectrum showing an asymmetric shape called the Fano profile. Here we triggered the He autoionization process by introducing high harmonic pulses produced in Ar. The 39th har-

monic with the photon energy of 60 eV, corresponding to the energy level of the 2s2p state of He, was used for the excitation. The photoelectron streaking was accomplished by a time-delayed femtosecond laser pulse in order to imprint the characteristics of the intermediate state in the photoelectron signal of the two-photon transition. This was, consequently, intended for revealing the characteristics of the 2s2p doubly excited state of He.

The 2s2p state of He was characterized in time by applying the FROG CRAB method to the measured photoelectron spectra. The FROG CRAB reconstruction was successfully demonstrated in experiment for the complete characterization of attosecond harmonic pulses and femtosecond laser pulses [3]. It could provide the information on the spectral phase as well as amplitude of the 2s2p state. The Fano asymmetric parameter was, hence, determined to be -1.7 ± 0.2 by extracting the resonant spectrum of the autoionization process from the phase-retrieved photoelectron spectra of He. From the temporal profile of the 2s2p state the decay time of the autoionization process in He was measured to be 18.0 ± 0.6 fs, close to the previously reported value of 17 fs [4]. The temporal reconstruction of ionized electron wave packets occurring through two ionization paths revealed the light-matter interaction of the autoionization process in time, which would be valuable for probing multi-electron relaxation dynamics in atoms and molecules.

References

- [1] M. Drescher *et al.* 2002 *Nature* **419**, 803.
- [2] K. T. Kim *et al.* 2012 *Phys. Rev. Lett.* **108**, 093001.
- [3] K. T. Kim *et al.* 2010 *New J. Phys.* **12**, 083019.
- [4] U. Fano 1961 *Phys. Rev.* **124**, 1866 (1961).

^{†1} E-mail: kyungtaec@gist.ac.kr

Probing molecules with photoelectron rescattering and harmonics generation

Serguei Patchkovskii^{*1}, Timm Bredtmann^{*}, Michael Schuurman[†]

^{*} Max-Born-Institut, Max-Born-Straße 2A, 12489 Berlin, Germany

[†] Dept. of Chemistry and Biomolecular Sciences, University of Ottawa, 10 Marie Curie, Ottawa, ON, Canada K1N 6N5

Synopsis We examine the influence of non-adiabatic vibronic dynamics on high-harmonics emission in molecules and the effects of the strong-field continuum structure on photoelectron rescattering. We discuss the consequences of both effects for practical applications of these experimental techniques.

The rapidly developing field of strong-field attosecond science offers a promise of observing and controlling electronic and nuclear motion *directly*, on their natural time scales. Understanding the underlying dynamics in molecules is difficult due to ubiquitous near-degeneracies of electronic states in molecules, particularly influential in the vicinities of conical intersections (CIs).

Short-time CI dynamics can be probed using isotope-specific high-harmonic spectroscopy (PACER)[1]. Description of PACER results in polyatomic species often assumes that the nuclear motion occurs on a single electronic energy surface[2, 3].

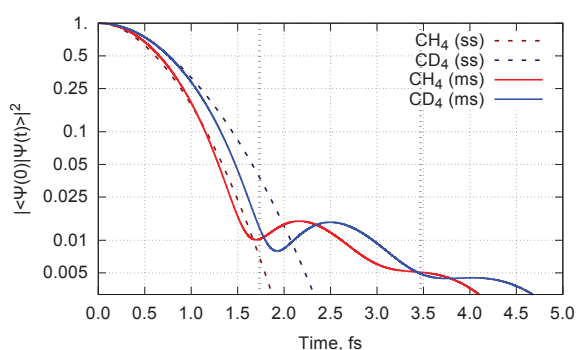


Figure 1. Nuclear autocorrelation functions for CH_4^+ (red) and CD_4^+ (blue). Dashed: single-surface simulation from Ref. [2]. Solid: full non-adiabatic simulation. Dotted vertical lines indicate time delays for the cut-off trajectories (≈ 1.7 fs at 800 nm; ≈ 3.5 fs at 1.6 μm).

We present our progress towards the full-dimensional description of the PACER experiments in polyatomic molecules, treating *all* degrees of freedom quantum-mechanically. We combine time-dependent vibronic Schrödinger equation in the basis of multi-dimensional harmonic oscillator functions[3] with the multi-state strong-field approximation for the continuum electron driven by the strong field.

Our preliminary results for the nuclear autocorrelation function in the methane cation are shown in Figure 1. Experimental results for this system are currently available for ionization–recollision delays

up to ≈ 1.5 fs. For these delays, multi-surface nuclear autocorrelation functions (and therefore the isotope effects) agree closely with single-surface simulations. At longer times, the multi-surface autocorrelation functions undergo revivals, which are associated with the wavepacket completing one (at ≈ 2.3 fs) and two (at ≈ 4.5 fs) orbits around the CI.

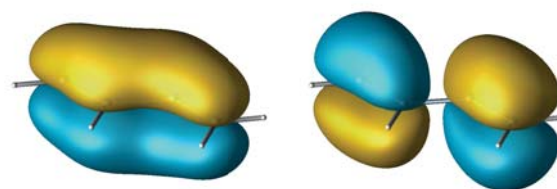


Figure 2. Dyson orbitals for ionization of the ground-state butadiene forming the ground (left) and the first excited (right) states of the butadiene cation.

The shape of the photoelectron wavepacket formed by strong-field ionization is sensitive to the final ion state it is correlated to. The common assumption underlying photoelectron holography[4] and self-imaging due to laser-induced electron diffraction is that most of this structure is erased due to strong-field dynamics in the continuum. Quantitative applications of these techniques requires an independent investigation of this critical assumption.

We use first-principles TD-RIS[5] simulations of butadiene to investigate the energy and ellipticity dependence of the recollision cross-section. We show that these cross-sections are sensitive to the final ion state. The dependence survives orientational averaging, and should be detectable in an unaligned target.

References

- [1] S. Baker *et al.* 2006 *Science* **312** 424
- [2] S. Patchkovskii 2009 *Phys. Rev. Lett.* **102** 253602
- [3] S. Patchkovskii *et al.* 2014 *J. Phys. Chem. A* **118** 12069
- [4] M. Meckel *et al.* 2014 *Nature Phys.* **10** 594
- [5] M. Spanner *et al.* 2009 *Phys. Rev. A* **80** 063411

¹E-mail: Serguei.Patchkovskii@mbi-berlin.de

Ultrafast imaging of isolated molecules with electron pulses

Jie Yang^{*,§}, Omid Zandi^{*}, Kyle Wilkin^{*}, Markus Guehr^{†,‡}, Xiaozhe Shen[§], Renkai Li[§], Theodore Vecchione[§], Ryan Coffee[§], Jeff Corbett[§], Alan Fry[§], Nick Hartmann[§], Carsten Hast[§], Kareem Hegazy[§], Keith Jobe[§], Igor Maksyuk[§], Joseph Robinson[§], Matthew S. Robinson^{*}, Sharon Vetter[§], Stephen Weathersby[§], Charles Yoneda[§], Xijie Wang[§], Martin Centurion^{*1}

^{*} University of Nebraska-Lincoln, 855 N 16th Street, Lincoln, Nebraska 68588, USA.

[†] PULSE, SLAC National Accelerator Laboratory, Menlo Park, California 94025, USA.

[‡] Physics and Astronomy, Potsdam University, 14476 Potsdam, Germany.

[§] SLAC National Accelerator Laboratory, Menlo Park, California 94025, USA.

Synopsis We have captured the dynamics of laser-excited molecules in the gas phase using ultrafast electron diffraction. First experiments observed a vibrational wavepacket in iodine with a resolution of 0.1 Å in space and 230 fs in time. This result, which was achieved with the MeV electron source at SLAC National Lab, opens the door to imaging structural dynamics in more complex molecules. We will also discuss a new table-top keV electron source that uses pulse compression to achieve femtosecond resolution with a high repetition rate.

Observing chemical reactions as they take place is essential for understanding, and eventually controlling the outcome of reactions. Measuring the dynamics in isolated molecules is important for understanding the intrinsic response of the molecules to excitation, and can provide a benchmark for quantum chemical simulations. Gas phase ultrafast electron diffraction (UED) has the advantage that the diffraction patterns are directly sensitive to the spatial distribution of the atoms in the molecule. In order to observe the dynamics of photo-induced reactions the temporal resolution needs to be on the femtosecond scale, while the spatial resolution needs to be sufficient to resolve individual atoms, on the sub-Angstrom scale. Previously, picosecond gas phase UED experiments have successfully captured the structure of long-lived intermediate states [1] but in order to observe the coherent motion of atoms femtosecond resolution is needed. Femtosecond UED has been achieved previously for condensed matter systems [2].

Recent experiments have achieved 230 fs resolution in gas phase UED [3,4]. These demonstration experiments captured a rotational wavepacket in nitrogen molecules [3] and a vibrational wavepacket in iodine molecules [4]. The iodine experiments were the first in which UED has been used to spatially and temporally resolve coherent nuclear motion, and open the door to capturing the dynamics in more complex molecules. These first results were achieved using the relativistic MeV electron source at SLAC National Laboratory. The use of relativistic electrons has the advantage that

the Coulomb broadening of the pulses is reduced, thus shorter electron pulses can be delivered on target. Experiments to image photodissociation and conformational changes in molecules on a time scale of 100 fs are currently ongoing.

We are also developing a table-top setup that will reach a resolution of around 400 fs by accelerating electrons to 90 keV in a static field and then using an RF field to compress the pulses. While the temporal resolution is higher with MeV electrons, the keV source has the advantage that it can operate at 5-10 kHz repetition rate (compared to 120 Hz for the MeV setup). The higher beam current will provide more signal at larger scattering angles, and thus better spatial resolution.

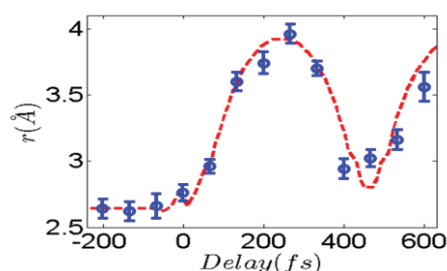


Figure 1. Bond length as a function of time in laser-excited iodine molecules, measured with gas phase UED.

References

- [1] A. H. Zewail 2006 *Annu. Rev. Phys. Chem.* 57 65
- [2] G. Sciaini *et al.* 2011 *Rep. Prog. Phys.* 74 096101
- [3] J. Yang *et al.* 2016 *Nat. Commun.* 7, 11232
- [4] J. Yang *et al.* 2016 *Phys. Rev. Lett.* 117, 15300

¹E-mail: martin.centurion@unl.edu

Molecular orbital and atomic motion imaging using time-resolved electron scattering

Masakazu Yamazaki*¹ and Masahiko Takahashi*²

* Institute of Multidisciplinary Research for Advanced Materials, Tohoku University, Sendai 980-8577, Japan

Synopsis We report recent progress in developing time-resolved (e, 2e) electron momentum spectroscopy as well as a multichannel apparatus to be used for time-resolved atomic momentum spectroscopy, both of which spectroscopies employ femtosecond laser and picosecond electron pulses in a pump-probe scheme. We have made an attempt to improve the signal intensities for these experiments. With further development, a joint use of these techniques will eventually serve as a momentum-space reaction microscope which enables one to take a series of snapshots of molecular orbitals and atomic motions changing rapidly during a unimolecular reaction.

Electron momentum spectroscopy (EMS [1, 2]) is a kinematically-complete electron-impact ionization experiment performed under the high-energy Bethe ridge conditions, where the collision kinematics can be described by electron Compton scattering that most nearly corresponds to the collision of two free electrons with the residual ion acting as a spectator. The remarkable feature of this technique is its ability to measure momentum distributions of each electron bound in matter or to look at molecular orbitals in momentum space.

Since the change of the electron motion in a molecular orbital is the driving force behind any chemical reactions, application of EMS to transient species is expected to provide new insights into ultrafast molecular dynamics. For this purpose, we have recently developed time-resolved EMS (TR-EMS) by combining EMS with a pump-probe experiment. Although the currently available data statistics are poor and the time-resolution is limited (± 35 ps), the potential ability of TR-EMS has already been demonstrated through molecular orbital imaging of the short-lived (13.5 ps), second excited state of deuterated acetone [4], an EMS study on the electronic structure of the relatively long-lived (86 ns), first excited state of toluene [5], and an attempt at a product vibrational analysis of a photo-induced chemical reaction [6]. We are going further towards one of the goals of TR-EMS, that is, to film *molecular orbital movies*, which might enable one to access the heart of chemical reactions.

Under the above-mentioned circumstances, we are, in parallel, going to develop a new experimental technique to afford a real-time measurement of *atomic* (nuclear) motions in chemical reactions. Measurements of the momentum distribution of atoms in a ground-state

molecule can be made by using electron-atom Compton scattering experiment, which we call atomic momentum spectroscopy (AMS). It is quasi-elastic electron scattering at high momentum transfer, in which the instantaneous motion of the scattering atom causes a Doppler broadening in the energy of the scattered electrons, as has beautifully been developed and demonstrated by Vos and his colleagues [7]. In order to advance this technique to a time-resolved regime (TR-AMS), we have recently developed a multi-channel AMS spectrometer [8], which has improved the signal count rate by a factor of 840 compared to that of the existing spectrometer [9].

In this contribution, some results of our recent studies of TR-EMS and AMS will be presented, which may examine the current status and future prospects of TR-EMS and TR-AMS. With these spectroscopies it might be possible to experimentally investigate how and how much the change in atomic motions are brought about by the change in electron motion during chemical reactions.

References

- [1] E. Weigold and I. E. McCarthy, 1999 *Electron Momentum Spectroscopy* (Kluwer/Plenum, New York)
- [2] M. Takahashi 2009 *Bull. Chem. Soc. Jpn.* **82** 751
- [3] M. Yamazaki, Y. Kasai, K. Oishi, H. Nakazawa, M. Takahashi 2013 *Rev. Sci. Instrum.* **84** 063105
- [4] M. Yamazaki, K. Oishi, H. Nakazawa, C.-Y. Zhu, M. Takahashi 2015 *Phys. Rev. Lett.* **114** 103005
- [5] M. Yamazaki *et al.* 2016 *Phys. Rev. A* **94** 052509
- [6] M. Yamazaki, H. Nakazawa, C.-Y. Zhu, M. Takahashi 2015 *J. Phys. Conf. Ser.* **635** 012010
- [7] M. Vos *et al.* 2005 *Inst. Phys. Conf. Ser.* **183** 81
- [8] M. Yamazaki *et al.*, *submitted*
- [9] M. Vos 2010 *J. Chem. Phys.* **132** 074306

¹ E-mail: masakazu@tagen.tohoku.ac.jp

² E-mail: masahiko@tagen.tohoku.ac.jp

Electron and positron scattering and transport in simple liquids

G. J. Boyle*¹, R. P. McEachran[†], D. G. Cocks* and R. D. White*

* College of Science & Engineering, James Cook University, Townsville QLD 4810, Australia

[†] Research School of Physical Sciences & Engineering, Australian National University, Canberra ACT 0200, Australia

Synopsis The formalism of Lekner and Cohen for electron scattering in liquids is generalized using modern scattering techniques, and was found to reproduce well transport quantities in liquid argon and liquid xenon. There is some difficulty in extending the same procedure to positron scattering.

The study of electron and positron transport in dense gases and non-polar liquids is of fundamental interest for understanding the dynamics of electron/positron processes in structured and disordered media, including dynamic and scattering processes. Applications to high-energy particle detectors, plasma medicine and medical imaging among others requires knowledge of charged particle transport through liquid noble gases, liquid water, and biomolecules, typically under non-equilibrium conditions.

In [1, 2] we generalized the formalism of Lekner and Cohen, in which they describe *ab initio* modifications to the microscopic processes to account for dense fluid effects, overcoming several approximations which are no longer necessary in modern day electron transport and scattering theory.

A numerical solver for the Boltzmann equation with a multi-term treatment of the velocity distribution, and which accounts for coherent scattering has been developed. When combined with the generalized Lekner and Cohen procedure, our model, which contained

no free parameters, was found to reproduce well experimental drift velocities and characteristic energies in liquid argon and liquid xenon.

We are now extending the Lekner and Cohen formalism from electron scattering to positron scattering. The key problem is how to determine the region “owned” by a single atom in a dense system, which cannot be defined using the original Lekner theory due to the static and polarisation potentials having opposite signs. The effect that different choices for this region has on scattering cross-sections, and hence macroscopic transport properties, including average Z_{eff} , has been investigated and compared with positron swarm experiments in dense helium and argon systems.

References

- [1] G. J. Boyle *et al.* 2015 *J. Chem. Phys.* [142](#)
[154507](#)
- [2] G. J. Boyle *et al.* 2016 *J. Phys. D: Appl. Phys.* [49](#)
[355201](#)

¹ E-mail: Gregory.Boyle@my.jcu.edu.au

Dissociative electron attachment to CO molecule probed by velocity slice imaging technique

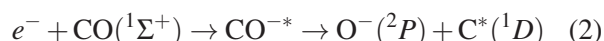
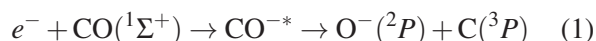
Pamir Nag¹ and Dhananjay Nandi²

Indian Institute of Science Education and Research Kolkata, Mohanpur 741246, India

Synopsis We have studied dissociative electron attachment to CO molecule using the well-established velocity slice imaging spectrometer. We have conclusively determined the symmetries of the TNI states involved in both the channels producing O^- ions. Also in contrast to a recent report we observed that there is no need to invoke coherent interference between different states. Recent calculations and experimental study by other groups also strongly support our claims.

Low-energy electron-molecule collision leading to dissociative electron attachment (DEA) is an important process from the fundamental as well as the application point of view. DEA is a two-step resonant process resulting into a final anionic and neutral fragments from a parent neutral molecule via intermediate temporary negative ion (TNI) state. DEA study of molecules are important starting from electrical discharges, atmospheric chemistry, installer medium chemistry to radiation induced damage of living cell and biologically important molecules.

Carbon monoxide (CO) is a simple but important heteronuclear diatomic molecule. But only few studies on DEA to CO exist in literature using modern techniques like velocity map imaging or momentum imaging. DEA to CO have two possible channels for O^- production with energy threshold 9.62 and 10.88 eV and are shown by equation 1 and 2 respectively.



From the angular distribution measurements over a limited angular range Hall *et al.* [1] concluded a TNI state with Π symmetry is responsible for both the processes. In contrast, Tian *et al.* [2] reported that for 10 eV incident electron energy Σ and Π two states are involved but, for 10.6 eV three TNI states, Π , Δ and Φ , with coherent interference between them are present. To address these issues we have studied DEA to CO [3] using a recently developed velocity slice imaging (VSI) spectrometer similar to that was reported by Nandi *et al.* [4] with few modifications. VSI technique is a well-established method for simultaneous measurement of the kinetic energy and angular distribution of the fragment anions produced due to DEA over the entire 2π angle.

From the systematic kinetic energy distribution measurements we have identified both the processes.

To determine the symmetry of the TNI states we have measured angular distributions of the O^- ions produced due to both the processes separately. We observed a Σ state is primarily responsible for both the processes. In addition a minor contribution from a Π state also exists for process 1 and the contribution increases with increasing incident electron energy. In a recent R-matrix calculation Dora *et al.* [5] also observed only a Σ resonant state. From the angular distribution measurements we also have observed that there is no need to invoke the coherent interference between different states as suggested by Tian *et al.* In a recent experimental study Gope *et al.* [6] also observed similar results and strongly supported our conclusions.

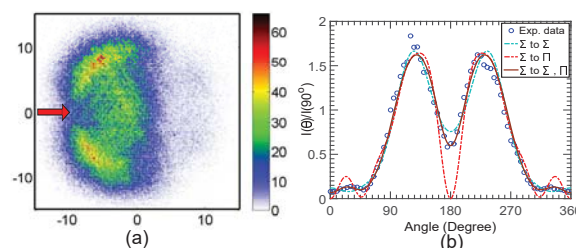


Figure 1. (a) The VSI of O^- ions for 11 eV beam energy and (b) angular distribution of the ions created due to process I for 11 eV beam energy along with fitted curves.

References

- [1] R. I. Hall *et al.* 1977 *Phys. Rev. A* **15** 599
- [2] S. X. Tian *et al.* 2013 *Phys. Rev. A* **88** 012708
- [3] P. Nag and D. Nandi 2015 *Phys. Chem. Chem. Phys.* **17** 7130
- [4] D. Nandi *et al.* 2005 *Rev. Sci. Instrum.* **76** 053107
- [5] A. Dora *et al.* 2016 *Eur. Phys. J. D* **70** 197
- [6] K. Gope *et al.* 2016 *Eur. Phys. J. D* **70** 134

¹E-mail: pamir1118@iiserkol.ac.in

²E-mail: ghananjay@iiserkol.ac.in

Imaging the Temporal Evolution of Molecular Orbitals during Ultrafast Dissociation

M. Weller^{*1}, H. Sann^{*}, T. Havermeier^{*}, C. Müller^{*}, H.-K. Kim^{*}, F. Trinter^{*}, M. Waitz^{*}, J. Voigtsberger^{*}, F. Sturm^{*}, T. Bauer^{*}, R. Wallauer[†], D. Schneider^{*}, C. Goihl^{*}, J. Tross^{*}, K. Cole^{*}, J. Wu^{*}, M. S. Schöffler^{*}, H. Schmidt-Böcking^{*}, T. Jahnke^{*}, M. Simon[‡] and R. Dörner^{*2}

^{*} Institut für Kernphysik, Universität Frankfurt, Max-von-Laue-Str. 1, 60438 Frankfurt, Germany,

[†] Fachbereich Physik, Philipps-Universität Marburg, Renthof 5, 35032 Marburg, Germany,

[‡] Sorbonne Universités, UPMC Université Paris 06, CNRS, UMR 7614, Laboratoire de Chimie Physique-Matière et Rayonnement, F-75005 Paris, France.

Synopsis We investigate the temporal evolution of molecular frame angular distributions of Auger electrons emitted during ultrafast dissociation of HCl following a resonant single-photon excitation. The electron emission pattern changes its shape from that of a molecular σ orbital to that of an atomic p state as the system evolves from a molecule into two separated atoms.

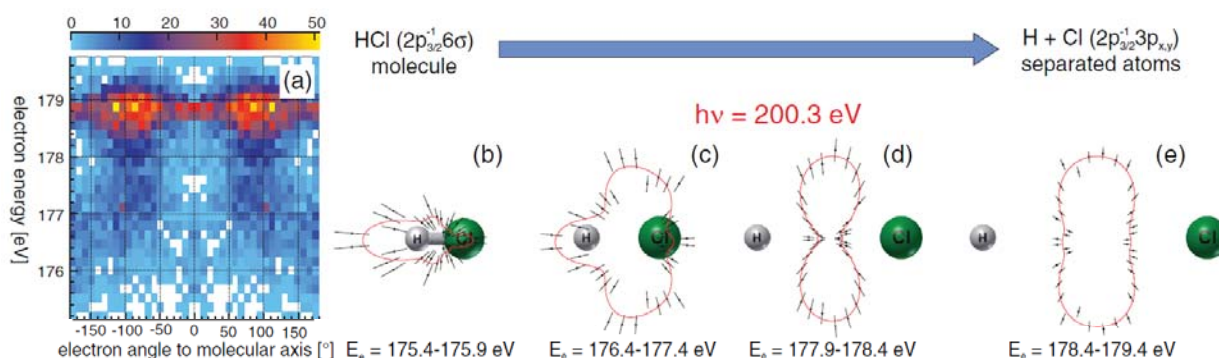


Figure 1. (a) Electron angular emission distribution with respect to the molecular axis as a function of electron energy. (b-e) Subsets of data shown in (a) for different regions of electron energy. (b) Corresponds to decay of the still intact molecule, (c,d) show emission patterns during bond breakage, (e) shows emission from the Cl^{*} fragment.

We investigate the breaking of chemical bonds and thus the transition of a molecular orbital to an atomic orbital. To realize this, we coincidentally measure the fragment momenta of the molecular decay of HCl through Ultrafast Dissociation with a COLTRIMS system.

Ultrafast Dissociation proceeds as follows: Using narrow-bandwidth synchrotron radiation, an inner shell electron is resonantly excited to an antibonding molecular σ^* -orbital in the pump step. The molecule now rapidly dissociates in the timescale of a few femtoseconds along the steeply repulsive potential energy surface. Competing with the molecular dissociation, Auger decay takes place. The Auger electron can be emitted either within the molecular Franck-Condon region, during bond breakage or when the molecule is already fragmented into two atoms. The Auger decay can thereby be used as a probe of the state of the decaying system. By coincidentally measuring the ionic fragment and the emitted electron, we gain information about internuclear distance and hence

the timespan from excitation to the point when each decay took place. The internuclear distance is encoded in the kinetic energy of the fragments as well as in the energy of the emitted Auger electron. For different time steps we can now investigate the Auger electron angular distribution in the molecular frame. These distributions are a fingerprint of the systems orbital structure.

In reality, the situation is considerably more complicated because many initial and final states are involved. In the analysis, these states as well as the two possible fragment channels could be separated by restricting to the channels of interest via coincident energy maps.

Figure 1 finally shows the transition of the molecular σ -type orbital (b) via bond breakage (c, d) to the atomic p -orbital (e) mapped in the Auger electron emission pattern.

Reference

[1] H. Sann *et al.* 2016 *Phys. Rev. Lett.* **117**, 243002

¹ E-mail: weller@atom.uni-frankfurt.de

² E-mail: doerner@atom.uni-frankfurt.de

New Physics with Advanced Positron Traps and Beams*

Clifford M. Surko^{1†}

Physics Department, University of California, San Diego
La Jolla, CA, 92093-0319, USA

Synopsis: The development of novel positron traps and beams has enabled new investigations of antimatter such as the creation and study of antihydrogen atoms, the positronium molecule (Ps_2), and Feshbach-resonances in annihilation that lead to positron-molecule bound states. This talk will discuss highlights of these and other successes and the critical tools that enabled them. It will conclude with a brief discussion of prospects for further progress on topics of keen interest including study of lepton many-body physics: Ps-atom BECs and classical ($e^+ - e^-$) "pair plasmas."

Study of antimatter is of interest for a range of scientific and technological applications, including fundamental tests of gravity and tests of symmetries predicted by field theories (e.g., CPT), understanding astrophysical processes, the characterization of materials, and positron emission tomography (PET) to study human metabolic processes.

Many applications benefit greatly from tailoring collections of the antiparticles to optimize them for a specific end use. The need to keep the antiparticles isolated from contact with matter has motivated the development of methods to manipulate them in vacuum in the form of single-component gases and plasmas [1].

This talk will describe the manner in which three decades of positron trap and beam development have enabled new investigations. Specific advances include specially designed electromagnetic traps for long-term (e.g., weeks or more) antimatter confinement, cryogenically cooled antiparticle gases and plasmas, high-density plasmas, finely focused antiparticle beams, and methods to deliver very large bursts of antiparticles.

Scientific and technological progress in several areas will be reviewed. It includes the creation and study of antihydrogen atoms (Fig. 1) for CPT

and gravity tests [2-5]; the formation of the positronium molecule (i.e., Ps_2 , the first many-electron, many-positron state, $e^+e^-e^+e^-$) [6]; and understanding Feshbach-resonances in positron annihilation and the nature of the resulting positron-molecule bound states [7].

A challenging goal for the future is study of many-body physics in the electron-positron system (Fig. 2) [8]. Prospects and progress on this topic will be reviewed in both the classical and quantum regimes – the creation of a positronium-atom Bose-Einstein condensed gas (BEC) [9], and the creation of a classical "pair" (i.e., $e^+ - e^-$) plasma [10].

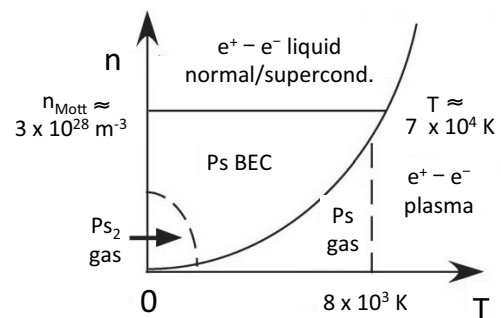


Fig. 2. Phase diagram of the electron-positron system [8].

* Supported by the U. S. NSF, grant PHY 14-01794.

[†] Recent work at UCSD was done in collaboration with J. R. Danielson, M. R. Natisin and N. C. Hurst.

References:

- [1] J. Danielson, *et al.*, *Rev. Mod. Phys.* **87**, 247 (2015).
- [2] M. Amoretti, *et al.*, *Nature* **419**, 456 (2002).
- [3] G. B. Andresen, *et al.*, *Nature* **468**, 673 (2010).
- [4] G. Gabrielse, *et al.*, *Phys. Rev. Lett.* **108**, 113002 (2012).
- [5] M. Ahmadi, *et al.*, *Nature* doi:10.1038/21040 (2016).
- [6] D. B. Cassidy, *et al.*, *Nature* **449**, 195 (2007).
- [7] G. Gribakin, *et al.*, *Rev. Mod. Phys.* **82**, 2557 (2010).
- [8] H. Yabu, *Nuc. Instrum. Meth. B* **221**, 144 (2004).
- [9] A. P. Mills, *Nucl. Instrum. Meth. B* **192**, 107 (2002).
- [10] T. S. Pedersen, *et al.*, *New J. Phys.* **14**, 035010 (2012).

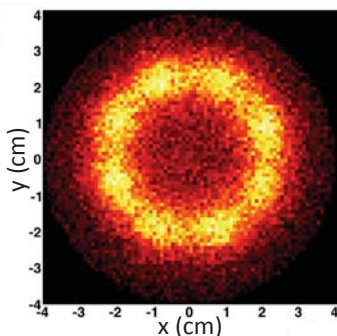


Fig. 1. Antihydrogen atoms annihilating on the surrounding electrodes in a minimum-magnetic-field atom trap. Courtesy of the ALPHA collaboration.

¹ E-mail: csurko@ucsd.edu

Ultrafast dynamics of atomic clusters proved by XFEL

Kiyonobu Nagaya¹

Department of Physics, Graduate School of Science, Kyoto University, Kyoto 606-8502, Japan

Synopsis We report the recent achievements of time-resolved experiments of atomic clusters carried out at SACLA in Japan. The first example is the time-resolved ion spectrometry of Xe clusters, which gives us the insight to the early stages of the XFEL-triggered nanoplasma formation. In the second example, we reveal the ultrafast destruction of atomic order in giant Xe clusters triggered by intense NIR laser pulses by using time-resolved x-ray scattering measurements.

The self-amplified spontaneous emission (SASE) based X-ray free electron laser (XFEL) facilities deliver spatially coherent, ultrashort and extremely intense X-ray pulses [1,2]. One promising application of XFEL is the observation of the ultrafast motion in the objects. Here we report the recent achievements of time-resolved experiments of clusters at SPring-8 Angstrom Compact free electron LAser (SACLA) in Japan [2] using an arrival timing monitor [3] that improves the time-resolution of the pump-probe experiment down to a few tens of femtoseconds by measuring the temporal jitters between the XFEL and NIR pulses on a shot-to-shot basis. Experiments were performed at the experimental hutch 2 and 4 of the beam-line 3 at SACLA.

In the first example, we carried out the time-resolved ion spectrometry of Xe clusters to observe the early stages of the XFEL-triggered nanoplasma formation. We irradiated Xe clusters beam (average size of 5000 atoms) by XFEL pulses (5.5 keV, 10 fs FWHM) and by NIR-probe laser (800 nm, 32 fs FWHM). We measured the Xe^{1+} yield as a function of the time delay between the XFEL and the NIR pulses. We found a clear enhance of the Xe^{1+} yields due to ionizing the excited Xe atoms created during the nanoplasma formation process, that suggest the importance of the electron collisions and interatomic relaxation processes for the primary mechanisms for nanoplasma formation triggered by intense hard X-rays pulses.

In the second example, we carried out the time-resolved x-ray scattering measurements of giant Xe clusters. We produced giant Xe clusters (average size of 10^6 atoms) and irradiated them with X-FEL pulses (11.2 keV, 10 fs FWHM, $\sim 60 \mu\text{J}$). Scattered x-ray photons were

recorded by the multi-port charge-coupled device (MPCCD) octal sensor [4] installed 100 mm downstream of the interaction point. Bragg spot signals corresponding to the fcc-crystalline structure of giant Xe clusters were observed on MPCCD sensor. With keeping the giant cluster condition, we irradiated intense NIR pulses (800 nm, 30 fs FWHM, 12mJ) to heat-up the Xe clusters. We observed a significant decrease in the number of the Bragg spots in sub-ps time scale after irradiation of NIR pulses, which suggest the ultrafast destruction of atomic order in xenon nano-crystals by intense NIR laser pulses.

Work done in collaboration with T. Nishiyama, K. Kumagai, A. Niozu, C. Bostedt, H. Fukuzawa, K. Motomura, M. Bucher, D. Iablonskyi, Y. Ito, T. Takanashi, K. Asa, Y. Sato, D. You, Y. Li, T. Ono, Y. Sakakibara, T. Umemoto, K. Kariyazono, E. Kukk, C. Miron, L. Neagu, C. Callegari, M. D. Fraia, D. Galli, G. Rossi, T. Pincelli, A. Colombo, K. Kooser, C. Nicolas, T. Asavei, L. Neagu, M. Schöffler, G. Kastirke, X-J Liu, S. Wada, S. Owada, K. Tono, T. Katayama, T. Togashi, M. Yabashi, K. Ueda.

This study was supported by the X-ray Free Electron Laser Utilization Research Project and the X-ray Free Electron Laser Priority Strategy Program of the MEXT, by JSPS, the Proposal Program of SACLA Experimental Instruments of RIKEN.

References

- [1] P. Emma et al., 2010 *Nat. Photonics* 4, 641.
- [2] T. Ishikawa et al., 2012 *Nat. Photonics* 6, 540.
- [3] T. Katayama et al., 2016 *Struct. Dyn.* 3 034031
- [4] T. Kameshima et al., 2014 *Rev. Sci. Instrum.* 85 033110

¹ E-mail: nagaya@scphys.kyoto-u.ac.jp

Attosecond coherent control at FELs

K. C. Prince¹

Elettra Sincrotrone Trieste, 34149 Trieste, Italy

Synopsis The fully coherent Free Electron Laser FERMI has demonstrated phase resolution of ~ 3 attoseconds, permitting new experiments in multicolour optics at short wavelength. Results of coherent control experiments are shown for ground state atoms, and prospects for further work discussed, including experiments not possible with optical lasers.

Pulsed optical lasers are characterized by high intensity, ultrashort duration, variable polarization, transverse coherence and longitudinal coherence. The majority of short wavelength Free Electron Lasers (FELs) possess the first four of these five characteristics, but lack the fifth. Most FELs are based on Self Amplified Spontaneous Emission (SASE), which is an intrinsically stochastic process, and produces pulses which are spiky in both the temporal and frequency domains.

Low longitudinal coherence limits SASE FELs for some experiments which can be done with HHG short-wavelength optical sources, which produce ultrashort coherent light, albeit with low energy/pulse. Using the methods of coherent control (control of the phase and amplitude), quantities can be measured on the time scale of the phase resolution, expressed in temporal terms. For example, Schultze et al [1] used an IR pulse of approximately 3 fs duration to measure a temporal delay of 21 as, only possible due to high precision phase locking.

The seeded FEL FERMI is the first FEL to produce fully coherent pulses. As well, we have demonstrated experimentally the longitudinal phase correlation between two colours (first and second harmonics), and applied it to coherently control a photoionization experiment [2]. Neon was ionized at wavelengths of 63.0 and 31.5 nm, and the asymmetry of the 2p photoelectron angular distribution (PAD) was manipulated by adjusting the phase, in a Brumer-Shapiro type experiment [3]. The outgoing 2p electrons, ionized by one (second-harmonic) photon or two (first-harmonic) photons interfere to give an asymmetric PAD whose asymmetry depends on the relative phase of the two photon fields.

The relative phase of the two wavelengths was locked and tuned with temporal resolution of ~ 3 as. The extremely precise manipulation of the phase in the present experiment is based on the use of phase shifters located between the radiators of FERMI. This innovative approach provides an extremely high degree of control.

The present results open the door to new coherent control experiments on atoms and molecules in the XUV and soft X-ray region, with ultrahigh time/phase resolution. The flexible design of FERMI has permitted new operating modes of the machine, such as double-pulse operation; production of two coherent, incommensurate colours; and single-colour, phase locked double pulses [4]. The latter open up the way to perform Tannor-Rice or pump-dump type experiments, and results will be shown. Other very recent results will be shown of an apparently unique application of Free Electron Lasers: coherent control of the decay of an excited state ion [5].

Acknowledgements. All of the authors of Refs. 2 and 5 contributed to this work. This work was supported by MEXT, JST, JSPS, IMRAM and NSF.

References

- [1] M. Schultze et al, *Science* 328 (2010) 1658.
- [2] K. C. Prince, E. Allaria, C. Callegari, R. Cucini, G. De Ninno, S. Di Mitri, B. Diviacco, E. Ferrari, P. Finetti, D. Gauthier, L. Giannessi, N. Mahne, G. Penco, O. Plekan, L. Raimondi, P. Rebernik, E. Roussel, C. Svetina, M. Trovò, M. Zangrando, M. Negro, P. Carpeggiani, M. Reduzzi, G. Sansone, A. N. Grum-Grzhimailo, E.V. Gryzlova, S.I. Strakhova, K. Bartschat, N. Douguet, J. Venzke, D. Iablonskyi, Y. Kumagai, T. Takanashi, K. Ueda, A. Fischer, M. Coreno, F. Stienkemeier, E. Ovcharenko, T. Mazza, M. Meyer, *Nature Photon.* 10, 176 (2016).
- [3] P. Brumer, and M. Shapiro. "Principles of the Quantum Control of Molecular Processes", Wiley-VCH, Berlin (2003).
- [4] E. Roussel et al, *Phys. Rev. Lett.* 115, 214801 (2015). D. Gauthier et al, *Phys. Rev. Lett.* 116, 024801 (2016).
- [5] D. Iablonskyi, K. Ueda, K. L. Ishikawa, A. Kheifets, G. Sansone, A. Comby, T. Csizmadia, S. Kuehn, E. Ovcharenko, T. Mazza, M. Meyer, A. Fischer, C. Callegari, O. Plekan, P. Finetti, E. Allaria, L. Giannessi, B. Diviacco, E. Ferrari, E. Roussel and K. C. Prince, to be published.

¹E-mail: Prince@Elettra.eu

Dichroism and resonances in intense radiation fields

Tommaso Mazza^{*}¹

^{*} European X-Ray Free Electron Laser Facility GmbH, Holzkoppel 4, 22869 Schenefeld, Germany

Synopsis Multi-photon excitation and ionization studies on dichroism and resonant excitations in atoms involving intense XUV and optical radiation are presented. This report focuses on the possibility given by light-matter interaction in the non-linear regime of unveiling otherwise hidden electronic properties and of steering the relaxation dynamics in the fs time range.

Dichroic and resonant phenomena in atoms can be regarded as a manifestation of the sensitivity of the interaction between light and matter to the spin and the energy of the exciting radiation, respectively. With the availability of ultra-fast and intense XUV light sources it is possible to observe and study these processes, involving inner-shell excitations, under non-linear photo-excitation conditions. This allows the unveiling of specific features which are hidden when restricting the investigations to the linear regime.

The non-linear conditions can be created by high XUV photon density or by an external intense optical field produced in short light pulses, that need to be synchronized to the XUV on a fs level.

In this paper, a few studies are presented exemplifying the above statement.

Specifically, using a 2-color multiphoton ionization scheme involving circularly polarized light I report on how dichroism can give information about the contribution of different electronic partial waves to the ionization process [1]; within the same scheme, I report on the intensity and polarization dependence of the ionization cross section of an oriented resonantly excited target in an intense optical field [2].

It is shown how non-linear XUV photoionization can unveil resonance substructures in collective excitations [3].

Finally, the application of a XUV-optical two-color scheme on closed shell systems [4] and on atomic radicals [5] involving the optical control of the relaxation dynamics of resonantly excited core-hole states is reported. This scheme gives the possibility of modifying the

ionization dynamics of resonantly excited atoms by an external optical field on a femtosecond timescale; in the case radicals, the open-shell configuration offers the possibility of investigating within the same system resonantly excited states with very different behavior. Experimental challenges and potential applications will be presented.

References

- [1] T. Mazza, M. Ilchen, A.J. Rafipoor, C. Callegari, P. Finetti, O. Plekan, K.C. Prince, R. Richter, A. Demidovich, C. Grazioli, L. Avaldi, P. Bolognesi, M. Coreno, P. O'Keeffe, M. Di Fraia, M. Devetta, Y. Ovcharenko, V. Lyamayev, S. Düsterer, K. Ueda, J.T. Costello, E.V. Gryzlova, S.I. Strakhova, A.N. Grum-Grzhimailo, A.V. Bozhevolnov, A.K. Kazansky, N.M. Kabachnik, M. Meyer 2016 *Journal of Modern Optics* **63** (4), 367-382.
- [2] M. Ilchen, N. Douguet, T. Mazza, A.J. Rafipoor, C. Callegari, P. Finetti, O. Plekan, K.C. Prince, A. Demidovich, C. Grazioli, L. Avaldi, P. Bolognesi, M. Coreno, M. Di Fraia, M. Devetta, Y. Ovcharenko, S. Düsterer, K. Ueda, K. Bartschat, A.N. Grum-Grzhimailo, A.V. Bozhevolnov, A.K. Kazansky, N.M. Kabachnik, M. Meyer 2017 *Physical Review Letters* **118**, 013002.
- [3] T. Mazza, A. Karamatskou, M. Ilchen, S. Bakhtiarzadeh, A.J. Rafipoor, P. O'Keeffe, T.J. Kelly, N. Walsh, J.T. Costello, M. Meyer, R. Santra 2015 *Nature Communications* **6**, 6799
- [4] T. Mazza, K.G. Papamihail, P. Radcliffe, W.B. Li, T.J. Kelly, J.T. Costello, S. Düsterer, P. Lambropoulos, M. Meyer *et al.* 2012 *J. Phys. B* **45** (14), 141001.
- [5] A. Achner *et al.* manuscript in preparation.

¹ E-mail: tommaso.mazza@xfel.eu

Footprints of electron correlation in strong field double ionization of Kr close to sequential ionization regime

Xiaokai Li*, Zongqiang Yuan†, Difa Ye†, Chuncheng Wang*¹, Pan Ma*, Wenhui Hu*, Sizuo Luo*, Libin Fu*² and Dajun Ding*³

* Institute of Atomic and Molecular Physics, Jilin University, Changchun 130012, P. R. China

† Laboratory of Computational Physics, Institute of Applied Physics and Computational Mathematics, Beijing 100088, P. R. China

‡ Science and Technology on Plasma Physics Laboratory, Research Center of Laser Fusion, China Academy of Engineering Physics, Mianyang 621900, P. R. China

With combination of kinematically complete measurement and semiclassical Monte Carlo simulation we study the correlated electron dynamics in strong field double ionization of Kr from nonsequential double ionization (NSDI) plateau to sequential double ionization (SDI) domain. In the NSDI regime, the measurements on Kr show consistent crossover behavior in comparison with early results on Ar and Xe, reveal the complex competition between the screening effect of inner-shell electrons and the Coulomb focusing of nuclei. In the SDI regime, we find that the electron correlation still gets involved in a subtle way.

Nonsequential double ionization (NSDI) always catches people's great attention because it contains electron correlation in the interaction between laser field and atoms or molecules. The well established recollision model[1] can explain the general feature of NSDI, however, more in-depth studies is needed to achieve a comprehensive understanding of the microscopic dynamics. Significant target dependence of SFDI does exist[2] and the role of the electron correlation in SDI regime is still debatable.

We have performed the differential measurements of SFDI of Kr in a Cold-Target Recoil-Ion-Momentum Spectroscopy (COLTRIM-S) at four typical laser intensities covering NSDI and sequential double ionization (SDI) regime. Figure 1 (A1-A4) shows the correlated electron momentum distributions which strongly depend on intensity. It evolves from a roughly round-shape distribution to an elongated pattern with substantially more population in the first and third quadrants, and this feature survived even for 3.5×10^{14} W/cm² which is expected to be in SDI regime. This clearly reveals the electron correlation still exist in the SDI regime.

To understand the experiment observations, we perform numerical simulations with the helium-like model and an improved Green-Sellin-Zachor (GSZ) model including screening effect. We find that the joint momentum spectra with the GSZ model agrees better with experiment at lower intensities, and it is more consistent with the helium-like model for higher intensities. This comparison reveals the competition between the screening effect of inner-shell electrons and the Coulomb focusing

of nuclei. Another strong evidence for the existence of electron correlation in SDI regime can be revealed by the sum-energy spectra of two electrons. Our experimental data show good match with the fitting[3] at energies lower than 4Up, but reveal upward long tails deviating the fittings, indicating the high probability of hard recollisions. Only the numerical simulations with GSZ model have reproduced this feature, which can be understood as a result of the fact that the GSZ core has a stronger Coulomb singularity[4] because the effective nuclear charge increases from 2 to Z as the radial position goes from infinity to zero.

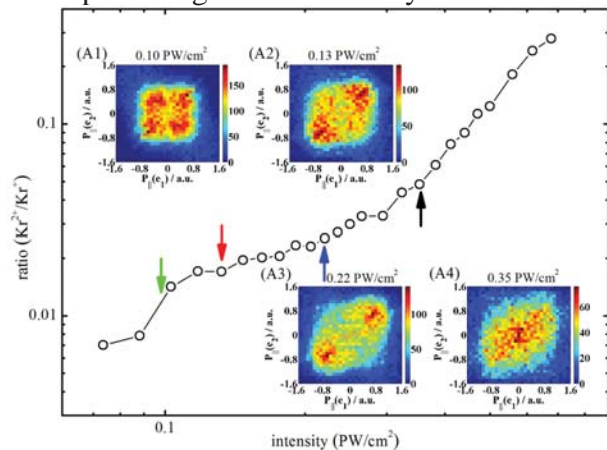


Figure 1. The measured ratio of doubly over singly ionization yield as a function of laser intensity and the correlated electron momentum spectrum.

References

- [1] P. B. Corkum 1993 *Phys. Rev. Lett.* 71 1994.
- [2] X. Sun *et al.* 2014 *Phys. Rev. Lett.* 113 103001.
- [3] D. F. Ye *et al.* 2015 *Phys. Rev. Lett.* 115 123001.
- [4] A. Rudenko *et al.* 2005 *J. Phys. B* 38 L191.

¹ E-mail: ccwang@jlu.edu.cn.

² E-mail: lbfu@iapcm.ac.cn ,

³ E-mail: dajund@jlu.edu.cn

Control of H₂ and D₂ dissociative ionization in the non-linear regime using EUV femtosecond pulses @FERMI

F. Holzmeier^{* 1}, M. Hervé^{*}, A. Achner[†], T. Baumann[†], M. Meyer[†], M. Di Fraia[‡], P. Finetti[‡], O. Plekan[‡], R. Richter[‡], C. Callegari[‡], K. C. Prince[‡], D. Gauthier[‡], E. Roussel[‡], R. Bello[§], A. Palacios[§], F. Martín[§], H. Bachau[¶], and D. Doweck^{* 2}

^{*} Institut des Sciences Moléculaires d'Orsay, Université Paris-Saclay, 91400 Orsay, France, [†] European XFEL, 22607 Hamburg, Germany, [‡] Elettra-Sincrotrone Trieste, 34149 Basovizza Trieste, Italy, [§] Universidad Autónoma de Madrid, 28049 Madrid, Spain, [¶] Université de Bordeaux, 33405 Talence, France

Synopsis Two-photon ionization via selected vibrational levels in neutral H₂ and D₂ intermediate states is demonstrated to control the dissociative ionization rate with femtosecond FEL pulses.

H₂ and D₂ molecules were photoionized in a non-linear 2-photon process via resonantly excited intermediate states thanks to the unique properties FERMI free electron laser (FEL) providing bright, coherent and tunable EUV femtosecond (fs) pulses. Selective excitation of the vibrationally resolved H₂^{*}(B ¹Σ_u⁺, v=8-17) and H₂^{*}(C ¹Π_u, v=2-4) states using 100 fs FEL pulses in the 12-15 eV range made it possible to investigate the influence of the nuclear degree of freedom (DOF) on the outcome of photoionization: depending on the intermediate state's internuclear distance expansion, absorption of the second photon leads to dissociative (DI) and/or non-dissociative ionization (NDI).

Time-of-flight (TOF) mass spectrometry, together with electron and ion velocity map imaging (VMI), were employed on the LDM beam-line [1] to analyze the DI/NDI ratio, kinetic energy spectra and angular distributions of photoelectrons and H⁺ fragment ions. DI was observed to be enhanced drastically by up to two orders of magnitude compared to one-photon ionization, as predicted by time-dependent Schrödinger equation calculations for 1-10 fs pulses and accounting for the DOF of electrons and nuclei [2,3]. Excitation of isolated H₂^{*}(B ¹Σ_u⁺, v) levels even leads to situations where DI dominates NDI, which is very unusual for valence shell ionization. For such cases, clear oscillations in the ion fragment energy spectra are discerned, which reflect a projection of the intermediate state vibrational wave function onto the ionic H₂⁺(2pσ_u) dissociative state. The photoelectron spectra feature the analogous structures for electrons correlated to DI. The latter spectra moreover yield access to the vibrational distribution of the H₂⁺(X ²Σ_g) ground state for NDI. As the distribution is quite sensitive to the vibronic intermediate state, it provides an additional probe of the induced nuclear dynamics.

New calculations based on time-dependent second order perturbation theory, well adapted to the 100 fs EUV pulses as utilized in the experiment, are in progress.

The remarkable anisotropies observed in the angular distributions complement the characterization of the photoionization dynamics. Furthermore, the electron angular distribution provides a sensitive means to characterize quantum interferences resulting from the coherent superposition of indistinguishable reaction paths. The study was extended to D₂ also and, beyond, a first experiment supports the feasibility for coherent control [4] of NDI involving two-EUV-photon resonant and one-XUV-photon non-resonant channels, relying on the variable controlled phase available at FERMI between the fundamental and second harmonic FEL pulses.

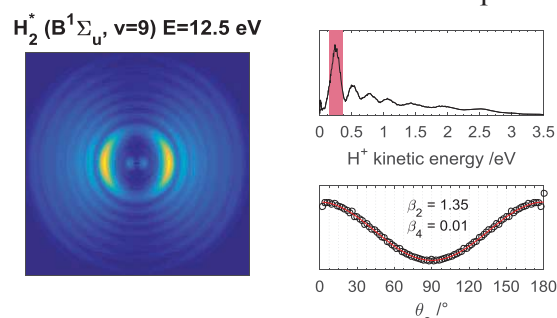


Figure 1. Inverted VMI, kinetic energy spectrum and angular distribution (highlighted band) for H⁺ ions from 2-photon ionization via H₂^{*}(B ¹Σ_u⁺, v=9).

References

- [1] V. Lyamayev *et al.* 2013 *J. Phys. B: At. Mol. Opt. Phys.* **46** 164007; C. Svetina *et al.* 2015 *J. Synchrotron Radiat.* **22** 538
- [2] A. Palacios *et al.* 2006 *Phys. Rev. Lett.* **96** 143001; 2007 *Phys. Rev. A* **75** 013408
- [3] J. F. Pérez *et al.* 2010 *J. Phys. B: At. Mol. Phys.* **43** 015204.
- [4] K. Prince *et al.* 2016 *Nat. Phot.* **10** 176

¹ E-mail: fabian.holzmeier@u-psud.fr

² E-mail: danielle.doweck@u-psud.fr

Fast interactions of atoms and laser pulses with crystal surfaces

M.S. Gravielle* ¹

* Instituto de Astronomía y Física del Espacio (IAFE, CONICET-UBA), Buenos Aires C1428 EGA, Argentina

Synopsis. For fast atom diffraction from crystal surfaces, the influence of coherence and decoherence effects produced by the collimation of the incident beam as well as by thermal vibrations of the crystal lattice is addressed. Additionally, effects due to long-range dispersive forces and the induced potential are analyzed.

In the last time fast interactions of atoms and laser pulses with crystal surfaces have emerged as promissory tools to investigate in detail the interface region of ordered materials.

Concerning heavy-particle interactions, grazing-incidence fast atom diffraction (GIFAD or FAD) has become a powerful surface analysis technique that allows one to inspect crystal surfaces, providing precise information on their morphological and electronic characteristics. The extreme sensitivity of FAD relies on the preservation of quantum coherence, which is affected by the initial conditions of the incoming projectiles as well as by thermal vibrations of the crystal lattice. Both aspects are addressed in this report.

In relation to collimation effects, we found that the collimating scheme of the incident beam influences strongly FAD patterns. By varying the size and shape of the collimating apertures it is possible to make different interference mechanisms alternately visible, as experimentally observed (see Fig. 1) [1]. On the contrary, at room temperature thermal effects play a minor role, introducing a slight widening of the interference peaks, which can be associated with decoherent processes (see Fig. 2) [2].

The sensitivity of FAD is also illustrated by investigating the influence of long-range van der Waals (vdW) forces in atom- LiF(001) interactions. While for multielectronic projectiles effects due to vdW contributions are negligible, for H projectiles the inclusion of vdW interactions in the potential model yields a great improvement of the description FAD patterns for low normal energies and incidence along the $\langle 100 \rangle$ channel [3]. It opens a window to scrutinize vdW approaches via FAD techniques.

On the other hand, the fast interaction of ultra-short laser pulses with metal surfaces allows us to study the contribution of the induced potential to the emergence of band-structure signatures in the near-threshold region of photoelectron spectra.

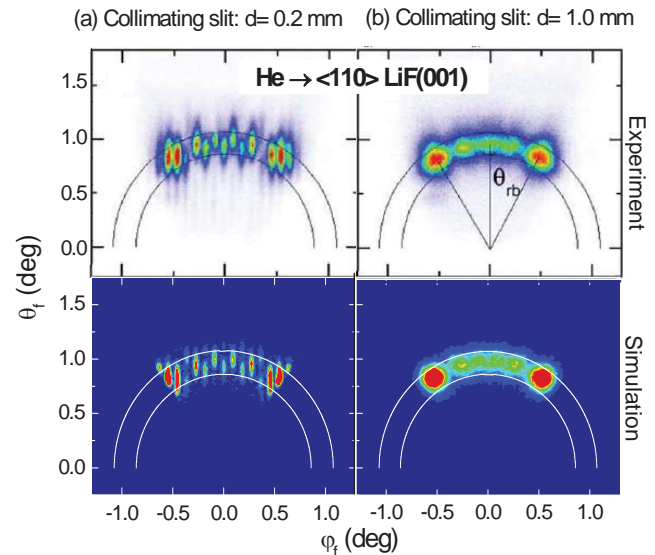


Figure 1. Projectile distribution, as a function of the polar (θ_f) and azimuthal (ϕ_f) angles, for ^4He atoms impinging on LiF(001) along the $\langle 110 \rangle$ channel, with a normal energy $E_{\perp} = 0.3$ eV. Simulations for a rectangular collimation slit with a width (a) $d = 0.2$ mm and (b) $d = 1$ mm are displayed.

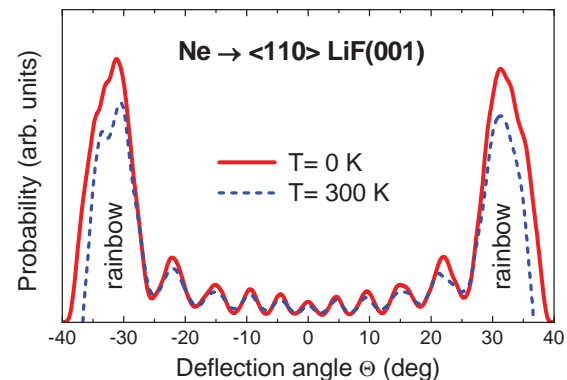


Figure 2. Projectile distribution, as a function of the deflection angle $\Theta = \arctan(\phi_f/\theta_f)$, for Ne atoms impinging on LiF(001) at a temperature T . The normal energy is $E_{\perp} = 0.3$ eV.

References

- [1] M.S. Gravielle *et al.* 2015 *Phys. Rev. A* **92** 062709; *ibid Nucl. Instrum. Meth. Phys. Res. B* 2016 **382** 42
- [2] J.E Miraglia *et al.* 2017 *Phys. Rev. A* in press
- [3] G.A. Bocan *et al.* 2016 *Phys. Rev. A* **94** 022711

Observation of the Efimov State of the Helium Trimer

M. Kunitski^{*}¹, S. Zeller^{*}, J. Voigtsberger^{*}, A. Kalinin^{*}, L. Ph. H. Schmidt^{*}, M. Schöffler^{*},
A. Czasch^{*}, W. Schöllkopf[†], R. E. Grisenti^{*}, T. Jahnke^{*}, D. Blume[‡] and R. Dörner^{*}² ¶

^{*} Institut für Kernphysik, Goethe-Universität, Max-von-Laue-Straße 1, 60438 Frankfurt am Main, Germany

[†] Department of Molecular Physics, Fritz-Haber-Institut, Faradayweg 4-6, 14195 Berlin, Germany

[‡] Department of Physics and Astronomy, Washington State University, Pullman, WA 99164-2814, USA

Synopsis We have observed the excited Efimov state of the helium trimer. The structure and the binding energy of this state have been revealed.

In 1970 Vitali Efimov predicted remarkable counterintuitive behaviour of a three-body system made up of identical bosons. Namely, a weakening of pair interaction in such a system brings about in the limit appearance of infinite number of bound states of a huge spatial extent [1]. The helium trimer has been predicted to be a molecular system having an excited state of this Efimov character under natural conditions.

Here we report experimental observation of the Efimov state of $^4\text{He}_3$ by means of Coulomb explosion imaging of mass-selected clusters [2].

Helium trimers were prepared under supersonic expansion of the gaseous helium through a $5\text{ }\mu\text{m}$ nozzle. The clusters were selected from the molecular beam by means of matter wave diffraction [3]. Each atom of a trimer was singly ionized by a strong ultrashort laser field resulting in Coulomb explosion of the cluster. The momenta, the ions acquired during Coulomb explosion, were measured by COLTRIMS. These momenta were utilized for reconstruction of the initial spatial geometry of the neutral trimer at the instant of ionization.

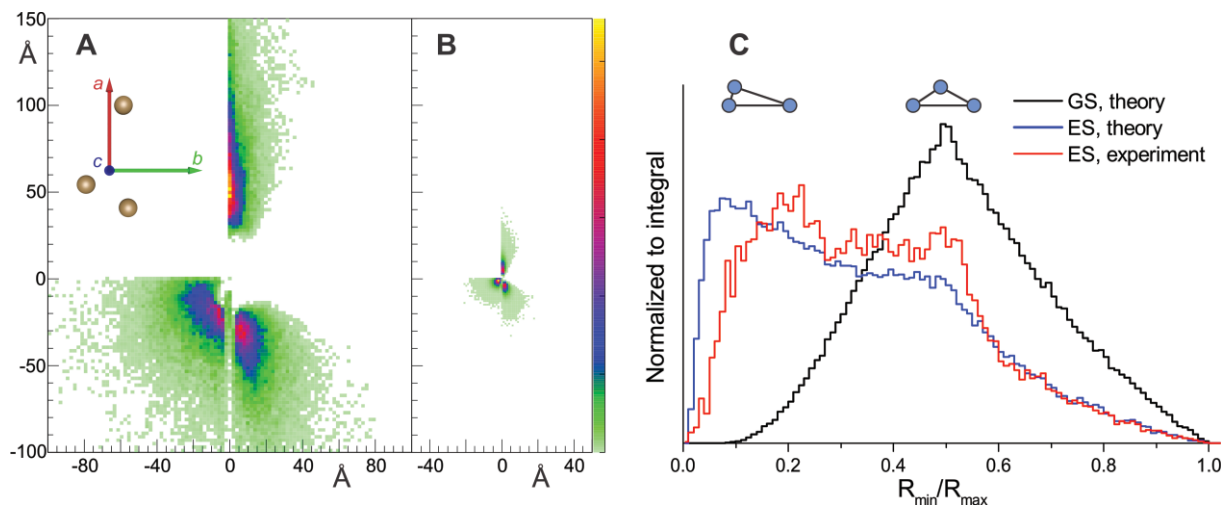


Figure 1. Structures of the helium trimer: A – excited state, experimental, B – ground state, theoretical. Three helium atoms of each trimer are plotted in the principal axis frame abc . C: Distributions of the ratio of the shortest interparticle distance to the longest interparticle distance for ground state structures (black), theoretical excited state structures (blue) and experimental excited state structures (red).

Structures of the excited Efimov state of the $^4\text{He}_3$ (Fig. 1A) are about eight times larger than those of the ground state (Fig. 1B), which is in accordance with theory. Whereas the ground state corresponds to an almost randomly distributed cloud of particles [4], the excited Efimov state is dominated by configurations in which two atoms are close to each other and the third one farther away (Fig. 1C).

References

- [1] V. Efimov 1970 *Phys. Lett. B* **33** 563
- [2] M. Kunitski *et al.* 2015 *Science* **348** 551
- [3] W. Schöllkopf, J. P. Toennies 1994 *Science* **266** 1345
- [4] J. Voigtsberger *et al.* 2014 *Nat. Comm.* **5** 5765

¹ E-mail: kunitski@atom.uni-frankfurt.de

² E-mail: doerner@atom.uni-frankfurt.de

H₂ ortho-para conversion on amorphous solid water

Naoki Watanabe*¹, Hirokazu Ueta*², Tetsuya Hama*, Akira Kouchi*

* Institute of Low Temperature Science, Hokkaido University, Sapporo, Hokkaido 060-0819, Japan

Synopsis Nuclear spin conversion of hydrogen molecules was monitored on amorphous solid water at very low temperatures with a combination of photostimulated desorption and resonance enhanced multiphoton ionization methods. The conversion rate steeply changed from 2.4×10^{-4} to $1.7 \times 10^{-3} \text{ s}^{-1}$ in the very narrow temperature window from 9.2 to 16 K. The observed strong temperature dependence can be explained by the energy dissipation model via two phonon process.

Since the radiative transformation of molecular nuclear spins is forbidden in the gas phase, the ortho-to-para abundance ratios (OPRs) of hydrogen molecule (H₂) observed toward various astronomical objects have been often considered as tracers of chemical history of the molecule. The OPR of H₂ is particularly crucial for chemical evolution and deuterium fraction of molecules in very cold region in space, so-called molecular clouds, because H₂ in the ortho-ground state ($J=1$) is more energetic (and thus reactive) than that in the para-ground state ($J=0$) by approximately 14.6 meV corresponding to 170 K, which is significantly higher than typical temperatures of molecular clouds.

In contrast to the gas phase, it was not obvious how the nuclear spins behave on cosmic ice dust. It was often assumed without the experimental evidences that the OPR of H₂ formed on the cosmic dust surface is statistical value of 3. Recently, our group has tackled this issue experimentally. Using experimental techniques of molecular beam, photostimulated-desorption, and resonance-enhanced multiphoton ionization, we measured the OPRs of H₂ photodesorbed from amorphous solid water (ASW) at around 10 K, which is an ice dust analogue. We obtained the clear evidence that the OPR of H₂ easily varies on ASW. Furthermore, it was first demonstrated that the rate of spin conversion from ortho to para drastically increases from 2.4×10^{-4} to $1.7 \times 10^{-3} \text{ s}^{-1}$ within the very narrow temperature window of 9.2 to 16 K and reach a plateau at temperatures above 12 K (See Figure 1) [2]. This temperature dependence cannot be explained solely by state-mixing models ever proposed. The data points for the conversion rate were fitted very well by the power law of T^7 where T is the surface temperature. This indicates that the conversion rate at lower temper-

atures is dominated by the two-phonon energy dissipation process (Raman process) for the excess energy ($\sim 14.6 \text{ meV}$) due to the conversion, and at higher temperatures the rate may be limited by a spin-flip transition rate.

From the present and our previous results, astrochemical history of interstellar H₂-OPR is depicted as follows. When H₂ molecule is produced by H-H recombination on cosmic ice dust, the OPR of nascent H₂ is 3 [1]. If the H₂ is immediately desorbed at the formation, the OPR of H₂ released should be near 3. However, if H₂ is trapped on the ice dust surface before desorption, the OPR at desorption strongly depends on the surface temperature and duration of trapped.

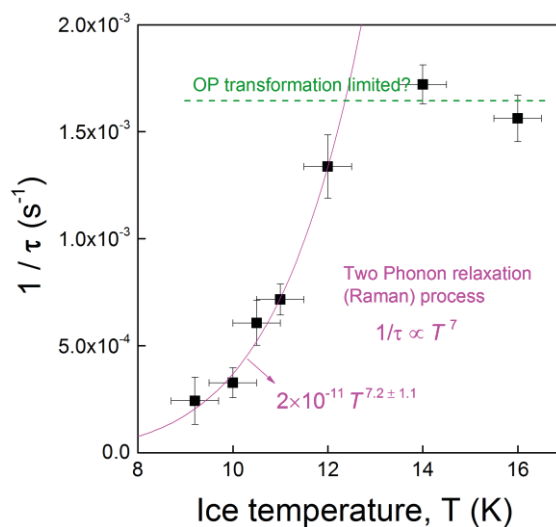


Figure 1. The rate of ortho-to-para nuclear spin conversion on ASW.

References

- [1] N. Watanabe *et al.* 2010 *Astrophys. J. Lett.* **714** L233
- [2] H. Ueta *et al.* 2016 *Phys. Rev. Lett.* **116** 253201

¹ E-mail: watanabe@lowtem.hokudai.ac.jp

² Present address, Department of Physics, Rikkyo University, Tokyo 171-8501, Japan

MeV ion beam extraction into air with a glass capillary filled with He

M. Asamura^{*1}, K. Ishii^{†2}, and H. Ogawa[†]

^{*} Graduate School of Humanities and Sciences, Nara Women's University, Nara, 630-8506, Japan

[†] Department of Physics, Nara Women's University, Nara, 630-8506, Japan

Synopsis In order to obtain intense ion beam in air, we have developed the He capillary, which is normal glass capillary filled with low pressure He gas. Energy spectra of ion beam via the He-capillary with and without He have been measured. Enhancement of peak intensity and suppression of low energy components have been observed for the He- capillary.

Developments of in-air-analysis method with MeV ion beam have been expected in various fields such as biology, nano-technology and archaeology. In particular, a technique to extract ion beam in air by a tapered glass capillary has been developed by Nebiki et al and they have performed in-air-PIXE (particle induced X-ray emission) for the sea sludge [1]. This technique was so simple and effective to obtain an in-air micro beam that this technique becomes to be used in various laboratories. We have also developed several in-air-analysis techniques using glass and metal capillaries [2] and reported transmission properties of ion beam through several capillaries [3]. It is concluded that an ion beam diameter in air via capillary is determined by the inner diameter of the capillary and its energies and intensities are spread by atmospheric gas inside and outside of the capillary. In this work, we have newly developed the capillary named He-capillary, which is normal glass capillary filled with low pressure He gas. It is expected that an ion beam spread in the capillary is suppressed since energy loss and struggling of ion beam in He atmosphere are smaller than that in air.

We have measured energy spectra of an ion beam via He capillary as a function of He pressure in the capillary by using the SSD (silicon semiconductor detector). Figure 1 shows energy spectra of 3 MeV proton beam via the He-capillary filled with and without He gas in the capillary. As is shown in Figure, peak intensity is more enhanced at He-capillary with He than without He although peak energy is shifted lower. Furthermore, low energy components of the energy spectra with He is much suppressed than that without He condition.

In the presentation, we will introduce the He- capillary and discuss transmission properties of ion beam via the capillary in detail.

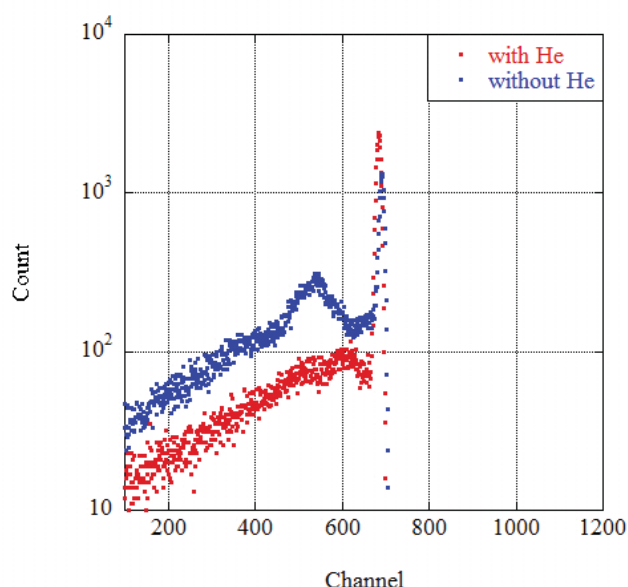


Figure 1. Energy spectra of 3.0 MeV proton beam via the He-capillary with and without He.

References

- [1] T. Nebiki, M. H. Kabir and T. Narusawa, Nucl. Instr. Meth. B **249**(2006) 226.
- [2] N. Fujita, K. Ishii and H. Ogawa, Nucl. Instr. Meth. B **269** (2011)1023. ; K. Ishii, N. Fujita and H. Ogawa, Nucl. Instr. Meth. B **269** (2011)1026.
- [3] N. Fujita, A. Yamaki, K. Ishii and H. Ogawa, Nucl. Instr. Meth. B **315** (2013)332.

¹E-mail: nam_amanura@cc.nra-wu.ac.jp

²E-mail: ishii@cc.nara-wu.ac.jp

Studying Molecular Structure and Dynamics via Coulomb Explosion Imaging with X-rays and Ultrafast Laser Pulses

U. Ablikim^{*†1}, C. Bomme[‡], E. Savelyev[‡], H. Xiong[§], R. Obaid[§], B. Kaderiya^{*}, S. Augustin^{*}, K. Schnorr^{††}, I. Dumitriu[¶], R. Bilodeau[†], D. Kilcoyne[†], V. Kumarappan^{*}, R. K. Kushawaha^{*}, F. Ziaee^{*}, T. Osipov[&], A. Rudenko^{*}, N. Berrah[§], and D. Rolles^{*2}

^{*}James R. Macdonald Laboratory, Department of Physics, Kansas State University, Manhattan, KS 66506, USA

[†]Advanced Light Source, Lawrence Berkeley National Laboratory, Berkeley, CA 94704, USA

[‡]Deutsches Elektronen-Synchrotron (DESY), Hamburg, 22607, Germany

[§]Department of Physics, University of Connecticut, Storrs, CT 06269, USA

^{††}Department of Chemistry, University of California, Berkeley, CA 94720, USA

[¶]Hobart and William Smith Colleges, Geneva, NY 14456, USA

[&]SLAC National Accelerator Laboratory, Menlo Park, CA 94025, USA,

Synopsis Coincidence momentum imaging is a powerful method to study molecular structure and dynamics. Here, we used the Coulomb explosion imaging method together with synchrotron radiation and ultrafast laser pulses in order to distinguish between geometric isomers of $C_2H_2Br_2$, $C_2H_2Cl_2$, and difluoroiodobenzene and to investigate their fragmentation dynamics following both strong-field and inner-shell photoionization.

Isomers, i.e. molecules with the same chemical formula but different geometric structures, play an important role in many biological processes [1]. Despite containing the same atomic constituents, isomers can have very different physical, chemical, and biological properties. Therefore, it is of particular interest to experimentally distinguish isomers in order to investigate isomer-specific reactions and to study the interconversion between different isomers in time-resolved experiments.

We have conducted coincidence momentum imaging measurements on gas-phase molecular isomers, such as dibromoethane ($C_2H_2Br_2$) and dichloroethene ($C_2H_2Cl_2$), using a double-sided velocity map imaging (VMI) spectrometer at the Advanced Light Source as well as using a COLTRIMS setup and an ultrafast near-infrared laser at the J.R. Macdonald Laboratory at Kansas State University. The goal of the studies is to experimentally identify and separate *cis* and *trans* isomers using the Coulomb Explosion Imaging (CEI) method. Our results show that the geometric structure of the isomers can be distinguished by triply ionizing the molecule into the $C_2H_2^+ + Br^+ + Br^+$ fragmentation channels via inner-shell photoionization using X-ray synchrotron beams [2] or via strong-field ionization with ultrafast femtosecond laser pulses. Furthermore, numerical simulations using a classical Coulomb explosion (CE) model for both isomers match closely with the kinetic energies of the ionic fragments and the momentum correlation between their momentum vectors.

In order to further extend our CEI studies to other types of isomers and more complex molecules, we

performed similar coincidence momentum imaging experiments on 2,6- and 3,5-difluoroiodobenzene (DFIB) [3]. Our experimental results and CE simulation indicate a fast charge migration along the phenyl ring after inner-shell photoionization of the iodine *4d* shell. Furthermore, we find that the majority of three-body fragmentation channels result from a sequential two-step fragmentation, where the iodine ion rapidly departs from the system after inner-shell ionization, leaving the remaining DFB dication in a rotationally excited metastable state, which subsequently fragments after a delay that is longer than its rotational period.

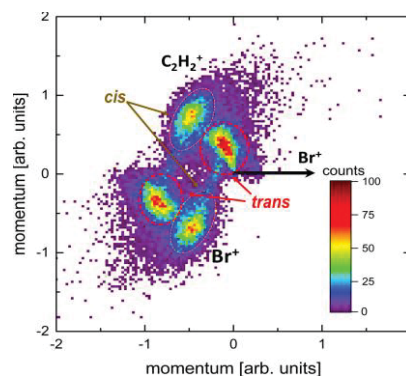


Figure 1. Newton plot of the three-body $C_2H_2^+ + Br^+ + Br^+$ coincidence channel created by inner-shell ionization of $C_2H_2Br_2$ (*cis/trans* mixture) at 140 eV photon energy.

References

- [1] U. K. Genick *et al.* 1998 *Nature* **392** 206-209
- [2] U. Ablikim *et al.* 2016 *Sci. Reports* **6** 38202
- [3] U. Ablikim *et al.* 2017 *submitted*

¹ E-mail: utuq@lbl.gov

² E-mail: rolles@phys.ksu.edu

Stimulating electron competition with XUV-initiated high harmonic generation

Andrew C. Brown¹, Kathryn R. Hamilton, Hugo W. van der Hart²,

Centre for Theoretical Atomic, Molecular and Optical Physics, Queen's University Belfast, Belfast BT7 1NN

Synopsis We demonstrate a new technique wherein a combination of XUV and Mid-IR laser pulses stimulates multielectron dynamics encoded in the high-harmonic spectrum. We address this 'XUV-initiated High Harmonic Generation' for both Ne and Ar. The contribution of inner and outer electrons to the spectrum is investigated with an emphasis on electron correlation arising from the interaction between the $3s^{-1}$ and $3p^{-1}$ hole states in Ar.

High harmonic generation (HHG) is the cornerstone of much of modern attoscience, not only as the driver for both high energy and ultrashort laser pulses [1], but also as an investigative tool in its own right. The so-called 'high harmonic spectroscopy' has been used to elucidate atomic and molecular structure and ultrafast electron dynamics in a variety of systems [2–4]. The well-known 'three-step' model provides a useful framework to understand the HHG process: an electron is tunnel-ionized and then driven by a strong laser pulse, before recombining with its parent ion, releasing its energy as a high-harmonic photon [5].

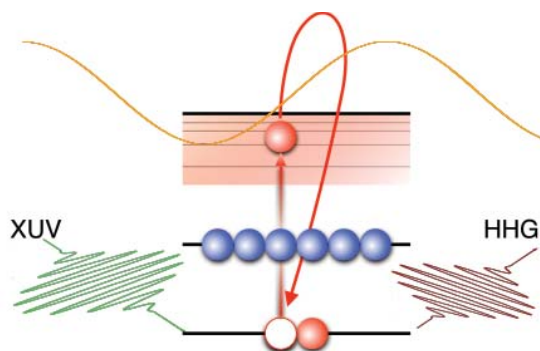


Figure 1. XIIHHG in noble gas atoms initiated by excitation of the inner-valence electron and subsequent tunnel-ionization.

Despite the ubiquity of HHG in attoscience, the process is actually severely limited by the initial, tunnel-ionization step. Tunnel ionization offers little or no temporal control of the ionization event, an extremely low conversion efficiency, and is limited to the ionization of only the outer-valence electron. XUV-initiated HHG (XIIHHG) could mitigate these factors: several theoretical studies have explored the efficiency question [6, 7] and one study probed core-hole dynamics in small molecules with XIIHHG [8].

Among theoretical models able to address the dynamics of atoms in strong-laser fields, only a handful also have the capability to describe multiple electrons and the interactions between them. The R-matrix with time-dependence (RMT) method has been established as a leading approach in this area, affording

a comprehensive description of atomic structure and electron correlation in multielectron atomic systems exposed to intense, long-wavelength light [9, 10].

In the two studies presented here, we employ a variation on the XIIHHG principle. The first stage of the process is not direct photo-ionization of the inner-valence electron, but excitation to a high-lying Rydberg state attached to the inner-valence hole. The inner-valence electron is then tunnel ionized by the IR field and driven in a three-step-like trajectory to elicit HHG. We first demonstrate the mechanism in Ne, resolving the contribution of the inner- and outer-valence electrons to the harmonic spectrum [11].

We will then show our most recent results for Ar where we observe a resonant boost in the cutoff harmonics. The feature appears in the spectra only for calculations where *both* the ionization of the $3s$ electron *and* the doubly excited $3s^2 3p^4 ndn\ell$ Rydberg states are included. We propose a mechanism which relies on the strong mixing of the $3s 3p^6 n\ell$ and $3s^2 3p^4 ndn\ell$ Rydberg states and is thus mediated by correlation between the $3s^{-1}$ and $3p^{-1}$ hole states.

References

- [1] K. Zhao *et al.* 2012, *Opt. Lett.* **37**, 3891
- [2] A. D. Shiner *et al.* 2011, *Nat. Phys.* **7**, 464
- [3] O. Smirnova *et al.* 2009, *Nature* **460**, 972
- [4] J. Itatani *et al.* 2004, *Nature* **432**, 867
- [5] P. B. Corkum, 1993 *Phys. Rev. Lett.* **71**, 1994
- [6] J. Biegert *et al.* 2006, *J. Mod. Opt.* **53**, 87
- [7] G. Gademann *et al.* 2011, *N. J. Phys.* **13**, 033002
- [8] J. Leeuwenburgh *et al.* 2013, *Phys. Rev. Lett.* **111**, 123002
- [9] T. Ding *et al.* 2016 *Opt. Lett.* **41**, 709
- [10] O. Hassounah, A. C. Brown, and H. W. van der Hart, 2014, *Phys. Rev. A* **90**, 043418
- [11] A. C. Brown and H. W. van der Hart, 2016, *Phys. Rev. Lett.* **117**, 093201

¹E-mail: andrew.brown@qub.ac.uk

²E-mail: h.vanderhart@qub.ac.uk

Precise attosecond pulse characterization using coherent bound wave packets

Jan Marcus Dahlström ^{*†1} and Stefan Pabst ^{†‡2}

^{*} Department of Physics, Stockholm University, AlbaNova University Center, SE-106 91 Stockholm, Sweden

[†] ITAMP, Harvard-Smithsonian Center for Astrophysics, 60 Garden Street, Cambridge, Massachusetts 02138, USA

[‡] Physics Department, Harvard University, 17 Oxford Street, Cambridge, Massachusetts 02138, USA

Synopsis This is a theoretical study of an attosecond pulse characterization method based on photoionization of coherent bound wave packets. It is shown that the influence of dipole phases can be eliminated, thus opening up for future attosecond experiments with increased precision in the XUV and soft x-ray range.

We investigate the PADA method (Pulse Analysis by Delayed Absorption) [1] for spectral phase characterization of pulses in the extreme ultraviolet (XUV) and soft x-ray regime. The basic idea of the method is illustrated in Fig. 1. We demonstrate that the dependence on dipole phases can be eliminated by performing both time-dependent simulations and calculations based on perturbation theory. The dipole phase elimination occurs if (i) the pump step (at τ_L) and probe step (at τ_X) are sequential, (ii) the intermediate wave packet, $\psi(t)$, is bound, and (iii) the photoelectron probability (or absorption of photons) is measured as a function of energy and delay, $P(\epsilon, \tau)$. This opens up for increased accuracy in pulse characterization beyond present-day methods based on laser-assisted photoionization, c.f. Ref. [2].

Photoionization of atomic Rydberg wave packets in both alkali and noble gas atoms have been considered. For example, we find that excited K atoms (in a coherent superposition of $4p$ and $5p$ Rydberg states) exhibit a 3 as delay with angle-resolved detection. This effect is attributed to Cooper minima in the partial photoionization cross sections. Fano resonances in photoionization from excited Ne atoms (in a coherent superposition of $2p^{-1}3s$ and $2p^{-1}4s$ states) exhibit a delay of -25 as with angle-resolved detection. Finally, we show that neither Cooper- nor Fano phase shifts affect the spectral-phase reconstruction procedure of the PADA method.

The energy spacing between Rydberg states decreases with $1/n^3$, offering high spectral energy shearing resolution and the possibility to bridge energy regions with no spectral weights (as in the case of pulse trains). Wave packets involving multiple electronic states provide redundant information that can be used to cross-check the consistency of the phase reconstruction. One downside of using Rydberg electrons, however, is that photoionization cross sections are small. This is a major concern for direct

application of the PADA method to the x-ray regime, where inner-shell photoionization is the dominant ionization mechanism. The sudden creation of an inner-core hole is followed by secondary processes like fluorescence, Auger decay, and shake-up that may create additional delay-dependent modulations due to interaction with the Rydberg wave packet [3].

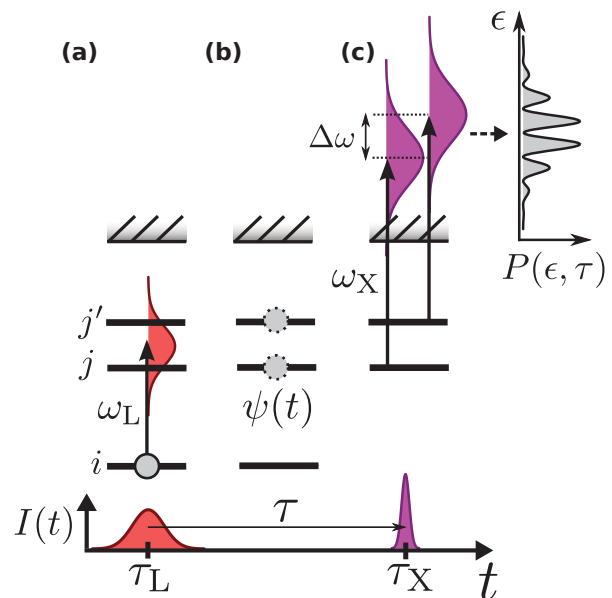


Figure 1. The PADA method for spectral shearing of XUV/x-ray pulses. (a) Initiation of bound wave packet. (b) Field free propagation. (c) Photoionization from bound excited states by the test pulse.

References

- [1] S. Pabst and J.M. Dahlström 2016 *Phys. Rev. A* **94** 013411
- [2] J.M. Dahlström *et al.* 2012 *J. Phys. B: At. Mol. Opt. Phys.* **45** 183001
- [3] S. Pabst and J.M. Dahlström 2017 *arXiv* :1702.04804 [physics.atom-ph]

¹E-mail: marcus.dahlstrom@fysik.su.se

²E-mail: stefan.pabst@cfa.harvard.edu

Strong Near-Field Induced Molecular Processes on Nanoparticles

Matthias F. Kling^{*,†}

^{*}Physics Department, Ludwig-Maximilians-Universität Munich, Garching, Germany

[†]Max Planck Institute of Quantum Optics, Garching, Germany

Synopsis We developed a nanotarget reaction microscope and investigated the strong near-field driven Coulomb explosion of ethanol and water molecules on silica nanoparticles in intense few-cycle laser fields. A strong spatial correlation between the electron and ion dynamics is found. The results open the door towards nanometer scale spatio-selective chemical analysis of aerosols.

The chemical composition of atmospheric aerosols is a crucial factor in their contribution to air pollution and their impact on health. Strong laser fields offer a route for single particle chemical analysis, where molecular fragments are created in the laser interaction and spectroscopically identified. Strong-field induced processes in molecules such as ionization and dissociation have been subject to theoretical and experimental investigations for many decades [1]. These processes include, e.g., above threshold ionization, high harmonic generation, and laser induced electron diffraction. Since these effects strongly rely on the exact spatial and temporal evolution of the electric fields, they are also influenced and controlled by the presence of enhanced near-fields in the proximity of a nanostructure [2].

Recent theoretical and experimental work focused mainly on either atomic processes in strong near-fields or near-field driven photoemission from nanostructures. Here, we investigated the near-field control of one of the most fundamental *molecular strong-field processes*, namely multiple ionization leading to Coulomb explosion (CI).

We have developed a nanotarget reaction-microscope based on recoil-ion-momentum spectroscopy (nanoTRIMS) [3], which permits recording both ions and electrons from the interaction of light pulses with molecules on a nanoparticle surface. Nanoparticles are injected into the interaction region using an aerosol technique and are illuminated by 5 fs laser pulses at 720 nm with a peak intensity of $\sim 3 \times 10^{13}$ W/cm². In particular, we have studied the Coulomb explosion of ethanol and water molecules on SiO₂ nanoparticles of various diameters, leading to the ejection of high-energy H⁺ ions (see Fig. 1(a)). For large nanoparticles (300 nm in Fig. 1), the data show a clear propagation effect [4] as well as indications of enhanced-field ionization of ethanol or water and the acceleration of H⁺ in the spatially varying near-field.

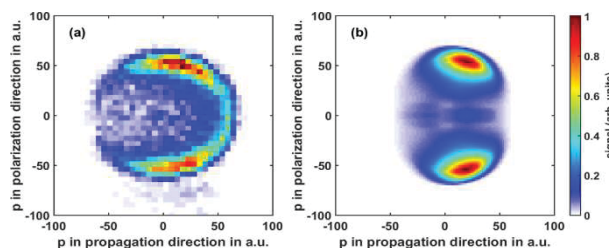


Figure 1 (a) Projected initial momenta of H⁺ ions from ethanol or water on 300 nm SiO₂ nanospheres. The propagation-induced near-field is clearly visible in the asymmetric distribution of signal along the propagation direction momenta. (b) Mie-Monte-Carlo simulations for the same experimental parameters.

The results from the nanoTRIMS experiment are modelled by a semi-classical Monte-Carlo trajectory simulation [4] including Mie fields and charged particle interactions, shown in Fig. 1(b). The simulations show a strong spatial correlation between the mean-field of emitted electrons and the trajectories of the much heavier ions, which are accelerated in the mean-field rather than in the pure Mie near-field.

The results open the door towards strong near-field induced chemical reactions on nanoparticles and a route towards nanometer-scale spatio-selective chemical analysis of molecular adsorbates on aerosols.

References

- [1] T. Brabec, *Strong Field Laser Physics* (Springer, New York, 2009)
- [2] P. Hommelhoff and M.F. Kling, *Attosecond Nanophysics: From Basic Science to Applications*, (Wiley, 2015)
- [3] P. Rupp *et al.*, *in preparation*.
- [4] F. Süßmann *et al.*, Nat. Commun. **6**, 8944, (2015).

E-mail: matthias.kling@lmu.de

Time-Dependent Two-Particle Reduced Density Matrix Theory: Application to High-Harmonic Generation

Fabian Lackner^{*1}, Iva Březinová^{*2}, Takeshi Sato^{†‡}, Kenichi L. Ishikawa^{†‡}, Joachim Burgdörfer^{*}

^{*} Institute for Theoretical Physics, Vienna University of Technology, Wiedner Hauptstraße 8-10/136, 1040 Vienna, Austria, EU

[†] Photon Science Center, School of Engineering, The University of Tokyo, 7-3-1 Hongo, Bunkyo-ku, Tokyo 113-8656, Japan

[‡] Department of Nuclear Engineering and Management, School of Engineering, The University of Tokyo, 7-3-1 Hongo, Bunkyo-ku, Tokyo 113-8656, Japan

Synopsis We follow a new approach for calculating high-harmonic spectra for multi-electron atoms and molecules by propagating the two-particle reduced density matrix. Calculated results are in very good agreement with state-of-the-art many-body wavefunction-based benchmark calculations.

High-harmonic generation (HHG) is one of the fundamental processes in strong field physics whose applications range from attosecond metrology [1], tunable table-top XUV/Soft X-ray sources [2] to high precision spectroscopy [3] and orbital imaging [4]. On the atomic level the theoretical description of HHG is challenging because of the multi-electron nature of the underlying process. While simple models such as the single-active-electron approximation (SAE) or time-dependent Hartree-Fock (TDHF) are well suited to describe qualitative features of HHG, advanced theories capable of correctly treating electron correlation are needed for a quantitative description [5]. However, with increasing system size conventional wavefunction-based methods such as the multi-configurational time-dependent Hartree-Fock (MCTDHF) method soon become unfeasible due to their exponential scaling with particle number. One way to overcome this exponential barrier is to abandon a wavefunction-based description and propagate time-dependent reduced densities instead. Considerable success along this line has been achieved by time-dependent density functional theory (TDDFT) [6]. However, accurate calculations in TDDFT face the difficulty of unknown exchange-correlation functionals that are difficult to improve systematically. We propose to go beyond the limitations of TDDFT by propagating the time-dependent two-particle reduced density matrix (TD-2RDM). As a hybrid between the electron density and the many-body wavefunction the 2RDM fully includes two-particle correlations. We have implemented the TD-2RDM method to describe high-harmonic generation of fully three-dimensional multi-electron atoms [7]. To obtain accurate results for the electronic response we use an advanced closure scheme [8] that is suited to conserve all constants of motion associated with symmetries of the Hamiltonian. We benchmark the

performance of the TD-2RDM method by comparing it to a state of the art MCTDHF calculation [9] as well as to TDDFT calculations (see Fig.1). We find very good agreement between the TD-2RDM and the MCTDHF method while TDDFT within the local density approximation shows clear deviations indicating that the correct treatment of two-particle correlations is essential to obtain accurate HHG spectra.

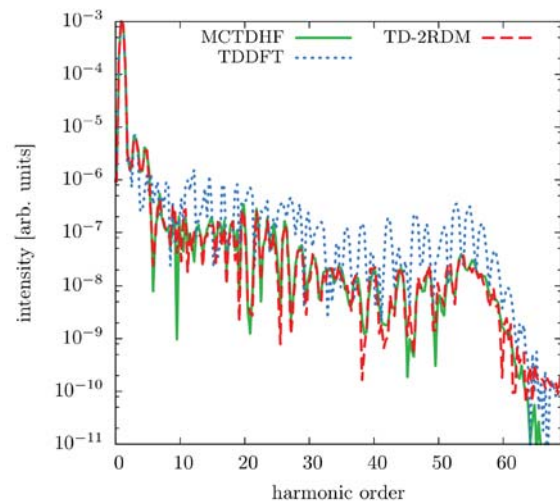


Figure 1. HHG spectrum of beryllium subject to a 3-cycle laser pulse with intensity $I = 4.0 \times 10^{14} \text{ W/cm}^2$. MCTDHF(—), TD-2RDM(---), TDDFT(····).

References

- [1] M. Hentschel *et al.* 2001 *Nature* **414** 509
- [2] Ph. Zeitoun *et al.* 2004 *Nature* **431** 426
- [3] A. D. Shiner *et al.* 2001 *Nature Phys.* **7** 464
- [4] J. Itatani *et al.* 2004 *Nature* **432** 867
- [5] S. Sukiasyan *et al.* 2009 *Phys. Rev. Lett.* **102** 223002
- [6] X. M. Tong *et al.* 2015 *Phys. Rev. A* **92** 043422
- [7] F. Lackner *et al.* *Phys. Rev. A* in press
- [8] F. Lackner *et al.* 2015 *Phys. Rev. A* **91** 023412
- [9] T. Sato *et al.* 2016 *Phys. Rev. A* **94** 023405

¹E-mail: fabian.lackner@tuwien.ac.at

²E-mail: iva.brezinova@tuwien.ac.at

Nonlinear resonant Auger spectra and transient x-ray absorption spectra in CO using an x-ray pump-control scheme

Song Bin Zhang^{* 1}, Victor Kimberg[†], and Nina Rohringer^{*}

^{*} School of Physics and Information Technology, Shaanxi Normal University, 710119 Xi'an, China

[†] Department of Theoretical Chemistry and Biology, Royal Institute of Technology, S-106 91 Stockholm, Sweden

^{*} Max Planck Institute for the Structure and Dynamics of Matter (MPSD), 22761 Hamburg, Germany

Synopsis In this work we propose nonlinear femtosecond x-ray pump-probe spectroscopy to study the vibrational dynamics of a core-excited molecular state and discuss numerical results in CO. A femtosecond pump resonantly excites the carbon core-excited $1s-1\pi^*$ state of the CO molecule. A second strong probe (control) pulse is applied at variable delay and is resonantly coupled to a valence excited state of the molecule (Fig. 1). The strong nonlinear coupling of the control pulse induces Rabi flopping between the two electronic states. During this process, a vibrational wave packet in the core-excited state is created, which can be effectively manipulated by changing the time delay between pump and control pulses. We present an analysis of the resonant Auger electron spectrum (Fig. 2) and the transient absorption or emission spectrum (Fig. 3) on the pump transition and discuss their information content for reconstruction of the vibrational wave packet [1].

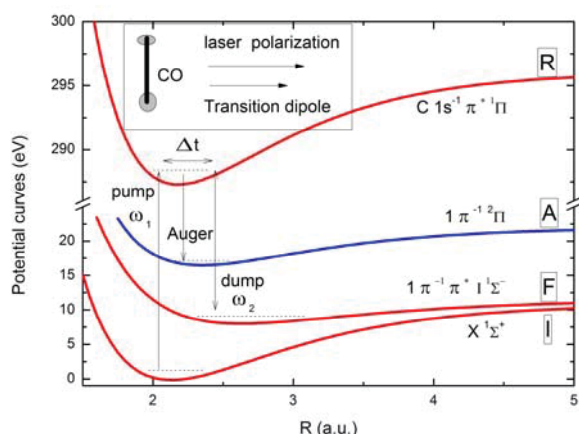


FIG. 1. Potential-energy curves for the four involved electronic states and the schematics of the present pump-probe scheme. The optical nonlinear interaction is caused by the strong probe (control) pulse on the transition between states R and F.

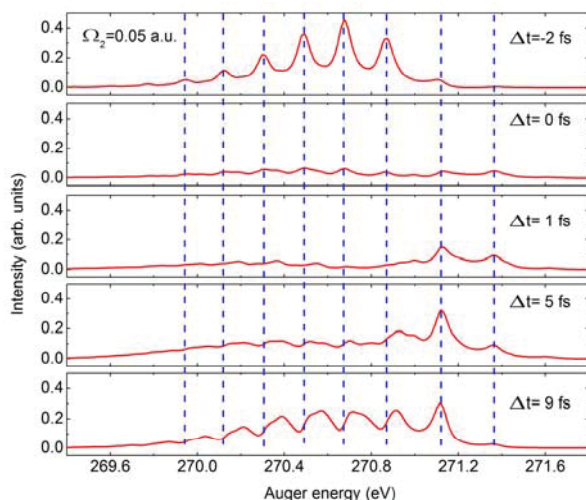


Fig. 2. The resonant Auger spectra for different Δt for a strong control pulse of $\omega_2 = 277.6$ eV and $\Omega_2 = 0.05$ a.u.

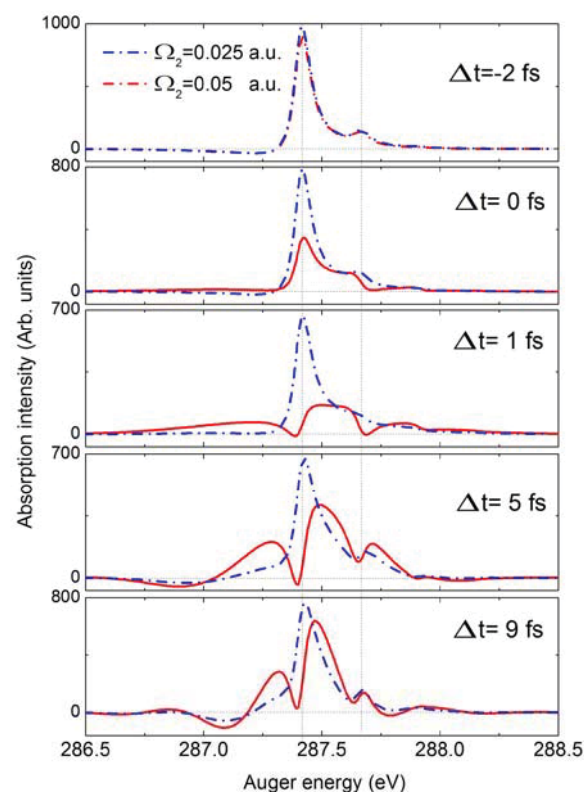


Fig. 3. X-ray transient absorption or emission spectra of CO for the pump field around 287.4 eV. Shown is a comparison for weak and strong control pulses. The absorption or emission peaks for the case of $\Delta t = -2$ fs are labeled as vertical dashed lines.

References

- [1] S. B. Zhang, V. Kimberg, and N. Rohringer, Phys. Rev. A **94**, 063413 (2016)

¹ E-mail: song-bin.zhang@snnu.edu.cn

Electron impact ionization of molecules and clusters

Alexander Dorn¹, Enliang Wang, Xueguang Ren

Max Planck Institute for Nuclear Physics, 69117 Heidelberg, Germany

Synopsis Kinematically complete (e,2e) experiments with coincident detection of the residual ion are performed on atomic and molecular targets (Ar, H₂O, tetrahydrofuran C₄H₈O). Data for the isolated target species are compared to those of small clusters in order to see the influence of the environment on the ionizing reactions. We observe the modification of fragmentation pathways due to the proximity of neighbors. We also observe energy transfer mechanisms like intermolecular coulombic decay (ICD) not only in van der Waals clusters but also in hydrated biomolecule clusters.

It is well known that primary ionizing radiation penetrating biological tissue produces large numbers of low-energy secondary electrons which effectively induce damages to the biological material. In order to understand the underlying reactions electron collisions with biomolecules are regularly studied in the gas phase, e.g. in kinematically complete (e,2e) experiments [1] or in experiments using mass spectrometers [2].

Here we combine both techniques by using a reaction microscope where the momentum vectors of two outgoing electrons (energies E_1 and E_2) are detected in coincidence with the residual ion. This enables, e.g., to correlate the ionized electron orbital (according to the measured binding energy) and the subsequent fragmentation pathway. A first demonstration was done for tetrahydrofuran (THF, C₄H₈O, see Figure 1) which is a surrogate for the sugar in the DNA backbone at $E_0 = 27$ eV impact energy [3]. Furthermore, we were interested in how the ionization and fragmentation dynamics of a monomer is modified if neighbors are present as in the aqueous environment in biological tissue. Thus, studies were extended to pure THF clusters and hydrated clusters produced in a supersonic gas jet.

Interestingly, we see a destabilizing effect of the environment as it is illustrated in Figure 1 where the binding energy (BE) of the ionized electron is shown for different residual ion species. For ionization of the HOMO orbital ($BE = 10$ eV) in the THF monomer the molecule stays intact leading to the parent ion (full squares). For the ring breaking reaction leading to C₂H₄O⁺ an inner orbital is ionized (HOMO-4,5) with BE around 13 eV (open squares). The required energy for this ring breaking reaction is strongly reduced for the dimers. For ionization of the hydrated dimer (H₂O)THF to 10.5 eV (open circles) and for the THF₂ dimer to 10 eV (open diamonds). In both cases no stable parent

ions are observed. From that and the binding energies we conclude that in the clusters HOMO ionization leads to ring breaking and not to the stable parent ion as in the monomer.

Furthermore, in hydrated THF clusters we observe intermolecular coulombic decay (ICD) reactions as it was observed before in pure water dimers [4]. Here energy from the water molecule ionized in the inner valence shell is transferred to THF ionizing it and leading to coulomb explosion. ICD is identified according to the projectile energy loss, the kinetic energy release of the ions and the low energy ICD electrons.

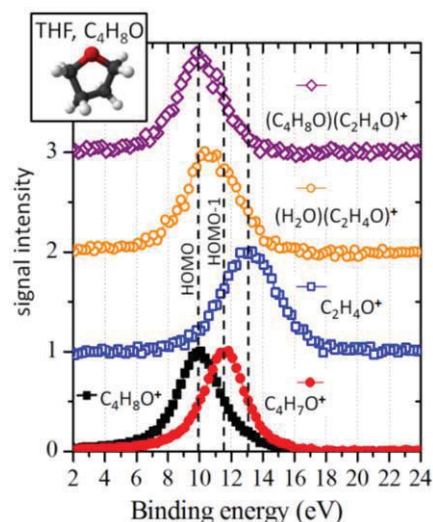


Figure 1. Binding energy spectra ($BE = E_0 - E_1 - E_2$) for ionization of THF monomers (three bottom curves) hydrated THF (second curve from top) and THF dimers (top curve) and fragmentation into the ion species given in the diagram.

References

- [1] D. B. Jones *et al* 2016 *J. Chem. Phys* 145, 164306
- [2] M. Dampc *et al* 2011 *J. Phys. B* 44, 055206
- [3] X. Ren *et al* 2014 *J. Chem Phys* 141, 134314
- [4] T. Jahnke *et al*, 2010 *Nat. Phys.* 6, 139
- [5] X. Ren *et al* 2016 *Nat. Commun.* 7 11093

¹ E-mail: Alexander.Dorn@mpi-k.de

Reactive collisions of electrons with molecular cations: multichannel fragmentation dynamics via super-excited states

J. Zs. Mezei^{a,b,c,d}, F. Colboc^a, Y. Moulane^{a,e}, D. A. Little^f, M. D. Epée Epée^g, S. Niyonzima^h, N. Popⁱ, D. O. Kashinski^j, K. Chakrabarti^k, O. Motapon^{g,l}, V. Laporta^{a,f,m}, R. Celiberto^{m,n}, D. Talbi^o, A. P. Hickman^p, J. Robert^c, O. Dulieu^c, X. Urbain^q, A. Wolf^r, J. Tennyson^f, I. F. Schneider^{a,c,1}

^a Laboratoire Ondes et Milieux Complexes UMR6294, Université du Havre, Normandie Université, France

^b Laboratoire des Sciences des Procédés et des Matériaux UPR3407, Université Paris 13, Villetaneuse, France

^c Laboratoire Aimé Cotton UMR9188 Université Paris-Sud/ENS Cachan, Orsay, France

^d Institute for Nuclear Research, Hungarian Academy of Sciences, Debrecen, Hungary

^e Oukaimeden Observatory, High Energy Physics and Astrophysics Lab., Cadi Ayyad University, Marrakech, Morocco

^f Department of Physics and Astronomy, University College London, UK

^g Faculty of Sciences, University of Douala, Cameroon

^h Faculté des Sciences, Université du Burundi, Bujumbura, Burundi

ⁱ Politehnica University of Timisoara, Fundamental of Physics for Engineers Department, Timisoara, Romania

^j Department of Physics and Nuclear Engineering, US Military Academy, West Point, NY, USA

^k Department of Mathematics, Scottish Church College, University of Calcutta, India

^l University of Maroua, Faculty of Science, Maroua, Cameroon

^m Istituto di Nanotecnologia, CNR, Bari, Italy

ⁿ Dipartimento di Ingegneria Civile, Ambientale, del Territorio, Edile e di Chimica, Politecnico di Bari, 70125 Bari, Italy

^o Laboratoire Univers et Particules de Montpellier, CNRS, Université de Montpellier, France

^p Department of Physics, Lehigh University, PA, USA

^q Institute of Condensed Matter and Nanosciences, Université Catholique de Louvain, Belgium

^r Max-Planck-Institut für Kernphysik, Stored and cooled ions division, Heidelberg, Germany

Synopsis The major mechanisms governing the dynamics of electron-driven reactions of molecular cations will be illustrated.

Electron-impact dissociative recombination, dissociative excitation (1) and ro-vibrational (de)excitation (2) of molecular cations:



occur in various ionized media of astrophysical, energetical and industrial interest [1].

These collisions are representative for a number of outstanding features: high reactivity, involvement of super-excited molecular states undergoing pre-dissociation and autoionization, and strong resonant character. Consequently, they are subject to beyond-Born-Oppenheimer theoretical approaches, and often require quasi-diabatic rather than adiabatic representations of the molecular states as well as particularly sophisticated methods for modeling the collisional dynamics, able to manage superposition of many continua and infinite series of Rydberg states.

We therefore use Multichannel Quantum Defect Theory (MQDT), capable to account the strong mixing between ionization and dissociative channels, open - direct mechanism - and closed - indirect mechanism, via capture into prominent Rydberg resonances [2, 3, 4, 5]. These features will be illustrated for H_2^+ [6], H_3^+ [7], BeH^+ [8], N_2^+ [9], BF^+ , NO^+ ,

CO^+ , SH^+ , CH^+ and ArH^+ , and the comparison of the theoretical data with the experimental ones - obtained in storage rings and flowing afterglows - will be given.

Perspectives on the advancement in the theoretical treatment - addressing polyatomic systems, predicting branching ratios, using time-dependent methods - and in the applications - ionic propulsion, industrial plasmas, novel laser devices, accurate astrophysical kinetical modeling - will be outlined.

References

- [1] I. F. Schneider, O. Dulieu, and J. Robert (editors) 2015 *Eur. Phys. J. Web of Conf.* **84**
- [2] Ch. Jungen 2011 in *Handbook of High-resolution Spectroscopy*, edited by M. Quack and F. Merkt (Wiley & Sons, New York) p.471
- [3] A. Giusti 1980 *J. Phys. B: At. Mol. Phys.* **13** 3867
- [4] F. O. Waffeu Tamo *et al.* 2011 *Phys. Rev. A* **84** 022710
- [5] K. Chakrabarti *et al.* 2013 *Phys. Rev. A* **87** 022702
- [6] O. Motapon *et al.* 2014 *Phys. Rev. A* **90** 012706
- [7] I. F. Schneider *et al.* 2012 *Phys. Rev. A* **86**, 062706
- [8] V. Laporta *et al.* 2017 *Pl. Phys. C. Fus.* **59** 045008
- [9] D. A. Little *et al.* 2014 *Phys. Rev. A* **90**, 052705

¹E-mail: ioan.schneider@univ-lehavre.fr

Resonant anion states of radiosensitizers

F. Kossoski^{*1}, J. Kopyra[‡], H. Aboul-Carime[§], M. A. P. Lima^{*}, M. T. do N. Varella[†]

^{*} Instituto de Física “Gleb Wataghin”, Universidade Estadual de Campinas, Campinas, Brazil

[‡] Chemistry Department, Siedlice University, Siedlice, Poland

[§] Institut de Physique Nucléaire de Lyon, Université de Lyon, Lyon, France

[†] Instituto de Física, Universidade de São Paulo, São Paulo, Brazil

Synopsis We present ongoing research concerning low-energy electron collisions with a series of potential radiosensitizers, including the 5-halouracils family, chlorinated adenine, thiolated uracil and guanine. Scattering calculations allow us to characterize the anion spectra of these compounds and to indicate possible electron-induced dissociation mechanisms. The biologically relevant fragmentation pathways should generally originate from mechanisms where long-lived π^* resonances are formed, and diabatic couplings to dissociative σ^* states follow.

One major strategy towards more efficient radio-therapeutic treatments lies in incorporating radiosensitizing drugs into the genetic material, which would sensitize the cell under the exposure to ionizing radiation. Some of these are currently under clinical use, while many others are under different stages of research, as there is still much to be learned about their mechanisms of action. It is now largely recognized that low-energy electrons should play a major role in starting off the damaging process [1]. These species efficiently induce dissociative electron attachment (DEA), such that the generated radicals further promote deleterious reactions to cellular DNA. However, the nascent molecular mechanisms that give rise to DEA and ultimately to their enhanced radiosensitivity remain under intense investigation.

Here we present recent theoretical results on the interaction of low-energy electrons with a series of modified nucleobases. In Fig. 1 the elastic integral cross sections for 5-chlorouracil [2], 2-thiouracil [3], 2-chloroadenine [4] and 6-thioguanine are shown, as computed by the Schwinger multichannel method. Overall, the anion spectra of these compounds comprise delocalized π^* resonances and dissociative σ^* states. Our results support that π^*/σ^* couplings should account for most of the fragmentation pathways observed below the excitation threshold.

For the well-known 5-halouracils [2, 5], we have shed some light into details of the underlying DEA mechanisms that give rise to halide and neutral hydrogen elimination. Besides the more familiar case of halogenated pyrimidines, purines also decomposes under the action of low-energy electrons, as we have demonstrated for 2-chloroadenine [4]. Moreover, we have found that the very rich anion spectra of 2-thiouracil [3] can promote complex rearrangement reactions at surprisingly low energies. Calculations for 6-thioguanine also suggests that π^*/σ^* couplings might account for DEA, indicating that thiolated

purines could likewise act as a potential radiosensitizers. As a whole, our results should be able to point out desired molecular features that make for a good radiosensitizer.

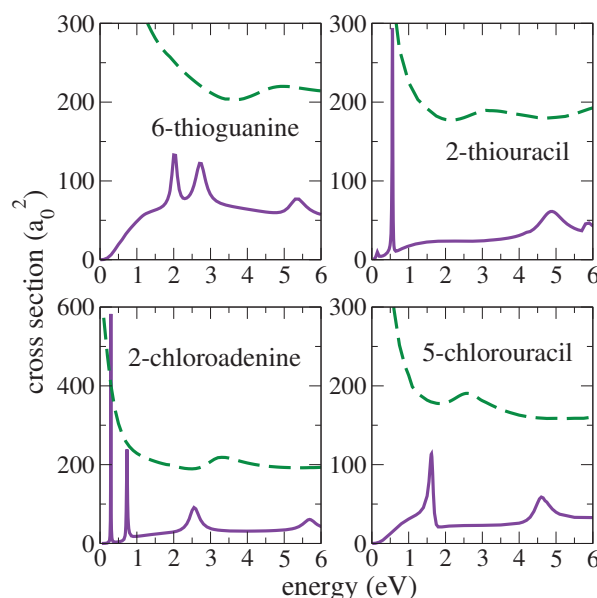


Figure 1. A' (green) and A'' (violet) components for the elastic integral cross section for electron scattering from a series of potential radiosensitizers.

The authors acknowledge financial support from Brazilian agencies FAPESP and CNPq.

References

- [1] B. Boudaïffa *et al.* 2000, *Science* **287** 1658
- [2] F. Kossoski *et al.* 2014, *J. Chem. Phys.* **140** 024317
- [3] J. Kopyra *et al.* 2014 *Phys. Chem. Chem. Phys.* **16** 25054
- [4] F. Kossoski *et al.* 2015 *Phys. Chem. Chem. Phys.* **17** 28958
- [5] F. Kossoski and M. T. do N. Varella 2015 *Phys. Chem. Chem. Phys.* **17** 17271

¹E-mail: fabris@if.usp.br

Evaluated electron scattering cross sections from furfural molecules for modelling particle transport in the energy range 0-10000 eV

A. Traore*, L. Ellis-Gibblings*, A. Lozano*, A. Roldán†, F. Blanco‡, D. Jones§, F. Ferreira da Silva¶, P. Limão-Vieira¶, M. Brunger§ and G. García*¹

* Instituto de Física Fundamental, Consejo Superior de Investigaciones Científicas, 28006 Madrid, Spain

† Centro de Investigaciones Energéticas Medioambientales y Tecnológicas, 28040 Madrid, Spain

‡ Facultad de Ciencias Físicas, Universidad Complutense de Madrid, 28040 Madrid, Spain

¶ Laboratório de Colisões Atômicas e Moleculares, CEFITEC, Departamento de Física, Faculdade de Ciências e Tecnologia, Universidade NOVA de Lisboa, 2829-516 Caparica, Portugal

§ School of Chemical and Physical Sciences, Flinders University, Adelaide SA 5001, Australia

Synopsis An evaluated set of electron scattering cross section data from furfural molecules is presented for incident energies ranging from 0.1 to 10000 eV. This comprises previous theoretical and experimental data, new calculations including interference effects and new total cross section measurements we performed for benchmarking purposes. Present scattering data is used for modelling electron transport in furfural and the influence of the input cross section values on the simulated track structure is discussed. Special attention was paid to evaluate low energy differential scattering cross section by comparing the predictions of the model with the transmission of 0-10 eV electrons through furfural under strong field confinement conditions.

There is an increasing interest in developing new technologies related to using biofuels and other biomaterials as alternative energy sources. Recently, furfural has been postulated as a precursor biofuel and several electron scattering studies have been carried out to determine relevant interaction cross section data (see Ref. [1] and references therein). We present in this study an evaluated data compilation including new differential and integral electron scattering calculations we have carried out with our improved IAM-SCAR method, accounting for interference terms [2], in the energy range 0.1-10000 eV. Recent electron scattering total cross section measurements [3] have been used to benchmark this calculation.

Energy loss spectra have also been measured for incident energies within 50 and 5000 eV with an energy resolved transmission beam apparatus operating at a constant energy resolution of 500 meV. Below 50 eV we used the spectra previously measured with a crossed beam apparatus in the range 20-40 eV with a typical energy resolution of 80 meV and for scattering angles between 10° and 90° [4].

The Low Energy Particle Track Simulation (LEPTS) code [5] has been used to simulate single electron tracks of 10 keV electron in liquid furfural. Electron scattering cross sections for single molecules have been corrected to account for the overlap of surrounding molecules

in the liquid phase according to the procedure described in Ref. [3]. Representative parameters, as the electron stopping powers and ranges, have been derived from the simulation and compared with available information. Dependence of these parameters on the input data, cross section and energy loss distribution functions, are analyzed and discussed in order to estimate the uncertainty limits of the simulated values.

In order to check the reliability of calculated DCS at low energies, where dipole interactions are dominant, we have simulated the transmission of low energy electrons (0-20 eV) through a low-pressure furfural gas under a strong axial magnetic field (0.05 T) confinement and compared with the observed transmission spectra. In these conditions, scattering angles are converted into energy loss in the forward direction being thus quantified by a retarding field energy analyzer.

References

- [1] R. F. da Costa *et al.* 2016 *J. Chem. Phys.* **144** 124310
- [2] F. Blanco and G. García 2016 *Chem. Phys. Lett.* **645** 71
- [3] A. Traore *et al.* 2016 *Phys. Rev. A* (to be submitted)
- [4] D. B. Jones *et al.* 2016 *J. Chem. Phys.* **144** 124309
- [5] F. Blanco *et al.* 2013 *Eur. Phys. J.* **67** 199

E-mail: g.garcia@csic.es

Dipolar quantum gases and liquids

Tilman Pfau* ¹

* 5. Physikalisches Institut and Center for Integrated Quantum Science and Technology (IQST),
Universität Stuttgart, Germany

Synopsis We review the physics and recent developments of magnetic dipolar quantum gases like Chromium or the Lanthanides and discuss the recent discovery of a dilute quantum liquid, which is forming stable self-bound droplets.

Dipolar interactions are fundamentally different from the usual van der Waals forces in real gases. Besides the anisotropy the dipolar interaction is nonlocal and as such allows for self organized structure formation. Candidates for dipolar species are polar molecules, Rydberg atoms and magnetic atoms. More than ten years ago the first dipolar effects in a quantum gas were observed in an ultracold Chromium gas. By the use of a Feshbach resonance a purely dipolar quantum gas was observed three years after [1]. By now dipolar interaction effects have been observed in lattices and also for polar molecules. Recently it became possible to study degenerate gases of lanthanide atoms among which one finds the most magnetic atoms. The recent observation of their collisional properties includes the emergence of quantum chaos and very broad resonances [2,3]. Similar to the Rosensweig instability in classical magnetic ferrofluids self-organized structure formation was expected. In our experiments with quantum gases of Dysprosium atoms we could recently observe the formation of a droplet crystal [4]. In contrast to theoretical mean field based predictions the superfluid droplets did not collapse. We find that this unexpected stability is due to beyond meanfield quantum corrections of the Lee-Huang-Yang type [5,6]. We observe and study self-bound droplets [7] which can interfere with each other. These droplets are 100 million times less dense than liquid helium droplets and open new perspectives as a truly isolated quantum system.

References

- [1] T. Lahaye, C. Menotti, L. Santos, M. Lewenstein, and T. Pfau, "The physics of dipolar bosonic quantum gases", *Rep. Prog. Phys.* **72**, 126401 (2009)
- [2] T. Maier, I. Ferrier-Barbut, H. Kadau, M. Schmitt, M. Wenzel, C. Wink, T. Pfau, K. Jachymski, P. S. Julienne, "Broad Feshbach resonances in collisions of ultracold Dysprosium atoms", *Phys. Rev. A* **92**, 060702(R) (2015)
- [3] T. Maier, H. Kadau, M. Schmitt, M. Wenzel, I. Ferrier-Barbut, T. Pfau, A. Frisch, S. Baier, K. Aikawa, L. Chomaz, M. J. Mark, F. Ferlaino, C. Makrides, E. Tiesinga, A. Petrov, S. Kotochigova, "Emergence of chaotic scattering in ultracold Er and Dy", *Phys. Rev. X* **5**, 041029 (2015)
- [4] H. Kadau, M. Schmitt, M. Wenzel, C. Wink, T. Maier, I. Ferrier-Barbut, T. Pfau, "Observing the Rosensweig instability of a quantum ferrofluid", *Nature* **530**, 194 (2016)
- [5] T. D. Lee, K. Huang, and C. N. Yang, "Eigenvalues and Eigenfunctions of a Bose System of Hard Spheres and Its Low-Temperature Properties", *Phys. Rev.* **106**, 1135 (1957). D.S. Petrov, "Quantum mechanical stabilization of a collapsing Bose-Bose mixture", *Phys. Rev. Lett.* **115**, 155302 (2015).
- [6] I. Ferrier-Barbut, H. Kadau, M. Schmitt, M. Wenzel, T. Pfau, "Observation of quantum droplets in a strongly dipolar Bose gas", *Phys. Rev. Lett.* **116**, 215301 (2016)
- [7] M. Schmitt, M. Wenzel, F. Böttcher, I. Ferrier-Barbut, and T. Pfau, "Self-bound droplets of a dilute magnetic quantum liquid", *Nature* **539**, 259 (2016)

¹ E-mail: t.pfau@physik.uni-stuttgart.de

Ion and photon interactions with trapped biomolecular ions

Thomas Schlathölter

Zernike Institute for Advanced Materials, University of Groningen, 9747AG Groningen, The Netherlands

Synopsis Energetic interactions involving complex biomolecular systems play a key role in fields such as radiotherapy, astrobiology, mass spectrometry and comparison to high level theory. For a long time, such studies were limited to biomolecular building blocks (amino acids and DNA bases), for which targets can be produced in a straightforward way. The combination of electrospray ionization and radio frequency ion trapping is a novel experimental approach that allows to experimentally investigate systems of virtually unlimited complexity.

Investigating the response of complex biological molecules upon interaction with energetic photons or keV ions is a very powerful approach to address the molecules' chemical and electronic structure and dynamics. To investigate such processes in the gas phase, we employ a combination of electrospray ionization (ESI) and radiofrequency (RF) ion guiding and trapping.

For instance, soft X-ray photoionization of the protonated peptide leucine enkephalin (555 amu, 5 amino acid residues) leads almost exclusively to extensive fragmentation dominated by loss of small amino acid sidechains [1]. The underlying process is likely due to fast dissociation through repulsive states, before internal vibrational redistribution (IVR) of the excitation energy. In contrast, for large proteins such as multiply protonated cytochrome c (~12 kDa, 104 residues) mainly non-dissociative single and double ionization is observed [2]. Due to the much larger heat capacity, photoabsorption only leads to small increase in internal temperature. Nevertheless, fast dissociation is never fully suppressed, even in the largest proteins under study. Very similar results are observed in keV ion collisions with protonated proteins/peptides [3]

The transition between both size and temperature regimes is gradual, with a co-existence of backbone scission, sidechain loss and non-dissociative ionization for intermediate size systems with a few kDa mass [4]. Rather than varying protein size, a variable photoabsorption-induced increase of internal temperature can be reached by variation of the number of absorbed photons. To this end, we have used the XUV/soft X-ray free electron laser FLASH to investigate photofragmentation of ubiquitin ions in intense 90 eV / 70 fs pulses as a func-

tion of intensity [5]. With increasing intensity, sidechain fragment yields increase linearly while backbone scission remains negligible. Ionization clearly triggers a localized molecular response that occurs before the excitation energy equilibrates. Consistent with this interpretation, the effect is barely affected by the initial charge state of the ubiquitin. The fragmentation patterns of sixfold deprotonated and tenfold protonated ubiquitin turn out to be very similar. Ubiquitin thus responds to EUV multiphoton ionization as an ensemble of small peptides.

In the context of radiotherapy, interactions of energetic photons with DNA are of fundamental relevance. In biological environments, DNA is present in multiply deprotonated form. We have recently investigated soft X-ray and VUV photoabsorption in multiply deprotonated gas-phase oligonucleotides that contain the human telomere sequence TTAGGG. First results indicate that although electron detachment is the dominating process for these systems, single strand breaks preferentially involve the GGG region. The telomere sequence seems to act like a hole trap, as recently predicted theoretically [6].

References

- [1] O. Gonzalez-Magaña et al., J. Phys. Chem. A, 116 (2012) 10745
- [2] A. R. Milosavljević et al., J. Phys. Chem. Lett., 3 (2012) 1191
- [3] S. Bari et al., Phys. Chem. Chem. Phys., 12 (2010) 3376 ; S. Martin et al., Phys. Rev. A 89 (2014) 012707
- [4] D. Egorov, et al., Phys. Chem. Chem. Phys., 18 (2016) 26213
- [5] T. Schlathölter, et al., Angew. Chem. Int. Ed., 55 (2016) 10741
- [6] E. Cauët, J. Biomol. Struct. & Dyn., 12 (2011) 557

Error! Reference source not

found. E-mail: t.a.schlatholter@rug.nl

Excitation, fragmentation and radiative decay of molecules studied with fast ion beams

L. Chen¹, J. Bernard, R. Brédy, S. Martin

Institut Lumière Matière, UMR5306,
Université Claude Bernard Lyon 1- CNRS,
Université de Lyon,
69622 Villeurbanne cedex, France

Charged atomic and molecular ions A^{q+} accelerated to about $1 \times q$ keV to $30 \times q$ keV provide a powerful tool for studying the fragmentation and relaxation of isolated molecules. In this report, we recall three types of experiments developed in our group in the past years: a multi-coincidence detection setup to study the fragmentation dynamics of multicharged C_{60} in collisions with highly charged ions; a collision chamber to study the collision induced dissociation of molecules under energy control, in collisions between singly charged ions and molecular targets; a small electrostatic storage ring (Mini-Ring) to study the cooling of charged molecules prepared in an electron cyclotron resonance (ECR) ion source.

A highly charged atomic ion for example Xe^{25+} accelerated to 100 keV offers a strong electric field of a point charge, which moves very fast in the space ($v \approx 0.18$ a.u.). Depending on the impact parameter, such an ion can capture several electrons from a neutral isolated target, for example C_{60} , leading to the formation of multicharged molecules C_{60}^{r+} . By coincidence analyses of the scattered projectile, the number of ejected electrons and all charged fragments resulting from the fragmentation of the target, we have studied the dissociation dynamics of C_{60}^{r+} ($r \leq 9$) as a function of the charge [1].

Using a singly charged projectile ion A^+ colliding on a molecular target M , two-electron capture process may lead to the formation of scattered anion, $A^+ + M \rightarrow A^- + M^{2+}$. By analyzing the kinetic energy loss of the anion and measuring in coincidence the target fragments, we have studied the fragmentation dynamics of doubly charged molecules as a function of the excitation energy deposited in the target during

the collision [2]. With this method, called CIDECE (Collision Induced Dissociation under Energy Control), we have studied the dissociation of doubly charged C_{60} , C_{70} , 2-Deoxy-D-Ribose, Adenine, Anthracene, HDO, $W(CO)_6$ and Porphyrine.

The above experiments are dedicated to study fast fragmentation processes (in the μs time scale) resulting from excitation of the molecular targets induced in collisions with fast atomic ions. In another type of experiments, the studied molecules were ionized and excited directly in an ECR source and accelerated to several keV. The fast molecular ions were injected into an electrostatic ring, the Mini-Ring. To study the cooling of the molecules, the evolution of the internal energy distribution of the stored population was probed with laser-induced dissociation. When a dissociation event occurs in the ring, the fast neutral fragment could fly along one of the six straight lines of the Mini-Ring, escape from the ring and be detected with good efficiency. Using this setup, we have studied the slow radiative decay of several molecules of the PAH family (Naphthalene, Anthracene, Pyrene...) in a time range up to several milliseconds [3].

References:

- [1] S.Martin, L.Chen, J.Bernard, R.Brédy and J.Désésquelles *Phys.Rev. A* 66, (2002), 063201
- [2] L. Chen, S. Martin, J. Bernard and R. Brédy *Phys. Rev. Lett.* 98, 193401 (2007)
- [3] S. Martin, J. Bernard, R. Brédy, B. Concina, C. Joblin, M. Ji, C. Ortega and L. Chen, *Phys. Rev. Letters*, 110, 063003 (2013)

¹E-mail: chen@univ-lyon1.fr

Machine-learning the best potential surfaces for polyatomic molecules and the error bars for non-adiabatic atomic collisions

Daniel Vieira, Rodrigo Vargas and Roman Krems¹

Department of Chemistry, University of British Columbia, Vancouver, BC V6T 1Z1, Canada

We will present the application of kernel methods of machine learning to two problems in atomic and molecular physics.

Problem I:

The accuracy of quantum calculations of collision rates for atoms and molecules is limited by the inherent uncertainty of underlying potential energy surfaces. It is often difficult to assess the errors stemming from this uncertainty. This is particularly true for non-adiabatic collision processes that are determined by multiple interaction potentials. In the present work, we introduce a machine-learning technique based on Gaussian process regression for computing the error bars of collision rates corresponding to simultaneous variations of multiple adiabatic interaction potentials within the uncertainty of quantum chemistry calculations [1]. We show that the method can be used to obtain the sensitivity of the collision observables to individual electronic potentials [2]. This illustrates how machine learning can provide information on the mechanisms of electronic transitions.

Problem II:

Constructing accurate potential energy surfaces for polyatomic molecules is a major challenge. For a molecule with a large number of degrees of freedom, the difficulty arises both from the large num-

ber of ab initio computations required and from the uncertainty as to where in the configuration space to place the ab initio points in order to obtain the most accurate representation of the surface. We will show that both of these problems can be addressed with a machine-learning technique based on Gaussian processes. We will first show that Gaussian process regression yields a qualitatively good representation of the surface with a rather small number of ab initio points (~ 200 for a 6D surface) [3]. We will then illustrate the application of Bayesian optimization with Gaussian processes as an efficient method for sampling the configuration space of polyatomic molecules. Bayesian optimization is based on an iterative procedure, where, at each iteration, the surface is constructed by Gaussian process regression and a small set of ab initio points is added in the part of space determined by maximizing the so-called acquisition function. The acquisition function quantifies the improvement of the accuracy of the potential energy surface thus obtained.

References

- [1] J. Cui and R. V. Krems, *Phys. Rev. Lett.* **115**, 073202 (2015)
- [2] D. Vieira and R. V. Krems, *Astrophys. J.* **835**, 255 (2017).
- [3] J. Cui and R. V. Krems, *J. Phys. B* **49**, 224001 (2016).

¹E-mail: rkrems@chem.ubc.ca

Tunneling ionization imaging of photoexcitation of NO by ultrafast laser pulses

Tomoyuki Endo^{*1}, Akitaka Matsuda[†], Mizuho Fushitani[‡], Tomokazu Yasuike[‡], Oleg I. Tolstikhin[§],
Toru Morishita[¶], Akiyoshi Hishikawa^{†&2}

^{*} INRS-EMT, Varennes, Québec J3X 1S2, Canada

[†] Department of Chemistry, Graduate School of Science, Nagoya University, Nagoya 464-8602, Japan

[‡] The Open University of Japan, Mihama, Chiba 261-8586, Japan

[§] Moscow Institute of Physics and Technology, Dolgoprudny 141700, Russia

[¶] Institute for Advanced Science, The University of Electro-Communications, Chofu, Tokyo 182-8585, Japan

[&] Research Center for Materials Science, Nagoya University, Nagoya 464-8602, Japan

Synopsis Tunneling ionization imaging of photoexcitation of NO has been demonstrated by using ultrafast intense laser pulses (8 fs, 800 nm, 1.1×10^{14} W/cm²). The distributions of N⁺ fragments produced by dissociative ionization of NO starting from the electronically ground ($X^2\Pi$) and excited ($A^2\Sigma^+$) states are in good agreement with theoretical tunneling ionization yields based on WFAT, showing that the fragment anisotropy reflects changes in the outermost molecular orbital by photoexcitation.

Visualization of the highest occupied molecular orbitals (HOMOs) of electronically ground states has been achieved by using the fact that the tunneling ionization rate strongly depends on the molecular alignment (orientation) with respect to the laser polarization direction [1, 2]. The extension to electronically excited states is important for a real-time observation of electron dynamics during chemical reactions. Recently, we investigated the fragment distribution produced by dissociative ionization (DI) of NO, $\text{NO} \rightarrow \text{NO}^+ + e^- \rightarrow \text{N}^+ + \text{O} + e^-$, in few-cycle intense laser fields (8 fs, 1.1×10^{14} W/cm²) from the ground state ($X^2\Pi$, $2\pi^13s\sigma^0$) and the excited state ($A^2\Sigma^+$, $2\pi^03s\sigma^1$) to demonstrate the applicability of tunneling ionization imaging to the excited states [3].

The output of a Ti:Sapphire laser system (800 nm, 1 kHz) was used to obtain pump DUV pulses (226 nm) tuned to the NO A-X (0, 0) transition and probe few-cycle NIR pulses (800 nm, 8 fs) to induce DI. Those pulses with a pump-probe time delay of 150 ps were focused on the molecular beam of NO by concave mirror ($f = 75$ mm) in an ultrahigh vacuum chamber. The produced ions were accelerated to a position sensitive detector by four electrodes in a velocity map configuration. The three-dimensional momentum vector of respective ions was obtained from the position (x, y) and the arrival time (t) at the detector. To obtain the net signals from the excited state, an optical chopper (0.5 kHz) was introduced to block the pump pulse in every other shot.

The N⁺ produced by DI from the ground state ($X^2\Pi$) via the dissociative state ($c^3\Pi$) of NO⁺ show the anisotropic distribution peaked at 45° with respect to the probe laser polarization direction (Fig. 1 (a), (c)). On the other hand, the fragments produced from the excited state ($A^2\Sigma^+$) form a weak peak at 0° (Fig. 1 (b), (d)), reflecting the change in the outer-

most molecular orbital from 2π to $3s\sigma$. These results show a good agreement with theoretical calculation based on WFAT [4] under the adiabatic approximation, which naturally includes the effects of the permanent dipole of a heteronuclear diatomic molecule. The present study demonstrates a readout of the electron distribution in the excited states and the change in the distribution by photoexcitation from fragment anisotropy produced by ultrafast intense laser pulses.

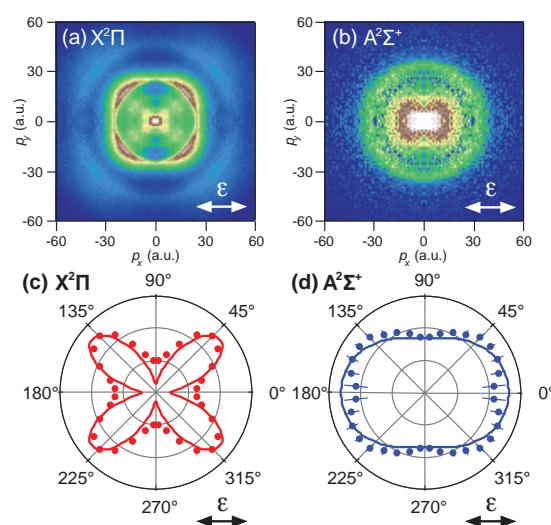


Figure 1. Momentum images of the N⁺ fragments produced by DI from (a) $X^2\Pi$ and (b) $A^2\Sigma^+$ states. Polar plots of the fragment angular distributions obtained for (c) $X^2\Pi$ and (d) $A^2\Sigma^+$ states. Solid lines are calculated by WFAT under the adiabatic approximation. The probe laser polarization direction is denoted with ϵ .

References

- [1] J. Itatani *et al.* 2004 *Nature* **432** 867
- [2] A.S. Alnaser *et al.* 2004 *Phys. Rev. Lett.* **93** 113003
- [3] T. Endo *et al.* 2016 *Phys. Rev. Lett.* **116** 163002
- [4] O. I. Tolstikhin *et al.* 2011 *Phys. Rev. A* **84** 053423

¹E-mail: tomoyuki.endo@emt.inrs.ca

²E-mail: hishi@chem.nagoya-u.ac.jp

Basic mechanisms of photon/ion induced fragmentation of molecules of biological interest

P. Bolognesi¹

CNR-ISM, Area della Ricerca di Roma 1, Via Salaria Km. 29300, 00015, Monterotondo, Italy

Synopsis The use of synchrotron radiation and photoelectron-photoion (PEPICO) coincidence techniques in gas phase experiments combined to *ab-initio* calculations provides detailed information on the photoionisation and photofragmentation mechanisms in molecules of increasing complexity. This approach has been applied to the study of radiation damage mechanisms in different classes of radiosensitisers and to develop a method to assess the energy transfer in ion collision experiments.

The tunability of synchrotron radiation and coincidence spectroscopic techniques enable a state- and sometime site-selective investigation of the energy deposition in relatively complex molecular species. Then the combination of the experimental results with *ab-initio* calculations can provide a comprehensive and highly detailed picture of the radiation induced photoionisation and photofragmentation.

This approach has been used to investigate the fundamental mechanisms of VUV induced fragmentation of two different classes of radiosensitising molecules, i.e. the halopyrimidines [1] and the three isomers of nitroimidazole [2].

fundamental role in the specific radiosensitisation during radiotherapy.

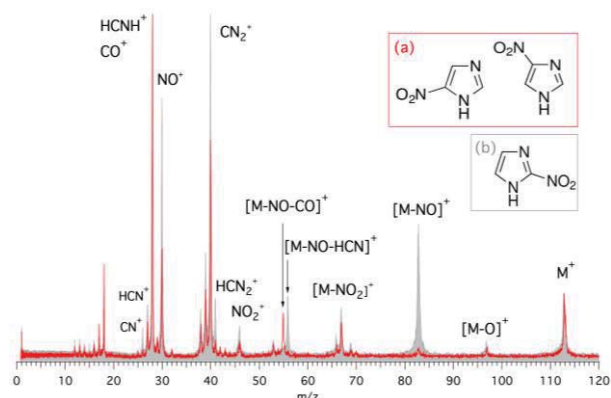


Figure 1. Mass spectra of 4(5)-nitroimidazole (red line, a) and 2-nitroimidazole molecules (gray, full, area and b) measured at 60 eV photon energy [2].

In the case of the halopyrimidines the role of the halogen atom and its position have been studied.

In the case of the three isomers of nitroimidazole the radiation-induced decomposition displays different features depending on the isomer (Figure 1). Based on DFT calculations (Figure 2), models are proposed which fully explain such differences and reveal the subtle and peculiar fragmentation mechanisms that may play a

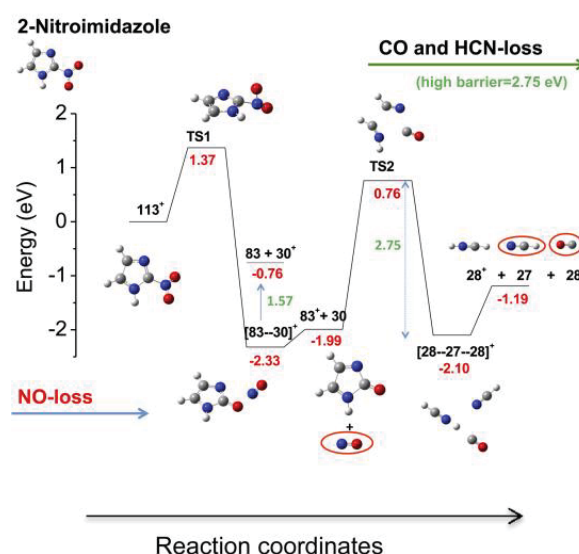


Figure 2. Potential energy profiles for 2-nitroimidazole.

In a third example it is shown how state-selected photofragmentation spectra can be used to estimate the distribution of the energy transfer in ion induced fragmentation. In collaboration with CIMAP CNRS and UAM [3], the method has been tested on thymidine

Acknowledgement. This work was partially supported by the Serbia–Italy Joint Research Project PGR220 ‘A nanoview of radiation-biomatter interaction’ and the XLIC COST Action CM1204 via the STSM program.

References

- [1] M.C. Castrovilli *et al.* 2014 *J. Am. Soc. Mass Spectrom.* **25**, 351-367.
- [2] P. Bolognesi *et al.* 2016 *J.Chem.Phys. Comm.* **145**, 191102.
- [3] S. Maclot *et al.* 2016 *Phys.Rev.Lett.* **117**, 073201

¹ E-mail: paola.bolognesi@cnr.it

Ultrafast dissociation induced by hard X-Rays

O. Travnikova^{*†}, N. Sisourat^{*◇}, K. Jänkälä[‡], T. Marchenko^{*◇}, G. Goldsztejn^{*◇}, R. Guillemin^{*◇}, L. Journel^{*◇}, D. Céolin[‡], R. Püttner[†], H. Iwayama[‡], A. F. Lago[⊗], E. Shigemasa[‡], S. Carniato^{*◇}, M. N. Piancastelli^{*◇‡} and M. Simon^{*◇‡}

^{*} CNRS, UMR 7614, Laboratoire de Chimie Physique-Matière et Rayonnement, F-75005 Paris, France

[◇] Sorbonne Universités, UPMC Univ Paris 06, UMR 7614, Laboratoire de Chimie Physique-Matière et Rayonnement, F-75005 Paris, France.

[‡] Department of Physics, University of Oulu, P. O. Box 3000, 90014 Oulu, Finland

[†] Institut für Experimentalphysik, Freie Universität Berlin, D-14195 Berlin, Germany

[‡] Synchrotron SOLEIL, l'Orme des Merisiers, Saint-Aubin, F-91192 Gif-sur-Yvette Cedex, France

[⊗] Centro de Ciências Naturais e Humanas, UFABC, 09210-170, Santo André, SP, Brazil

[‡] Department of Physics and Astronomy, Uppsala University, SE-75120 Uppsala, Sweden

[‡] Ultraviolet Synchrotron Orbital Radiation Facility, Institute for Molecular Science, Okazaki 444-8585, Japan

Synopsis Absorption of hard X-Ray photons leads to creation of deep electron vacancies, which have a very short lifetime on the order of 1 fs or below. In the case of molecules, ultrafast dissociation may take place in the course of a relaxation decay cascade, typically occurring on a timescale of few femtoseconds. This report describes a mechanism of multi-step ultrafast dissociation, using the example of HCl following Cl 1s → σ^* excitation. We demonstrate that by tuning the photon energy multi-step ultrafast dissociation can be controlled.

Creation of deep core holes leads to extensive nuclear dynamics on a few-femtosecond timescale despite the very short ($\tau \leq 1$ fs) lifetime of such states. The decay of a deep core hole is very complex, and occurs via a series of subsequent relaxation steps. Recently, we demonstrated a general multi-step ultrafast dissociation on example of HCl following Cl 1s → σ^* excitation (~ 2.8 keV). Intermediate states with one or multiple holes in the shallower core electron shells are generated in the course of the cascade decays (Fig. 1) [1]. The longer lifetime and steep potential energy surfaces of these intermediates enable the ultrafast fragmentation. Consequently, atomic-like Auger electrons are detected for the 3 possible LMM decay channels. Despite its very short lifetime, a dissociative deep-core-hole state is impetus to create the domino effect of the bond elongation in the following Auger cascades leading to abundant dissociation on a femtosecond timescale..

Furthermore, tuning hard X-ray excitation energy along Cl 1s → σ^* resonance in HCl allows *manipulating* molecular fragmentation [2]. Remarkably, the nuclear dynamics, taking place during the first hundreds of attoseconds, affects drastically the spread of the nuclear wave packets in the subsequent relaxation steps. Energy dependent atomic contributions relative to the molecular ones are observed and explained by a strong interplay between the topology of the potential energy curves, involved in the Auger-cascades, and the so-called *core-hole-clock*, which determines the time, spent by the system in the very first step [3].

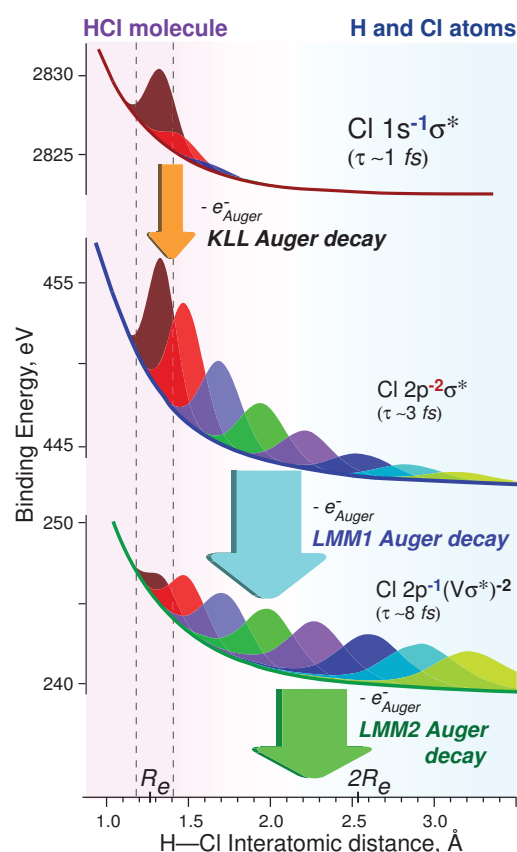


Figure 1. Schematic representing KLL Auger decay cascade in HCl. Wave-function distributions after x-ray photon absorption are shown in different colors with 1 fs increments.

References

- [1] O. Travnikova *et al* 2016 *Phys. Rev. Lett.* **116** 213001
- [2] O. Travnikova *et al* submitted
- [3] M.N. Piancastelli *et al* 2014 *J. Phys. B* **47** 124031

[†]E-mail: oksana.travnikova@upmc.fr

Polychromatic resonant ionization of many-electron atoms

E. V. Gryzlova¹

Skobeltsyn Institute of Nuclear Physics, Lomonosov Moscow State University, Moscow 119991, Russia

Synopsis Coherent control of the photoelectron angular distribution in bichromatic ionization of neon is studied, thereby providing a method to determine the relative phase of amplitudes for different ionization channels. A fundamental problem of phase variation between one- and two-photon ionization amplitudes in the cases of isolated and doublet intermediate resonance(s) is investigated.

The study of quantum interference is a powerful tool to demonstrate fundamental principles of quantum mechanics as well as to disclose the structure and dynamics of atoms, molecules, and clusters. When angle-differential parameters, e.g., photoelectron angular distributions (PADs), are determined, the relative phases of amplitudes in the various reaction channels may be deduced.

The present research is devoted to interference of two-pathway ionization in neon irradiated by the bichromatic electromagnetic field

$$\mathbf{E}(t) = \mathbf{E}_0(t)[\cos(\omega t) + \eta \cos(2\omega t + \phi)]. \quad (1)$$

We choose the fundamental frequency ω close to the energy of the $(2p^6)^1S \rightarrow 2p^5[{}^2P]4s_{J=1}$ transition. This choice, which was inspired by a recent measurement at FERMI [1], allows for determining the relative phase of the two-photon resonant (by the fundamental) and one-photon direct (by the second harmonic) ionization channels in the important case of two overlapping fine-structure sublevels.

When both harmonics are linearly polarized, the PAD is described by four angular anisotropy parameters β_k as

$$dW/d\Omega = W_0/(4\pi) \sum_{k=1}^4 \beta_k P_k(\cos \theta). \quad (2)$$

The odd-rank Legendre polynomials $P_k(\cos \theta)$ lead to an asymmetry with respect to the plane orthogonal to the laser polarization vector. Measurements of β_1 , β_3 , and the asymmetry as function of the phase ϕ provide a way to determine the relative phase and the absolute ratio of the ionization amplitudes. It is expected that the phase of the two-photon amplitude jumps by π in the vicinity of a resonance [2]. In our case, the two fine-structure levels $2p^5[{}^2P]4s_{J=1}$ are unresolved for a pulse duration of $N \approx 100$ optical cycles, while they are resolved for $N \approx 500$.

Our particular interest is to investigate the phase dependence in the case of partially unresolved fine-

structure sublevels. Figure 1 shows the asymmetry as function of photon energy and pulse duration (in N). For short pulses the asymmetry exhibits only one extremum near the $4s$ state, while for longer pulses several much more distinct structures can be seen. The above discrete states become noticeable at 20 eV.

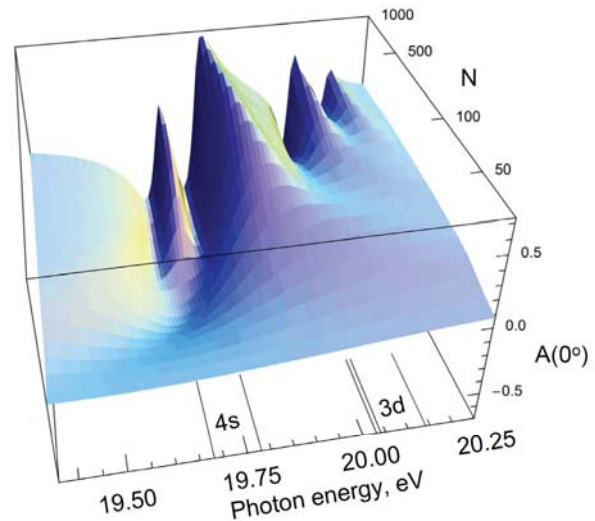


Figure 1. PAD asymmetry in the laser polarization direction as function of photon frequency and length of pulse for $\eta = 0.02215$, $\phi = 3\pi/4$, and peak intensity $I = 10^{12} \text{ W/cm}^2$

The investigation of the PAD as function of the pulse duration, accompanied by a detailed amplitude analysis, clarifies a fundamental problem of the behavior of the relative phase between the amplitudes of one- and two-photon ionization in the region of a double resonance.

The author would like to acknowledge K. Bartschat, N. Douguet, A. N. Grum-Grzhimailo, E. I. Staroselskaya, G. Sansone, K. Prince, and K. Ueda for fruitful discussions.

References

- [1] K. C. Prince *et al.* 2016 *Nature Phot.* **10** 176
- [2] J. R. Taylor 1972 *Scattering Theory: the quantum theory of nonrelativistic collisions* J. Wiley & Sons

¹E-mail: gryzlova@gmail.com

Attosecond soft x-rays in the water window

Zenghu Chang*¹

* Institute for the Frontier of Attosecond Science and Technology, CREOL and Department of Physics,
University of Central Florida, Orlando, Florida 32816, USA

Synopsis Isolated X-ray pulses as short as 53 as with photon energy extending to more than 400 eV were produced by using a mid-infrared driving laser.

Millijoule level, few-cycle, carrier-envelope phase (CEP) stable Ti:Sapphire lasers have been the workhorse for the first generation attosecond light sources for the last sixteen years [1]. The spectral range of isolated attosecond pulses with sufficient photon flux for time-resolved pump-probe experiments has been limited to extreme ultraviolet (10 to 150 eV). The shortest pulses achieved are 67 as [2]. The center wavelength of Ti:Sapphire lasers is 800 nm. It was demonstrated in 2001 that the cutoff photon energy of the high harmonic spectrum can be extended by increasing the center wavelength of the driving lasers [3].

In recent years, mJ level, two-cycle, carrier-envelope phase stabilized lasers at 1.6 to 2.1 micron have been developed by compressing pulses from Optical Parametric Amplifiers with gas-filled hollow-core fibers or by implementing Optical Parametric Chirped Pulse Amplification (OPCPA) techniques [4]. Recently, when long wavelength driving was combined with polarization gating, isolated soft x-rays in the water window (280-530 eV) were generated in our laboratory. The number of x-ray photons in the 120–400 eV range is comparable to that generated with Ti:Sapphire lasers in the 50 to 150 eV range [5]. The yield of harmonic generation depends strongly on the ellipticity of the driving fields, which is the foundation of polarization gating.

When the width of the gate was set to less than one half of the laser cycle, a soft x-ray supercontinuum was generated. The intensity of the gated x-ray spectrum is sensitive to the carrier-envelope phase of the driving laser, which indicates that single isolated attosecond pulses were generated. The ultrabroadband isolated x-ray pulses with 53 as duration were characterized by attosecond streaking measurements.

It is expected that the photon energy of the attosecond X-ray pulses can be further increased to keV by driving high harmonic generation with two-cycle, CEP stable mid-infrared lasers [6]. Such ultrabroadband light sources can be used in time-resolved X-ray absorption near edge structure measurements for studying charge migration and other electron/nuclear dynamics in molecules.

This work has been supported Army Research Office (W911NF-14-1-0383, W911NF-15-1-0336); Air Force Office of Scientific Research (FA9550-15-1-0037, FA9550-16-1-0013); the DARPA PULSE program by a grant from AMRDEC (W31P4Q1310017). This material is also based upon work supported by the National Science Foundation under Grant Number (NSF Grant Number 1506345).

References

- [1] Zenghu Chang, Paul. B. Corkum and Stephen R. Leone, 2016, *Journal of the Optical Society of America B* **33**, [1081-1097](#).
- [2] Michael Chini, Kun Zhao and Zenghu Chang, 2014, *Nature Photonics* **8**, [178 - 186](#).
- [3] B. Shan, Z. Chang, 2001, *Phys. Rev. A* **65**, [011804\(R\)](#).
- [4] Yanchun Yin, Jie Li, Xiaoming Ren, Kun Zhao, Yi Wu, Eric Cunningham, Zenghu Chang, 2016, *Optics Letters* **41**, [1142-1145](#).
- [5] Jie Li, Xiaoming Ren, Yanchun Yin, Yan Cheng, Eric Cunningham, Yi Wu, and Zenghu Chang, 2016, *Applied Physics Letters* **108**, [231102](#).
- [6] Yanchun Yin, Jie Li, Xiaoming Ren, Yang Wang, Andrew Chew, and Zenghu Chang, 2016, *Optics Express* **24**, [24989-24998](#).

¹ E-mail: Zenghu.Chang@ucf.edu

Imaging molecular bond breaking with one electron

B. Wolter¹, M. G. Pullen¹, A.-T. Le², M. Baudisch¹, K. Doblhoff-Dier³, A. Senftleben⁴, M. Hemmer^{1,5}, C. D. Schröter⁶, J. Ullrich^{6,7}, Thomas Pfeifer⁶, R. Moshhammer⁶, S. Gräfe^{8,9}, O. Vendrell^{5,10}, C.D. Lin², J Biegert^{1,11,*}

¹ICFO–Institut de Ciències Fòniques, The Barcelona Institute of Science and Technology, 08860 Castelldefels, Barcelona, Spain. ²J. R. Macdonald Laboratory, Physics Department, Kansas State University, Manhattan, KS 66506-2604, USA. ³Leiden Institute of Chemistry, Leiden University, 2300 RA Leiden, Netherlands. ⁴Universität Kassel, Institut für Physik und CINSaT, Heinrich-Plett-Str. 40, 34132 Kassel, Germany. ⁵Center for Free-Electron Laser Science, Deutsches Elektronen-Synchrotron (DESY), Centre for Ultrafast Imaging (CUI), 22607 Hamburg, Germany. ⁶Max-Planck-Institut für Kernphysik, Saupfercheckweg 1, 69117 Heidelberg, Germany. ⁷Physikalisch-Technische Bundesanstalt (PTB), Bundesallee 100, 38116 Braunschweig, Germany. ⁸Institute for Physical Chemistry, Friedrich-Schiller University Jena, 07743 Jena, Germany. ⁹Abbe Center of Photonics, Friedrich-Schiller-University Jena, 07743 Jena, Germany. ¹⁰Department of Physics and Astronomy, Aarhus University, 8000 Aarhus C, Denmark. ¹¹ICREA, Pg. Lluís Companys 23, 08010 Barcelona, Spain.

Synopsis We apply laser-induced electron diffraction to visualize bond scission in acetylene with 0.6 fs temporal and 6 pm spatial resolution.

Chemical processes are typically understood in terms of reactants and products. To understand the underlying mechanism and to possibly control them, tools are required which capture molecular dynamics in real time and real space, i.e. on the picometer spatial and femtosecond temporal scale.

An imaging technique that can simultaneously achieve the required spatial and temporal resolutions and image gas-phase molecules is laser-induced electron diffraction (LIED) [1]. Moreover, disentangling information from concurrent processes requires many capabilities that standard experimental apparatuses do not possess.

Our group developed a methodology for LIED with coincidence detection with which we could extract multiple bond lengths in acetylene molecules (C_2H_2) [2]. To apply the method to complex molecules and to image a specific reaction pathways, we utilize electron recollisions from C_2H_2 fragmentation pathways to resolve different dynamics and to capture bond scission for the first time [3].

Our experimental methodology for imaging polyatomic molecules combines a few-cycle 160-kHz, 3.1- μ m laser source with a reaction microscope (ReMi) detection system. The mid-IR radiation accelerates rescattering electrons to core-penetrating velocities while keeping the ionization fraction low. The reaction microscope permits coincident detection of fragments, and hence the identification of a specific fragmentation channel.

Selecting the deprotonation channel $C_2H_2^{++} \rightarrow H^+ + C_2H^+$ we demonstrate imaging of bond scission in real time and real space. The snapshots of the spatiotemporal structure were taken

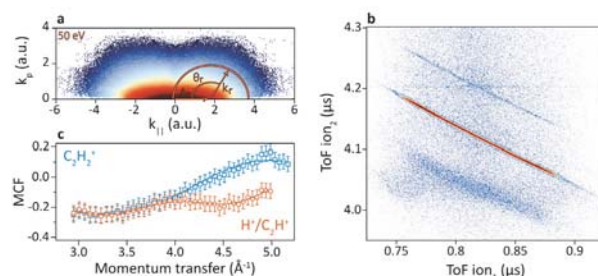


Figure 1. (a) 3D electron momentum distribution of C_2H_2 ; (b) PiPiCo of the deprotonation reaction products of C_2H_2 ; (c) molecular contrast factors (MCFs).

with an estimated 0.6-fs temporal resolution and can distinguish the different kinetic behaviours of the molecule when field-ionized parallel or perpendicular to the LIED field. Moreover, changing the orientation of the molecule, we capture different dynamics and show that the perpendicular case reveals the molecular structure in the quasi-field-free scenario for the dissociative dication.

References

- [1] T. Zuo, A. D. Bandrauk, P. B. Corkum, Chem. Phys. Lett. 259, 313–320 (1996).
- [2] M. G. Pullen et al., Nat. Commun. 6, 7262 (2015).
- [3] B. Wolter et al. Science 354, 3-8 (2016).

E-mail: jens.biegert@icfo.eu

Attosecond Physics gets Nano

M. F. Ciappina^{*1}, F. Krausz^{†,‡} and M. Lewenstein^{§,¶}

^{*} Institute of Physics of the ASCR, ELI-Beamlines project, Na Slovance 2, 182 21 Prague, Czech Republic

[†] Max-Planck-Institut für Quantenoptik, Hans-Kopfermann-Str. 1, D-85748 Garching, Germany

[‡] Fakultät für Physik, Ludwig-Maximilians-Universität München, Am Coulombwall 1, D-85748 Garching, Germany

[§] ICFO - Institut de Ciències Fotòniques, The Barcelona Institute of Science and Technology, Av. Carl Friedrich Gauss 3, 08860 Castelldefels (Barcelona), Spain

[¶] ICREA - Pg. Lluís Companys 23, 08010 Barcelona, Spain

Synopsis One of the main theoretical assumptions in the modelling of laser-matter phenomena is that the laser field is spatially homogeneous in the region where the electron dynamics takes place. When the laser field presents spatial variations at a nanometric scale, we open a new and unexplored scenario until now.

Recently two emerging areas of research, attosecond and nanoscale physics, have started to come together. Attosecond physics deals with phenomena occurring when ultrashort laser pulses, with duration on the femto- and sub-femtosecond time scales, interact with atoms, molecules or solids. The laser-induced electron dynamics occurs natively on a timescale down to a few hundred or even tens of attoseconds (1 attosecond = 1 as = 10^{-18} s), which is comparable with the optical field. For comparison, the revolution of an electron on a 1s orbital of a hydrogen atom is ~ 152 as. On the other hand, the second branch involves the manipulation and engineering of mesoscopic systems, such as solids, metals and dielectrics, with nanometric precision. Although nano-engineering is a vast and well-established research field on its own, the merger with intense laser physics is relatively recent.

We present in this Progress Report a comprehensive experimental and theoretical overview of physics that takes place when short and intense laser pulses interact with nanosystems, such as metallic and dielectric nanostructures. In particular we elucidate how the spatially inhomogeneous laser induced fields at a nanometer scale modify the laser-driven electron dynamics (see Fig. 1 for a sketch of conventional and plasmonic-enhanced strong field processes).

Consequently, this field characteristic has important impact on pivotal processes such as above-threshold ionization (ATI) and high-order harmonic generation (HHG). The deep understanding of the coupled dynamics between these spatially inhomogeneous fields and matter configures a promising way to new avenues of research and applications. Thanks to the maturity that attosecond physics has reached,

together with the tremendous advance in material engineering and manipulation techniques, the age of atto-nano physics has begun, but it is in the initial stage. We present thus some of the open questions, challenges and prospects for experimental confirmation of theoretical predictions, as well as experiments aimed at characterizing the induced fields and the unique electron dynamics initiated by them with high temporal and spatial resolution [1].

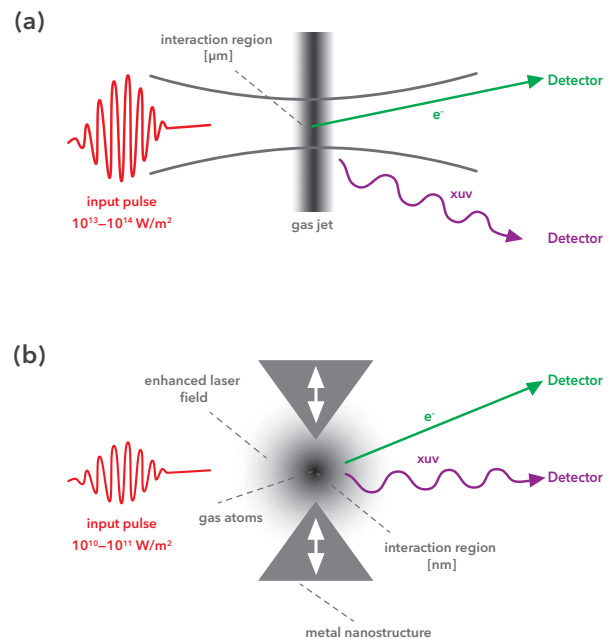


Figure 1. Sketch of conventional (a) and plasmonic-enhanced (b) strong field processes.

References

- [1] M. F. Ciappina *et al.* 2017 *Rep. Prog. Phys.* (in press)

¹E-mail: marcelo.ciappina@eli-beams.eu

Observing the ultrafast buildup of a Fano resonance

Alexander Blättermann^{* 1}, Andreas Kaldun^{*}, Veit Stooß^{*}, Stefan Donsa[†], Hui Wei[‡], Renate Pazourek[†], Stefan Nagele[†], Christian Ott^{*}, Chii-Dong Lin[‡], Joachim Burgdörfer[†] and Thomas Pfeifer^{* 2}

^{*} Max Planck Institute for Nuclear Physics, 69118 Heidelberg, Germany, EU

[†] Institute for Theoretical Physics, Vienna University of Technology, 1040 Vienna, Austria, EU

[‡] Department of Physics, Kansas State University, 66506 Manhattan KS, USA

Synopsis We report the experimental observation of the buildup of the 2s2p Fano resonance in helium, which has been under theoretical investigation for more than a decade. The emergence of the absorption line is temporally resolved by interrupting the natural decay of the excited state via saturated strong-field ionization at variable time delay.

Asymmetric Fano line shapes occur in a variety of research fields ranging from nuclear and atomic physics to condensed matter physics and photonics. Among the most well-known examples are the resonances in the extreme ultraviolet (XUV) absorption spectrum of doubly excited helium. From the early works on attosecond dynamics until today, theorists have been investigating how these spectral lines emerge and evolve after the transition is triggered and the subsequent process of autoionization takes place.

Here, we report for the first time the experimental observation of the ultrafast formation of a Fano resonance, namely the helium 2s2p spectral line via high-resolution XUV absorption spectroscopy [1]. In order to monitor the buildup of the absorption line, we apply an intense few-cycle near-infrared (NIR) laser pulse, which rapidly depletes the excited state via strong-field ionization. This in turn terminates the optical response of the atom, and therefore limits the atom's contribution to the measured absorption spectrum to a temporal gate between XUV excitation and NIR depletion. By establishing rise/fall times of the gate much shorter than the lifetime of the state, and by controlling the time delay between the XUV and NIR pulses with sub-femtosecond precision, we are able to sample the transient buildup of the 2s2p line.

A complementary study by an independent team of researchers allowed to observe the formation of the Fano resonance in the photoelectron spectrum of the very same transition, which has been reported simultaneously [2].

Figure 1 depicts the formation of the 2s2p spectral line. For small time delays, the measured spectrum is very broad since the XUV-optical response of doubly excited helium contributes only very briefly to the formation of the line. Extending the duration of the gate by increasing the NIR delay the excited atom is allowed to

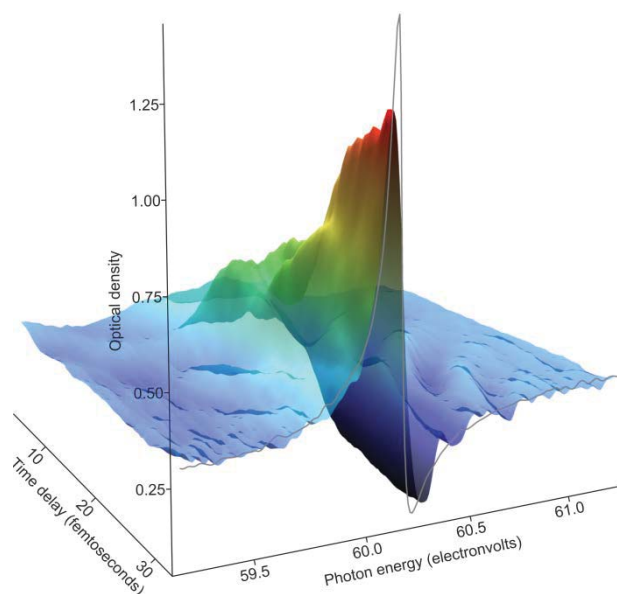


Figure 1. Experimental buildup of the 2s2p absorption line in terms of the time-resolved absorption spectrum (colored surface). The reference (gray line) was recorded with minimum NIR laser influence.

contribute to the absorption spectrum for longer and longer times, causing the resonance line to become more and more pronounced. At the maximum experimentally accessible delay of 32 fs, the observed line shape already closely resembles the natural Fano resonance line. Our measurements are compared with and confirmed by *ab-initio* calculations and an analytic theory of Fano resonances [1].

The presented method of establishing a temporal gate by excitation and laser-driven saturated ionization is also a promising technique for future studies of ultrafast phenomena, e.g. the creation of quasi particles in solids and the emergence of electron—electron or electron—internuclear correlations in molecules.

References

- [1] A. Kaldun *et al.* 2016 *Science*. [354 738](#)
- [2] V. Gruson *et al.* 2016 *Science*. [354 734](#)

¹ E-mail: blaetter@mpi-hd.mpg.de

² E-mail: thomas.pfeifer@mpi-hd.mpg.de

Attosecond Time Delay in Photoemission and Electron Scattering near Threshold

A. W. Bray^{*1}, A. S. Kheifets^{*2}, I. Bray^{†3}

^{*} Research School of Physics and Engineering, Australian National University, Canberra ACT 2601, Australia

[†] Department of Physics, Astronomy and Medical Radiation Science, Curtin University, WA 6845 Perth, Australia

Synopsis We study the time delay in the primary photoemission channel near the opening of an additional channel and compare it with the Wigner time delay in elastic scattering of the photoelectron near the corresponding inelastic threshold. The photoemission time delay near threshold is significantly enhanced, to a measurable 40 as, in comparison to the corresponding elastic scattering delay. This opens the possibility of studying threshold behaviour utilizing attosecond chronoscopy.

Attosecond time delay in atomic photoemission can provide an alternative route for observing threshold effects. The opening of a new channel corresponds to a branching point of the scattering amplitude in the complex energy plane because the number of physically available quantum states of the system changes. Hence, the behaviours present around such a branching point brings significantly richer information in comparison to any other regular energy point.

The time delay in photoemission is interpreted in terms of the Wigner time delay introduced for particle scattering in external potential [1]. It is a delay, or advance, of a particle travelling through a potential landscape in comparison with the same particle travelling in a free space. The Wigner time delay is calculated as an energy derivative of the scattering phase in a given partial wave. A similar definition is adopted in photoemission, where the time delay is related to the photoelectron group delay, and evaluated as an energy derivative of the phase of the complex ionization amplitude [2].

Here we report on the recently published work [3] where we investigated the time delay in the primary photoemission channel near the opening of an additional channel and compared it with the Wigner time delay in the elastic scattering of the photoelectron near the corresponding inelastic threshold. We do so by considering photodetachment from the H^- negative ion and comparing it with electron scattering on the hydrogen atom near the first excitation threshold. Additionally, we consider the equivalent processes on the He atom for the purpose of contrast and comparison.

Our numerical results are obtained within the convergent close-coupling (CCC) formalism [4]. In the case of He, all three calculated time delays closely approximate one another. This means that the independent electron Hartree-Fock basis represents both the scattering and ionization processes very ac-

curately and correlations are negligible. In the case of H^- , above the $n = 2$ (10.2 eV) excitation threshold, both the photodetachment and elastic scattering amplitudes experience rapid growth of their phases. However, this growth is an order of magnitude larger in photodetachment in comparison with photoelectron scattering. This results in an order of magnitude enhancement of the photoemission time delay near threshold, reaching a readily measurable $\simeq 40$ as. We attribute this large deviation between the time delay in photoemission and electron scattering to the different lowest orders of interelectron interaction mixing the ground state and excitation channels.

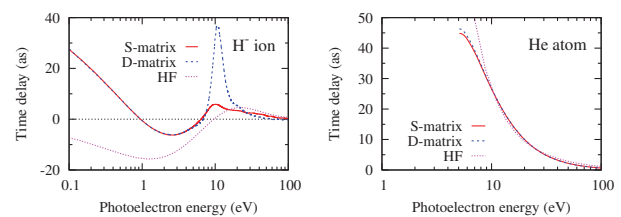


Figure 1. Left: The calculated time delay for the photodetachment of H^- labelled *D*-matrix (red), elastic scattering of an electron on H in the dipole singlet channel labelled *S*-matrix (blue), and this elastic scattering delay as calculated by a frozen core Hartree-Fock approach (cyan) [5]. Right: Equivalent, but for a He atomic target.

References

- [1] L. Eisenbud, Ph.D. thesis, Princeton University (1948)
- [2] M. Schultze *et al.*, *Science* **328**, 1658 (2010)
- [3] A. S. Kheifets, A. W. Bray, and I. Bray, *Phys. Rev. Lett.* **117**, 143202
- [4] I. Bray *et al.* *Phys. Rep.* **520**, 135 (2012)
- [5] L. V. Chernysheva, N. A. Cherepkov, and V. Radojevic, *Comp. Phys. Comm.* **18**, 87–100 (1979)

¹E-mail: Alexander.Bray@anu.edu.au

²E-mail: A.Kheifets@anu.edu.au

³E-mail: Igor.Bray@curtin.edu.au

Inelastic electron scattering from biologically important molecules and radicals

D. B. Jones,^{a,1} R. F. da Costa,^{b,c} M. T. do N. Varella,^d M. H. F. Bettega,^e M. A. P. Lima,^c F. Blanco,^f G. García,^g P. Limão-Vieira,^h O. Ingólfsson,ⁱ G. B. da Silva^j and M. J. Brunger^a

^a School of Chemical and Physical Sciences, Flinders University, Adelaide SA 5001, Australia

^b Centro de Ciências Exatas, Departamento de Física, Universidade Federal do Espírito Santo, 29075-910, Vitória, Espírito Santo, Brazil

^c Instituto de Física “Gleb Wataghin,” Universidade Estadual de Campinas, Campinas, São Paulo 13083-859, Brazil

^d Instituto de Física, Universidade de São Paulo, CP 66318, 05315-970, São Paulo, Brazil

^e Departamento de Física, Universidade Federal do Paraná, CP 19044, 81531-990, Curitiba, Paraná, Brazil

^f Departamento de Física Atómica, Molecular y Nuclear, Universidad Complutense de Madrid, Madrid E-28040, Spain

^g Instituto de Física Fundamental, CSIC, Serrano 113-bis, 28006 Madrid, Spain

^h Laboratório de Colisões Atômicas e Moleculares, CEFITEC, Departamento de Física, Faculdade de Ciências e Tecnologia, Universidade NOVA de Lisboa, 2829-516 Caparica, Portugal

ⁱ Science Institute and Department of Chemistry, University of Iceland, Dunhagi 3, 107 Reykjavík, Iceland

^j Universidade Federal de Mato Grosso, Barra do Garcas, Mato Grosso, Brazil

Synopsis We report on experimental measurements of cross sections for electron impact excitation and ionization of molecules that are key subunits of biological systems.

Electron impact excitation and ionization processes can initiate and drive chemical reactions in plasma and plasma-like environments. These processes influence the energy deposition in radiation-based medical therapies and the production of active species for technological plasmas. Understanding fundamental electron-interactions with key molecular species found within biological system is important in building and developing models for these physical systems, and adapting technologies to advance medical and industrial plasma processes.

We have performed experimental investigations using electron energy loss spectroscopy to measure differential cross sections for electron impact excitation of molecular species. Here we will discuss results from our experimental investigations into electron scattering from phenol [1,2], furfural [3,4], and quinone [5]. These molecules are key structural subunits of complex biomass. The performance of theoretical calculations aiming to describing electron scattering behavior under our experimental conditions will also be discussed.

We are particularly interested in understanding how the geometric configuration and electronic structure of molecules contributes to electron scattering behaviour. The present measurements are therefore compared to previous measurements performed on structurally similar systems. This enables a qualitative assessment of how chemical structure contributes to scattering dynamics, and assesses the limitation in ap-

proximating biomolecular complexes as a collection of molecular subunits.

Lastly, an experimental apparatus for performing electron scattering experiments from molecular radicals has also been developed at Flinders [6]. This facility has been used for measuring elastic scattering differential cross sections from radical species, such as CF₂ [7], CF₃ [8] and I [9]. We are currently expanding the range of molecular radical targets that can be investigated with this system through the development of a new radical source and mass spectrometer system. The existing electron scattering spectrometer is also being replaced to allow for experimental investigations of electron impact excitation of molecular radical species. The progress and details of these developments will also be discussed.

References

- [1] R. Neves *et al.* 2015 J. Chem. Phys. 142, 104305
- [2] G. da Silva *et al.* 2014 J. Chem. Phys. 141, 124307
- [3] D. B. Jones *et al.* 2016 J. Chem. Phys. **144**, 124309.
- [4] D. B. Jones *et al.* 2015 J. Chem. Phys. **143**, 184310.
- [5] D. B. Jones *et al.* 2016 J. Chem. Phys. **145**, 164306.
- [6] T. M. Maddern *et al.* 2008, Meas. Sci. Technol. **19**, 085801.
- [7] T. M. Maddern *et al.* 2008 Phys. Rev. Lett. **100**, 063202.
- [8] J. R. Brunton *et al.* 2013 J. Phys. B: At. Mol. Opt. Phys. **46**, 245203.
- [9] O. Z. Zatsarinny *et al.* 2011 Phys. Rev. A **83** 042702.

¹ E-mail: darryl.jones@flinders.edu.au

Low Energy Electron interaction with DNA and Protein*

S. V. K. Kumar¹

1114, Sobha Eternia, Haralur Road, Bengaluru 560 102, India

Synopsis The experimental results of damage caused by low energy electron interaction with pQE30 and Φ X174 dsDNAs and first results with full protein Cytochrome *c* is presented.

Radiation used for treatment of tumours, viz., X-ray, γ -ray, proton and carbon ion beams, generate secondary particles such as ions, radicals, excited neutrals and ballistic electrons with energies below 100 eV (e.g. $\sim 40\,000$ secondary electrons/MeV photon) [1]. It has been shown that these secondary low energy electrons (LEEs) can damage DNA and its constituents [2,3]. However, no experiments have been reported on the damage caused to other biomolecules, like proteins, in the cell. The results of the experiments on damage induced by LEEs to DNA, Oligonucleotides and **proteins** using a specially designed dose controlled electron irradiator [4] is presented here.

Plasmid dsDNAs pQE30 and Φ X174 have been used as models for double stranded DNA-LEE interaction experiments. Single Strand Breaks (SSB) induced to Φ X174 RF1 dsDNA by electrons over the energy range 0.5 to 500 eV show SSB yield at 0.5 eV is the lowest and it increases as function of electron energy till 500 eV. Detailed measurements conducted in the 0.5 To 25 eV range show resonance peaks, which shift at higher irradiation doses. In addition, DNA suspended in TE buffer at a pH of 7.5 show that LEE interaction results only in the formation of relaxed form. When the DNA is suspended in 0.001 mM NaOH and irradiated similarly, linear form and cross links are also formed, in addition to relaxed form, which may be attributed to the to the secondary electrons interacting with Na^+ ions that are bound to the DNA causing a second strand break in the opposite strand.

Measurements on single strand TT(ATA)₃TT Oligonucleotide (as a model) origami nanostructures, show that the energy dependence of strand break (SB) cross section not only show resonances but also demonstrate, for the first time [5], the influence of the potential radiosensitizer 8-Bromo adenine (⁸BrA) for the configuration TT(⁸BrATA)₃TT by enhancing the SB cross section up to 2.3 ± 0.7 at an electron energy as low as 0.5 eV, 2.8 ± 0.6 at 3 eV, and 2.4 ± 0.6 at 7 eV respectively.

LEE-Oligo nucleotide interaction studies were done in collaboration with Ilko Bald's group, University of Potsdam, Germany.

We have studied electron and photon interactions with proteins for the first time, using Cytochrome *c*, an important heme protein, which is involved not only in electron transport but also in the apoptotic pathway that can be triggered during radiation therapy. Irradiated Cytochrome *c* was analysed by using the molecular biology technique Enzyme-Linked Immunosorbent Assay (ELISA). Second method of analysis was by using Mass Spectrometry, which helps in identifying the actual bond/s that are broken during irradiation, while such an identification has not been possible till now for DNA or Oligonucleotides. Both photons and electrons break the protein except that the electrons cleave the prosthetic heme group while the photons cleave the peptide backbone between the 18th and the 19th amino acid residues. Similar experiments on the apo protein *i.e.* the protein without the heme group show no damage. It is clear from the above experiments that the heme group plays a vital role in the interaction process with both electrons and photons. As the sulfurs in the two cysteines also have an affinity for electrons, the electron can also interact them leading to structural changes and subsequent dissociation.

References

- [1] Sanche L. Nanoscale Dynamics of Radiosensitivity: Role of Low Energy Electrons in García G. G. & Fuss M. C. editors Radiation Damage in Biomolecular Systems, Heidelberg, Springer, 2012, p. 3.
- [2] Zheng Y. & Sanche L. 2013 *Rev. Nanosci. Nanotechnol.* **2**, 1.
- [3] Kumar S. V. K. *et al.* 2015 *Eur. Phys. J. D* **69** 204
- [4] Kumar S. V. K. *et al.* 2016 *Rev. Sci. Instrum.*, **87**, 034302.
- [5] Schürmann R. *et al.* (manuscript under preparation)

E-mail: svkk@tifr.res.in

*Work done at Tata Institute of Fundamental Research, Homi Bhabha Road, Colaba, Mumbai 400 005, India

Low energy electron interaction with molecules of biological interest

M. A. Śmialek^{1,‡,¶}, A. Ribar,^{†,*} S. E. Huber,[†] M. Neustetter,[†] R. Schürmann,[§] I. Bald,[§] and S. Denifl[†]

[‡]Faculty of Ocean Engineering and Ship Technology, Gdansk University of Technology, Gabriela Narutowicza 11/12, 80-233 Gdansk, Poland

[¶]School of Physical Sciences, The Open University, Walton Hall, Milton Keynes MK7 6AA, United Kingdom

[†]Center of Molecular Biosciences Innsbruck, Leopold Franzens University of Innsbruck, Technikerstr. 25, 6020 Innsbruck, Austria

^{*}Faculty of Mathematics, Physics and Informatics, Comenius University in Bratislava, Mlynská dolina F2, 842 48 Bratislava, Slovakia

[§]Institut für Chemie, Universität Potsdam, Karl-Liebknecht-Str. 24-25, D-14476 Potsdam, Germany

Synopsis Electron impact ionization and low energy electron attachment to 2-amino-2-(hydroxymethyl)-1,3-propanediol (TRIS) and methyliminodiacetic acid (MIDA), an analogue of ethylenediaminetetraacetic acid (EDTA), were investigated experimentally complemented by thermochemical calculations. Both compounds are components of biological buffers and often are used as DNA stabilizers in irradiation studies. Thus it is of importance to understand their potential interactions with radiation and their eventual influence on experimental results. The most prominent dissociation channel for TRIS is associated with hydroperoxyl radical formation, whereas dissociation of MIDA results mainly in the formation of formic and acetic acid.

Understanding the interactions of various types of radiation with the constituent cellular molecules (DNA in particular) underlies the formulation of DNA damage models. Such models should be able to predict not only the patterns of ionizations but also the spectra of damage complexity that different types of radiation can induce in DNA. Hence, knowledge of the relationship between the amount of energy deposited within a given region of the DNA helix and the type and severity of the damage that is produced is required [1]. Among others, low energy electrons are the most abundant secondary species that are produced upon impact of highly energetic photons, electrons or ions on biological matter.

In most *in vitro* irradiation studies, extracted plasmid DNA is used requiring stabilization, e.g. by suspension in EDTA solution [2] or in TRIS-EDTA buffer [3] that is later lyophilized or used in aqueous phase, depending on the specific type of undertaken irradiation study. TRIS buffer has also been used as hydroxyl radical scavenger [4]. In order to adequately assess experimental outcomes of studies employing these compounds, controlling their eventual influence on the results is highly desirable [5].

We attempted to investigate interactions between electrons and the two most popular stabilisers used in DNA irradiation studies: TRIS and EDTA, by means of electron attachment in the energy range of 0–20 eV. However due to the thermal decomposition of EDTA upon heating, methyliminodiacetic acid (MIDA) was investigated instead of EDTA. The molecules are depicted in Figure 1 with MIDA being half of

EDTA, having the other half replaced by a hydrogen atom.

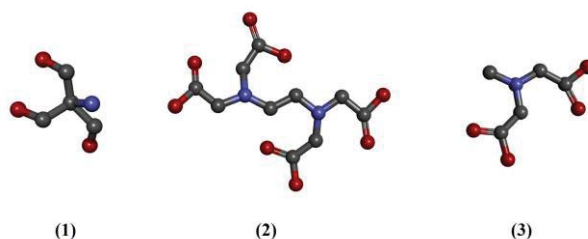


Figure 1. (1) TRIS, (2) EDTA and (3) MIDA molecules. Hydrogens are omitted for convenience.

The most prominent channels observed during molecular fragmentation upon low energy electron attachment resulted in formation of hydroperoxyl radical and hydroxyl anion for TRIS and formic and dehydrogenated acetic acids along with hydroxyl anion for MIDA in line with theoretical considerations of the reaction energetics.

On balance, these results support the request to scrutinize the eventual, indirect influence of substances used to stabilize plasmid DNA on outcomes of DNA irradiation studies.

References

- [1] M. A. Śmialek *et al.* 2015 *Radiat. Res.* **172** 529
- [2] K. Prise *et al.* 2000 *Int. J. Radiat. Biol.* **76** 881
- [3] (a) K. Pachnerová Brabcová, *et al.* 2014 *Radiat Environ Biophys.* **53** 705 (b) L. Vyšín *et al.* 2015 *Radiat Environ Biophys* 2015 **54** 343
- [4] M. Folkard *et al.* 1999 *J. Phys. B* **32** 2753
- [5] (a) M. A. Śmialek *et al.* 2010 *Eur. Phys. J. D* **60** 31 (b) M. A. Śmialek *et al.* 2011 *Eur. Phys. J. D* **62** 197 (c) O. Boulanouar *et al.* 2013 *J. Chem. Phys.* **139** 055101

¹ E-mail: smialek@pg.gda.pl

Energy Flow Between Pyrimidines and Water Triggered by Low Energy Electrons

Jaroslav Kočišek^{*1}, Juraj Fedor^{*}, Andriy Pysanenko^{*}, Mateusz Zawadzki^{*}, Michal Fárník^{*}, Jan Poštulka[†], Petr Slavíček^{†2}

^{*} J. Heyrovský Institute of Physical Chemistry v.v.i., The Czech Academy of Sciences, Dolejškova 3, 18223 Prague, Czech Republic

[†] Department of Physical Chemistry, University of Chemistry and Technology, Technická 5, Prague 6, Czech Republic

Synopsis Substituted pyrimidines form a base of several cancer chemotherapeutics. Their effective dissociation by low energy electrons was identified to be a source of their radiosensitizing properties in combined chemo-radiation treatments. Here we combine experiment and theory to explore the energetics of the low energy electron interaction with these molecules in a solution. Novel approach enables estimation of the total energy flow between pyrimidines and water.

We present the results of experiments with molecular beams of microhydrated pyrimidines uracil, 5-Fluorouracil and 5-Bromouracil. Microhydrated pyrimidines are prepared by recently described gas humidification technique [1]. The molecules interact with low energy 1.5 eV or 70 eV electrons and reaction products are analyzed by the means of negative or positive ion mass spectrometry, respectively. Control over the hydration process enables the change of hydration level of the neutral microhydrated pyrimidines in molecular beam. The combination of two different ionization techniques with theory then allows us to estimate absolute energy flow from pyrimidines to water after electron attachment and electron ionization.

In a good agreement with the interpretation of our previous work on uracil and thymine [1], water reduces the dissociation of pyrimidines by caging of the dissociation products. The energy transferred to the cage is released by evaporation of individual water molecules. Number of evaporated molecules can be used to estimate the total energy transferred to the solvent. In our experiment, number of evaporated water molecules is not measured directly but estimated from the comparison of positive and negative ion mass spectra.

The amount of energy transferred to the solvent after electron attachment copies the trend of rising electron affinity of the pyrimidines from uracil to 5-bromouracil. On the other side, the energy transferred to the solvent after electron ionization is nearly constant. On the basis of our previous studies with pure water clusters [2] one can expect that after the ionization, the energy transferred to solvent should be high. However, the experiments show that it is actually low and comparable to the energy transferred to the solvent after electron attachment

to 5-bromouracil. This indicates that stable cluster cations are formed only after ionization of pyrimidines within the cluster, while ionization of water results in prompt fragmentation and possible pyrimidine dissociation after proton transfer reaction.

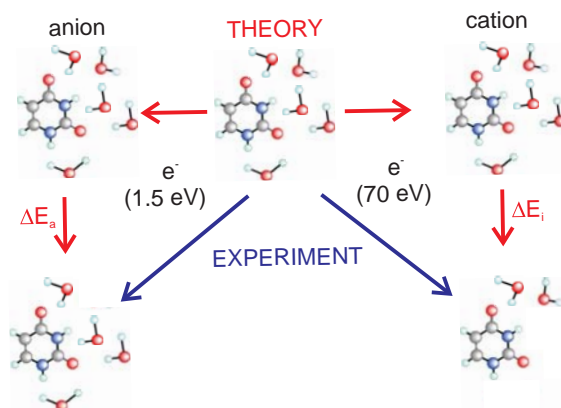


Figure 1. Sketch of the present approach. Experiment provides information about distributions of microhydrated cations and anions formed after electron ionization and electron attachment, respectively. Theory is then used to estimate the amount of energy needed to evaporate the water molecules as observed for electron attachment (ΔE_a) and electron ionization (ΔE_i). Experiments with different pyrimidines and at different level of hydration were done to validate the approach.

ACKNOWLEDGMENT: This work was supported by Czech Science Foundation grant no. 16-10995Y.

References

- [1] J. Kočišek *et al.* 2016 *J. Phys. Chem. Lett.* **7** 3401
- [2] J. Lengyel *et al.* 2014 *Chem. Phys. Lett.* **612** 256

¹E-mail: jaroslav.kocisek@jh-inst.cas.cz

²E-mail: petr.slavicek@vscht.cz

NOO peroxy isomer discovered in the velocity-map imaged photoelectron spectrum of NO_2^-

Benjamin A Laws^{*1}, Steven J Cavanagh^{*}, Brenton R Lewis^{*}, Stephen T Gibson^{*2},

^{*} Research School of Physics and Engineering, Australian National University, Canberra ACT 2601, Australia

Synopsis Photoelectron spectra of NO_2^- measured with ANU's state of the art velocity-map imaging spectrometer have revealed unexpected, additional high energy electron structure that cannot arise from detachment of C_{2v} NO_2^- . Our work shows that this additional structure must instead be a signature of a new peroxy NOO isomer, a molecule which has not previously been observed.

NO_2 , a toxic gas formed in most combustion processes, is a key component of photochemical smog and an important molecule in the Earth's atmosphere. Photoelectron spectroscopy allows for the structural and photophysical properties of this important molecule, and its parent negative ion, to be studied in detail. By employing the ANU's state of the art spectrometer, this information may be obtained with high resolution.

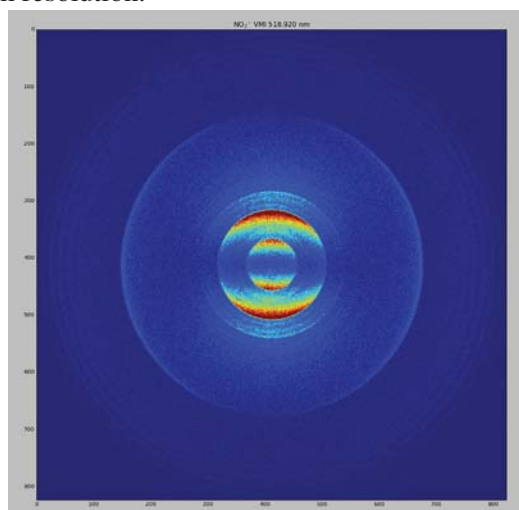
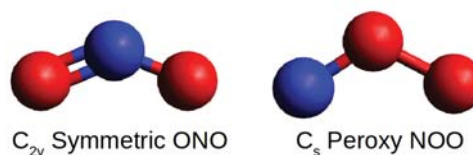


Figure 1. Velocity-map image of NO_2^- at 518.920nm, showing unexpected high eKE structure.

Through the implementation of velocity-map imaging, both the energetic and the angular information from the observed photodestruction events are acquired with 100% electron collection efficiency, allowing for multiple detachment/dissociation channels to be observed simultaneously. This benefit is highlighted in our measurements of NO_2^- , where unexpected additional high eKE photoelectrons are revealed. The surprising high eKE structure persists at detachment energies lower than the EA of ONO^- (2.273eV) [1], confirming that this previously unseen

electron structure can not arise from the standard C_{2v} isomer of NO_2^- . Furthermore, the corresponding angular distribution has a negative anisotropy parameter β , opposite in sign to detachment from ONO^- .

Through further experimentation, combined with *ab-initio* calculations, it can be shown that this additional photoelectron structure is the result of another isomer of NO_2^- . The possible existence of a peroxy NOO isomer was first suggested in 1961, however despite numerous theoretical and experimental studies since then, there has been no previous conclusive evidence that a stable NOO isomer exists [2, 3, 4].



This work provides the first direct measurement of the NOO isomer, along with determination of multiple spectroscopic constants. This may have a significant impact on our understanding of this vital NO_2 molecule, a result with many possible implications in atmospheric science.

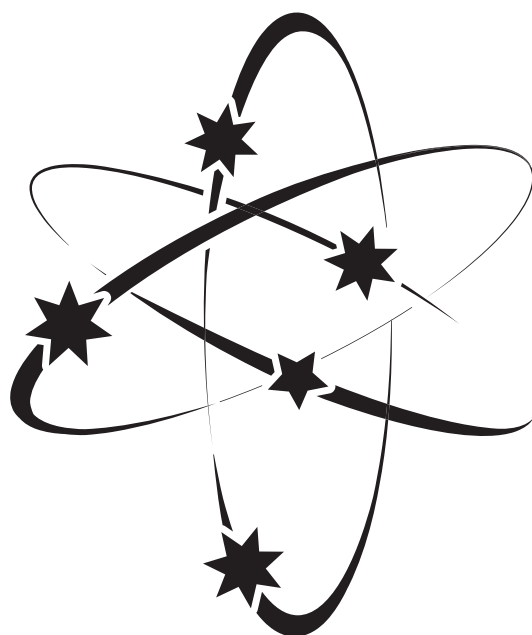
References

- [1] K. M. Ervin, J. Ho, and W. C. Lineberger 1988 *J. Phys. Chem.* **92** 5405
- [2] E. Herbst, T. A. Patterson, and W. C. Lineberger 1974 *J. Chem. Phys.* **61** 1300
- [3] C. Meredith, R. D. Davy, G. E. Quelch, and H. F. Schaefer 1991 *J. Chem. Phys.* **94** 1317
- [4] S. P. Walch 1995 *J. Chem. Phys.* **102** 4189

Research supported by the Australian Research Council Discovery Project Grant DP160102585

¹E-mail: ben.laws@anu.edu.au

²E-mail: stephen.gibson@anu.edu.au



ICPEAC **2017**

Cairns, Australia

XXX INTERNATIONAL CONFERENCE
ON PHOTONIC, ELECTRONIC
AND ATOMIC COLLISIONS



poster sessions

Poster abstracts can be found at
<http://icpeac30.edu.au/posterlist.php>
and on the USB memory stick

POSTER LIST SCHEDULE

TOPICS	WEDNESDAY 26 JULY	THURSDAY 27 JULY	FRIDAY 28 JULY	MONDAY 31 JULY	TUESDAY 1 AUGUST
1a. Photon - Atom / Ion Weak field processes	WE01 - WE32				
1b. Photon - Atom / Ion Strong field and ultrafast processes		TH01 - TH20		MO01 - MO62	
1c. Photon - Atom / Ions Structure and spectroscopy			FR01 - FR22		
2a. Photon - Molecule Weak field processes		TH21 - TH44			
2b. Photon - Molecule Small Cluster Strong field and ultrafast processes	WE33 - WE52		FR23 - FR63 FR141		
2c. Photon - Molecule - Small Cluster Cold species - Storage - Clusters					TU01 - TU18
3-4 Photon - Condensed Matter Other					TU19 - TU50

TOPICS	WEDNESDAY 26 JULY	THURSDAY 27 JULY	FRIDAY 28 JULY	MONDAY 31 JULY	TUESDAY 1 AUGUST
5. Lepton - Atom / Ion	WE53 - WE072		FR64 - FR93	MO63 - MO109	
6. Lepton - Molecule / Small Cluster	WE73 - WE101	TH45 - TH74	FR137 - FR140 FR142 - FR145		TU51 - TU93
7. Lepton - Condensed Matter Large Cluster - Other	WE103 - WE115				
8. Heavy Particle - Cold		TH75 - TH108			
9. Heavy Particle - Atom / Ion	WE117 - WE145		FR94 - FR135		
10. Heavy Particle - Molecule / Small Cluster		TH109 - TH142		MO110 - MO143	
11. Heavy Particle - Condensed Matter + Other					TU94 - TU126
12. Other processes and post-deadline			FR136		TU127 - TU133

POSTER LIST

1. PHOTON - ATOM/ION (WEAK FIELD PHENOMENA)

- WE-001 **Autoionization of very-high-n strontium Rydberg atoms**
F. Barry Dunning, Xinyue Zhang, Gavin Fields, Shuhei Yoshida, Joachim Burgdorfer
- WE-002 **Photoionization of neutral iron from ground and metastable states**
Oleg Zatsarinny, Luis Fernández-Menchero, Klaus Bartschat
- WE-003 **Low-energy outer-shell photodetachment of the negative ion of aluminum**
Oleg Zatsarinny, Klaus Bartschat, Elizabeth Nagy, Sergey Gedeon, Viktor Gedeon, Vladimir Lazur
- WE-004 **Photoexcitation of atoms by Laguerre-Gaussian beams**
Stephan Fritzsche, Anton Peshkov
- WE-005 **Multi-electron processes in K-shell double and triple photodetachment of oxygen anions**
Stefan Schippers, Randolph Beerwerth, Levente Abrok, Sadia Bari, Michael Martins, Sandor Ricz, Jens Viehhaus, Stephan Fritzsche, Alfred Müller
- WE-007 **Two-photon K-shell ionization cross sections for neutral atoms**
Stephan Fritzsche, Jiri Hofbrucker
- WE-008 **Atomic photoionisation calculated using the singularity-free convergent close-coupling method**
Alexander Bray, Anatoli Kheifets, Igor Bray
- WE-009 **Photoionization of atomic fluorine**
Jiayu Sun, Jinlei Liu, Jianhua Wu, Jianmin Yuan, Zengxiu Zhao
- WE-010 **Photodetachment microscopy in time-dependent fields**
Ilya Fabrikant, Harindranath Ambalampitiya
- WE-011 **Relativistic Effects in Photoionization of Outer ns Subshells of Heavy Atoms**
David Keating, Pranawa Deshmukh, Steven Manson
- WE-012 **Decay of inner-shell holes in potassium and rubidium investigated by multielectronspectroscopy**
Mehdi Khalal, Pascal Lablanquie, Francis Penent, Jérôme Palaudoux, Lidija Andric, Jean-Marc Bizau, Denis Cubaynes, Kenji Ito, Kari Jänkälä
- WE-013 **K-shell Excitation in the Photoionization of the Open-shell Cl Atom**
Zineb Felfli, Steven Manson, Alfred Msezane
- WE-014 **Calculations of electron shakeoff probabilities using pseudostates**
Takeshi Mukoyama and Nobuyuki Tamura
- WE-015 **Photodetachment Spectroscopy of Bound and Quasibound States of the Negative Ion of Lanthanum**
C.W. Walter, N.D. Gibson, N.B. Lyman, J. Wang
- WE-016 **Photoionization and Photoabsorption in the Rydberg resonance region**
Jacques Dubau, Igor Ivanov
- WE-017 **Fully differential single photon double photoionization of atomic magnesium**
Frank Yip, Thomas N. Rescigno, C. William McCurdy
- WE-018 **PCI Recapture of Photoelectrons: Conjugate Processes and Angular correlations**
Yoshiro Azuma, Satoshi Kosugi, Norihiro Suzuki, Naoki Kumagai, Fumihiro Koike,

Hiroshi Iwayama, Eiji Shigemasa

- WE-019 **Limitations in photoionization of helium by an extreme ultraviolet vortex**
Tatsuo Kaneyasu, Yasumakasa Hikosaka, Masaki Fujimoto, Taro Konomi, Masahiro Katoh, Hiroshi Iwayama, Eiji Shigemasa
- WE-020 **Observation of electron back-to-back emission from the quasifree mechanism of helium at 800 eV photon energy**
Sven Grundmann, Florian Trinter, Sebastian Eckart, Jonas Rist, Gregor Kastirke, Daniel Metz, Jens Viefhaus, Till Jahnke, Lothar Ph. H. Schmidt, Reinhard Dörner, Markus S. Schöffler
- WE-021 **Distorted wave photoionization cross sections for use in NLTE model atmospheres: Ni^+ - Ni^{10+}**
Simon Preval, Nigel Badnell
- WE-023 **Double Photoionization of Atomic Oxygen: Feshbach Resonances in the Two-Electron Continuum**
Madhushani Wickramarathna, Thomas Gorczyca, Connor Ballance, Wayne Stolte
- WE-024 **Photoionization of polarized Ne II in the region of autoionizing states**
Alexei Grum-Grzhimailo, Elena Gryzlova, Svetlana Strakhova, Sergej Burkov, Kiyoshi Ueda, Michael Meyer, Giuseppe Sansone
- WE-025 **Measurement and analysis of EUV emission spectrum from laser produced Pr plasma**
Shiquan Cao, Maogen Su, Qi Min, Duixiong Sun, Chenzhong Dong
- WE-026 **Radiation properties and hydrodynamics evolution of highly charged ions in laser-produced silicon plasma**
Qi Min, Maogen Su, Shiquan Cao, Duixiong Sun, Chenzhong Dong
- WE-027 **The influence of ambient gas on laser produced plasmas and the crater morphology of laser-ablated Al**
Duixiong Sun, Yongqiang Wang, Maogen Su, Qi Min, Shiquan Cao, Chenzhong Dong
- WE-028 **Low-energy photon-alkali atom scattering cross-sections**
Michael Bromley, Swaantje Grunefeld, Emily Kahl, Julian Berengut, Jun Jiang
- WE-029 **Photodetachment of O^- : the complete picture**
Matthieu G  n  vriez, Arnaud Dochain, Xavier Urbain
- WE-030 **Time-Resolved Two-Colour Photoionization from the 5P and 6P states of Rb**
James Pursehouse, Andrew Murray
- WE-031 **Resonance induced population transfer of Fe XVII ions in plasma environment**
Chensheng Wu, Xiang Gao
- WE-032 **Towards understanding the Auger cascade following Xe $3d_{5/2}$ photoionisation**
Boon Lee, Tibor Kibedi, Andrew Stuchbery, Maarten Vos

2. PHOTON - MOLECULE (STRONG FIELD AND ULTRAFAST PHENOMENA)

- WE-033 **Observing electron localization in a dissociating molecule in real time**
Han Xu, X. Wang, A. Atia-Tul-Noor, D. Kielpinski, R. T. Sang, and I. V. Litvinyuk
- WE-034 **Imaging ultrafast molecular wave-packets with a single chirped UV pulse**
Denis Jelovina, Johannes Feist, Fernando Mart  n, Alicia Palacios
- WE-035 **Role of electron-nuclear coupled dynamics on charge migration in glycine induced by attosecond pulses**

Manuel Lara-Astiaso, Alicia Palacios, Piero Decleva, Ivano Tavernelli, Fernando Martín

WE-036 **Modelling laser-matter interactions for simple molecules**

Alexander Galstyan, Yuri Popov, Franciska Mota-Furtado, Patrick O'Mahony, Bernard Piraux

WE-037 **Perturbative expansions for laser-atom interactions**

Yuri Popov, Alexander Galstyan, Franciska Mota-Furtado, Patrick O'Mahony, Bernard Piraux

WE-039 **Enhanced ionization of acetylene in intense laser pulses is due to energy up-shift and field coupling of multiple orbitals**

Sonia Erattupuzha, Cody L. Covington, Arthur Russakoff, Erik Lötstedt, Seyedreza Larimian, Vaclav Hanus, Markus Schöffler, Sergiy Bubin, Markus Koch, Stefanie Gräfe, Andrius Baltuska, Xinhua Xie, Kaoru Yamanouchi, Kálmán Varga, Markus Kitzler

WE-040 **Selective bond breaking of CO_2^{2+} in phase-locked two-color intense laser fields**

Tomoyuki Endo, Hikaru Fujise, Yuuna Kawachi, Ayaka Ishihara, Akitaka Matsuda, Mizuho Fushitani, Hirohiko Kono, Akiyoshi Hishikawa

WE-041 **Above-threshold ionization processes in diatomic molecules driven by strong laser fields**

Noslen Suárez, Alexis Chacón, Marcelo F. Ciappina, Jens Biegert, Maciej Lewenstein

WE-042 **High-order harmonic generation in polyatomic systems**

Noslen Suárez, Alexis Chacón, Jose A. Pérez-Hernández, Jens Biegert, Maciej Lewenstein, Marcelo F. Ciappina

WE-043 **High-Order Harmonic Generation of hydrogen molecule ions in a large internuclear distance**

Xiao-xin Zhou, Ling-Ling Du, Peng-Cheng Li, Hong-Shan Chen

WE-044 **Imaging the Temporal Evolution of Molecular Orbitals during Ultrafast Dissociation**

Miriam Weller, Hendrik Sann, Thilo Havermeier, Christian Müller, Hong-Keun Kim, Florian Trinter, Markus Waitz, Jörg Voigtsberger, Felix Sturm, Tobias Bauer, Robert Wallauer, Deborah Schneider, Christoph Goihl, Jan Tross, Kyra Cole, Jian Wu, Markus S. Schöffler, Horst Schmidt-Böcking, Till Jahnke, Marc Simon, Reinhard Dörner

WE-045 **Commissioning a new COLTRIMS-Reaction Microscope for the SQS instrument at European XFEL**

Gregor Kastirke, Markus Schöffler, Miriam Weller, Kilian Fehre, Lothar P.H. Schmidt, Juliane Siebert, Joseph Hoehl, Isabel Vela-Perez, Daniel Trabert, Yannick Hermann, Sven Grundmann, Markus Waitz, Till Jahnke, Etienne Bloch, Markus Ilchen, Yevheniy Ovacharenko, Thomas Baumann, Daehyun You, Brandon Griffin, Marc Simon, Michael Meyer, Reinhard Dörner

WE-046 **Real Time Observation of the Ultrafast Dynamics Induced by XFEL Pulses in CH_2I_2 Molecule**

T. Takanashi, H. Fukuzawa, K. Motomura, K. Nagaya, S. Wada, Y. Kumagai, D. Iablonskyi, S. Mondal, Y. Ito, T. Tachibana, S. Yamada, Y. Sakakibara, D. You, T. Nishiyama, K. Matsunami, T. Sakai, K. Asa, Y. Sato, T. Umemoto, K. Kariyazono, Y. Takahashi, M. Kanno, K. Nakamura, K. Yamazaki, S. Kajimoto, H. Sotome, E. Kukk, K. Kooser, C. Nicolas, C. Miron, M. Schöffler, G. Kastirke, P. Johnsson, T. Asavei, L. Neagu, X.-J. Liu, S. Molodtsov, T. Togashi, K. Ogawa, S. Owada, T. Katayama, K. Tono, M. Yabashi, A. Rudenko, H. Fukumura, M. Yao, H. Kono and Kiyoshi Ueda

- WE-047 **A dressed harmonic study in laser-assisted photoionization of water molecules by attopulses**
Lara Martini, Diego Boll, Omar Fojón
- WE-049 **Dynamical origin of below- and near-threshold harmonic generation of H_2^+ in an intense NIR laser field**
John Heslar, Shih-I Chu
- WE-050 **Rydberg-state excitation suppression of diatomic molecules in strong near-infrared laser fields**
Hang Lv, Lei Zhao, Haifeng Xu, Mingxing Jin, Dajun Ding, Shilin Hu, Jing Chen
- WE-051 **Strong-field ionization and dissociation of linear triatomic molecules irradiated by 800-nm and 400nm femtosecond laser fields**
Wanlong Zuo, Hang Lv, Lei Zhao, Qi Zhang, Li Yang, Haifeng Xu
- WE-052 **The Role of Super-Atom Molecular Orbitals in Doped Fullerenes in a Femtosecond Intense Laser Field**
Nora Berrah, H. Xiong, B. Mignolet, L. Fang, T. Osipov, T. J. A. Wolf, E. Sistrunk, M. Gühr, and F. Remacle

5. LEPTON - ATOM/ION

- WE-053 **Doubly-differential cross sections for electron and positron impact ionization of argon**
Radu Campeanu
- WE-057 **Study of multiply charged Argon-ions formed by decay of 2p-hole state under e^- -Ar collision employing energy selected ion coincidence technique**
Sunil Kumar, Suman Prajapati, Bhupendra Singh, B.K.Singh, R.Shanker
- WE-058 **Electron impact L and M-subshell ionization cross sections for atoms ($14 \leq Z \leq 92$) including the relativistic effects**
B. C. Saha, A. K. Basak, M. A. Uddin, A. K. F. Haque, M. A. R. Patoary, M. M. Haque, M. Ismail Hossain, M. Maaza
- WE-059 **Electron impact excitation of O III**
Swaraj Tayal, Oleg Zatsarinny
- WE-060 **Benchmark calculations for electron-impact excitation of Mg^{4+}**
Kedong Wang, Luis Fernández-Menchero, Oleg Zatsarinny, Klaus Bartschat
- WE-061 **B-spline R-matrix with pseudo-states calculations for electron-impact excitation and ionization of magnesium**
Oleg Zatsarinny, Klaus Bartschat
- WE-062 **Low-energy collisions of excited positronium with antiprotons**
Ilya Fabrikant, Alisher Kadyrov, Igor Bray, Michael Charlton
- WE-063 **On the mean kinetic energy of recoil ions produced in 3.5keV electron-argon collisions**
Suman Prajapati, Sunil Kumar, Bhupendra Singh, Bhartendu K Singh, Rama Shanker
- WE-064 **Photorecombination of berylliumlike and boronlike silicon ions**
Dietrich Bernhardt, Arno Becker, Carsten Brandau, Manfred Grieser, Michael Hahn, Claude Krantz, Michael Lestinsky, Oldrich Novotný, Roland Reponow, Daniel Wolf Savin, Kaija Spruck, Andreas Wolf, Alfred Müller, Stefan Schippers
- WE-065 **Electron shakeoff subsequent to β^+ decay of trapped $^{35}Ar^+$ and $^{19}Ne^+$ trapped ions**

Xavier Fléchar, Bernard Pons, Gilles Ban, Martin Breitenfeldt, C. Couratin, P. Delahaye, D. Durand, X. Fabian, B. Fabre, P. Finlay, A. Leredde, E. Liénard, A. Méry, O. Naviliat-Cuncic, T. Porobic, G. Quemener, D. Rodriguez, N. Severjins, J-C. Thomas, S. Van Gorp

- WE-066 **Study on KLL dielectronic recombination for highly charged tungsten ions at Shanghai EBIT**
Bingsheng Tu, Jun Xiao, Ke Yao, Yang Yang, Baoren Wei, Roger Hutton, Yamin Zou
- WE-067 **Spin evolution of two valence electrons in two separated ions**
Biplab Goswami, Stephan Fritzsche
- WE-068 **Electron impact ionization of calcium atoms inside quadrupole trap**
Lukasz Klosowski, Mariusz Piwinski, Szymon Wojtewicz, Daniel Lisak, Michael Drewsen, Katarzyna Pleskacz, Stanislaw Chwiot
- WE-069 **Energy and momentum transfer in electron-ion elastic collisions**
Lukasz Klosowski, Mariusz Piwinski
- WE-070 **Electronic excitation of P-state of cadmium and zinc atoms**
Mariusz Piwinski, Lukasz Klosowski, Dariusz Dziczek, Stanislaw Chwiot
- WE-071 **Benchmark calculations of double ionization of Ne in Graphics Processing Units**
Flavio Colavecchia, Michael Schulz, T Kirchner, Marcelo Ciappina
- WE-072 **Multiple scattering of slow muons in an electron gas**
Claudio Archubi, Diego Arbó, Néstor Arista

6. LEPTON - MOLECULE

- WE-073 **Isotopical effects in electron and atom molecular scattering**
Serguey Pozdneev
- WE-074 **Resonances in Electron Scattering by Molecules**
Serguey Pozdneev
- WE-075 **Application of few-body approximation to the scattering hydrogen halide molecules by slow electron**
Serguey Pozdneev
- WE-076 **Dissociative electron attachment**
Serguey Pozdneev
- WE-077 **Application quantum theory of scattering for guided control of chemical reaction and creation of the new molecular structures**
Serguey Pozdneev
- WE-078 **The peak shape of electrons scattered 'elastically' from H₂ not a delta function or a Gaussian but almost a cusp**
Maarten Vos
- WE-079 **N (²P) Production in electron-N₂ Collisions.**
J William Mcconkey, Wladek Kedzierski, Jeffery Dech
- WE-080 **A novel approach to deconvolve overlapping features in molecular spectra: Monte Carlo random walk routine and its application**
Weiqing Xu, Xiao-Xun Mei, Ya-Wei Liu, Lin-Fan Zhu
- WE-081 **Electron Impact Ionization Cross Sections and Rate Coefficients For C₂H₄ Molecule**
Neeraj Kumar, Satyendra Pal

- WE-082 **Low energy elastic cross section of fluoroacetylene by electron impact**
Dhanoj Gupta, Heechol Choi, Mi-Young Song
- WE-083 **(e, 2e) Impact ionization cross section of biomolecules**
Prithvi Singh, G. Purohit and C. Champion
- WE-084 **Ultrafast gas electron diffraction by THz-wave assisted electron scattering: Numerical simulations of time-resolved electron diffraction patterns**
Reika Kanya, Kaoru Yamanouchi
- WE-085 **Low-energy electron interactions with chromium hexacarbonyl $\text{Cr}(\text{CO})_6$**
J. Khreis, J. Ameixa, M. Neustetter, J. Reitshammer, Filipe Ferreira Da Silva and S. Denifl
- WE-086 **Shake-up processes in Auger Cascades of Light and Medium Elements**
Stephan Fritzsche, Randolph Beerwerth
- WE-087 **Electron-Impact Ionization of Laser-Aligned Atoms – Contributions from both Natural and Unnatural-Parity States.**
Andrew Murray, James Colgan, Don Madison, Matthew Harvey, Ahmad Sakaamini
- WE-088 **(e,2e) Ionization Studies of N_2 at Low to Intermediate Energies from a Coplanar Geometry to the Perpendicular Plane**
Ahmad Sakaamini, Matthew Harvey, Sadek Amami, Andrew Murray, Don Madison, Chuangang Ning
- WE-089 **Dissociative electron attachment to CO molecule probed by velocity slice imaging technique**
Pamir Nag, Dhananjay Nandi
- WE-090 **Dipolar dissociation dynamics in electron collisions with carbon monoxide**
Dipayan Chakraborty, Pamir Nag, Dhananjay Nandi
- WE-091 **New insights in low-energy electron-fullerene interactions**
Alfred Msezane, Zineb Felfli
- WE-092 **Binding energies of fullerene and complex atomic negative ions**
Alfred Msezane, Zineb Felfli
- WE-093 **Resonances in low-energy electron elastic scattering from Fullerenes**
Zineb Felfli, Alfred Msezane
- WE-094 **Integral cross sections of the dipole-allowed excitations of nitrogen studied by fast electron scattering and X-ray scattering**
Ya-wei Liu, Long-Quan Xu, Dong-Dong Ni, Xin Xu, Xin-Chao Huang, Lin-Fan Zhu
- WE-095 **Electron scattering from molecular hydrogen**
Dmitry Fursa, Mark Zammit, Jeremy Savage, Igor Bray
- WE-096 **Electron stopping powers in H_2**
Dmitry Fursa, Robert Threlfall, Mark Zammit, Igor Bray
- WE-098 **Positive ion mass spectrometry for fragmentation of anthracene by low energy electron impact**
Melissa Dunne, Marcin Gradziel, Peter van der Burgt
- WE-099 **Positive ion mass spectrometry for fragmentation of 5-fluorouracil by low energy electron impact**
Michael Brown, Peter van der Burgt
- WE-100 **Differential Measurements of Ionization and Excitation of H_2 by 250 eV Positrons**
Oscar G de Lucio, Robert D DuBois

WE-101 **Investigation of low energy electron interaction with silane molecules**

Arvind Kumar Jain

7 LEPTON - CONDENSED MATTER

WE-103 **Electron impact secondary electron emissions from atomic and molecular solid targets**

Abul Kalam Fazlul Haque, M. A. Uddin, A. K. Basak, B. C. Saha, M. Maaza, M. A. R. Patoary, M. M. Haque, M. Ismail Hossain

WE-104 **Measurement of angular distributions of K x-ray intensity of Ti and Cu thick targets following impact of 10-25 keV electrons**

Bhupendra Singh, Sunil Kumar, Suman Prajapati, Bhartendu K Singh, Xavier Llovet, Rama Shanker

WE-105 **Transmission of electrons through a conical glass capillary**

Hongqiang Zhang, Libing Qian, Pengfei Li, Bo Jin, Dingkun Jin, Guangyin Song, Qi Zhang, Long Wei, Ben Niu, Chenliang Wan, Zhangyong Song, Zhihu Yang, Reinhold Schuch, Ximeng Chen

WE-106 **Diffraction in matter-antimatter binding: Positronium formation from C60**

Himadri Chakraborty, Anzumaan Chakraborty, Paul-Antoine Hervieux

WE-107 **Fragmentation of condensed diazenes**

Lilian Ellis-gibbings, Andrew Bass, Pierre Cloutier, Gustavo Garcia, Leon Sanche

WE-108 **Electron transmission through macroscopic metallic capillaries**

Dusko Borka, Karoly Tokesi, Christoph Lemell

WE-109 **Novel Plasmon-Coupling Theory of the Electron Inelastic Mean Free Path**

Christopher Chantler, Jay Bourke

WE-110 **The nonlinear electron scattering spectroscopy of the surface plasmon resonance for Au nano-structures on graphite surface**

Chunkai Xu, Meng Li, Zhean Li, Yi Luo, Xiangjun Chen

WE-111 **Characterization measurements with a transverse electron target at a crossed-beams setup**

Sabrina Geyer, Sarah Lamprecht, Thorsten Conrad, Holger Podlech, Oliver Kester

WE-112 **Theoretical dielectronic recombination rate coefficients for lowly charged tungsten ions**

Duck-Hee Kwon

WE-113 **The Monte Carlo simulation of electron transmission through Al₂O₃ nanocapillary**

Ai-xiang Yang, B. H. Zhu, X. M. Chen, J. X. Shao

WE-114 **The investigation of quasi-characteristic radiation of electrons channeled along the charged axes in the crystals of zinc blende**

Mykola Maksyuta, Volodymyr Vysotskii, Svitlana Efimenko, Vladislav Syshchenko, Artur Tarnovsky, Alexandr Isupov

9 HEAVY PARTICLE - ATOM/ION

WE-117 **APPA R&D - BMBF collaborative research at FAIR**

Stefan Schippers, Thomas Stöhlker

WE-118 **Mitigation of EUV emission from laser-induced oxygen plasmas for**

- atom-surface interaction studies in a simulated space environment**
Kumiko Yokota, Junki Ohira, Yugo KImoto, Hiroaki Nlshimura, Masahito Tagawa
- WE-119 **EUV spectra from laser-induced argon/oxygen mixed plasmas: Gas mixture dependence of EUV emission relevance to space environmental simulation**
Masahito Tagawa, Junki Ohira, Yugo Kimoto, Hiroaki Nishimura, Kumiko Yokota
- WE-120 **On the beam emittance/brilliance of highly charged ions extracted from the Frankfurt 14GHz Electron-Cyclotron-Resonance-Ion-Source in standard and enhanced (MD) mode**
Jan Müller, Reinhard Dörner, Frederik King, Leo Schaechter, Kurt Ernst Stiebing
- WE-121 **Measurements of the kinetic-energy-release (KER) of vibrational cooled HeH⁺ and H³⁺ at the electrostatic Frankfurt low energy storage ring (FLSR)**
Jan Müller, Reinhard Dörner, Frederik King, Lothar Schmidt, Markus Schöffler, Kurt Ernst Stiebing
- WE-122 **Asymmetries of the electron cusp in heavy-ion atom collisions**
Pierre-Michel Hillenbrand, Siegbert Hagmann, Yuri A. Litvinov, Thomas Stöhlker
- WE-123 **Towards laser-controlled generation of hydrogen-like ions in Rydberg states**
Joan Dreiling, Aung Naing, Joseph Tan
- WE-124 **Universal empirical and theoretical fits to K- and L-shell x-ray production cross sections by protons**
Gregory Lapicki
- WE-125 **Multiple ionization effects on L X-ray in Bi by proton impact**
Sunita Sharma
- WE-126 **Determination of the ⁴P/²P ratio in single electron capture of C⁴⁺(1s²/1s2s ³S) ion beams in 6-18 MeV collisions with gas targets**
Ioannis Madesis, Aggelos Laoutaris, Emmanuel Benis, Tom Kirchner, Theo Zouros
- WE-127 **Effective solid angle correction factors for long-lived Auger states populated in low-Z ion collisions with gas targets**
Emmanuel Benis, Stefanos Nanos, Ioannis Madesis, Aggelos Laoutaris, Tom Gorczyca, Theo Zouros
- WE-128 **Investigation of 2s2p ^{3,1}P excitation and (1s2s ³S)nl capture lines in 6-18 MeV C⁴⁺ (1s²,1s2s ³S) collisions with gas targets**
Aggelos Laoutaris, Ioannis Madesis, Emmanuel Benis, Theo Zouros
- WE-129 **A 150 kV Highly Charged Ions Research Platform in Shanghai**
Baoren Wei, Xincheng Wang, Yu Zhang, Di Lu, Ke Yao, Roger Hutton, Yaming Zou
- WE-130 **Electron capture and subsequent radiative decay of fast Xe⁵⁴⁺ ions in collisions with Kr and Xe gaseous targets**
Bian Yang, Deyang Yu, Caojie Shao, Yingli Xue, Wei Wang, Junliang Liu, Rongchun Lu, Mingwu Zhang, Zhangyong Song, Fangfang Ruan, Xiaohong Cai
- WE-131 **Atomic structure calculations of He and Li-like Ti ions for interpreting astrophysical spectra**
Gajendra Singh, Ajay Kumar Singh
- WE-132 **Theoretical study on projectile coherence effects in fully differential ionization cross sections**
Ladislau Nagy, Borbély Sándor, Ferenc Járαι-szabó
- WE-133 **Studies of single- and double-electron capture by highly charged ions isolated at very low energy in a Penning trap**
Joseph Tan, Joan Dreiling, Shannon Hoogerheide, Aung Naing, David Schultz, Yuri

Ralchenko

- WE-134 **Radiative Double Electron Capture (RDEC) in $F^{9+} + Ne$, He Collisions**
David La Mantia, P. N. S. Kumara, Asghar Kayani, Anna Simon, John Tanis
- WE-135 **Production of low energy “cusp” electrons in slow ion-atom collisions**
Roger Hutton, Baoren Wei
- WE-136 **Two-centre Born approach to fully differential proton-impact ionisation of hydrogen: coherent versus incoherent combination of amplitudes**
Jackson Bailey, Ilkhom Abdurakhmanov, Alisher Kadyrov, Igor Bray
- WE-137 **Calculations of stopping power for protons in hydrogen**
Jackson Bailey, Ilkhom Abdurakhmanov, Alisher Kadyrov, Igor Bray
- WE-138 **Competition between radiative and Auger decay processes of doubly excited Li-like C, N and O ions**
Naoki Numadate, Yoshiyuki Uchikura, Kento Shimada, Takuto Akutsu, Hajime Tanuma
- WE-139 **The effect of coupled states on the differential and total cross section in excitation channel**
Mohammad Bolorizadeh
- WE-140 **A Quasi Four-Body FWL Treatment of Single Charge Transfer in Energetic Proton-Helium Collisions**
Mohammad Bolorizadeh, Zohre Safarzade, Reza Fathi, Farideh Shojaei Akbarabadi, Michael Brunger
- WE-141 **Single electron transfer in the collision of He^+ ion with Hydrogen atom**
Mohammad Bolorizadeh, Sh Azizan, Reza Fathi, Farideh Shojaei
- WE-142 **Single ionization of Helium at 0.5 - 2 MeV proton impact: On the quest for projectile coherence effects**
J. Gatzke, F. Navarrete, M. Ciappina, H. Gatzke, O. Chuluunbaatar, S. A. Zaytsev, A. A. Bulychev, K. A. Kouzakov, A. Galstyan, M. Waitz, H.-K. Kim, T. Bauer, A. Laucke, S. Eckart, G. Kastirke, J. Müller, M. Ritzer, E. Bloch, M. Richter, K. Fehre, M. Kunitski, Ch. Müller, J. Voigtsberger, J. Rist, K. Pahl, M. Honig, M. Pitzer, M. Weller, I. Vela Pérez, J. Hoehl, G. Nalin, S. Grundmann, H. Maschkiwitz, C. Janke, S. Zeller, C. Goihl, Y. Herrman, D. Trabert, T. Jahnke, L. Ph. H. Schmidt, Yu. V. Popov, R. Dörner, R. O. Barrachina, and Markus Schöffler
- WE-143 **Time evolution of the population distribution in charge exchange collisions**
Kento Shimada, Naoki Numadate, Yoshiyuki Uchikura, Takuto Akutsu, Ling Liu, Jian-guo Wang, Hajime Tanuma
- WE-144 **Single Ionization of Helium atoms in the collision of fast protons**
Mohammad Bolorizadeh, Farideh Shojaei, Reza Fathi, Sh Azizan, M Rahmanian
- WE-145 **Prior collision interactions in differential cross sections for charge transfer processes**
Mohammad Bolorizadeh, Farideh Shojaei, Reza Fathi, M Rahmanian

9 HEAVY PARTICLE - ATOM/ION

- TH-001 **PENNING-TRAP EXPERIMENTS FOR EXTREME-FIELD PHYSICS**
Manuel Vogel, Z Andelkovic, G Birkel, M Ebrahimi, Z Guo, T Murböck, W Nörtershäuser, W Quint, S Ringleb, S Schmidt, N Stallkamp, Th Stöhlker, M Wiesel
- TH-002 **Correlation Dynamics in Double Photoionization of Excited Helium Atom by a Single Ultrashort XUV Pulse**
Aihua Liu, Dajun Ding, Uwe Thumm
- TH-003 **Observing the ultrafast buildup of a Fano resonance**
Alexander Blättermann, Andreas Kaldun, Veit Stooß, Stefan Donsa, Hui Wei, Renate Pazourek, Stefan Nagele, Christian Ott, Chii-Dong Lin, Joachim Burgdörfer, Thomas Pfeifer
- TH-004 **Electron Matter-Wave Vortices in Double Photoionization of Helium by Attosecond Pulses**
J. M. Ngoko Djiokap, A. V. Meremianin, N. L. Manakov, S. X. Hu, L.B. Madsen, Anthony F Starace
- TH-005 **Impact of fullerene polarizability on Wigner time delay in photodetachment of fullerene anions CN^-**
Valeriy Dolmatov
- TH-006 **Coherence effects in laser-induced ultrafast response of complex atoms**
Yongqiang Li and Jianmin Yuan
- TH-007 **Disentangling intracycle interferences in the photoelectron spectrum of argon using orthogonally polarized two-colour laser pulses**
Xinhua Xie, Tian Wang, ShaoGang Yu, XuanYang Lai, Stefan Roither, Daniil Kartashov, Markus Schöffler, XiaoJun Liu, André Staudte, Markus Kitzler
- TH-008 **Mechanisms of near-threshold harmonic generation in atoms**
Wei-Hao Xiong, Qihuang Gong, Liang-You Peng
- TH-009 **Perspectives of AMO endstation at Shanghai XFEL**
Yizhu Zhang, Jing Zhu, Xincheng Wang, Yuhai Jiang
- TH-010 **Attosecond time delays in the valence photoionization of xenon and iodine at energies degenerate with core emissions**
Maia Magrakvelidze, Himadri Chakraborty
- TH-011 **Localizing High-Lying Rydberg Wave Packets with Orthogonally-Polarized Two-Color Laser Fields**
Seyedreza Larimian, Ji-Wei Geng, Stefan Roither, Daniil Kartashov, Li Zhang, Mu-Xue Wang, Qihuang Gong, Liang-You Peng, Christoph Lemell, Shuhei Yoshida, Joachim Burgdörfer, Andrius Baltuška, Markus Kitzler, Xinhua Xie
- TH-013 **Sideband and streaking regimes in two-color photoionization by twisted X-waves in strong infrared fields**
Birger Böning, Stephan Fritzsche
- TH-014 **Intracycle interference in laser assisted XUV atomic hydrogen ionization**
Ana Gramajo, Renata Della Picca, Roberto Garibotti, Diego Arbó
- TH-015 **Non-perturbative semiclassical model for strong-field ionization**
Nikolay Shvetsov-Shilovski, Manfred Lein, L Madsen, E Räsänen, Christoph Lemell, Joachim Burgdörfer, Diego Arbó, Károly Tokesi
- TH-016 **Intensity-dependent shift in transverse electron momentum distribution for strong field ionization**

Nida Haram, Han Xu, Atia-tu-Noor Atia-tul-Noor, Sainadh Satya Undurti, Igor Ivanov, Igor Litvinyuk, R. T. Sang

TH-017 **Attosecond Time Delay in Photoemission and Electron Scattering near Threshold**

Alexander Bray, Anatoli Kheifets, Igor Bray

TH-018 **Study of atomic delays in negative ions**

Jan Marcus Dahlström, Eva Lindroth

TH-019 **Tunneling ionization imaging of photoexcitation of NO by ultrafast laser pulses**

Tomoyuki Endo, Akitaka Matsuda, Mizuho Fushitani, Tomokazu Yasuike, Oleg I. Tolstikhin, Toru Morishita, Akiyoshi Hishikawa

TH-020 **Two-center interferences in atomic RABBIT-like experiments**

Diego Boll, Omar Fojón

2. PHOTON - MOLECULE (WEAK FIELD PHENOMENA)

TH-021 **Enhanced chiral asymmetries in the inner-shell photoionization of uniaxially oriented methyloxirane enantiomers**

Maurice Tia, Martin Pitzer, Gregor Kastirke, Janine Gatzke, Hong-Keun Kim, Florian Trinter, Jonas Rist, Alexander Hartung, Daniel Trabert, Juliane Siebert, Kevin Henrichs, Jasper Becht, Stefan Zeller, Helena Gassert, Florian Wiegandt, Robert Wallauer, Andreas Kuhlins, Carl Schober, Tobias Bauer, Natascha Wechselberger, Philipp Burzynski, Jonathan Neff, Miriam Weller, Daniel Metz, Max Kircher, Markus Waitz, Joshua Williams, Lothar Schmidt, Anne Müller, André Knie, Arno Ehresmann, Andreas Hans, Ltaief Ben Ltaief, Robert Berger, Hironobu Fukuzawa, Kiyoshi Ueda, Horst Schmidt-Böcking, Reinhard Dörner, Till Jahnke, Philipp Demekhin, Markus Schöffler

TH-022 **Disentangling energy transport in photosynthetic proteins using action spectroscopy on fast ions beams**

Mark Stockett, Christina Kjær, Jørgen Houmøller, Bjarke Pedersen, Lihi Musbat, Yoni Toker, Bruce Milne, Angel Rubo, Steen Brøndsted Nielsen

TH-023 **Inelastic squared form factors of the valence-shell excitations of hydrogen studied by high-resolution inelastic x-ray scattering**

Long-Quan Xu, Ya-Wei Liu, Lin-Fan Zhu

TH-024 **The observation of the pair of Lyman-a and Lyman-b photons produced in the photodissociation of H₂**

Kouichi Hosaka, Yutaro Torizuka, Philipp Schmidt, Takeshi Odagiri, Andre Knie, Kari Jankala, Arno Ehresmann, Masashi Kitajima, Noriyuki Kouchi

TH-025 **Comparative study of carbon dioxide by high-resolution inelastic x-ray and electron scattering**

Dongdong Ni, Longquan Xu, Yawei Liu, Linfan Zhu

TH-026 **Electron pair escape from fullerene cage via collective modes**

Paola Bolognesi, Emma Sokell, Michael Schuler, Yaroslav Pavlyukh, Jamal Berakdar, Lorenzo Avaldi

TH-027 **Dynamics of ion-molecule reactions of SO₂⁺ with H₂O and CH₄**

Antonella Cartoni, Daniele Catone, Paola Bolognesi, Mauro Satta, Pal Markus, Lorenzo Avaldi

TH-028 **Evidence for Efficient Pathway to Produce Slow Electrons by Ground-state**

Dication in Clusters

Daehyun You, Hironobu Fukuzawa, Yuta Sakakibara, Tsukasa Takanashi, Yuta Ito, Gianluigi G. Malinar, Koji Motomura, Kiyonobu Nagaya, Toshiyuki Nishiyama, Kazuki Asa, Yuhiro Sato, Norio Saito, Masaki Oura, Markus Schöffler, Gregor Kastirke, Uwe Hergenbahn, Vasili Stumpf, Kirill Gohkberg, Alexander I. Kuleff, Lorenz S. Cederbaum, and Kiyoshi Ueda

TH-030 **Vector correlation**

F. Trinter, L. Ph. H. Schmidt, T. Jahnke, M. S. Schöffler, O. Jagutzki, A. Czasch¹, J. Lower, T. A. Isaev, R. Berger, A. L. Landers, Th. Weber, R. Dörner, and Horst Schmidt-Böcking

TH-031 **Disentangling sequential from concerted three-body fragmentation of molecules**

Jyoti Rajput, T Severt, B Berry, B Jochim, P Feizollah, P Kanaka Raju, M Zohrabi, U Ablikim, F Ziaee, B Kaderiya, D Rolles, A Rudenko, K D Carnes, B D Esry, I Ben-Itzhak

TH-032 **Photoionisation of allene and propyne**

John Neville, Priya Bhutani, Egill Antonsson, Safia Benkoula, Christophe Nicolas, Minna Patanen, Catalin Miron

TH-033 **Single-or double-electron emission within the Keldysh nonequilibrium Green's function – a diagrammatic approach**

Yaroslav Pavlyukh, Michael Schueler, Jamal Berakdar

TH-034 **Direct monitoring of photon induced isomerization, dissociation and electron detachment of the green fluorescent protein chromophore anion**

Eduardo Carrascosa, Michael S. Scholz, James N. Bull, Evan J. Bieske

TH-035 **Spectator Auger decays of cis-1,1,2,2,3,4-hexafluorocyclobutane in the F 1s region**

Kazumasa Okada, Takuma Kaneda, Hiroshi Iwayama, Eiji Shigemasa

TH-036 **Multicoincidence Studies of Ionization of Chiral Molecules in Strong Laser Fields**

Kilian Fehre, Maksim Kunitski, Lothar Ph. Schmidt, Christian Janke, Stefan Zeller, Martin Pitzer, Till Jahnke, Reinhard Dörner, Markus Schöffler

TH-037 **A method to determine the energy-transfer distribution in ion-molecule collisions via PEPICO experiments: the case of glycine**

Paola Bolognesi, Jacopo Chiarinelli, Alicja Domaracka, Patrick Rousseau, Robert Richter, Lorenzo Avaldi

TH-038 **PLEIADES: an ultra-high resolution soft x-ray beamline for spectroscopy of dilute species**

John Bozek, Christophe Nicolas, Aleksandar Milosavljevic, Emmanuel Robert, Jean-Marc Bizau, Catalin Miron

TH-039 **X-ray absorption spectra of excited triplet states of organic molecules**

Atsunari Hiraya, Haruka Inui, Sho Yamahira, Osamu Takahashi

TH-040 **“Position” does matter : the photofragmentation of the nitroimidazole isomers**

Jacopo Chiarinelli, Paola Bolognesi, Annarita Casavola, Antonella Cartoni, Matteo Castrovilli, Daniele Catone, Robert Richter, Stefano Borocci, Sanja Tosic, Hanan Sa'adeh, Masa Masic, Bratislav Marinkovic, Kevin Prince, Lorenzo Avaldi

TH-041 **Photodetachment cross sections for molecular anions of astrophysical interest**

Lorenzo Ugo Ancarani, Carlos Mario Granados-Castro, Miguel Lara, Thierry Stoecklin

TH-042 **NOO peroxy isomer discovered in the velocity-map imaged photoelectron spectrum of NO₂⁻**

Benjamin Laws, Steven Cavanagh, Brenton Lewis, Stephen Gibson

TH-044

Shallow Core Ionization of the Tetrachloroethene Molecule

Antonio Santos, Michael MacDonald, Alexandre Rocha, Narayan Appathurai, Marcelo Sant'Anna, William Holetz, Ralph Wehlitz, Lucia Zuin

6. LEPTON - MOLECULE

TH-045

Single and Double differential cross sections for ionization of water molecules in the liquid state by fast electrons.

Maria Laura De Sanctis, Marie-Françoise Politis, Rodolphe Vuilleumier, Carlos Raúl Stia, Omar Ariel Fojón

TH-046

Development of the Time-Resolved Electron Momentum Spectroscopy Apparatus in Hefei

Yaguo Tang, Xu Shan, Zhaohui Liu, Shanshan Niu, Enliang Wang, Xiangjun Chen

TH-047

Electron Momentum Spectroscopy Investigation of Valence Electronic Structures of CH₃I

Yaguo Tang, Shanshan Niu, Zhaohui Liu, Yufeng Shi, Enliang Wang, Xu Shan, Xiangjun Chen

TH-048

Positron scattering upon a "simple" endohedral

Miron Amusia, Larissa Chernysheva

TH-049

N₂ dissociative ionization by electron impact

Y. Zhang, X. Wang, L. F. Zhu, D. Lu, R. Hutton, Y. Zou, B. Wei

TH-051

Electron Interactions with Plasma Feed Gases

Chetan Limbachiya, Rakesh Bhavsar, Mohit Swadia

TH-052

Resonances in low-energy electron scattering from para-Benzoquinone

Alexandra Loupas, Jimena D. Gorfinkiel

TH-053

Computation of electron impact total cross sections for Glycine over an extensive range of impact energy (0.1 – 5000 eV)

Mohit Swadia, Ashok Chaudhary, Minaxi Vinodkumar, Chetan Limbachiya

TH-054

Cross sections calculations for electron interaction with astrocompounds

Yogesh Thakar, Rakesh Bhavsar, Mohit Swadia and Chetan Limbachiya

TH-055

Electron Interactions with Furan (C₄H₄O), Tetrahydrofuran (C₄H₈O) and 2, 5-Dimethylfuran (C₆H₈O) Molecules

Rakesh Bhavsar, Yogesh Thakar, Mohit Swadia and Chetan Limbachiya

TH-056

Effect of microhydration on the resonances of pyridine and thymine

Jimena D. Gorfinkiel, Agnieszka Sieradzka

TH-057

Excitation of guanine molecules in gas phase under the low energy electron beam

Svida Yu.Yu., Shafranyosh M.I., Margitich M.O., Sukhoviya and Miroslav Shafranyosh

TH-058

High resolution measurements of positron and electron scattering from water

Rina Kadokura, Andrea Loreti, Samuel Fayer, Ákos Kövér, Gaetana Laricchia

TH-059

Spectroscopic wavelength shifts characterizing the phase transition of helium adsorbed on fullerene cations

Yang Wang, M. Kuhn, M. Renzler, J. Postler, S. Ralser, S. Spieler, M. Simpson, H. Linnartz, A. G. G. M. Tielens, J. Cami, A. Mauracher, M. Alcamí, F. Martín, M. K. Beyer, R. Wester, A. Lindinger, Paul Scheier

- TH-060 **A space-charge-effect-compensated electron monochromator for electron-impact multi-coincidence measurements**
Takuma Okumura, Yuma Mori, Hirofumi Akasaka, Kouichi Hosaka, Masashi Kitajima, Noriyuki Kouchi
- TH-061 **Dissociative electron attachment experiments with biomolecular targets**
Michal Ryszka, Sylwia Ptasińska
- TH-062 **Positron and Electron Scattering with Biological Molecules**
Joshua Machacek, David Stevens, Tamara Babij, Michael Brunger, Stephen Buckman, James Sullivan
- TH-063 **Kinetic energy release of fragments from electron impact dissociation of the molecular hydrogen ion**
Liam Scarlett, Mark Zammit, Dmitry Fursa, Igor Bray
- TH-064 **Valence electronic structures of isopropyl iodide investigated by using electron momentum spectroscopy**
Minfu Zhao, Xu Shan, Shanshan Niu, Yaguo Tang, Zhaohui Liu, Xiangjun Chen
- TH-065 **Molecular-frame EELS experiment on inner-valence ionization of N₂**
Noboru Watanabe, So Yamada, Masahiko Takahashi
- TH-066 **Relationship between interference pattern and molecular orbital shape: a binary (e, 2e) study on SF₆**
Noboru Watanabe, Masakazu Yamazaki, Masahiko Takahashi
- TH-067 **Absolute cross sections for silver clusters (Ag_n, n=1-4) by electron impact**
Paresh Modak, Bobby Antony
- TH-068 **Coherence and symmetry breaking in dissociative electron attachment to molecular hydrogen**
Erumathadathil Krishnakumar, Vaibhav S Prabhudesai, Nigel J Mason
- TH-069 **Precise variational calculations for few-body systems using Hylleraas-type basis sets**
Jayanta Kumar Saha
- TH-070 **Experimental scaling of plane-Born cross sections for the electron-impact excitation to the b¹Π_u state of N₂ molecule**
Atsuya Tanaka, Hidetoshi Kato, Masamitsu Hoshino, Hiroshi Tanaka
- TH-071 **Electron impact scattering study of H₂ molecule**
Hitesh Yadav, Minaxi Vinodkumar, Chetan Limbachiya, P. C. Vinodkumar
- TH-072 **Study of dissociative electron attachment of H⁻ from HCl**
Minaxi Vinodkumar, Hitesh Yadav, P. C. Vinodkumar
- TH-073 **Theoretical investigation of water ionization by electron impact at low energies**
István Tóth, Ladislau Nagy
- TH-074 **Absolute elastic differential cross sections for PF₃ molecule by electron impact: A comparative study with XF₃ (X=B,C,N and CH) molecules**
Naoki Hishiyama, Masamitsu Hoshino, Francisco Blanco, Gustavo Garcia, Hiroshi Tanaka

8. HEAVY PARTICLES (COLD COLLISIONS)

- TH-075 **Universal Properties of p-Wave Fermi Gases**
Zhenhua Yu

- TH-076 **Lifetimes of ultralong-range strontium Rydberg molecules in a dense BEC**
F. Barry Dunning, Francisco Camargo, Joseph Whalen, Roger Ding, Thomas Killian, Jesus Perez-Rios, Shuhei Yoshida, Joachim Burgdorfer
- TH-077 **Rydberg atom scattering in $K(12p)-CH_3NO_2$ collisions: role of transient ion pair formation**
F. Barry Dunning, Michael Kelley, Sitti Buathong
- TH-078 **Fermi liquid nature in one-dimensional strongly attractive Hubbard model**
Xiwen Guan
- TH-079 **Optical fields to control ultracold atomic/molecular collisions**
A. Orbán, O. Dulieu, and Nadia Bouloufa-maafa
- TH-081 **Universal Behavior of Spin Dipolar Relaxation in Atomic Condensates**
Yuangang Deng, Yiquan Zhou, Min Deng, Qi Liu, Mengkhon Tey, Bo Gao, Li You
- TH-082 **Anisotropic blockade using pendular long-range Rydberg molecules**
Matthew Eiles, Hyunwoo Lee, Jesus Perez-Rios, Chris Greene
- TH-083 **Ultracold Collision between Spin-Orbit-Coupled Dipoles**
Christiaan Hougaard, Jia Wang, Brendan Mulkerin, Xia-ji Liu, Hui Hu
- TH-084 **Calculations of long-range three-body interactions for $He(n_0\ ^1S) - He(n_0\ ^1S) - He(n_0\ ^1P)$**
Pei-Gen Yan, Li-Yan Tang, Zong-Chao Yan, James F Babb
- TH-085 **Creation of Rydberg Polarons in a Bose Gas**
F. Camargo, R. Schmidt, J. D. Whalen, R. Ding, G. Woehl Jr., S. Yoshida, J. Burgdorfer, F. B. Dunning, H. R. Sadeghpour, E. Demler, Thomas Killian
- TH-086 **Direct Photoassociation of Halo Molecules in ^{86}Sr**
J. A. Aman, J. C. Hill, Thomas Killian
- TH-087 **Development of a linear wave Stark velocity filter for studying cold ion-polar molecule reactions in interstellar clouds**
Kunihiro Okada, Yusuke Takada, Naoki Kimura, Michiharu Wada, Hans A. Schuessler
- TH-088 **Ultracold molecules strongly coupled to a nanophotonic crystal: an universal platform for ultracold chemistry experiments**
Jesus Perez Rios, May Kim, Chen-Lung Hung
- TH-089 **Heteroisotopic Feshbach resonances in collisions of cold Ca and Ca^+**
Marko Gacesa, Robin Cote
- TH-090 **Using trilobite-like Rydberg trimers to probe Efimov states**
Robin Cote and Jovica Stanojevic
- TH-091 **Rubidium Magnetic-Optical-Trap Reaction Microscope**
Renyuan Li, Qiuxiang Meng, Junyang Yuan, ‡, Yizhu Zhang, Xincheng Wang, Matthias Weidemüller, Y.H. Jiang
- TH-092 **Observation of atom-surface interaction near dielectric surface using ultracold rubidium atoms**
Go Tanaka, Yutaka Kobayashi, Kosuke Shibata, Satoshi Tojo
- TH-093 **Zeeman and Paschen-Back spectra of rubidium 5S-5D two-photon excitation**
Ryohei Itoyama, Yuta Komiyama, Kousuke Shibata, Satoshi Tojo
- TH-095 **Scattering of two particles in a one-dimensional lattice incorporating multi-band effects**
Seth Rittenhouse, P. Giannakeas, Nirav Mehta

- TH-096 **Dynamic behavior of Bose-Einstein condensates in optical lattices with two- and three-body interactions**
Yan Chen, KeZhi Zhang
- TH-098 **Towards laser cooling of atomic negative ions**
Giovanni Cerchiari, Stefan Erlewein, Alban Kellerbauer
- TH-099 **Emerging novel phases of Bose-Einstein Condensate for various topology**
Priyam Das, Ayan Khan, Prasanta K. Panigrahi
- TH-100 **Elementary excitation of spin-orbit coupled Bose-Einstein condensates in optical lattice**
Ju-kui Xue, Xu-Dian Chai
- TH-101 **Phase transition of soft-core bosons in disordered optical lattice**
Ju-kui Xue, Ji-Ming Gao
- TH-102 **Internal cooling of cold Rb_2^+ ions with cold Rb atoms**
Humberto da Silva Jr, Maurice Raoult, Olivier Dulieu
- TH-103 **Characterization of charge-exchange collisions between ultracold 6Li atoms and $^{40}\text{Ca}^+$ ions**
Ryoichi Saito, Shinsuke Haze, Mizuki Sasakawa, Ryosuke Nakai, Maurice Raoult, Humberto Jr. Da Silva, Olivier Dulieu, Takashi Mukaiyama
- TH-104 **Photodissociation of cold RbBa^+ ions produced in a hybrid cold atom-ion trap**
Humberto da Silva Jr, Maurice Raoult, Amir Mohammadi, Johannes Hecker Denchlag, Olivier Dulieu
- TH-105 **Quantum-State Resolved Study of the Ultracold $\text{K} + \text{KRb}$ Reaction**
J. F. E. Croft, C. Makrides, M. Li, A. Petrov, S. Kotochigova, B. K. Kendrick, N. Balakrishnan
- TH-106 **Beam lifetime measurement and longitudinal dynamics investigation for laser cooling at the CSRe**
Hanbing Wang, Weiqiang Wen, Zhongkui Huang, Dacheng Zhang, Bang Hai, Xiaolong Zhu, Dongmei Zhao, Jie Li, Xiaoni Li, Lijun Mao, Ruishi Mao, Jiancheng Yang, Youjin Yuan, Lewin Eidam, Danyal Winters, Tobias Beck, Daniel Kiefer, Benjamin Rein, Thomas Walther, Markus Loeser, Ulrich Schramm, Mathias Siebold, Michael Bussmann, Xinwen Ma
- TH-107 **Long-range dispersion interactions between excited states of K and rare-gas atoms**
Denghong Zhang, Yabin Xu, Jun Jiang, Li Jiang, Luyou Xie, Chenzhong Dong
TH-108 Preparation for laser cooling of relativistic Li-like O^{5+} at the CSRe
Weiqiang Wen, Hanbing Wang, Zhongkui Huang, Dacheng Zhang, Danyal Winters, Michael Bussmann, Bang Hai, Jie Yang, Xiaolong Zhu, Dongmei Zhao, Xiaoni Li, Jie Li, Lijun Mao, Ruishi Mao, Jiancheng Yang, Youjin Yuan, Xinwen Ma
- TH-108 **Preparation for laser cooling of relativistic Li-like O_5^+ at the CSRe**
Weiqiang Wen, Hanbing Wang, Zhongkui Huang, Dacheng Zhang, Danyal Winters, Michael Bussmann, Bang Hai, Jie Yang, Xiaolong Zhu, Dongmei Zhao, Xiaoni Li, Jie Li, Lijun Mao, Ruishi Mao, Jiancheng Yang, Youjin Yuan, Xinwen Ma

10. HEAVY PARTICLE - MOLECULE

- TH-109 **Near-cold inelastic collisions of $\text{He}(1\text{S})$ with the smallest astrophysical anion observed, $\text{CN}-(1\text{S}^+)$: an accurate quantum dynamical study.**

Fabio Carelli, Francesco Gianturco, Roland Wester

- TH-110 **Probing anion resonances in FeO^- : a species of astrophysical relevance**
Roby Chacko, Shreyak Banhatti, Anit K Gupta, Aravind Gopalan
- TH-111 **Rotationally cold ($>99\%$ $J = 0$) OH^- molecular ions in a cryogenic storage ring**
Henning T Schmidt, Gustav Eklund, Kiattichart Chartkunchand, Emma Anderson, Magdalena Kaminska, Nathalie de Ruelle, Michael Gatchell, Henning Zettergren, Sven Mannervik, Richard Thomas, Henrik Cederquist
- TH-112 **Impulse driven fragmentation of biomolecules**
Linda Giacomozi, Michael Gatchell, Nathalie de Ruelle, Michael Wolf, Giovanna D'Angelo, Henning Schmidt, Henrik Cederquist, Henning Zettergren
- TH-113 **Reactions of O^- with D_2 at low temperatures 10 – 300 K**
Radek Plasil, Thuy Dung Tran, Stepan Roucka, Pavol Jusko, Dmytro Mulin, Illia Zymak, Petr Dohnal, Juraj Glosik
- TH-114 **Contour of full potential energy curves of molecular hydrogen ($N \leq 3$)**
Xianfang Yue, Xiang Gao, and Jia-Ming Li
- TH-115 **Charge dependence of fragmentation process induced by ion collisions with furan molecule**
Ewa Erdmann, Marta Łabuda, Sergio Díaz-Tendero, Néstor Fabián Aguirre, Manuel Alcamí
- TH-116 **Excitation and fragmentation in high velocity $\text{CnN}^+ - \text{He}$ collisions**
Thejus Mahajan, Tijani Id Barkach, Nestor Fabian Aguirre, Manuel Alcamí, Maëlle Bonnin, Marin Chabot, Sergio Diaz-Tendero, Florian Geslin, Thibaut Hamelin, Fairouz Hammache, Clara Illescas, Aurélie Jallat, Alba Jorge, Thibaut Launoy, Thi-Kim-Cuong Le, Arnaud Le Padellec, Fernando Martin, Anne Meyer, Luc Perrot, Thomas Pino, Bernard Pons, Nicolas de Séréville, Karine Béroff
- TH-117 **Development of transferable water-halide potentials**
Raúl Rodríguez-Segundo, Daniel J. Arismendi-Arrieta, Rita Prosmi
- TH-118 **Total cross sections for proton induced electron emission from pyrimidine, THF, and TMP in a screened independent atom model**
Hans Juergen Luedde, Tom Kirchner
- TH-119 **K-K electron transfer and K-ionization in fast ion collisions with adenine and water using KLL Auger electron technique**
Chandan Bagdia, S. Bhattacharjee M. Roychowdhury, A. Mandal and Lokesh Tribedi
- TH-120 **Ionization of water molecules by fast neutral H and He impact**
Juan Manuel Monti, Michele Arcangelo Quinto, Christophe Champion, Roberto Rivarola
- TH-121 **Machine-learning the best potential surfaces for polyatomic molecules and the error bars for non-adiabatic atomic collisions**
Daniel Vieira, Rodrigo Vargas and Roman Krems
- TH-122 **Conformation analysis and semiclassical dynamics study of charge exchange process induced by collision of C_2^+ ions with tetrahydrofuran**
Marta Łabuda, Ewa Erdmann
- TH-123 **Benchmarking the performance of density-functional-based approaches on intermolecular interactions of Helium--water complexes**
Maria Blanco de Paz, Daniel J. Arismendi-Arrieta, Rita Prosmi
- TH-124 **Fully Differential Study of Capture with Vibrational Dissociation in $p + \text{H}_2$ Collisions**

Michael Schulz, Basu Lamichhane, Thusitha Arthanayaka, Ahmad Hasan, Daniel Fischer, Ramaz Lomsadze, Marcelo Ciappina, Francisco Navarrete, Raul Barrachina

- TH-125 **Laboratory Measurements for Deuterated Astrochemistry**
Xavier Urbain, Kyle P. Bowen, Pierre-Michel Hillenbrand, Kenneth A. Miller, Nathalie de Ruelle, Daniel W. Savin
- TH-126 **Electron emission in ionization of bromouracil by fast bare carbon ions**
Madhusree Roy Chowdhury, S. Bhattacharjee, C. Bagdia and Lokesh Tribedi
- TH-127 **Electron emission from water molecule in collisions with fast highly charged C, O and Si-ions and scaling law**
Shamik Bhattacharjee, C. D. Bagdia, M. R. Chowdhury, J. Monti, R. D. Rivarola, D. Misra, L. C. Tribedi
- TH-128 **Bare C-ion impact ionization of adenine molecules : DDCS and TCS measurements**
Shamik Bhattacharjee, C. D. Bagdia, M. R. Chowdhury, J. Monti, R. D. Rivarola, L. C. Tribedi
- TH-129 **Knockout fragmentation and endohedral formation in collisions between C_{60}^+ and noble gas atoms**
Mark Stockett, Michael Gachell, Henning Zettergren, Henning Schmidt, Henrik Cederquist
- TH-130 **Investigation of fragmentation dynamics of nitrogen dimers by collisions with highly charged ions**
Xiaolong Zhu, Shuncheng Yan, Wentian Feng, Dalong Guo, Yong Gao, Shaofeng Zhang, Zhongkui Huang, Hanbing Wang, Dongbin Qian, Dongmei Zhao, Dapu Dong, Xinwen Ma
- TH-131 **Orientation effects in ionisation of CO by proton and ion impact**
Bhas Bapat, Deepak Sharma, Ajit Kumar, Pragya Bhatt, C P Savvan
- TH-133 **Development of a cryogenic linear RF ion trap for the TMU E-Ring**
Hiromasa Yanagase, Takeshi Furukawa, Hajime Tanuma, Haruo Shiromaru, Jun Matsumoto, Toshiyuki Azuma
- TH-134 **Formation of covalent carbon molecules inside clusters of C_{60} molecules after collisions with slow Ar^+ ions**
Rudy Delaunay, Michael Gatchell, Arkadiusz Mika, Alicja Domaracka, Lamri Adoui, Henning Zettergren, Henrik Cederquist, Patrick Rousseau, Bernd A. Huber
- TH-135 **Stereodynamics of asymmetric ion-pair formation in collisions of highly-charged ions with rare gas dimers**
Tomoko Ohyama-Yamaguchi, Atsushi Ichimura
- TH-136 **Quantum-mechanical calculations of rovibrationally resolved cross sections for the charge transfer and excitation in $H^+ + H_2$ and $H + H_2^+$ collisions**
Fuyang Zhou, Yong Wu, Jianguo Wang and Predrag Krstic
- TH-137 **Orientation-dependent dissociation dynamics of H_2O_2**
Nrisimha Murty Madugula, Chandan Bagdia, Lokesh C. Tribedi, Deepankar Misra
- TH-138 **Theoretical study for the exchange reactions of $H^+ + NH \rightarrow NH^+ + H$ and $D + NH \rightarrow ND + H$**
Xianfang Yue
- TH-139 **Rotational energy transfer in collisions of ammonia with rare gas atoms and H_2**
Jérôme Loreau and Ad van der Avoird

- TH-140 **Effect of SWCNT charge on a carbon adatom diffusion**
Longtao Han, Predrag Krstic
- TH-141 **Electron Loss and Capture from Low-Charge-State Oxygen projectiles in Water**
Antonio Santos, Vitor Oliveira, Anderson Gomes, Karoly Tokesy
- TH-142 **Isotope effect in reactive collisions of O^- with H_2 , D_2 and HD**
Martin Cizek, Karel Houfek, Jirí Táborský
- TH-143 **Interference effect in e-emission spectrum from a molecular (N_2) double slit in collisions with fast electrons**
Madhusree Roy Chowdhury, C. R. Stia, O. A. Fojon, R. D. Rivarola and Lokesh Tribed

1. PHOTON - ATOM/ION (STRUCTURE AND SPECTROSCOPY)

- FR-001 **Inelastic x-ray scattering technique and its application on determining the electronic structures of atoms and molecules**
Lin Fan Zhu
- FR-002 **Photodissociation of sympathetically crystallized CaH⁺**
Naoki Kimura, Masatoshi Kajita, Kunihiro Okada
- FR-003 **Accessing the hyperfine splitting in highly charged helium-like ions via angle-resolved x-ray spectroscopic analysis**
Stephan Fritzsche, Zhongwen Wu
- FR-004 **REGLIS3: Rare Elements in-Gas Laser Ionization and Spectroscopy at S3**
Xavier Fléchar, B. Bastin, P. Creemers, P. de Groote, P. Delahaye, R. Ferrer, S. Franchoo, L. P. Gafney, L. Ghys, W. Gins, M. Herbane, M. Huyse, Yu. Kudryavtsev, N. Lecesne, Y. Martinez, E. Mogilevskyi, J. Piot, S. Raeder, H. Savajol, S. Sels, J.-C. Thomas, E. Traykov, C. Van Beveren, P. Van den Bergh, P. Van Duppen, A. Zadvornaya
- FR-005 **Photoionization of Ne⁺ ions and Ne atoms near the K edge**
Alfred Mueller, Dietrich Bernhardt, Alexander Borovik Jr., Ticia Buhr, Jonas Hellhund, Kristof Holste, Arthur Lewis David Kilcoyne, Stephan Klumpp, Michael Martins, Sandor Ricz, Jörn Seltsmann, Jens Viehhaus, Stefan Schippers
- FR-006 **Impact of laser polarization on spectra of Eu 4f⁷6p_{3/2} nl autoionizing states**
Chang-jian Dai, Xin-xin Chang, Jing Wang
- FR-007 **Studying Cold Potassium Rydberg Atoms with an AC-MOT**
Matthew Harvey, John Agomuo, Ahmad Sakaamini, Andrew Murray
- FR-008 **Critical free electron densities and temperatures for spectrum lines in hot and dense plasmas**
Xiang-Fu Li, Gang Jiang, Lu-You Xie
- FR-009 **High precision laser spectroscopy of Li-like Kr³³⁺ at 136eV and perspectives for hyperfine structure studies at highest Z with FLASH**
Günter Brenner, Sven Bernitt, Michael Blessenohl, André Cieluch, Stepan Dobrodey, Zachary Hockenbery, Steffen Kühn, Janko Nauta, Miguel-Angel Sanchez, René Steinbrügge, Sascha Epp, José Ramon Crespo López-Urrutia
- FR-010 **Infrared Photodetachment Spectroscopy Measurement of the Electron Affinity of Gallium and the Fine Structure of Ga⁻**
N.D. Gibson, C.W. Walter, C.T. Crocker, W. Nakayama, J. Wang, J.N. Yukich
- FR-011 **Evolution analysis of EUV radiation from laser-produced tin plasmas**
Maogen Su, Qi Min, Shiquan Cao, Duixiong Sun, P Hayden, Gerry O'Sullivan, Chenzhong Dong
- FR-012 **Radiative lifetime of metastable Xe³⁺ measured using an electrostatic ion beam trap**
Manabu Saito, Asahi Chikaoka, Takuya Majima, Makoto Imai, Hidetsugu Tsuchida
- FR-013 **Hyperfine stark shifts of ground states of ⁸⁷Rb, ⁸⁵Rb**
Xia Wang, Jun Jiang, Luyou Xie, Denghong Zhang, Chenzhong Dong
- FR-014 **Magic wavelengths for the 6s²1S₀ - 6s6p 3P₁ transition in ytterbium atom**
Zhiming Tang, Yanmei Yu, Jiguang Li, Chenzhong Dong
- FR-015 **Lifetimes of bound excited states of Pt⁻**
Kiattichart Chartkunchand, Magdalena Kamińska, Emma K Anderson, Moa K Kristiansson, Gustav Eklund, Odd M Hole, Rodrigo F Nascimento, Mikael Blom, Mikael

Björkhage, Anders Källberg, Patrik Löfgren, Peter Reinhed, Stefan Rosén, Ansgar Simonsson, Richard D Thomas, Sven Mannervik, Vernon T Davis, Paul A Neill, Jeffrey S Thompson, Dag Hanstorp, Henning Zettergren, Henrik Cederquist, Henning T Schmidt

FR-016 Lamb shifts and many-body effects in neutral atoms

Jacinda Ginges, Julian Berengut

FR-017 Analytical Property of Scattering Matrix: Spectroscopy Phenomena and Sharp Overlapping Autoionization Resonances

Rui Jin, Xiao-Ying Han, Xiang Gao, De-Ling Zeng, Jia-Ming Li

FR-018 Laser cooling and spectroscopy of trapped isotope ions injected through Mass Spectrometer

Shuichi Hasegawa, Kyunghung Jung, Yoshihiro Iwata, Kazuhiro Yamamoto, Yuta Yamamoto, Masabumi Miyabe, Ikuo Wakaida

FR-019 Observation of the 1S - 2S transition in trapped antihydrogen

Stefan Eriksson

FR-020 Extended Calculations of Spectroscopic Data for Highly-Charged Ions: Comparison study using MCDHF and RMBPT methods

Chong-yang Chen, Kai Wang, Ran Si, Chun-Yu Zhang, Yao-Wu Liu, Shuang Li, Xue-Ling Guo, Yan Jun

FR-021 Influence of distance between lens and target on emission intensity of neutral and ionic lines in laser-induced silicon plasma

Anmin Chen, Suyu Li, Mingxing Jin

FR-022 Lamb shift measurement of antihydrogen for determining the charge radius of antiproton and a stringent test of CPT symmetry

Naofumi Kuroda, David A. Cooke, Paolo Crivelli, Hiroyuki Higaki, Gianluca Janka, Yasuyuki Matsuda, Balint Radics, Christian Regenfus

2. PHOTON - MOLECULE (STRONG FIELD AND ULTRAFAST PHENOMENA)

FR-023 The possibility for calibrating laser intensity in strong-field-ionization experiments

Song-Feng Zhao, Anh-Thu Le, Cheng Jin, Xu Wang, Xiao-Xin Zhou, Chii-Dong Lin

FR-024 Attosecond time delay in harmonic emissions of H₂ and D₂

Mumta Hena Mustary, Dane Edward Laban, James Barry Oszko Wood, Igor Litvityuk, Robert Sang

FR-025 Observation quasi-periodic structures of laser-air plasma

Xiao-xin Zhou, Zhi-Hong Jiao, Yan-Lei Zuo

FR-026 Reveal multi-channel dynamics from high-harmonic and terahertz-wave spectroscopy (HATS)

Yindong Huang, Chao Meng, Jing Zhao, Xiaowei Wang, Zhihui Lv, Dongwen Zhang, Jianmin Yuan, Zengxiu Zhao

FR-027 Ionization with tailored laser fields from multi-harmonic field synthesizer

Christian Burger, Wilhelm Frisch, Boris Bergues, Pawel Wnuk, Matthias Kling

FR-028 Nanoplasma formed by an ultrashort hard x-ray pulse in Xe clusters

Y. Kumagai, H. Fukuzawa, †, K. Motomura, D. Iablonskyi, K. Nagaya, S. Wada, Y. Ito, T. Takanashi, Y. Sakakibara, D. You, T. Nishiyama, K. Asa, Y. Sato, T. Umemoto, K. Kariyazono, E. Kukkk, K. Kooser, C. Nicolas, C. Miron, T. Asave, L. Neagu, M. Schöffler,

- G. Kastirke, X-J Liu, S. Owada, T. Katayama, T. Togashi, K. Tono, M. Yabashi, K. Gokhberg, L. S. Cederbaum, A.I. Kuleff, and Kiyoshi Ueda*
- FR-029 **Charge migration dynamics after xuv photo excitation of small iodine containing molecules**
Karolin Mertens, Maximilian Hollstein, Kay Bestmann, Stephan Klumpp, Daniela Pfannkuche, Michael Martins
- FR-030 **Time-resolved measurement of Interatomic Coulombic Decay in small helium clusters**
Max Kircher F. Trinter, M. Weller, J. B. Williams, N. Sisourat, S. Kazandjian, M. Waitz, C. Goihl, A. Hartung, H. Sann, A. Schottelius, G. Kastirke, M. Pitzer, D. You, T. Deselaers, Y. Herrmann, M. Tia, M. Schöffler, R. Dörner, T. Jahnke
- FR-031 **Intense-Field Photoionization of Molecules using Ultrashort Radiation Pulses: REMPI in Toluene, Aniline, Phenol, and Fluorobenzene**
Cornelis Uiterwaal, Joshua Beck, Collin McAcy, Timothy Scarborough
- FR-032 **Femtosecond dynamics of correlated many-body states in C₆₀ fullerenes**
Sergey Usenko, Michael Schueler, Armin Azima, Markus Jakob, Leslie Lazzarino, Yaroslav Pavlyukh, Andreas Przystawik, Markus Drescher, Tim Laarmann, Jamal Berakdar
- FR-033 **Self-consistent 2D-Bohmian description of photoelectron holography**
Baptiste Fabre, Bernard Pons
- FR-034 **Dissociative ionization processes of D₂ molecule investigated with a-few-pulse attosecond pulse train**
Tomoya Okino, Yasuo Nabekawa, Katsumi Midorikawa
- FR-035 **Effect of hydrogen bond on the charge transfer dynamics in the excited state of coumarin 343: experimental and theoretical study**
XiaoChun Liu, Hang Yin, Hui Li, DaJun Ding, Ying Shi
- FR-036 **Diffraction Imaging of Coherent Nuclear Motion in I₂**
Chaochao Qin and Yuhai Jiang
- FR-037 **High-Harmonic Generation from Aligned N₂ Molecules Reveals Angle-Resolved Molecular Structures**
Ri Ma, Dajun Ding
- FR-038 **Strong held theories beyond the dipole approximation in nonrelativistic regimes**
Pei-Lun He, Feng He
- FR-039 **Enhanced ionization of C₂H₂ as a function of CC inter-nuclear separation**
Atia Tul Noor, Han Xu, Nida Harem, Robert Sang, I.V. Litvinyuk
- FR-040 **Site-specific production of H₃⁺ by core ionization of CH₃Cl**
Hikaru Fujise, Hiroshi Iwayama, Eiji Shigemasa
- FR-041 **Nonlinear resonant Auger spectra and transient x-ray absorption spectra in CO using an x-ray pump-control scheme**
Song Bin Zhang, Victor Kimberg, Nina Rohringer
- FR-042 **Stereochemical configuration and selective excitation of the chiral molecule halothane**
Martin Pitzer, Gregor Kastirke, Phillip Burzinsky, Miriam Weller, Daniel Metz, Jonathan Neff, Markus Waitz, Florian Trinter, Lothar Ph H Schmidt, Joshua B Williams, Till Jahnke, Horst Schmidt-Böcking, Robert Berger, Reinhard Dörner and Markus Schöffler

- FR-043 **Laser-Induced Oxygen Formation from Carbon Dioxide**
Seyedreza Larimian, Sonia Erattupuzha, Markus Schöffler, Sebastian Mai, Philipp Marquetand, Leticia González, Andrius Baltuška, Markus Kitzler, Xinhua Xie
- FR-044 **Static Exchange in the High-harmonic Generation of N₂**
Yan Yang, Lu Liu and Zengxiu Zhao
- FR-045 **Dissociation of H₂⁺ in strong inhomogeneous near-fields**
Ilhan Yavuz, Marcelo F. Ciappina, Alexis Chacon, Zikri Altun, M. Lewenstein, Matthias F. Kling
- FR-046 **Control of H₂ and D₂ dissociative ionization in the non-linear regime using EUV femtosecond pulses @FERMI**
Fabian Holzmeier, Marius Hervé, Alexander Achner, Thomas Baumann, Michael Meyer, Michele Di Fraia, Paola Finetti, Oksana Plekan, Robert Richter, Carlo Callegari, Kevin C. Prince, David Gauthier, Eleonore Roussel, Roger Bello, Alicia Palacios, Fernando Martín, Henri Bachau, Danielle Doweck
- FR-047 **Structural retrieval of C₂H₄ molecules by laser induced rescattering photoelectron spectroscopy**
Yuta Ito, Richard Carranza, Misaki Okunishi, Robert R. Lucchese, Kiyoshi Ueda
- FR-048 **Intramolecular interference effects in photoelectron momentum distributions arising due to strong-field molecular ionization**
Vladimir Usachenko, Pavel Pyak
- FR-049 **Theory of X-ray photoelectron diffraction from molecules undergoing an ultrafast photochemical reaction**
Shota Tsuru, Tokuei Sako, Takashi Fujikawa, Akira Yagishita
- FR-050 **Orientation-selective molecular tunneling ionization by four-color Fourier-synthesized laser fields**
Hideki Ohmura
- FR-051 **Observation of molecular rotation during femtosecond laser filamentation in air by a pump-probe longitudinal diffraction method**
Qingyi Li, Suyu Li, Anmin Chen, Laizhi Sui, Yuanfei Jiang, Mingxing Jin
- FR-052 **Studying Molecular Structure and Dynamics via Coulomb Explosion Imaging with X-rays and Ultrafast Laser Pulses**
Utug Ablikim, Cedric Bomme, Evgeny Savelyev, Hui Xiong, Razib Obaid, Balram Kaderiya, Sven Augustin, Ileana Dumitriu, Rene Bilodeau, David Kilcoyne, Vinod Kumarappan, Rajesh Kushawaha, Farzaneh Ziaee, Timur Osipov, Artem Rudenko, Nora Berrah, Daniel Rolles
- FR-053 **Laser polarization effect on nitrogen fluorescence emission induced by femtosecond filament in air**
Suyu Li, Anmin Chen, Yuanfei Jiang, Hang Liu, Mingxing Jin
- FR-054 **Strong Field dissociative ionization of D₂⁺**
Sándor Borbély, Attila Tóth, Gábor József Halász, Ágnes Vibók
- FR-055 **Hybrid Basis Close-Coupling Interface to Quantum Chemistry Packages for the Treatment of Ionization Problems**
Carlos Marante, Inés Corral, Luca Argenti, Fernando Martin, Markus Klinker, Jesús González-Vázquez
- FR-056 **Mapping the Evolution of the Coherent Vibrational Wavepacket of Molecules**
Bing Zhang, Shuai Li, Xinli Song, Ying Tang, Bing Zhang

- FR-057 **Ultrafast dynamics in CO₂ studied by XUV-pump – NIR-probe experiments**
Seyyed Javad Robatjazi, Shashank Pathak, W. Lee Pearson, Kanaka Raju Pandiri, Jeffrey Powell, Xiang Li, Balram Kaderiya, Itzhik Ben-Itzhak, Daniel Rolles, Artem Rudenko
- FR-058 **Molecular movies and geometry reconstruction using Coulomb explosion imaging and Bayesian inference**
Ali Ramadhan, Benji Wales, Shoja'eddin Chenouri, Joseph Sanderson
- FR-059 **Contribution of resonance excitation on ionization of OCS molecules in a strong laser field**
Jiaqi Yu, Wenhui Hu, Lanhai He, Chuncheng Wang, Sizuo Luo, Dajun Ding
- FR-060 **Two-color wavemixing in Secondary Ion Mass Spectrometry**
Dusan Lorenc, Monika Jerigova, Dusan Velic
- FR-061 **Adaptive Control-based Femtosecond Laser Post-ionization in Secondary Neutral Mass Spectrometry**
Dusan Velic, Dusan Lorenc, Monika Jerigova, Monika Stupavska
- FR-062 **Mapping the secondary neutral emission in Secondary Ion Mass Spectrometry**
Monika Jerigova, Dusan Lorenc, Dusan Velic
- FR-063 **THz Streaking of the Autoionization Dynamics of O₂ at the Free-Electron-Laser FLASH**
Yifan Liu, Kirsten Schnorr, Georg Schmid, Sven Augustin, Severin Meister, Hannes Lindenblatt, Artem Rudenko, Matthias Kübel, Christian Burger, Nikola Stojanovic, Rolf Treusch, Stefan Düsterer, Till Jahnke, Matthias Kling, Claus Dieter Schröter, Thomas Pfeifer, Robert Moshhammer

5. LEPTON - ATOM/ION

- FR-064 **Spin entanglement in elastic electron scattering from quasi-one electron atoms**
Klaus Bartschat, Samantha Fonseca dos Santos
- FR-065 **Novel mechanism for creating long-lived metastable atomic negative ions**
Zineb Felfli, Alfred Msezane
- FR-066 **Simulating Low Temperature Maxwellian Plasma using SH-HtscEBIT**
Bingsheng Tu, Meichun Li, Zhongzheng Zhao, Yang Shen, Yang Yang, Di Lu, Jun Xiao, Chongyang Chen, Roger Hutton, Yaming Zou
- FR-068 **Low-Cost Computer-Controlled Power Supplies for Optimization and Control of Electron Spectrometers**
Ahmad Sakaamini, Matthew Harvey, Andrew Murray
- FR-069 **Many-body theory of positronium-atom scattering and pick-off annihilation**
Dermot Green, A. R. Swann, G. F. Gribakin
- FR-070 **Positronium formation in positron-hydrogen collisions in Debye plasma**
Jia Ma, Yuancheng Wang
- FR-071 **Positronium formation in positron-lithium collisions with Debye potentials**
Yuancheng Wang, Jia Ma, Liguang Jiao, Yajun Zhou
- FR-072 **Collisional-radiative model for EUV spectra of Pm-like ions in EBIT**
Daiji Kato, Hiroyuki A. Sakaue, Izumi Murakami, and Nobuyuki Nakamura
- FR-073 **Visible M1 transitions in 4f open shell heavy ions observed with an electron beam ion trap**
Shunichi Murata, Takayuki Nakajima, Marianna Safronova, Ulyana Safronova,

Nobuyuki Nakamura

FR-074 **Resonant excitation of highly charged Fe ions observed with a compact electron beam ion trap**

Takashi Tsuda, Erina Shimizu, Safdar Ali, Hiroyuki Sakaue, Daiji Kato, Izumi Murakami, Hirohisa Hara, Tetsuya Watanabe, Nobuyuki Nakamura

FR-075 **Cross sections for electrons scattering from silver at low energies**

Harsh Mohan

FR-076 **Measurements of time-resolved EUV spectra for studying the population kinetics in an electron beam ion trap plasma**

Masashi Monobe, Daiji Kato, Nobuyuki Nakamura

FR-077 **Extreme ultraviolet spectra of multiply charged tungsten ions**

Momoe Mita, Hiroyuki Sakaue, Daiji Kato, Izumi Murakami, Nobuyuki Nakamura

FR-078 **Vortex rings in the ionization of atoms by positron impact**

Francisco Navarrete, Raul Oscar Barrachina

FR-079 **Dielectronic Recombination Rate Coefficient of Si-like ions Ni¹⁴⁺**

Altun Zikri, Erdi Bleda

FR-080 **Electron-impact ionization cross-sections and rate coefficients for the Si-like ions Se²⁰⁺**

Altun Zikri, Erdi Bleda

FR-081 **The AC-MOT Cold Atom Electron Source (CAES)**

Michael Jones, Matthew Harvey, William Bertsche, Guoxing Xia, Swapan Chattopadhyay, Andrew Murray, Robert Appleby

FR-082 **Effect of exchange and absorption potentials in distorted wave calculations for electron impact excitation of autoionizing states of alkali atoms**

Chandra Singh, Aguyo Ochieng, Vincent Agutu, John Okumu

FR-083 **Ionization of rubidium by electron impact**

Karoly Tokesi, Takeshi Mukoyama

FR-084 **Dielectronic Recombination of Tungsten Ions**

Bowen Li, Gerry O'Sullivan, Chenzhong Dong, Yang Li, Xiaokai Xu, Ximeng Chen

FR-085 **Absolute excitation-emission cross section of electron induced argon excitation**

Juraj Országh, Michal Durian, Stefan Matejcik

FR-086 **Measurement of the Integrated Stokes Parameters for Zn 468 nm Florescence Excited by Polarized-Electron Impact**

Nathan Clayburn, Timothy Gay

FR-088 **The Tungsten Project: A complete set of isonuclear dielectronic recombination rate coefficients for use in magnetically confined fusion plasmas**

Simon Preval, Nigel Badnell, Martin O'Mullane

FR-089 **Dielectronic resonances in highly-charged heavy ions observed in ion traps**

Alexander Borovik, Joan Dreiling, Roshani Silwal, Dipti Dipti, Endre Takács, John Gillaspay, Ramaz Lomsandze, Vladimir Ovsyannikov, Kurt Huber, Stefan Schippers, Alfred Müller, Yuri Ralchenko

FR-090 **Guiding of high-current electron beam by macro-insulating units**

Mingwu Zhang, Yingli Xue, Xin Li, Junliang Liu, Bian Yang, Wei Wang, Yipan Guo, Wei Xi, Xiaona Zhu, Liping Yang, Deyang Yu, Caojie Shao, Xiaohong Cai

- FR-091 **Ionization of noble gases by positron impact - threshold studies and progress towards a “complete” experiment**
Tamara Babij, J. R. Machacek, D. J. Murtagh, E. Knudsen, D. W. Mueller, S. J. Buckman, J. P. Sullivan
- FR-092 **X-ray measurements in exotic atoms increase discrepancy in QED tests**
Christopher Chantler, Lucas Smale
- FR-093 **Emission line spectra of the 2s-2p transitions of S VIII-S XIII in the extreme ultraviolet region 160–300 Å**
Safdar Ali, Hiroyuki Kato, Nobuyuki Nakamura

9 HEAVY PARTICLE - ATOM/ION

- FR-094 **MeV ion beam extraction into air with a glass capillary filled with He**
Moemi Asamura, Kunikazu Ishii, Hidemi Ogawa
- FR-095 **Stereoscopic collisions of MeV molecular ion with atom and molecule**
Misaki Masatsugu, Ai Takahashi, Kunikazu Ishii, Hidemi Ogawa
- FR-096 **Time-dependent quantum wave packet dynamics to study charge transfer in heavy particle collisions**
Song Bin Zhang, Yong Wu, Jian Guo Wang
- FR-097 **SPARC experiments with highly charged ions at the HESR of FAIR**
Oleksandr Kovalenko, Yuri Litvinov, Thomas Stöhlker
- FR-098 **Influence of nuclear interaction on atomic ionization during ion-atom collisions**
Prashant Sharma, Tapan Nandi
- FR-099 **Polarisabilities and long-range atom-atom interactions of atoms and ions**
Michael Bromley, Swaantje Grunefeld, Jun Jiang, Yongjun Cheng, Jim Mitroy
- FR-100 **Radiative electron capture: a tool for studying the charge changing processes during the Heavy ion-atom collisions**
Prashant Sharma, Tapan Nandi
- FR-101 **Effects of autoionization in electron loss from helium-like highly charged ions in fast collisions with light atoms**
Konstantin Lyashchenko, Oleg Andreev, Alexander Voitkiv
- FR-102 **Storage test of a table-top electrostatic ion storage ring**
Jun Matsumoto, Ryujiro Saiba, Haruo Shiromaru
- FR-103 **State-selective electron capture in He⁺ + He collisions at intermediate energies**
Dalong Guo, Xinwen Ma, Ruitian Zhang, Shaofeng Zhang, Xiaolong Zhu, Wentian Feng, Yong Gao, Bang Hai, Min Zhang, Hanbing Wang, Zhongkui Huang
- FR-104 **Relativistic coupled-channel calculations of differential ionization cross sections**
Andrey I Bondarev, Yury S Kozhedub, Ilya I Tupitsyn, Vladimir M Shabaev, Guenter Plunien
- FR-105 **Frontiers of atomic physics with highly charged heavy ions at HIAF**
Xinwen Ma, Weiqiang Wen, Shaofeng Zhang, Zhongkui Huang, Hanbing Wang, Jie Yang, Xiaolong Zhu, Rui Cheng, Xiaohong Cai, Lijun Mao, Jiancheng Yang, Lina Sheng, Bo Wu, Xiaohong Zhou, Hushan Xu, Youjin Yuan, Jiawen Xia, Hongwei Zhao, Guoqing Xiao, Wenlong Zhan
- FR-106 **Electromagnetic non-destructive detectors for storage rings**
Shahab Sanjari, Yuri A. Litvinov, Thomas Stöhlker

- FR-107 **Proton and alpha capture studies for nuclear astrophysics at GSI storage rings**
Jan Glorius, Yuri Litvinov, Christoph Langer, Zuzana Slavkovska, René Reifarth
- FR-108 **Wave-packet continuum-discretisation approach to helium single ionisation by energetic protons**
Ilkhom Abdurakhmanov, Alisher Kadyrov, Igor Bray
- FR-109 **Molecular effects in M-shell ionization by slow light ions**
Marek Pajek, Dariusz Bana, Łukasz Jabłoski, Takeshi Mukoyama
- FR-110 **Electron-positron pair creation in collisions of heavy bare nuclei: One-center approach**
Ilia Maltsev, Roman Popov, Andrey Bondarev, Irina Ivanova, Yury Kozhedub, Vladimir Shabaev, Ilya Tupitsyn, Xinwen Ma, Guenter Plunien, Thomas Stöhlker
- FR-111 **Pair creation in low-energy collisions of heavy nuclei beyond the monopole approximation**
Ilia Maltsev, Vladimir Shabaev
- FR-112 **Experimental and Theoretical Study of Projectile Coherence Effects in Ionization of Helium by Ion Impact**
Michael Schulz, Thusitha Arthanayaka, Basu Lamicchane, Ahmad Hasan, Daniel Fischer, Sandor Borbély, Ferenc Járαι-Szabó, Ladislau Nagy
- FR-113 **He⁺-He collisions described within a time-dependent spin-density functional theory approach**
Matthew Baxter, Tom Kirchner, Eberhard Engel
- FR-114 **Numerical Simulations of purification and final charge state analysis of the slow ion beam for the FISIC project**
Ajit Kumar, Alain Méry, Lamri Adoui, Jean-Yves Chesnel, Anna Levy, Stéphane Macé, Christophe Prigent, Jean-Marc Ramillon, Jimmy Rangama, Jean-Pierre Rozet, Patrick Rousseau, Sébastien Steydli, Martino Trassinelli, Dominique Vernhet, Emily Lamour
- FR-115 **Uncertainty Quantification of theoretical atomic and molecular collisional data**
Hyun Kyung Chung, B. J. Braams, K. Bartschat, A. G. Császár, G. W. F. Drake, T. Kirchner, V. Kokoouline, J. Tennyson
- FR-116 **Energy straggling cross section for antiproton-atom collisions**
Xiao-min Tong, Sandor Borbely, Iva Brezinova, F. Lackner, S. Nagele, J. Feist, L. Nagy, K. Tokesi, N. Toshima, J. Burgdorfer
- FR-117 **The role of angular momentum in the spontaneous decay of small copper cluster anions measured on long timescales at DESIREE**
Mark Stockett, Klavs Hansen, Magdalena Kaminska, Rodrigo Nascimento, Emma Anderson, Michael Gatchell, Kiattichart Chartkunchand, Gustav Eklund, Henning Zettergren, Henning Schmidt, Henrik Cederquist
- FR-118 **Mutual Neutralization Studies of O⁻ and N⁺/O⁺ ions at Subthermal Collision Energies**
Mark Stockett, Nathalie de Ruelle, Arnaud Dochain, Magdalena Kaminska, Thibaut Launoy, Rodrigo Nascimento, Henning Schmidt, Henrik Cederquist, Xavier Urbain
- FR-119 **Two-centre convergent close-coupling approach to scattering of multiply-charged ions on atomic hydrogen**
Alisher Kadyrov, Ilkhom Abdurakhmanov, Joshua Faulkner, Kym Massen-Hane, Igor Bray
- FR-120 **Exploring different momentum-transfer regimes in proton-helium collisions**
Antonio Gómez, Marcelo Ambrosio, Lorenzo Ancarani, Darío Mitnik

- FR-121 **Helium double ionization by neutronic impact**
Antonio Gómez, Marcelo Ambrosio, Darío Mitnik, Lorenzo Ancarani
- FR-122 **Upgrade of the Main Magnetic Focus Ion Trap in Giessen**
Marc Keil, Stefan Schippers, Alfred Müller, Alexander Borovik
- FR-123 **Charge-exchange, ionization and excitation processes in low-energy Li⁺-Ar, K⁺-Ar, and Na⁺-He collisions**
Ramaz Lomsadze, Malkhaz Gochitashvili, Giorgi Takadze, Roman Kezerashvili, Michael Schulz
- FR-124 **Cold highly charged ions for highest precision spectroscopy**
Lisa Schmoeger, Oscar Versolato, Maria Schwarz, Julian Stark, Janko Nauta, Jofre Pedregosa, Tobias Leopold, Peter Micke, Thomas Baumann, Alexander Windberger, Thomas Pfeifer, Joachim Ullrich, Piet Schmidt, José Ramon Crespo López-Urrutia
- FR-125 **The controlled excitation of the ²²⁹Th nucleus via atomic processes**
Robert A. Müller, Andrey V. Volotka, Stephan Fritzsche, Andrey Surzhykov
- FR-126 **Post collision interactions in differential and total cross-sections for four-body charge transfer processes**
Malay Purkait, K Purkait, S Halder, A Mondal
- FR-127 **The formation of the protonium atoms at capture of protons by the antiprotons channeled in hydrogenous crystals**
Mykola Maksyuta, Volodymyr Vysotskii
- FR-128 **The investigation of a wake potential of protons channeled in an axial regime in ionic crystals**
Mykola Maksyuta, Volodymyr Vysotskii, Yevgen Martysh
- FR-129 **Time-dependent study of laser-assisted charge transfer in low energy ion-atom collisions**
Cong-zhang GAO, Yong Wu, Song-bin Zhang, Jian-Guo Wang
- FR-130 **Stopping and charge state revolution of low-energy ion beam in plasma**
Yongtao Zhao, Rui Cheng, Xianming Zhou, Yuyu Wang, Yu Lei, Ge Xu, Jieru Ren, Dieter Hoffmann, S. Savin, Roman Gavrilin, Alexander Golubev, Zhanghu Hu, Fei Gao, Younian Wang, Guoqing Xiao
- FR-132 **Injection of cold antiprotons for the ASACUSA antihydrogen experiment**
Minori Tajima, Naofumi Kuroda, Yugo Nagata, Horst Breuker, Pierre Dupré, Tatsuhito Kobayashi, Volkhar Maeckel, Takuya Matsudate, Hiroyuki A. Torii, Hiroyuki Higaki, Yasuyuki Kanai, Yasuyuki Matsuda, Stefan Ulmer, Yasunori Yamazaki
- FR-134 **Molecular Orbital interpretation to the couplings in collisions of 2.5 and 3 MeV Xe^{10+, 12+} - Au and Zr systems**
Punita Verma, Kajol Chakraborty, Ruchika Gupta, Sarvesh Kumar, Gaurav Sharma, Deepak Swami, Samit K. Mandal, C. P. Safvan
- FR-135 **Synthesis of antihydrogen with adiabatically transported cold antiprotons**
Naofumi Kuroda, Minori Tajima, Yugo Nagata, Horst Breuker, Pierre Dupré, Tatsuhito Kobayashi, Volkhard Mäckel, Takuya Matsudate, Hiroyuki A. Torii, Hiroyuki Higaki, Yasuyuki Kanai, Yasuyuki Matsuda, Stefan Ulmer, and Yasunori Yamazaki
- FR-136 **Model for plasma jet-driven magneto-inertial fusion**
Sergei V. Ryzhkov, Victor V. Kuzenov
- FR-137 **Electron attachment studies with 2,3-dimethoxy-5-methyl-1,4-benzoquinone**
Filipe Ferreira Da Silva, João Ameixa, Jusuf Khreis, Stephan Denifl

- FR-138 **Pt(CO)₂Cl₂ fragmentation upon low energy electron interactions**
Filipe Ferreira da Silva, Rachel Thorman, Hang Lu, Lisa McElwee-White, Oddur Ingolfsson
- FR-139 **Elastic Differential Cross Sections for Electron Scattering with Dichloromethane**
Emanuele Lange, Katherina Kruppa, João Ameixa, Alessandra Barbosa, Diego Pastega, Paulo Limão-Vieira, Marcio H. F. Bettega, F. Blanco, Gustavo García, Filipe Ferreira da Silva
- FR-140 **Dissociative electron attachment to 3-bromopyruvic acid**
Filipe Ferreira Da Silva, Stephan Denifl, Ilko Bald, Janina Kopyra
- FR-141 **Localized or delocalized K holes in N₂: Photoelectron Auger electron coincidence experiments with high energy resolution**
G. Nalin, S. Grundmann, I. Vela-Perez, H. Kang, F. Trinter, M. Schöffler, T. Jahnke and R. Dörner
- FR-142 **A combined gas phase and surface study on electron induced decomposition of the heteronuclear FEBID precursor; CpFe(CO)₂Mn(CO)₅**
Oddur Ingolfsson, Rachel M. Thorman, Ilyas Unlu, Julie Spencer, Kelsea R. Johnson, Lisa McElwee-White, Howard Fairbrother
- FR-143 **A combined experimental and theoretical study on dissociative ionization and dissociative electron attachment to the heteronuclear FEBID precursor; HFeCo₃(CO)₁₂**
Oddur Ingolfsson, Ragesh Kumar TP, Ragnar Bjornsson, Sven Barth
- FR-144 **Electron induced fragmentation and deposit formation from nano-meter thin surface layers of HFeCo₃(CO)₁₂ adsorbed on gold surfaces.**
Oddur Ingolfsson, Ragesh Kumar TP, Ilyas Unlu, D. Howard Fairbrother, Sven Barth
- FR-145 **Low energy ELEctron driven chemistry for the advantage of emerging NAno-fabrication methods (ELENA); a Marie Skłodowska-Curie Innovative Training Network.**
Oddur Ingolfsson

1. PHOTON - ATOM/ION (STRONG FIELD AND ULTRAFAST PHENOMENA)

- MO-001 **Multiphoton Ionization in Counter Rotating Circularly Polarized Two-Color Laser Fields**
Nikolai Schlott, Sebastian Eckart, Maksim Kunitski, Martin Richter, Lothar Ph. H. Schmidt, Markus Schöffler, Till Jahnke and Reinhard Dörner
- MO-002 **Photoionization Time delay of Atomic Barium**
Aarthi Ganesan, P.C. Deshmukh, A.S. Kheifets, V.K. Dolmatov, S.T. Manson
- MO-003 **The influence of gas-jet position on the macroscopic high-order harmonic generation**
Guoli Wang, Penghao Zhao, Xiaoxin Zhou
- MO-004 **Angular dependence of Wigner-Eisenbud-Smith time delay in photoionization: A case study on 4 f subshell of atomic mercury**
Ankur Mandal, Pranawa Deshmukh, Valeriy Dolmatov, Anatoli Kheifets, Steven Manson
- MO-005 **Confinement effects and angular dependence of Wigner-Eisenbud-Smith time delay**
Ankur Mandal, Pranawa Deshmukh, Valeriy Dolmatov, Anatoli Kheifets, Steven Manson
- MO-006 **HILITE - High-intensity laser experiments on stored ions**
Stefan Ringleb, Nils Stallkamp, Sugam Kumar, Manuel Vogel, Wolfgang Quint, Gerhard G. Paulus, Thomas Stöhlker
- MO-007 **Multi-electron effects in the photo-emission from few-electron systems - He attoclock, IR-double emission, and molecular ionization**
Armin Scrinzi, Vinay Pramod Majety, Jinzhen Zhu
- MO-008 **Polarization effects in above-threshold ionization of Mg with a mid-infrared strong laser field**
Huipeng Kang, SongPo Xu, YanLan Wang, XuanYang Lai, Thomas Pfeifer, XiaoJun Liu, Jing Chen, Ya Cheng, and ZhiZhan Xu
- MO-009 **Exploration of spectral and temporal fine structures of high-order harmonic generation**
Peng-cheng Li, Xiong-Yuan Lei, Xiao-Xin Zhou, Shih-I Chu
- MO-010 **Observation and coherent control of single-photon laser-enabled Auger decay using the free-electron laser FERMI**
Kenichi Ishikawa, Denys Iablonskyi, Kiyoshi Ueda, Anatoli Kheifets, Giuseppe Sansone, Ant Comby, Tamas Csizmadia, Sergei Kühn, Yevheniy Ovcharenko, Tommaso Mazza, Michael Meyer, Andreas Fischer, Carlo Callegari, Oksana Plekan, Paola Finetti, Enrico Allaria, Luca Giannessi, Kevin C Prince
- MO-011 **Study of angular dependence of photoionization time delay in $(n-1)d \rightarrow \epsilon f$ channels for Zn, Cd and Hg**
Sourav Banerjee, Pranawa Deshmukh, Anatoli Kheifets, Valeriy Dolmatov, Steve Manson
- MO-014 **Strong-field ionization inducing multi-electron-hole coherence probed by attosecond pulses**
Jing Zhao, Jianmin Yuan, Zengxiu Zhao
- MO-015 **Improving harmonic conversion efficiency via optimizing macroscopic properties of the gas medium**

Xiaoyong Li, Guoli Wang, Juan Fan, Jinyu Ma, and Yawen Jiang

MO-016 Nonsequential Double Ionization by Counterrotating Circularly Polarized Two-Color Laser Fields

Sebastian Eckart, Martin Richter, Maksim Kunitski, Alexander Hartung, Jonas Rist, Kevin Henrichs, Nikolai Schlott, Huipeng Kang, Tobias Bauer, Hendrik Sann, Lothar Ph. H. Schmidt, Markus Schöffler, Till Jahnke, Reinhard Dörner

MO-017 Ring Currents in Single Atoms – Ultrafast Preparation and Detection using Strong Field Ionization

Sebastian Eckart, Maksim Kunitski, Martin Richter, Jonas Rist, Alexander Hartung, Florian Trinter, Kilian Fehre, Nikolai Schlott, Kevin Henrichs, Lothar Ph. H. Schmidt, Till Jahnke, Markus Schöffler, Reinhard Dörner

MO-018 Ionization of atoms by few-cycle laser pulses: spatial and temporal interference effects

Sándor Borbély, Attila Tóth, Ladislau Nagy

MO-019 Lithium atom photoionization by ultrashort photo-pulse

Anna Kozhina, Dmitry Arkhipov, Stanislav Borovikh, Alla Mityureva, Valery Smirnov

MO-020 Modification of high-order harmonic generation by an XUV field: retrieving the XUV-assisted photorecombination cross section

Tatiana S. Sarantseva, Mikhail V. Frolov, Nilolay L. Manakov, Nikolay V. Vvedenskii, Anthony F. Starace

MO-021 Circular Dichroism in the Multi-Photon Ionization of Oriented Helium Ions

Markus Ilchen, Nicolas Douquet, Tommaso Mazza, Jones Rafipoor, Carlo Callegari, Paola Finetti, Oksana Plekan, Kevin Prince, Alexander Demidovich, Cesare Grazioli, Lorenzo Avaldi, Paola Bolognesi, Marcello Coreno, Michele DiFraia, Michele Devetta, Yevheniy Ovcharenko, Stefan Duesterer, Kiyoshi Ueda, Klaus Bartschat, Alexei Grum-Grzhimailo, Astislav Bozhevolnov, Andrey Kazansky, Nikolay Kabachnik, Michael Meyer

MO-022 Few-cycle strong-field ionization of atomic hydrogen with elliptically polarized infrared light

Nicolas Douquet, Klaus Bartschat

MO-023 Relativistic ionization probabilities of hydrogenlike ions exposed to intense laser pulses

Irina Ivanova, Alejandro Saenz, Andrey Bondarev, Ilya Maltsev, Vladimir Shabaev, Dmitry Telnov

MO-024 Symmetry Breaking in the Sequential Photoionization of Argon

Markus Ilchen, Gregor Hartmann, Alexei Grum-Grzhimailo, Elena Gryzlova, Alexander Achner, Andreas Beckmann, Jens Buck, Carlo Callegari, Ricardo Cucini, Alberto DeFanis, Eugenio Ferrari, Paola Finetti, Leif Glaser, André Knie, Anton Lindahl, Oksana Plekan, Tommaso Mazza, E. Roussel, Frank Scholz, Ivan Shevchuk, Joern Seltmann, Peter Walter, Jens Viefhaus, Michael Meyer

MO-025 Reconstructing real-time quantum dynamics in strong and short laser fields

Veit Stooss, Stefano M. Cavaletto, Alexander Blättermann, Paul Birk, Christoph H. Keitel, Christian Ott, Thomas Pfeifer

MO-026 Metastable argon production via strong-field excitation

Rohan Glover, Adam Palmer, Milad Dakka, John Holdsworth, Philip Light, Igor Litvinyuk, Andre Luiten, Robert Sang

- MO-027 **Time-Dependent Two-Particle Reduced Density Matrix Theory: Application to High-Harmonic Generation**
Fabian Lackner, Iva B. Bezinová, Takeshi Sato, Kenichi Ishikawa, Joachim Burgdörfer
- MO-028 **Superfluorescence (collective spontaneous emission) observed from helium atoms following excitation using an extreme-ultraviolet free-electron laser**
James Harries, Hikaru Fujise, Ichiro Inoue, Hiroshi Iwayama, Susumu Kuma, Yuki Miyamoto, Kyo Nakajima, Chiaki Ohae, Shigeki Ohwada, Noboru Sasao, Kenji Tamasaku, Tadashi Togashi, Eiji Shigemasa, Makina Yabashi
- MO-029 **Next-level electron dynamics through optimal control or plasmonic fields**
Janne Solanpää, Daniel Reich, Esteban Goetz, Marcelo Ciappina, Christiane Koch, Esa Räsänen
- MO-030 **Footprints of electron correlation in strong field double ionization of Kr close to sequential ionization regime**
Xiaokai Li, Zongqiang Yuan, Difa Ye, Chuncheng Wang, Pan Ma, Wenhui Hu, Sizuo Luo, Libin Fu and Dajun Ding
- MO-031 **Attosecond Streaking of Soft-X-ray Pulses Generated by a mid-IR Laser**
Thomas Gaumnitz, Martin Huppert, Inga Jordan, Yoann Pertot, Arohi Jain, Hans Jakob Wörner
- MO-032 **Unified Time and Frequency Picture of Ultrafast Atomic Excitation in Strong Laser**
H. Zimmermann, S. Patchkovskii, M. Ivanov, and Ulli Eichmann
- MO-033 **Intracycle interference in ionization of Ar by a laser assisted XUV pulse**
Diego Arbó, Sebastián López, Markus Kubin, J. Hummert, Marc Vrakking, Oleg Kornilov
- MO-034 **Manipulating dynamical interference in photoionization processes by inhomogeneous strong-field**
Hicham Agueny, Jan Petter Hansen
- MO-035 **Experimental evidence for Wigner's tunneling time**
Nicolas Camus, Enderalp Yakaboylu, Lutz Fechner, Michael Klaiber, Martin laux, Yonghao Mi, Karen Z. Hatsagortsyan, Thomas Pfeifer, Christoph H. Keitel, Robert Moshhammer
- MO-036 **Generation of few-cycle electromagnetic pulses at combination frequencies of two-color ionizing laser field**
Nikolay Vvedenskii, Vasily Kostin
- MO-037 **Theoretical studies on the fluorescence spectra of solid density Al plasma heated by intense X-ray free electron laser**
Rui Jin, Xiang Gao, Pei-Hong Zhang, Fei-Lu Wang, Xiao-Ying Han, Jia-Ming Li
- MO-039 **Coherent control of the photoelectron angular distribution in photoionization of neon**
Nicolas Douguet, Alexei N. Grum-Grzhimailo, Elena V. Gryzlova, Ekaterina I. Staroselskaya, Klaus Bartschat
- MO-040 **Convergence properties of the separable potential model applied to strong field Hydrogen ionization**
Vladimir Daniel Rodríguez
- MO-041 **Evolution operator technique for strong field atomic ionization with separable potential model**
Vladimir Daniel Rodríguez

- MO-042 **Long-range Coulomb effect in intense laser-driven photoelectron dynamics**
Wei Quan, XiaoLei Hao, SongPo Xu, XuanYang Lai, XiaoJun Liu, Jing Chen
- MO-043 **Alignment dependent spectral modulation in molecular high-order harmonic generation**
Mu-Zi Li Guang-rui Jia and Xue-Bin Bian
- MO-044 **j-resolved measurement of spin polarized electrons produced by strong-field ionization**
Daniel Trabert, Alexander Hartung, Sebastian Eckart, Markus Schöffler, Lothar Schmidt, Anton Kalinin, Florian Trinter, Maksim Kunitski, Reinhard Dörner
- MO-045 **High resolution measurement of isotopic shift in singly charged argon ions**
Sofia Botsi, Nicolas Camus, Lutz Fechner, Thomas Pfeifer, Robert Moshhammer
- MO-046 **Coherent control of the THz radiation in an inhomogenous plasma channel**
Ju-kui Xue, Xiao-Bo Zhang, Xin Qiao, Li-Hong Cheng, Ai-Xia Zhang
- MO-047 **Laser-electron interaction in plasma channel with dispersion effect**
Ju-kui Xue, Li-Hong Cheng
- MO-049 **Attoclock using atomic Hydrogen**
Satya Sainadh Undurti, Han Xu, Atia-Tul Noor, Xionshan wang, William Wallace, Nicolas Douguet, Igor Ivanov, Klaus Bartschat, Anatoli Kheifets, Robert Sang, Igor Litvinyuk
- MO-050 **Sequential ejection of the two valence electrons of beryllium by ultrashort laser pulses**
Samira Barmaki, Marc-André Albert, Stéphane Laulan
- MO-051 **Impact of Coulomb collisions on laser-plasma interaction processes at high densities and relativistic intensities**
Armenuhi Ghazaryan, S.S. Israelyan, H.H. Matevosyan, and Kh.V. Sedrakian
- MO-052 **Two-electron autoionization dynamics in helium driven by intense XUV fields of a free-electron-laser radiation source**
Christian Ott, Lennart Aufleger, Thomas Ding, Marc Rebholz, Maximilian Hartmann, Alexander Magunia, David Wachs, Veit Stooß, Paul Birk, Gergana Borisova, Andrew Attar, Thomas Gaumnitz, Zhi Heng Loh, Stefan Düsterer
- MO-053 **Ab initio simulations of multielectron dynamics in intense laser fields with infinite-range exterior complex scaling**
Yuki Orimo, Takeshi Sato, Kenichi L. Ishikawa
- MO-054 **Near-threshold photoelectron holography beyond the strong-field approximation**
XuanYang Lai, ShaoGang Yu, Carla Figueira de Morisson Faria, XiaoJun Liu
- MO-055 **Resolving forward rescattering photoelectron holography of Ar by phase-controlled two-color femtosecond lasers**
Wenhui Hu, Jiaqi Yu, Lanhai He, Chuncheng Wang, Sizuo Luo, Dajun Ding
- MO-056 **Control of photoemission delay in resonant two-photon transitions**
Luca Argenti, Álvaro Jiménez-Galán, Richard Taïeb, Jérémie Caillat, Alfred Maquet, Fernando Martín
- MO-057 **Analytical model for the calculation of the attosecond transient absorption spectrum of argon**
Coleman Cariker, Tor Kjellsson, Eva Lindroth, Luca Argenti
- MO-060 **Momentum mapping of continuum electron wave packet interference**
Guanghan Ge, Huatang Zhang, Cheng Lin, Jingwen Xu, Jing Chen, Xiaohong Song,

Weifeng Yang

- MO-061 **Double photoionization in vicinity of K-shell resonances and direct double Auger decay of K-shell excited states of O^+-O^{4+} ions**

Jiaolong Zeng, Yongjun Li, Liping Liu, Pengfei Liu, Cheng Gao, and Jianmin Yuan

- MO-062 **The mechanism of high-harmonic generation from solids under intense laser pulses**

Lu Liu, Jing Zhao, Z.X Zhao

5. LEPTON - ATOM/ION

- MO-063 **Theoretical study on the soft X-ray spectra of E1 transition of W LV ion**

Jiaoxia Yang, Xiaobin Ding, Rui Sun, Fumihiro Koike, Izumi Murakami, Daiji Kato, Hiroyuki Sakaue, Nobuyuki Nakamura, Chenzhong Dong

- MO-064 **Dielectronic Recombination of Be-like $^{40}\text{Ar}^{14+}$ at the CSRm**

Zhongkui Huang, Weiqiang Wen, Xin Xu, Tianheng Xu, Hanbing Wang, Lijun Dou, Shuxing Wang, Nadir Khan, Linfan Zhu, Weiqing xu, Ke Yao, Yang Yang, Xiaolong Zhu, Lijun Mao, Xiaoming Ma, Youjin Yuan, Jiancheng Yang, Xinwen Ma

- MO-065 **Calculations of dielectronic recombination of Li-Like Ar^{15+} and Xe^{51+} ions**

Lijun Dou, Weiqiang Wen, Zhongkui Huang, Hanbing Wang, Luyou Xie, Chenzhong Dong, Xinwen Ma

- MO-066 **Influence of Breit interaction on the linear polarization of radiation following electron impact excitation of B-like ions**

Cheng Ren, Fei Jiao, Xia Wang, Jun Jiang, Luyou Xie, Denghong Zhang, Chenzhong Dong

- MO-067 **A coupled rearrangement channel analysis of positronium antihydride PsH**

Takuma Yamashita, Yasushi Kino, Emiko Hiyama, Svante Jonsell, Piotr Froelich

- MO-068 **Analysis of time-of-flight spectra in electron acetylene collision experiment**

Dan Luo, Xincheng Wang, Baoren Wei, Yu Zhanbg, Roger Hutton, Yaming Zou

- MO-069 **Dielectronic recombination of open L-shell argon**

Gang Xiong, Zhimin Hu, Jun Xiao, Ke Yao, Jiyan Zhang, Jiamin Yang, Baohan Zhang, Yaming Zou

- MO-070 **Binding energies of C^{5+} ion under Quantum and Maxwellian Dusty Plasma Environment**

Sayantan Dutta, Jayanta K. Saha and T. K. Mukherjee

- MO-071 **Metastable-bound and Resonance energies of doubly excited $1,3\text{F}^e$ states of two-electron atoms**

Tapan Mukhopadhyay, S. Dutta, A. N. Sil and Jayanta K. Saha

- MO-072 **KLL-dielectronic recombination and polarization of X-ray emissions of H-like to B-like barium ions**

Qianqian Man, Luyou Xie, Haiyue Cui, Jun Jiang, Denghong Zhang, ChenZhong Dong

- MO-073 **Metastable-bound $2p\text{nf}$ (1F^e) states of helium like systems under Debye plasma**

Amar Nath Sil, S. Dutta and T. K. Mukhopadhyay

- MO-074 **Two-electron correlated integrals in finite domain: application in strongly coupled plasma environment**

Sukhamoy Bhattacharyya, Jayanta Kumar Saha and Tapan Kumar Mukhopadhyay

- MO-075 **The influence of Breit interaction and E1-M2 quantum interference on polarization following inner-shell electron-impact excitation of Li-like ions**

- Luyou Xie, Yulong Ma, Qianqian Man, Jun Jiang, Denghong Zhang, ChenZhong Dong
- MO-076 **Dipole transition of two-electron ions under pressure confinement**
Bibhas Dutta, Sukhamoy Bhattacharyya, Jayanta Kumar Saha and Tapan Kumar Mukhopadhyay
- MO-077 **The reliability evaluation on atomic collision measurement by ISO guide 98-3 (Guide to the expression of Uncertainty in Measurement)**
Chang Geun Kim, Kyun Shik Chae, Hyung Seok Shim
- MO-078 **Determination of ion temperature in shanghai Electron Beam Ion Trap, by measuring X-ray spectral line-width and the electron beam width**
Yang Yang, Jun Xiao, Di Lu, Yang Shen, Chongyang Chen, Roger Hutton, Yaming Zou
- MO-079 **Manipulating quantum interferences in laser dressed-helium by the transferred momentum between the electron projectile and helium target**
Hicham Agueny, Abdelkader Makhoute, Alain Dubois
- MO-080 **Electron impact ionization of He(1s2s ³S) and He(1s2s2p ⁴P)**
Matthieu Génévriez, Jozo J. Jureta, Pierre Defrance, Xavier Urbain
- MO-081 **Electron transfer processes in potassium collision with nitroimidazoles: the role of methylation at N1 site**
Mónica Mendes, Filipe Ferreira da Silva, Gustavo García, Paulo Limão-Vieira
- MO-082 **New numerical techniques to determine ionization cross sections: series representation for r_{12}^{-1} integrals and Bohm's velocity field**
Juan Martin Randazzo, Lorenzo Ugo Ancarani
- MO-083 **Commissioning of a high-power electron gun for electron-ion crossed-beams experiments**
Benjamin Ebinger, Alexander Borovik Jr., B. Michel Döhring, Tobias Molkentin, Alfred Müller, Stefan Schippers
- MO-084 **Laser-assisted free-free experiments: the search for dressed-atom effects**
C.M. Weaver, B.N. Kim, N.L.S. Martin, B.A. deHarak
- MO-085 **Strong higher-order resonant contribution to Fe Ka x-ray line polarization in hot anisotropic plasmas**
Chintan Shah, Pedro Amaro, Rene Steinbruegge, Sven Bernitt, Stephan Fritzsche, Andrey Surzhykov, Jose R. Crespo Lopez-Urrutia, Stanislav Tashenov
- MO-086 **Laboratory measurements compellingly support a charge-exchange mechanism for the "Dark matter" » 3.5 keV X-ray line**
Chintan Shah, Stepan Dobrodey, Sven Bernitt, Rene Steinbruegge, Liyi Gu, Jelle Kaastra, Jose R. Crespo Lopez-Urrutia
- MO-087 **Developments towards a transverse free-electron target for the storage ring CRYRING@ESR**
Carsten Brandau, Alexander Borovik, Michel Döhring, Benjamin Ebinger, Christophor Kozhuharov, Tobias Molkentin, Alfred Müller, Thomas Stöhlker, Stefan Schippers
- MO-088 **Inner Shell Excitations through Laser Induced Electron Recollision**
Gilad Marcus, Yunpei Deng, Zhinan Zeng, Zhengmao Jia, Pavel Komm, Yinhui Zheng, Xiaochun Ge and Ruxin Li
- MO-089 **A Perturbative Treatment For the Dielectronic Recombination of the Si-Like Isoelectronic Sequence**
Jagjit Kaur, Thomas Gorczyca, Nigel Badnell
- MO-090 **Accurately determining the number of Auger electrons per nuclear decay for medical isotopes**

Mohammed Alotibi, Maarten Vos, Tamas Torny, Tibor Kibedi, Boon Lee, Andrew Stuchbery, Maxime Roberts, Gregor Greguric

- MO-091 **Positronium impact Single Ionization of Alkali atoms**
Dipali Ghosh, Chandana Sinha
- MO-092 **Accurate Electron Spin Optical Polarimetry (AESOP)**
Timothy Gay
- MO-093 **Relativistic Atomic Structure Calculations of F-like ions**
Nupur Verma, Arun Goyal, Man Mohan
- MO-094 **Calculations of positron cooling and annihilation in noble gases**
Dermot Green, P. Mullan, M. Lee and G. F. Gribakin
- MO-095 **Nuclear reaction in muon atomic collision**
Yasushi Kino
- MO-096 **Kinematically complete scattering cross sections in positron and hydrogen atom collisions**
Alisher Kadyrov, Karoly Tóth
- MO-097 **The 1s Lamb Shift in hydrogen-like Gold by X-Ray Spectrometry with FOCAL**
Tobias Gassner, Martino Trassinelli, Regina Heß, Uwe Spillmann, Dariusz Banas, Karl-Heinz Blumenhagen, Fritz Bosch, Carsten Brandau, Weidong Chen, Christina Dimopoulou, Eckhart Förster, Robert Grisenti, Alexandre Gumberidze, Siegbert Hagmann, Pierre-Michel Hillenbrand, Paul Indelicato, Pawel Jagodzinski, Tino Kämpfer, Christophor Kozhuharov, Michael Lestinsky, Dieter Liesen, Yuri Litvinov, Robert Löttsch, Bruno Manil, Renate Martin, Fritz Nolden, Nikos Petridis, Mohammad Shahab Sanjari, Kai Sven Schultze, Max Schwemlein, Alexandre Simionovici, Markus Steck, Thomas Stöhlker, Csilla Szabo, Sergiy Trotsenko, Ingo Uschmann, Günter Weber, O. Wehrhan, Nicolas Winckler, Danyal Winters, Natalya Winters
- MO-098 **On e + Mn elastic scattering at $\epsilon = 20$ eV impact energy**
Valeriy Dolmatov
- MO-099 **CoBIT Spectroscopy of Mo and Y ions relevant to beyond EUV source development**
Emma Sokell, Safdar Ali, John Sheil, Hiroyuki Kato, Nobuyuki Nakamura
- MO-100 **Theoretical study on the angular distribution of Auger electron emission from highly charged Be-like ions**
Yinglong Shi, Xiaobin Liu, Feiping Lu, Denghong Zhang, Luyou Xie, Chenzhong Dong
- MO-101 **Resonant excitation of electronic transitions in highly charged ions with x-ray radiation from ultrabright light sources**
Sven Bernitt, René Steinbrügge, Stepan Dobrodey, Steffen Kühn, Peter Micke, Jan K. Rudolph, Sascha W. Epp, Thomas Stöhlker, José R. Crespo López-Urrutia
- MO-102 **Positronium Scattering from Hydrogen and Helium Atoms at Low Energies**
Mengshan Wu, Jun-Yi Zhang, Ying Qian, Zong-Chao Yan, Udo Schwingenschlogl
- MO-103 **On the effects of Orbital Angular Momentum (OAM) and impact parameters on (e, 2e) process on atoms by twisted electron**
Aditi Mandal and Rakesh Choubisa
- MO-104 **The S-EBIT Facility at the Helmholtz Institute Jena**
Sergiy Trotsenko, Weidong Chen, Jessica Menssen, Gleb Vorobjev, Alexandre Gumberidze, Christophor Kozhuharov, Frank Herfurth, Reinhold Schuch, and Thomas Stöhlker
- MO-105 **Equipment development for muon mobility measurement in rare gases**

Shiro Matoba, Naritoshi Kawamura, and Kenji Kojima

MO-106 **Prominent role of indirect processes in electron-impact ionization of Xe^{24+} ions**

Pengfei Liu, Jiaolong Zeng, Alexander Borovik, Stefan Schippers, Alfred Müller

MO-107 **Higher-order contribution in the resonance recombination of electron-ion interaction**

Guiyun LIANG, J.R. Crespo Lopez-Urrutia, C. Beilmann, H.G. Wei, G Zhao

MO-108 **Unified quantum theory on atomic multielectron processes: direct multiple ionization by an Auger decay, an electron or photon impact**

Jiaolong Zeng, Pengfei Liu, Cheng Gao, and Jianmin Yuan

MO-109 **A new generation of room-temperature electron-beam ion traps with straight-through, on-axis optical access**

Sven Bernitt, Klaus Blaum, Lisa F Buchauer, Thore M Bucking, Andre Cieluch, Alexander Egl, James R Harries, Sandro Kraemer, Steffen Kuehn, Peter Micke, Rima X Schussler, Christoph Schweiger, Sven Sturm, Robert N Wolf, Jose Crespo Lopez-Urrutia

10 HEAVY PARTICLE - MOLECULE

MO-110 **Double differential cross sections for ion impact ionization of ammonia(NH_3) and methane (CH_4) molecules**

Malay Purkait

MO-111 **Interference in fast bare ions colliding with diatomic molecules**

Malay Purkait, Saheb Halder, Abhoy Mondal

MO-112 **Fragmentation of N_2O under 15-30keV H^- , C^- and O^- negative ions impact**

Xuemei Zhang, Dedong Wang, Guannan Guo

MO-113 **Anisotropic two-body dissociation by highly charged ion impact**

Jyoti Rajput, A Agnihotri, A Cassimi, X Flechard, S Guillous, W Iskandar, A Mery, J Rangama, C. P. Safvan

MO-114 **Dissociation dynamics of NH_3 under slow highly charged ion impact**

C P Safvan, Pragya Bhatt, T Sairam

MO-115 **Bond rearrangement in NH_3 under slow highly charged ion impact**

Pragya Bhatt, T. Sairam, C. P. Safvan

MO-116 **Improved model for the interference effects in the ionization of H_2 by fast ions**

Ladislau Nagy, Lorand Czipa

MO-117 **Fragmentation dynamics of nitrogen dimers: role of the neighbor and access to the 3D geometry**

Xavier Fléhard, A. Méry, A. N. Agnihotri, J. Douady, B. Gervais, S. Guillous, W. Iskandar, E. Jacquet, J. Matsumoto, J. Rangama, F. Ropars, C.P. Safvan, H. Shiromaru, D. Zanuttini, A. Cassimi

MO-118 **Angular distributions in two body breakup of OCS^{q+} ions**

Herendra Kumar, Pragya Bhatt, C. P. Safvan, Jyoti Rajput

MO-119 **Three-body dissociation of OCS^{3+} : separating sequential and concerted pathways**

Herendra Kumar, Pragya Bhatt, C. P. Safvan, Jyoti Rajput

MO-120 **Excitation of diatomic carbon molecules by collision**

Aurelie Jallat, Marin Chabot, Karine Béroff, Sandra Bouneau, Florian GESLIN, Thibaut Hamelin, Arnaud Le Padellec, TKC Le, Guillaume Martinet, Luc Perrot, Van tiep

Phung, Thomas Pino

- MO-121 **Chiral Effects in Collisions of Protonated Amino Acids and Amino Acid Inclusive Diastereomeric Complexes with Chiral and Achiral Molecules**
Oleksii Rebrov, Kostiantyn Kulyk, Mauritz Ryding, Richard D. Thomas, Einar Uggerud, Mats Larsson
- MO-122 **Stability of dimer and trimer of Naphthalene studied in electrostatic storage Miniring.**
Serge Martin, L. Chen, J. Bernard, G. Montagne, C. Joblin and A. Cassimi
- MO-123 **Ab initio study of proton collisions with BeH**
Ismanuel Rabadan, Luis Mendez, Junwen Gao, Yong Wu, Jianguo Wang
- MO-124 **A non-adiabatic wave packet study of the post-collisional fragmentation of H₂O**
Ismanuel Rabadan, Jaime Suarez, Luis Mendez
- MO-125 **Proton impact fragmentation of water molecules**
Pavel Nikolaevich Terekhin, Michele Arcangelo Quinto, Juan Manuel Monti, Omar Ariel Fojón, Roberto Daniel Rivarola
- MO-126 **Multiple electron processes from H₂O by He²⁺ and Li³⁺ impact**
Pavel Nikolaevich Terekhin, Michele Arcangelo Quinto, Juan Manuel Monti, Omar Ariel Fojón, Roberto Daniel Rivarola
- MO-127 **Charge transfer cross sections of slow light element ions in collisions with carbon tetrafluoride and sulfur hexafluoride molecules**
Toshio Kusakabe, Toshiki Asai
- MO-128 **Analysis of radiative emissions from collisions of O⁶⁺ with Ar, H₂O, and CH₄**
Anthony Leung, Tom Kirchner
- MO-129 **Electron emission from water and nucleobases with radio-sensitizer**
Lokesh Tribedi, M. Roy Chowdhury, S. Bhattacharjee, C. Bagdia, A. Mandal, D. Misra, C. Champion, J. Monti, R.D. Rivarola
- MO-130 **Quantum calculations of the O(³P)+CO scattering**
Marko Gacesa, David W. Schwenke
- MO-131 **Radiative double electron capture (RDEC) in F⁹⁺ + N₂ collisions**
Nuwan Kumara, David La Mantia, Asghar Kayani, Anna Simon, John Tanis
- MO-132 **Comparison between anion and cation emission from CH₄ molecules colliding with 10.5-keV C⁺ ions: fragment-energy aspects**
John Tanis, Jean-Yves Chesnel, Zoltan Juhasz, E Lattouf, Bernd Huber, S. Kovacs, Peter Herczku, E Bene, V Vizcaino, Alain Mery, J.-C. Pouilly, Jimmy Rangama, Bela Sulik
- MO-133 **Three-body fragmentation dynamics of N₂O induced by 56 keV/u Ne⁸⁺ collision**
Xu Shan, Xi Zhao, Xiaolong Zhu, Wentian Feng, Enliang Wang, Zhenjie Shen, Lei Chen, Dalong Guo, Yong Gao, Ruitian Zhang, Shuncheng Yan, Shenyue Xu, Bang Hai, Hanbing Wang, Zhongkui Huang, Xinwen Ma, Xiangjun Chen
- MO-134 **Vibrational radiative cooling of isolated C⁴⁻ and C⁶⁻**
Ryuta Suzuki, Naoko Kono, Reito Andou, Takeshi Furukawa, Jun Matsumoto, Hajime Tanuma, Toshiyuki Azuma, Klavs Hansen, Haruo Shiromaru
- MO-135 **Electron-transfer studies in potassium collisions with tetrachloromethane**
Khrystyna Regeta, Tiago Cunha, Filipe Ferreira da Silva, Gustavo García and Paulo Lima-Vieira
- MO-136 **Detection of recurrent fluorescence photons emitted from C⁴⁻**

Mai Yoshida, Takeshi Furukawa, Jun Matsumoto, Hajime Tanuma, Toshiyuki Azuma, Haruo Shiromaru, Klavs Hansen

MO-137 Importance of the Auger electron emission in proton-induced interactions in biological medium: a TILDA-V Monte Carlo tracking

Michele Arcangelo Quinto, J. M. Monti, P. F. Weck, O. A. Fojón, R. D. Rivarola and C. Champion

MO-138 TILDA-V: a full-differential Monte Carlo for describing the energy deposition at the nanometer scale for protons in biological matter

Michele Arcangelo Quinto

MO-139 Commissioning of a new cryogenic ion storage ring RICE

Yuji Nakano, Yoshinori Enomoto, Takuya Masunaga, Sebastian Menk, Paul Bertier, Toshiyuki Azuma

MO-140 Total cross sections of ionization and electron capture for DNA nucleobases impacted by light ions

Michele Arcangelo Quinto, J. M. Monti, P. F. Weck, O. A. Fojón, R. D. Rivarola and C. Champion

MO-141 Multiple ionization and dissociation of ethylene induced by collision of Xe⁹⁺

Kiichi Yokokawa, Jun Matsumoto, Haruo Shiromaru, Pragya Bhatt, Herendra Kumar, Cholakka Safvan

MO-142 Spontaneous decay of hot Ag_n⁻ clusters in a cryogenic environment

Emma Anderson, Magdalena Kaminska, Kiattichart Chartakunchand, Gustav Eklund, Michael Gatchell, Klavs Hansen, Henning Zettergren, Henrik Cederquist, Henning Schmidt

MO-143 Fragmentation dynamics of multiply ionized acetylene: dependence on the charge state of intermediate ions

Takuya Majima, Shintaro Yoshida, Masaya Matsubara, Hidetsugu Tsuchida, Manabu Saito

2. PHOTON - MOLECULE (COLD SPECIES, STORAGE AND CLUSTERS)

- TU-001 **Spin-polarized electrons upon nondipole photodetachment of fullerene anions**
Alexander Edwards, Caleb Lane, Valeriy Dolmatov
- TU-002 **Photoionization and photofragmentation of $\text{Sc}_3\text{N@C}_{80}^+$ at energies from the carbon K edge to the scandium L and nitrogen K edges**
Alfred Mueller, Sadia Bari, Ticia Buhr, Jonas Hellhund, Kristof Holste, Arthur Lewis, David Kilcoyne, Michael Martins, Sandor Ricz, Kaja Schubert, Stefan Schippers
- TU-003 **Photoionization and photofragmentation of $\text{Lu}_3\text{N@C}_{80}^{q+}$ ions ($q = 1, 2, 3$)**
Jonas Hellhund, Alexander Borovik Jr., Kristof Holste, Stephan Klumpp, Michael Martins, Sandor Ricz, Stefan Schippers, Alfred Mueller
- TU-004 **A Single Atom Antenna**
Florian Trinter, Christiane Rauch, Joshua B. Williams, Miriam Weller, Markus Waitz, Martin Pitzer, Jörg Voigtsberger, Carl Schober, Gregor Kastirke, Christian Müller, Christoph Gohl, Phillip Burzynski, Florian Wiegandt, Robert Wallauer, Anton Kalinin, Lothar Ph. H. Schmidt, Markus S. Schöffler, Ying-Chih Chiang, Kirill Gokhberg, Till Jahnke, Reinhard Dörner
- TU-005 **A molecular movie of Interatomic Coulombic Decay in NeKr**
Florian Trinter, Tsveta Miteva, Miriam Weller, Sebastian Albrecht, Alexander Hartung, Martin Richter, Joshua Williams, Averell Gatton, Bishwanath Gaire, Thorsten Weber, James Sartor, Allen Landers, Ben Berry, Vasili Stumpf, Kirill Gokhberg, Reinhard Dörner, Till Jahnke
- TU-006 **Photodissociation of orange I monoanion studied using an electrostatic storage ring**
Manabu Saito, Tetsumi Tanabe, Masami Lintuluoto, Evgeni Starikov, Koji Noda, Takuya Majima, Shigeo Tomita, Katsutoshi Takahashi
- TU-007 **Investigation of environmental effects in prototypical noble gas clusters using fluorescence spectroscopy**
Andreas Hans, Xaver Holzapfel, Philipp Schmidt, Christian Ozga, Uwe Hergenbahn, Till Jahnke, Reinhard Dörner, Arno Ehresmann, André Knie
- TU-008 **A comprehensive study of Interatomic Coulombic Decay in argon dimers: Extracting R-dependent absolute decay rates from the experiment**
Jonas Rist, Tsveta Miteva, Bishwanath Gaire, Hendrik Sann, Florian Trinter, Marco Keiling, Nele Gehrken, Ali Moradmand, Ben Berry, Mohammad Zohrabi, Maksim Munitski, Itzik Ben-Itzhak, Ali Belkacem, Thorsten Weber, Allen Landers, Markus Schöffler, Joshua B. Williams, Premysl Koloren, Kirill Gokhberg, Till Jahnke, Reinhard Dörner
- TU-009 **Interatomic Coulombic Decay of HeNe dimers after ionization and excitation of He and Ne**
Jonas Rist, Hendrik Sann, Hong-Keun Kim, Felix Sturm, Florian Trinter, Markus Waitz, Stefan Zeller, Birte Ulrich, Moritz Meckel, Stefan Voss, Tobias Bauer, Deborah Schneider, Horst Schmidt-Böcking, Robert Wallauer, Markus Schöffler, Joshua B. Williams, Reinhard Dörner, Till Jahnke
- TU-010 **Angle-resolved Auger electron spectroscopy providing a sensitive access to a hidden vibronic coupling**
Andre Knie, Minna Patanen, Ivan Petrov, John Bozek, Arno Ehresmann, Philipp Demekhin

- TU-011 Mapping the entirety of optical transitions in the singly excited regime of hydrogen and its isotopes with rotational resolution**
Philipp Schmidt, Andreas Hans, Christian Ozga, Arno Ehresmann, André Knie
- TU-012 Photodetachment thermometry of stored OH⁻ at the Cryogenic Storage Ring**
Christian Meyer, Arno Becker, Klaus Blaum, Christian Breitenfeldt, Sebastian George, Jürgen Göck, Manfred Grieser, Florian Grussie, Elisabeth Guerin, Robert von Hahn, Philipp Herwig, Jonas Karthein, Claude Krantz, Holger Kreckel, Jorrit Lion, Svenja Lohmann, Preeti Mishra, Olda Novotný, Aodh O'Connor, Roland Repnow, Sunny Saurabh, Dirk Schwalm, Lutz Schweikhard, Kaija Spruck, Sudhakaran Sunil Kumar, Stephen Vogel, Andreas Wolf
- TU-013 Cross sections for the formation of H(2p) atom via doubly excited states in photoexcitation of rotationally cold H₂**
Yuta Abe, Takeshi Odagiri, Takuro Taniguchi, Takahisa Shiratori, Masashi Kaida, Kazufumi Yachi, Yoshiaki Kumagai, Koichi Hosaka, Masashi Kitajima, Noriyuki Kouchi
- TU-014 Photo induced dissociation of hydrogenated pyrene molecules**
Michael Wolf, Hjalte Kiefer, Jeppe Langeland, Lars Andersen, Henning Schmid, Henrik Cederquist, Henning Zettergren, Mark Stockett
- TU-015 MFPADs as tool to experimentally prove O K-shell hole localization in CO₂ due to asymmetric stretching**
Isabel Vela-Perez, Florian Trinter, Giammarco Nalin, Etienne Bloch, Huipeng Kang, Markus S. Schöffler, Martin Pitzer, Abir Mhamdi, Philipp Demekhin, Till Jahnke, Reinhard Dörner
- TU-016 Multicoincidence studies of resonant Interatomic Coulombic Decay in Ne₂**
Derya Aslitürk, Jonas Rist, Markus Waitz, Daniel Trabert, Sebastian Eckart, Pia Huber, Christian Janke, Sven Grundmann, Miriam Weller, Darja Trojanowskaja, Kevin Henrichs, Gregor Kastirke, Christoph Goihl, Max Kircher, Nikolai Schlott, Maurice Tia, Markus Schöffler, Hendrik Sann, Florian Trinter, Till Jahnke, Reinhard Dörner
- TU-017 Surface chemistry of colloidal surfactant-free gold nanoparticles generated by laser ablation**
Anna Levy, Jerome Gaudin, Martino Trassinelli, David Amans, Manuel De Anda Villa, John Bozek, Valérie Blanchet, Sophie Cervera, Robert Grisenti, Emily Lamour, Stéphane Macé, Christophe Nicolas, Irene Papagiannouli, Minna Patanen, Christophe Prigent, Jean Pierre Rozet, Sébastien Steydli, Dominique Vernhet

3. PHOTON - CONDENSED MATTER AND OTHER TARGETS

- TU-018 Terahertz generation in crystal driven by two-color laser pulses**
Xiao-xin Zhou, Lei Zhang, Zhong Guan, Guo-Li Wang
- TU-020 Bohmian-trajectories analysis of high harmonic generation from solids**
Jinlei Liu, Lu Liu, Wenpu Dong, Yindong Huang, Jing Zhao, Jianmin Yuan, Zengxiu Zhao
- TU-021 Improvement of MCP detectors to achieve a dead-time-free measurement of groups of charged particles**
Christian Janke, Achim Czasch, Dennis Schmidt, Gregor Kastirke, Juliane Siebert, Kilian Fehre, Lothar Schmidt, Markus Schöffler, Stefan Zeller, Sven Schöbller, Till Jahnke, Reinhard Dörner

- TU-022 **Effects due to the induced potential in ultrashort laser interactions with Al(100) and Al(111) surfaces**
Carlos Alberto Rios Rubiano, Renata Della Picca, Dario M. Mitnik, Vyacheslav M. Silkin, Maria Silvia Gravielle
- TU-023 **Mapping and control of ultrafast plasmons with PEEM**
B. Ji, J. Qin, P. Lang, A. Koya, H. Tao, X. Song, X. Gao, Z. Hao and Jingquan Lin
- TU-024 **Photoionization of open-shell halogen atoms endohedrally confined in C₆₀**
Dakota Shields, Ruma De, Mohamed Madjet, Steven T. Manson, Himadri Chakraborty
- TU-025 **Absolute detection efficiencies for multi coincidence studies**
Kilian Fehre, Darja Trojanowskaja, Maksim Kunitski, Lothar Ph. Schmitt, Janine Gatzke, Till Jahnke, Ottmar Jagutzki, Achim Czasch, Jürgen Stohner, Robert Berger, Reinhard Dörner, Markus Schöffler
- TU-026 **Comparative time-resolved photoelectron spectroscopy from Cu(100) and Cu(111) surfaces**
Marcelo Ambrosio, Uwe Thumm
- TU-027 **RABBITT spectroscopy of transition-metal surface states**
Marcelo Ambrosio, Uwe Thumm
- TU-028 **Electron-positron pair production in space-time-dependent colliding laser pulses**
Ivan Aleksandrov, Guenter Plunien, Vladimir Shabaev
- TU-029 **Coherent control of two-color above-threshold photoemission from tungsten nanotips**
Timo Paschen, Michael Förster, Michael Krüger, Christoph Lemell, Georg Wachter, Florian Libisch, Thomas Madlener, Joachim Burgdörfer, Peter Hommelhoff
- TU-030 **Simulation of High Harmonic Generation in Solids**
Isabella Floss, Georg Wachter, Christoph Lemell, Shunsuke Sato, Xiao-Min Tong, Kazuhiro Yabana, Joachim Burgdörfer
- TU-031 **Optimization of laser plasma dynamics towards high order harmonic generation applications**
Smijesh Nadarajan Achary, Kavya Hemantha Rao, Dashavir Chetty, Robert Sang, Igor Litvinyuk
- TU-032 **Plume dynamics of a laser produced plasma: Single and double pulse schemes**
Kavya Hemantha Rao, Smijesh Nadarajan Achary, Dashavir Chetty, Igor Litvinyuk, Robert Sang
- TU-033 **Soft X-ray induced ultraviolet fluorescence emission from bulk and interface of a liquid water microjet**
Andreas Hans, Christian Ozga, Robert Seidel, Philipp Schmidt, Timo Ueltzhöffer, Xaver Holzapfel, Marvin N. Pohl, Philip Wenzel, Isaak Unger, Philipp Reiß, Emad F. Aziz, Arno Ehresmann, Petr Slavíček, Bernd Winter, André Knie
- TU-034 **Does Heisenbergs Uncertainty Relation really limits the precision of Quantum Measurements**
Horst Schmidt-Böcking, Hans Jürgen Lüdde, Gernot Gruber, and John S. Briggs
- TU-035 **Controlled samples for single-particle x-ray diffraction**
Daniel Horke, Salah Awel, Zhipeng Huang, Tim Ossenbrüggen, Nils Roth, Igor Rubinsky, Amit Samanta, Vijay Singh, Xiaoyan Sun, Nicole Teschmit, Lena Worbs, Jochen Küpper

- TU-036 Optical focusing of isolated particles for diffractive imaging experiments**
Daniel Horke, Salah Awel, Nils Roth, Xiaoyan Sun, Richard Kirian, Henry Chapman, Andrei Rode, Jochen Küpper
- TU-037 Time-resolved wide-angle x-ray scattering measurements of Xe clusters by XFEL pulses**
Toshiyuki Nishiyama, Yoshiaki Kumagai, Akinobu Niozu, Hironobu Fukuzawa, Koji Motomura, Max Bucher, Yuta Ito, Tsukasa Takanashi, Kazuki Asa, Yuhiro Sato, Daehyun You, Yiwen Li, Taishi Ono, Edwin Kukk, Catalin Miron, Liviu Neagu, Carlo Callegari, Michele Fraia, Giorgio Rossi, Davide Galli, Tommaso Pincelli, Alessandro Colombo, Sigeki Owada, Tadashi Togashi, Kensuke Tono, Makina Yabashi, Kazuhiro Matsuda, Christoph Bostedt, Kiyonobu Nagaya, Kiyoshi Ueda
- TU-038 Attosecond interferometry with free-electron laser pulses**
Sergey Usenko, Andreas Przystawik, Markus Jakob, Leslie Lamberto Lazzarino, Günter Brenne, Sven Toleikis, Christian Haunhorst, Detlef Kip, and Tim Laarmann
- TU-039 Measurement of low cross section transition using versatile absorption technique**
Gaurav Sharma T. Nandi and Nitin K. Puri
- TU-040 Ortho-to-para ratio of water desorbed from ice and its implications for astronomy and planetary science**
Tetsuya Hama, Akira Kouchi, Naoki Watanabe
- TU-041 Ultrafast structural dynamics of metallic materials studied by photoelectron spectroscopy**
Manuel De Anda Villa, Anna Lévy, Jérôme Gaudin, Sophie Cervera, Benoît Chimier, Patrick Combis, Dominique Descamps, Nikita Fedorov, Robert Grisenti, Yuta Ito, Emily Lamour, Stéphane Macé, Patrick Martin, Stéphane Petit, Christophe Prigent, Vanina Recoules, Jean-Pierre Rozet, Laurent Soulard, Sébastien Steydli, Martino Trassinelli, Kiyoshi Ueda, Laurent Videau, Dominique Vernhet
- TU-042 Interaction of femtosecond structured beams with transparent dielectrics**
Andrei V. Rode, Ludovic Rapp, Eugene Gamaly, Remo Giust, Luca Furfaro, Pierre-Ambroise Lacourt, John M. Dudley, Saulius Juodkazis, Francois Courvoisier
- TU-043 Streaked photoelectron spectra from polycrystalline gold**
Marcelo Ambrosio, Uwe Thumm
- TU-044 Design of a charge sensitive spectroscopy amplifier for Compton camera**
Wei Wang, Junliang Liu, Deyang Yu, Xin Li, Xiaohong Cai
- TU-045 Gold nanoparticles and their coatings, their effect on cells and their interaction with radiation**
Sophie Grellet, Małgorzata Smiatek-Telega, Nigel Mason, Jon Golding
- TU-046 Mechanisms of the high-order harmonic generation from solids**
X. B. Bian, T. Y. Du
- TU-047 Coherence of Nonlinear Process**
磊 沈 (ShenLei)
- TU-048 Nuclear excitation by two-photon electron transition**
Stephan Fritzsche, Andrey Volotka
- TU-049 Characteristic X-ray Spectra and relativistic quantum mechanical theory**
Christopher Chantler, Truong Nguyen
- TU-050 Temperature effects on the isomer's stability of van der Waals clusters**
Orlando Carrillo-Bohórquez, Álvaro Valdés de Luxán, Rita Prosimi

6. LEPTON - MOLECULE

- TU-051 **Ionization of NH_3 by Electron and Photon Impact**
Carlos Mario Granados-Castro, Alessandro Genoni, Lorenzo Ugo Ancarani
- TU-052 **Bimodel distribution of vibrationally excited states in NO via DEA to NO_2**
Krishnendu Gope, Vaibhav Prabhudesai, E Krishnakumar
- TU-053 **Dissociation dynamics of transient anion formed via electron attachment to sulphur dioxide (SO_2)**
Krishnendu Gope, Vaibhav Prabhudesai, Nigel Mason, E Krishnakumar
- TU-054 **Electron Induced chemistry of Chlorobenzene**
Dinesh Prajapati, Minaxi Vinodkumar, Chetan Limbachiya, Pothodichackara Vinodkumar
- TU-055 **Electron Impact Ionization of CH_4 for Different Momentum Transfers**
Carlos Mario Granados-Castro, Lorenzo Ugo Ancarani
- TU-056 **Direct evidence of Interatomic Coulombic Decay in electron impact ionization of Ne dimer**
Shuncheng Yan, Pengju Zhang, Xinwen Ma, Shenyue Xu, Bin Li, Xiaolong Zhu, Wentian Feng, Dongmei Zhao, Lili Shen
- TU-059 **Study of inelastic processes for beryllium and its hydrides upon electron impact**
Ashok Chaudhari, Harshad Bhutadia, Chetan Limbachiya
- TU-060 **Molecular frame (e , $2e$ + ion) studies of CH_4 and CF_4**
Alexander Dorn, Khokon Hossen
- TU-061 **Electron impact ionization and total cross section for Pyrimidine**
Chetan Limbachiya, Harshad Bhutadia, Ashok Chaudhari
- TU-062 **Electron-Collision Induced Interatomic Coulombic Decay in Argon Clusters: from Dimers to Trimers**
Xueguang Ren, Alexander Dorn
- TU-063 **Tracing Young-type Interference Effects in Electron-Impact Ionization of Aligned H_2 Molecule**
Xueguang Ren, Enliang Wang, Khokon Hossen, Xingyu Li, Xiangjun Chen, Alexander Dorn
- TU-064 **Electron-Collision Induced Ionization and Fragmentation in Hydrated Biomolecule Clusters**
Xueguang Ren, Alexander Dorn
- TU-065 **Observation of Intermolecular Coulombic Decay in Water-Tetrahydrofuran Dimers Induced by Electron-Impact Ionization**
Xueguang Ren, Alexander Dorn
- TU-067 **Computation of Electron Impact Ionization Cross sections for Diborane - B_2H_6**
Umang Patel, K N Joshipura, H N Kothari
- TU-068 **Electron induced dissociation of Pyrrole molecule**
Hardik Desai, Minaxi Vinodkumar, Hitesh Yadav, P.C. Vinodkumar
- TU-072 **Anionic states of 5-cyaniteuracil (5-OCNU) and 5-thyocyaniteouracil (5-SCNU)**
Lucas Cornetta, Márcio Varella
- TU-077 **Dynamics of Dissociative Electron Attachment to Furan and Pyridine**
Alexander Dorn, Marvin Weyland
- TU-078 **Angle-resolved $e^- + \text{C}_{60}$ elastic scattering cross section versus Ramsauer**

minima in partial elastic scattering cross sections*Valeriy Dolmatov, Miron Amusia, Larissa Chernysheva*

- TU-079 **Total cross sections of $C_n H_6$ ($n = 2, 3, 4$) molecules by e^- and e^+ impact**

Harshit N Kothari, K N Joshipura, Umang R Patel

- TU-080 **Non-resonant vibrational excitation of N_2 by electron impact**

Keir Wren-little, Jonathan Tennyson

- TU-081 **Path integral simulation on the hyperfine coupling constants of the muoniated and hydrogenated acetone radicals**

Yuki Oba, Tsutomu Kawatsu, and Masanori Tachikawa

- TU-082 **Total cross section for low-energy electron scattering from formic acid, (HCOOH), molecules**

Paweł Możejko, Alicja Domaracka, Mateusz Zawadzki, Elżbieta Ptasińska-Denga, Czesław Szmytkowski

- TU-083 **Cross sections calculations for electron scattering from dimethylamine, $NH(CH_3)_2$, molecule**

Paweł Możejko, Bożena Żywicka, Alicja Domaracka

- TU-084 **Energy Flow Between Pyrimidines and Water Triggered by Low Energy Electrons**

Jaroslav Kočišek, Juraj Fedor, Andriy Pysanenko, Mateusz Zawadzki, Michal Fárník, Jan Poštulka, Petr Slavíček

- TU-085 **Dissociation of 2-oxopropanoic acid by low energy electrons.**

Mateusz Zawadzki, Jaroslav Kočišek, Juraj Fedor

- TU-086 **Electron impact study of H_2 and D_2 continuum radiation**

Michal Durian, Marian Danko, Juraj Orszagh, Stefan Matejcik

- TU-087 **Low-energy electron scattering from cyanamide using R-matrix method**

Kedong Wang, Shuangcheng Guo, Ju Meng, Xiaotian Huang and Yongfeng Wang

- TU-088 **Experimental and theoretical progress in time-resolved (e , $2e$) electron momentum spectroscopy of photodissociation dynamics of acetone at 195 nm**

Shotaro Nakayama, Masakazu Yamazaki, Masahiko Takahashi

- TU-089 **Observation of indirect (e , $3e$) of CO induced by electron impact**

Pengju Zhang, Shuncheng Yan, Xinwen Ma and Lili Shen

- TU-090 **Introducing a phase factor for the two-electron continuum representation**

Lorenzo Ugo Ancarani, A S Zaytsev, S A Zaytsev

- TU-091 **Electron Scattering Studies of atomic Mo and MoS_2**

Foram Milind Joshi, Minaxi Vinodkumar, K N Joshipura

- TU-092 **Excitation of Guanine Molecules in Gas Phase under the Low Energy Electron Beam**

Yuri Svyda, Myroslav Shafranyosh, Mykola Margitych, Maria Sukhoviya, Ivan Shafranyosh

- TU-093 **Electron impact scattering study of H_2 molecule**

*Hiteshkumar Yadav, Minaxi Vinodkumar, P.C. Vinodkumar***11 HEAVY PARTICLE - CONDENSED MATTER AND OTHER TARGETS**

- TU-095 **Charge equilibration times for slow highly charged ions in single layer graphene**

Elisabeth Gruber, Richard A. Wilhelm, Janine Schwestka, Valerie Smejkal, Roland

Kozubek, Arkady V. Krasheninnikov, Marika Schleberger, Stefan Facsko, Friedrich Aumayr

- TU-096 **Synthesis of boron-nitride nanostructures in plasma volume**
Predrag Krstic, Longtao Han
- TU-097 **Role of ion impact ionization cross sections in the irradiation of swift heavy ions into condensed matter**
Kengo Moribayashi
- TU-098 **Radiative de-excitation channel of slow highly charged ions transmitted through freestanding single layer graphene**
Richard A. Wilhelm, Janine Schwestka, Elisabeth Gruber, René Heller, Roland Kozubek, Marika Schleberger, Stefan Facsko, Friedrich Aumayr
- TU-099 **From Chains to Rings: Impulse Driven Molecular Growth in C_4H_6 Clusters**
Michael Gatchell, Rudy Delaunay, Arkadiusz Mika, Giovanna D'Angelo, Kostiantyn Kulyk, Alicja Domaracka, Patrick Rousseau, Henning Zettergren, Bernd Huber, Henrik Cederquist
- TU-100 **van der Waals effects in GIFAD for light atoms on insulating surfaces**
G.A. Bocan, J.D. Fuhr, M.S. Gravielle
- TU-101 **Energy loss due to plasmon excitation by the impact of charged particles on solid surfaces: Beyond an standard approximation**
Juana Luisa Gervasoni, Raul Oscar Barrachina, Silvina Segui, Francisco Navarrete, Nestor Arista
- TU-102 **New formula for the electronic stopping power of ions in an electron gas system**
Pedro Luis Grande
- TU-103 **Development of laser target sight-on system based on multiple transmission through a tapered glass capillary for ion microbeam irradiation**
Mikiko Koushima, Tokihiro Ikeda, Mitsuyoshi Matsubara, Takafumi Masuyama, Tatsuya Minowa, Wei-Guo Jin
- TU-105 **Stern-Gerlach-Experiment revisited**
Horst Schmidt-Böcking, Lothar Schmidt, Hans Jürgen Lüdde, Wolfgang Trageser, Gernot Gruber, and Tilman Sauer
- TU-106 **Shaping surface landscapes with molecules: rotationally induced diffractive scattering of H_2 on LiF(001) under fast grazing incidence conditions**
Fernando Martin, Marcos del Cueto, Alberto S. Muzas, Mark F. Somers, Geert-Jan Kroes, Cristina Diaz
- TU-107 **XMCD going ultra-cold: Experiments at 100 mK and 7 T**
Ivan Baev, Torben Beeck, M. Benedetta Casu, Michael Martins, Wilfried Wurth
- TU-108 **Energy deposition around swift proton and carbon ion tracks in biomaterials**
Rafael Garcia-Molina, Maurizio Dapor, Pablo de Vera, Isabel Abril
- TU-109 **Simulation of the energy loss of proton beams interacting with few layer graphene foils**
Juan José Esteve-Paredes, Jorge E. Valdés, Jaime Sánchez-Claros, Isabel Abril, Rafael Garcia-Molina
- TU-110 **Mass spectrometric study of negative secondary ions emitted from ethanol microdroplet surfaces by fast heavy ions**
Kensei Kitajima, Takuya Majima, Shiori Mizutani, Manabu Saito, Hidetsugu Tsuchida
- TU-111 **Active discharging method for stable sub-micron sized beams of slow highly charged ions using tapered glass capillary with electrodes**

Tokihiro Ikeda, Takao M. Kojima, Yoshio Natsume, Jun Kimura, Tomoko Abe

- TU-112 **Collision induced dissociation of the retinal protonated Schiff base**
Michael Wolf, Kostiantyn Kulyk, Linda Giacomozzi, Michael Gatchell, Nathalie de Ruelle, Akos Vegvari, Roman A. Zubarev, Mats Larsson, Henrik Cederquist, Henning T. Schmidt, Henning Zettergren
- TU-113 **M-X-ray emission in interaction of slow highly charged Xe^{q+} ions (q=26-40) with metallic foils**
Łukasz Jabłoński, Dariusz Banaś, Janusz Braziewicz, Joanna Czub, Paweł Jagodziński, Aldona Kubala-Kukuś, Daniel Sobota, Ilona Stabrawa, Marek Pajek
- TU-114 **Electric-field noise and carbon diffusion on Au(110)**
Eunja Kim, A. Safavi-Naini, D. A. Hite, K. S. McKay, D. P. Pappas, P. F. Weck, H. R. Sadeghpour
- TU-115 **Rb adsorbate-induced negative electron affinity on quartz**
Eunja Kim, J. A. Sedlacek, S. T. Rittenhouse, P. F. Weck, H. R. Sadeghpour, J. P. Shaffer
- TU-116 **Defects induced by ion collisions to control the thermal hysteresis in magnetocaloric thin films**
Sophie Cervera, Martino Trassinelli, Louis Bernard Carlsson, Mahmoud Eddrief, Victor Edtgens, Vasilica Gafton, Emily Lamour, Anna Lévy, Stéphane Macé, Massimiliano Marangolo, Christophe Prigent, Jean-Pierre Rozet, Sébastien Steydli, Dominique Vernhet
- TU-117 **Detection of Circular Rydberg states in lifetime measurements**
Gaurav Sharma and Nitin K. Puri
- TU-118 **First-step benchmark of collision cross-sections for heavy ions using charge-state evolutions after target penetration**
Makoto Imai, Viatcheslav Shevelko
- TU-119 **Charge-patch enhanced surface scattering in the transmission of hundred-keV proton through tapered glass capillary**
Jian-Xiong Shao, A. X. Yang, B. H. Zhu, X. M. Chen
- TU-120 **Electrostatic models for fullerene-fullerene interactions**
Michael Gatchell, Stefan Huber, Fredrik Lindén, Henrik Cederq, Andreas Mauracher, Henning Zettergren
- TU-122 **Experimental study of the interaction of ions with metallic nano-particles with sizes up to 10 nm**
Arkadiusz Mika, Rudy Delaunay, Alicja Domaracka, Patrick Rousseau*, Lamri Adoui and Bernd A. Huber*
- TU-123 **Non-radioactive electron source for atmospheric pressure ionization**
Matus Samel, Michal Stano, Miroslav Zahoran, and Štefan Matejčík
- TU-124 **Density-functional approximations on CO₂/sl clathrate hydrate interactions**
Daniel J. Arismendi- Arrieta, Álvaro Valdés de Luxán, Rita Prosimi
- TU-125 **Evolution of the electric potential of an insulator under charged particle impact**
Eric Giglio, Amine Cassimi, Karoly Tökési
- TU-126 **Magnetic resonance of rubidium atoms passing through a multi-layered transmission magnetic grating**
Yugo Nagata, Shutaro Kurokawa, Atsushi Hatakeyama

12. OTHER PROCESSES AND POST-DEADLINE ABSTRACTS

- TU-127 **Description of an elastic scattering process in the pilot-wave formulation**
Ditmar Ciro Cordeiro Ballesteros, Marcos Feole, Clement Collet, Francisco Navarrete, Raul Oscar Barrachina
- TU-129 **Shannon and Fisher entropies as indicators of atomic avoided crossings for Stark states of Rydberg atoms**
Yong Lin He, Yan Chen, Jiu Ning Han, Zhi Bin Zhu, Geng Xiang Xiang, Huai Dong Liu, Bao Hong Ma, De Chun He
- TU-130 **Magic wavelengths of Ca⁺ ion for linearly and circularly polarized light**
Jun Jiang, Li Jiang, Xia Wang, Peter Shaw, Denghong Zhang, Luyou Xie, Chenzhong Dong
- TU-131 **Structures and bonding features of Al_nC_m (n=4, 6; m=1-4) clusters**
Ning Du, Hongshan Chen
- TU-132 **Exploring metastable decay dynamics of polycyclic aromatic nitrogen containing hydrocarbons upon HCN evaporation**
Najeeb P. K, Turaga Sairam, Vinitha M. V, Anudit Kala, Sarita Vig, Pragya Bhatt, Safvan C. P, Umesh Kadhane
- TU-133 **Imaging the three-dimensional shapes and light induced dynamics of rotating helium nanodroplets**
Plekan O, Cucini R, Stienkemeier F, Callegari C, Ueda K, Nishiyama T, Di Fraia M, Fennel T, Clark A, Rupp D, Ovcharenko Y, LaForge A, Coreno M, Langbehn B, Finetti P, Oliver Álvarez de Lara V, Sander K, Piseri P, Möller T, Peltz C, Prince K, Grazioli C, Iablonskyi D

POSTER AUTHOR INDEX



Abdurakhmanov, I.....WE-136, WE-137, FR-108,
FR-119

Abe, T.....TU-111

Abe, Y.....TU-13

Ablikim, U.....TH-31, FR-52

Abril, I.....TU-108, TU-109

Abrok, L.....WE-5

Achner, A.....FR-46, MO-24

Adoui, L.....TH-134, FR-114

Agnihotri, A.....MO-113, MO-117

Agomuo, J.....FR-7

Agueny, H.....MO-34, MO-79

Aguirre, N.....TH-115, TH-116

Agutu, V.....FR-82

Akasaka, H.....TH-60

Akutsu, T.....WE-138, WE-143

Albert, M.....MO-50

Albrecht, S.....TU-05

Alcamí, M.....TH-59, TH-115, TH-116

Aleksandrov, I.....TU-28

Ali, S.....FR-74, FR-93, MO-99

Allaria, E.....MO-10

Alotibi, M.....MO-90

Altun, Z.....FR-45

Amami, S.....WE-88

Aman, J.....TH-86

Amans, D.....TU-17

Amaro, P.....MO-85

Ambalampitiya, H.....WE-10

Ambrosio, M.....FR-120, FR-121, TU-26, TU-27,
TU-43

Ameixa, J.....FR-137, FR-139

Amusia, M.....TH-48, TU-78

Ancarani, L.....TH-41, FR-120, FR-121, MO-82,
TU-51, TU-55, TU-90

Andelkovic, Z.....TH-1

Andersen, L.....TU-14

Anderson, E.....TH-111, FR-15, FR-117, MO-142

Andou, R.....MO-134

Andreev, O.....FR-101

Andric, L.....WE-12

Antonsson, E.....TH-32

Antony, B.....TH-67

Appathurai, N.....TH-44

Appleby, R.....FR-81

Arbó, D.....WE-72, TH-14, TH-15, MO-33

Archubi, C.....WE-72

Argenti, L.....FR-55, MO-56, MO-57

Arismendi- Arrieta, D.....TU-124, TH-117, TH-123

Arista, N.....WE-72, TU-101

Arkhipov, D.....MO-19

Arthanayaka, T.....TH-124, FR-112

Asa, K.....TU-37

Asai, T.....MO-127

Asamura, M.....FR-94

Aslitürk, D.....TU-16

Atia-tul-Noor, A.....TH-16, FR-39

Attar, A.....MO-52

Aufleger, L.....MO-52

Augustin, S.....FR-52, FR-63

Aumayr, F.....TU-95, TU-98

Avaldi, L.....TH-26, TH-27, TH-37, TH-40, MO-21

Awel, S.....TU-35, TU-36

Azima, A.....FR-32

Aziz, E.....TU-33

Azizan, S.....WE-141, WE-144

Azuma, T.....TH-133, MO-134, MO-13
MO-139

Azuma, Y.....WE-18

B

Babb, J.....TH-84
 Babij, T.....H-62, FR-91
 Bachau, H.....FR-46
 Badnell, N.....WE-21, FR-88, MO-89
 Baev, I.....TU-107
 Bagdia, C.....TH-137
 Bagheri, M.....MO-12
 Bailey, J.....WE-136, WE-137
 Balakrishnan, N.....TH-105
 Bald, I.....FR-140
 Ballance, C.....WE-23
 Baltuška, A.....WE-39, TH-11, FR-43
 Ban, G.....WE-65
 Banaś, D.....FR-109, MO-97, TU-113
 Banerjee, S.....MO-11
 Banhatti, S.....TH-110
 Bapat, B.....TH-131
 Barbosa, A.....FR-139
 Bari, S.....WE-5, TU-02
 Barmaki, S.....MO-50
 Barrachina, R.....TH-124, FR-78, TU-127, TU-101
 Barth, S.....FR-143, FR-144
 Bartschat, K.....WE-60, WE-61, WE-2, WE-3,
 FR-64, FR-115, MO-21, MO-22, MO-39, MO-49
 Basak, A.....WE-103, WE-58
 Bass, A.....WE-107
 Bastin, B.....FR-4
 Bauer, T.....WE-44, TH-21, MO-16, TU-09
 Baumann, T.....WE-45, FR-46, FR-124
 Baxter, M.....FR-113
 Becht, J.....TH-21
 Beck, J.....FR-31
 Beck, T.....TH-106
 Becker, A.....WE-64, TU-12
 Beckmann, A.....MO-24
 Beeck, T.....TU-107
 Beerwerth, R.....WE-86, WE-5

Beilmann, C.....MO-107
 Belkacem, A.....TU-08
 Bello, R.....FR-46
 Ben Ltaief, L.....TH-21
 Bene, E.....MO-132
 Benis, E.....WE-126, WE-127, WE-128
 Ben-Itzhak, I.....TH-31, FR-57, TU-08
 Benkoula, S.....TH-32
 Berakdar, J.....TH-26, TH-33, FR-32
 Berengut, J.....WE-28, FR-16
 Berger, R.....TH-21, TU-25
 Bergues, B.....FR-27
 Bernard Carlsson, L.....TU-116
 Bernhardt, D.....WE-64, FR-5
 Bernitt, S.....FR-9, MO-109, MO-85, MO-86,
 MO-101
 Béroff, K.....TH-116, MO-120
 Berrah, N.....WE-52, FR-52
 Berry, B.....TH-31, TU-05, TU-08
 Bertier, P.....MO-139
 Bertsche, W.....FR-81
 Bestmann, K.....FR-29
 Bettega, M.....FR-139
 Beyer, M.....TH-59
 Bhatt, P.....TH-131, MO-114, MO-115, MO-118,
 MO-119, MO-141, TU-132
 Bhattacharjee, S.....TH-127, TH-128
 Bhattacharyya, S.....MO-74
 Bhavsar, R.....TH-51, TH-55
 Bhutadia, H.....TU-59, TU-61
 Bhutani, P.....TH-32
 Bian, X.....TU-46
 Biegert, J.....WE-41, WE-42
 Bieske, E.....TH-34
 Bilodeau, R.....FR-52
 Birk, P.....MO-25, MO-52
 Birkl, G.....TH-1
 Bizau, J.....WE-12, TH-38
 Björkhage, M.....FR-15
 Bjornsson, R.....FR-14

Blanchet, V.....TU-17
 Blanco de Paz, M.....TH-123
 Blanco, F.....TH-74, FR-139
 Blättermann, A.....TH-3, MO-25
 Blaum, K.....MO-109, TU-12
 Bleda, E.....FR-79, FR-80
 Blessenohl, M.....FR-9
 Bloch, E.....WE-45, TU-15
 Blom, M.....FR-15
 Blumenhagen, K.....MO-97
 Bocan, G.....TU-100
 Boll, D.....WE-47, TH-20
 Bolognesi, P.....TH-26, TH-27, TH-37, TH-40, MO-21
 Bolorizadeh, M.....WE-139, WE-140, WE-141,
 WE-144, WE-145
 Bomme, C.....FR-52
 Bondarev, A.....FR-104, FR-110, MO-23
 Böning, B.....TH-13
 Bonnin, M.....TH-116
 Borbély, S.....FR-112, FR-116, FR-54, MO-18
 Borisova, G.....MO-52
 Borka, D.....WE-108
 Borocci, S.....TH-40
 Borovik, A.....FR-5, FR-89, FR-122, MO-83,
 MO-87, MO-106, TU-03
 Borovikh, S.....MO-19
 Bosch, F.....MO-97
 Bostedt, C.....TU-37
 Botsi, S.....MO-45
 Bouloufa-maafa, N.....TH-79
 Bouneau, S.....MO-120
 Bourke, J.....WE-109
 Bowen, K.....TH-125
 Bozek, J.....TH-38, TU-10, TU-17
 Bozhevolnov, A.....MO-21
 Braams, B.....FR-115
 Brandau, C.....WE-64, MO-87, MO-97
 Bray, A.....WE-8, TH-17
 Bray, I.....WE-62, WE-95, WE-96, WE-8, WE-136,
 WE-137, TH-17, TH-63, FR-108, FR-119

Braziewicz, J.....TU-113
 Breitenfeldt, C.....TU-12
 Breitenfeldt, M.....WE-65
 Brenner, G.....FR-9
 Březinová, I.....MO-27, FR-116
 Bromley, M.....WE-28, FR-99
 Brøndsted Nielsen, S.....TH-22
 Brown, M.....WE-99
 Brunger, M.....WE-140, TH-62
 Buathong, S.....TH-77
 Bubin, S.....WE-39
 Bučar, K.....MO-48
 Buchauer, L.....MO-109
 Bucher, M.....TU-37
 Buck, J.....MO-24
 Bucking, T.....MO-109
 Buckman, S.....TH-62
 Buhr, T.....FR-5, TU-02
 Bull, J.....TH-34
 Burgdörfer, J.....FR-116, MO-27, WE-1, TH-76,
 TH-85, TH-3, TH-11, TH-15, TU-29, TU-30
 Burger, C.....FR-27, FR-63
 Burkov, S.....WE-24
 Burzynski, P.....TH-21, TU-04
 Bussmann, M.....TH-106, TH-108



Cai, X.....WE-130, FR-90, FR-105, TU-44
 Caillat, J.....MO-56
 Callegari, C.....FR-46, MO-10, MO-21, MO-24,
 TU-37
 Camargo, F.....TH-76, TH-85
 Cami, J.....TH-59
 Camus, N.....MO-35, MO-45
 Cao, S.....WE-25, WE-26, WE-27, FR-11
 Carelli, F.....TH-109
 Cariker, C.....MO-57

Carnes, K.....	TH-31	Chen, X.....	WE-105, WE-110, TH-46, TH-47, TH-64, FR-84, TU-63
Carranza, R.....	FR-47	Chen, Y.....	TH-96
Carrascosa, E.....	TH-34	Cheng, L.....	MO-46, MO-47
Carrillo-Bohórquez, O.....	TU-50	Cheng, R.....	FR-105, FR-130
Cartoni, A.....	TH-27, TH-40	Cheng, Y.....	FR-99
Casavola, A.....	TH-40	Chenouri, S.....	FR-58
Cassimi, A.....	MO-113, MO-117, TU-125	Chernysheva, L.....	TH-48, TU-78
Castrovilli, M.....	TH-40	Chesnel, J.....	FR-114, MO-132
Casu, M.....	TU-107	Chetty, D.....	TU-31, TU-32
Catone, D.....	TH-27, TH-40	Chiang, Y.....	TU-04
Cavaletto, S.....	MO-25	Chiarinelli, J.....	TH-37, TH-40
Cavanagh, S.....	TH-42	Chikaoka, A.....	FR-12
Cederquist, H.....	TH-111, TH-112, TH-129, TH-134, FR-15, FR-117, FR-118, MO-142, TU-99, TU-14, TU-112, TU-120	Chimier, B.....	TU-41
Cerchiari, G.....	TH-98	Choi, H.....	WE-82
Cervera, S.....	TU-41, TU-116, TU-17	Choubisa, R.....	MO-103
Chabot, M.....	TH-116, MO-120	Chu, S.....	WE-49, MO-9
Chacko, R.....	TH-110	Chung, H.....	FR-115
Chacón, A.....	WE-41, WE-42, FR-45	Chwiot, S.....	WE-68, WE-70
Chae, K.....	MO-77	Ciappina, M.....	WE-41, WE-42, WE-71, TH-124, FR-45, MO-29
Chai, X.....	TH-100	Cieluch, A.....	FR-9, MO-109
Chakraborty, A.....	WE-106	Cizek, M.....	TH-142
Chakraborty, D.....	WE-90	Clayburn, N.....	FR-86
Chakraborty, H.....	WE-106, TH-10, TU-24	Cloutier, P.....	WE-107
Chakraborty, K.....	FR-134	Colavecchia, F.....	WE-71
Champion, C.....	TH-120	Cole, K.....	WE-44
Chang, X.....	FR-6	Colgan, J.....	WE-87
Chantler, C.....	WE-109, FR-92, TU-49	Collet, C.....	TU-127
Chapman, H.....	TU-36	Colombo, A.....	TU-37
Charlton, M.....	WE-62	Combis, P.....	TU-41
Chartkunchand, K.....	TH-111, FR-15, FR-117, MO-142	Comby, A.....	MO-10
Chattopadhyay, S.....	FR-81	Conrad, T.....	WE-111
Chaudhari, A.....	TH-53, TU-59, TU-61	Cordeiro Ballesteros,.....	TU-127
Chen, A.....	FR-21, FR-51, FR-53	Coreno, M.....	MO-21
Chen, C.....	FR-66, FR-20, MO-78	Cornetta, L.....	TU-72
Chen, H.....	WE-43, TU-131	Corral, I.....	FR-55
Chen, J.....	WE-50, MO-42	Côté, R.....	TH-89, TH-90
Chen, W.....	MO-97	Couratin, C.....	WE-65
		Courvoisier, F.....	TU-42

Covington, C.....WE-39
 Creemers, P.....FR-4
 Crespo López-Urrutia,.....MO-109, MO-85,
 MO-86, MO-107, FR-9, FR-124, MO-101
 Crocker, C.....FR-10
 Croft, J.....TH-105
 Császár, A.....FR-115
 Csizmadia, T.....MO-10
 Cubaynes, D.....WE-12
 Cucini, R.....MO-24
 Cui, H.....MO-72
 Czasch, A.....TU-21, TU-25
 Czipa, L.....MO-116
 Czub, J.....TU-113

D

da Silva, H.....TH-102, TH-103, TH-104
 Dahlström, J.....TH-18
 Dai, C.....FR-6
 Dakka, M.....MO-26
 D'Angelo, G.....TH-112, TU-99
 Danko, M.....TU-86
 Dapor, M.....TU-108
 Das, P.....TH-99
 Davis, V.....FR-15
 De Anda Villa, M.....TU-41, TU-17
 de Groote, P.....FR-4
 de Harak, B.....MO-84
 de Lucio, O.....WE-100
 de Ruelle, N.....TH-111, TH-112, TH-125,
 FR-118, TU-112
 De Sanctis, M.....TH-45
 de Séreville, N.....TH-116
 de Vera, P.....TU-108
 De, R.....TU-24
 Dech, J.....WE-79
 Decleva, P.....WE-35

DeFanis, A.....MO-24
 Defrance, P.....MO-80
 del Cueto, M.....TU-106
 Delahaye, P.....WE-65, FR-4
 Delaunay, R.....TH-134, TU-99
 Della Picca, R.....TH-14, TU-22
 Demekhin, P.....TH-21, TU-10, TU-15
 Demidovich, A.....MO-21
 Demler, E.....TH-85
 Deng, M.....TH-81
 Deng, Y.....TH-81
 Denifl, S.....FR-137, FR-140
 Desai, H.....TU-68
 Descamps, D.....TU-41
 Deshmukh, P.....WE-11, MO-2, MO-4, MO-5, MO-11
 Devetta, M.....MO-21
 Di Fraia, M.....FR-46
 Diaz, C.....TU-106
 Díaz-Tendero, S.....TH-115, TH-116
 DiFraia, M.....MO-21
 Dimopoulou, C.....MO-97
 Ding, D.....WE-50, TH-2, FR-35, FR-37,
 FR-59, MO-55
 Ding, R.....TH-76, TH-85
 Ding, T.....MO-52
 Ding, X.....MO-63
 Dipti, D.....FR-89
 Dobrodey, S.....FR-9, MO-86, MO-101
 Dochain, A.....WE-29, FR-118
 Dohnal, P.....TH-113
 Döhning, B.....MO-83
 Döhning, M.....MO-87
 Dolmatov, V.....TH-5, MO-2, MO-4, MO-5, MO-11,
 MO-98, TU-01, TU-78
 Domaracka, A.....TH-37, TH-134, TU-99, TU-82,
 TU-83
 Dong, C.....WE-25, WE-26, WE-27, TH-107,
 FR-84, FR-11, FR-13, FR-14, MO-63, MO-65,
 MO-66, MO-72, MO-75, MO-100, TU-130
 Dong, D.....TH-130

Dong, W.....TU-20
 Donsa, S.....TH-3
 Dorn, A.....TU-60, TU-62, TU-63, TU-64, TU-65,
 TU-77
 Dörner, R.....WE-120, WE-121, WE-44, WE-45,
 WE-20, TH-21, TH-36, MO-16, MO-17, MO-44,
 TU-21, TU-04, TU-05, TU-07, TU-08, TU-09, TU-25,
 TU-15, TU-16
 Dou, L.....MO-64, MO-65
 Douady, J.....MO-117
 Douguet, N.....MO-21, MO-22, MO-39, MO-49
 Dowek, D.....FR-46
 Drake, G.....FR-115
 Dreiling, J.....WE-123, WE-133, FR-89
 Drescher, M.....FR-32
 Drewsen, M.....WE-68
 Du, L.....WE-43
 Du, N.....TU-131
 Du, T.....TU-46
 Dubau, J.....WE-16
 Dubois, A.....MO-79
 DuBois, R.....WE-100
 Dudley, J.....TU-42
 Duesterer, S.....MO-21
 Dulieu, O.....TH-102, TH-103, TH-104
 Dumitriu, I.....FR-52
 Dunne, M.....WE-98
 Dunning, F.....WE-1, TH-76, TH-77, TH-85
 Durand, D.....WE-65
 Durian, M.....FR-85, TU-86
 Düsterer, S.....FR-63, MO-52
 Dutta, B.....MO-76
 Dutta, S.....MO-70
 Dziczek, D.....WE-70



Ebinger, B.....MO-83, MO-87

Ebrahimi, M.....TH-1
 Eckart, S.....WE-20, MO-16, MO-17, MO-44,
 TU-16
 Eddrief, M.....TU-116
 Edtgens, V.....TU-116
 Edwards, A.....TU-01
 Efimenko, S.....WE-114
 Egl, A.....MO-109
 Ehresmann, A.....TH-21, TH-24, TU-07, TU-10,
 TU-11, TU-33
 Eichmann, U.....MO-32
 Eidam, L.....TH-106
 Eiles, M.....TH-82
 Eklund, G.....TH-111, FR-15, FR-117, MO-142
 Ellis-Gibblings, L.....WE-107
 Endo, T.....WE-40, TH-19
 Engel, E.....FR-113
 Enomoto, Y.....MO-139
 Epp, S.....FR-9, MO-101
 Erattupuzha, S.....WE-39, FR-43
 Erdmann, E.....TH-115, TH-122
 Eriksson, S.....FR-19
 Erlewein, S.....TH-98
 Esry, B.....TH-31
 Esteve-Paredes, J.....TU-109



Fabian, X.....WE-65
 Fabre, B.....WE-65, FR-33
 Fabrikant, I.....WE-62, WE-10
 Facsko, S.....TU-95, TU-98
 Fairbrother, H.....FR-142, FR-144
 Fárnik, M.....TU-84
 Fathi, R.....WE-140, WE-141, WE-144, WE-145
 Faulkner, J.....FR-119
 Fausto, R.....TU-18
 Fayer, S.....TH-58

Fechner, L.....MO-35, MO-45
 Fedor, J.....TU-84, TU-85
 Fedorov, N.....TU-41
 Fehre, K.....WE-45, TH-36, MO-17, TU-21,
 TU-25
 Feist, J.....WE-34, FR-116
 Feizollah, P.....TH-31
 Felfli, Z.....WE-91, WE-92, WE-93, WE-13,
 FR-65
 Feng, W.....TH-130, FR-103, TU-56
 Feole, M.....TU-127
 Fernández-Menchero.....WE-60, WE-2
 Ferrari, E.....MO-24
 Ferreira Da Silva, F.....MO-81, FR-138, FR-139,
 WE-85, FR-137, FR-140
 Ferrer, R.....FR-4
 Fields, G.....WE-1
 Figueira de Morisson.....MO-54
 Finetti, P.....FR-46, MO-10, MO-21, MO-24
 Finlay, P.....WE-65
 Fischer, A.....MO-10
 Fischer, D.....TH-124, FR-112
 Fléchar, X.....WE-65, FR-4, MO-113, MO-117
 Floss, I.....TU-30
 Fojón, O.....WE-47, TH-20, TH-45, MO-125,
 MO-126
 Fonseca dos Santos, S.....FR-64
 Förster, E.....MO-97
 Förster, M.....TU-29
 Fraia, M.....TU-37
 Franchoo, S.....FR-4
 Frisch, W.....FR-27
 Fritzsche, S.....WE-86, WE-4, WE-5, WE-67,
 WE-7, TH-13, FR-3, FR-125, MO-85, TU-48
 Froelich, P.....MO-67
 Frolov, M.....MO-20
 Fuhr, J.....TU-100
 Fujikawa, T.....FR-49
 Fujimoto, M.....WE-19
 Fujise, H.....WE-40, FR-40, MO-28

Fukuzawa, H.....TH-21, TU-37
 Furfaro, L.....TU-42
 Fursa, D.....WE-95, WE-96, TH-63
 Furukawa, T.....TH-133, MO-134, MO-136
 Fushitani, M.....WE-40, TH-19

G

Gacesa, M.....TH-89, MO-130
 Gachell, M.....TH-129
 Gafney, L.....FR-4
 Gafton, V.....TU-116
 Gaire, B.....TU-05, TU-08
 Galli, D.....TU-37
 Galstyan, A.....WE-36, WE-37
 Gamaly, E.....TU-42
 Ganesan, A.....MO-2
 Gao, B.....TH-81
 Gao, C.....FR-129
 Gao, F.....FR-130
 Gao, J.....TH-101, MO-123
 Gao, X.....WE-31, FR-17, MO-37
 Gao, Y.....TH-130, FR-103
 García, G.....WE-107, TH-74, MO-81
 Garcia-Molina, R.....TU-108, TU-109
 Garibotti, R.....TH-14
 Gassert, H.....TH-21
 Gassner, T.....MO-97
 Gatchell, M. TH-111, TH-112, TH-134, FR-117,
 MO-142, TU-99, TU-112, TU-120
 Gatton, A.....TU-05
 Gatzke, J.....TH-21, TU-25
 Gaudin, J.....TU-41, TU-17
 Gaumnitz, T.....MO-31, MO-52
 Gauthier, D.....FR-46
 Gavrilin, R.....FR-130
 Gay, T.....FR-86, MO-92
 Gedeon, S.....WE-3

Gedeon, V.....	WE-3	Gope, K.....	TU-52, TU-53
Gehrken, N.....	TU-08	Gorczyca, T.....	WE-127, WE-23, MO-89
Génévriez, M.....	WE-29, MO-80	Gorfinkiel, J.....	TH-52, TH-56
Geng, J.....	TH-11	Goswami, B.....	WE-67
Genoni, A.....	TU-51	Goyal, A.....	MO-93
George, S.....	TU-12	Gradziel, M.....	WE-98
Gervais, B.....	MO-117	Gräfe, S.....	WE-39
Gervasoni, J.....	TU-101	Gramajo, A.....	TH-14
Geslin, F.....	TH-116, MO-120	Granados-Castro, C.....	TH-41, TU-51, TU-55
Geyer, S.....	WE-111	Grande, P.....	TU-102
Ghazaryan, A.....	MO-51	Gravielle, M.....	TU-100, TU-22
Ghosh, D.....	MO-91	Grazioli, C.....	MO-21
Ghys, L.....	FR-4	Green, D.....	FR-69, MO-94
Giacomozzi, L.....	TH-112	Greene, C.....	TH-82
Giannakeas, P.....	TH-95	Greguric, G.....	MO-90
Giannessi, L.....	MO-10	Grellet, S.....	TU-45
Gianturco, F.....	TH-109	Grieser, M.....	WE-64, TU-12
Gibson, N.....	WE-15, FR-10	Griffin, B.....	WE-45
Gibson, S.....	TH-42	Grisenti, R.....	MO-97, TU-41, TU-17
Giglio, E.....	TU-125	Gruber, E.....	TU-95, TU-98
Gillaspy, J.....	FR-89	Grum-Grzhimailo, A.....	WE-24, MO-21, MO-24, MO-39
Ginges, J.....	FR-16	Grundmann, S.....	WE-45, WE-20, TU-16
Gins, W.....	FR-4	Grunefeld, S.....	WE-28, FR-99
Giust, R.....	TU-42	Grussie, F.....	TU-12
Glaser, L.....	MO-24	Gryzlova, E.....	WE-24, MO-24, MO-39
Glorius, J.....	FR-107	Gu, L.....	MO-86
Glosik, J.....	TH-113	Guan, X.....	TH-78
Glover, R.....	MO-26	Guan, Z.....	TU-19
Gochitashvili, M.....	FR-123	Guerin, E.....	TU-12
Göck, J.....	TU-12	Guillous, S.....	MO-113, MO-117
Goetz, E.....	MO-29	Gumberidze, A.....	MO-97
Goihl, C.....	WE-44, TU-04, TU-16	Guo, D.....	TH-130, FR-103
Gokhberg, K.....	TU-04, TU-05, TU-08	Guo, G.....	MO-112
Golding, J.....	TU-45	Guo, X.....	FR-20
Golubev, A.....	FR-130	Guo, Y.....	FR-90
Gómez, A.....	TH-141, FR-120, FR-121	Guo, Z.....	TH-1
Gong, Q.....	TH-8, TH-11	Gupta, A.....	TH-110
González, L.....	FR-43	Gupta, D.....	WE-82
González-Vázquez, J.....	FR-55	Gupta, R.....	FR-134
Gopalan, A.....	TH-110		



Hagmann, S.....WE-122, MO-97
 Hahn, M.....WE-64
 Hai, B.....TH-106, TH-108, FR-103
 Halász, G.....FR-54
 Halder, S.....FR-126, MO-111
 Hama, T.....TU-40
 Hamelin, T.....TH-116, MO-120
 Hammache, F.....TH-116
 Han, L.....TH-140, TU-96
 Han, X.....FR-17, MO-37
 Hans, A.....TH-21, TU-07, TU-11, TU-33
 Hansen, J.....MO-34
 Hansen, K.....FR-117, MO-134, MO-136, MO-142
 Hanstorp, D.....FR-15
 Hanus, V.....WE-39
 Hao, X.....MO-42
 Haque, A.....WE-103, WE-58
 Haque, M.....WE-103, WE-58
 Hara, H.....FR-74
 Haram, N.....TH-16
 Harries, J.....MO-28, MO-109
 Hartmann, G.....MO-24
 Hartmann, M.....MO-52
 Hartung, A.....TH-21, MO-16, MO-17, MO-44,
 TU-05
 Harvey, M.....WE-87, WE-88, FR-68, FR-7, FR-81
 Hasan, A.....TH-124, FR-112
 Hasegawa, S.....FR-18
 Hatakeyama, A.....TU-126
 Hatsagortsyan, K.....MO-35
 Havermeier, T.....WE-44
 Hayden, P.....FR-11
 Haze, S.....TH-103
 He, F.....FR-38
 He, L.....FR-59, MO-55
 He, P.....FR-38
 He, Y.....TU-129

Hecker Denchlag, J.....TH-104
 Heller, R.....TU-98
 Hellhund, J.....FR-5, TU-02, TU-03
 Hemantha Rao, K.....TU-31, TU-32
 Henrichs, K.....TH-21, MO-16, MO-17, TU-16
 Herbane, M.....FR-4
 Herczku, P.....MO-132
 Hergenhausen, U.....TU-07
 Hermann, Y.....WE-45
 Hervé, M.....FR-46
 Hervieux, P.....WE-106
 Herwig, P.....TU-12
 Heslar, J.....WE-49
 Heß, R.....MO-97
 Hikosaka, Y.....WE-19
 Hill, J.....TH-86
 Hillenbrand, P.....WE-122, TH-125, MO-97
 Hiraya, A.....TH-39
 Hishikawa, A.....WE-40, TH-19
 Hishiyama, N.....TH-74
 Hite, D.....TU-114
 Hiyama, E.....MO-67
 Hockenbery, Z.....FR-9
 Hoehl, J.....WE-45
 Hofbrucker, J.....WE-7
 Hoffmann, D.....FR-130
 Holdsworth, J.....MO-26
 Hole, O.....FR-15
 Holetz, W.....TH-44
 Hollstein, M.....FR-29
 Holste, K.....FR-5, TU-02, TU-03
 Holzapfel, X.....TU-07, TU-33
 Holzmeier, F.....FR-46
 Hommelhoff, P.....TU-29
 Hoogerheide, S.....WE-133
 Horke, D.....TU-35, TU-36
 Hosaka, K.....TH-24, TH-60, TU-13
 Hoshino, M.....TH-70, TH-74
 Hossain, M.....WE-103, WE-58
 Hossen, K.....TU-60, TU-63

Hougaard, C.....TH-83
 Houmøller, J.....TH-22
 Hu, H.....TH-83
 Hu, S.....WE-50, TH-4
 Hu, W.....FR-59, MO-55
 Hu, Z.....FR-130, MO-69
 Huang, Y.....FR-26, TU-20
 Huang, Z.....TH-106, TH-108, TH-130, FR-103,
 FR-105, MO-64, MO-65, TU-35
 Huber, B.....TH-134, MO-132, TU-99
 Huber, K.....FR-89
 Huber, P.....TU-16
 Huber, S.....TU-120
 Hummert, J.....MO-33
 Hung, C.....TH-88
 Huppert, M.....MO-31
 Hutton, R.....WE-66, WE-129, WE-135, TH-49,
 FR-66, MO-68, MO-78
 Huyse, M.....FR-4

I

Iablonskyi, D.....MO-10
 Ichimura, A.....TH-135
 Id Barkach, T.....TH-116
 Ikeda, T.....TU-103, TU-111
 Ilchen, M.....WE-45, MO-21, MO-24
 Illescas, C.....TH-116
 Imai, M.....FR-12, TU-118
 Indelicato, P.....MO-97
 Ingolfsson, O.....FR-138, FR-142, FR-143, FR-144,
 FR-145
 Inoue, I.....MO-28
 Inui, H.....TH-39
 Ishihara, A.....WE-40
 Ishii, K.....FR-94, FR-95
 Ishikawa, K.....MO-10, MO-27, MO-53
 Iskandar, W.....MO-113, MO-117

Isupov, A.....WE-114
 Ito, K.....WE-12
 Ito, Y.....FR-47, TU-37, TU-41
 Itoyama, R.....TH-93
 Ivanov, I.....WE-16, TH-16, MO-49
 Ivanova, I.....FR-110, MO-23
 Iwayama, H.....WE-18, WE-19, TH-35, FR-40,
 MO-28

J

Jabłoński, Ł.....FR-109, TU-113
 Jacquet, E.....MO-117
 Jagodziński, P.....MO-97, TU-113
 Jagutzki, O.....TU-25
 Jahnke, T.....WE-44, WE-45, WE-20, TH-21,
 TH-36, FR-63, MO-16, MO-17, TU-21, TU-04,
 TU-05, TU-07, TU-08, TU-09, TU-25, TU-15, TU-16
 Jain, A.....WE-101, MO-31
 Jakob, M.....FR-32
 Jallat, A.....TH-116, MO-120
 Jänkälä, K.....WE-12, TH-24
 Janke, C.....TH-36, TU-21, TU-16
 Járαι-Szabó, F.....WE-132, FR-112
 Jelovina, D.....WE-34
 Jerigova, M.....FR-60, FR-61, FR-62
 Jia, G.....MO-43
 Jiang, G.....FR-8
 Jiang, J.....WE-28, TH-107, FR-13, FR-99,
 MO-66, MO-72, MO-75, TU-130
 Jiang, L.....TH-107, TU-130
 Jiang, Y.....TH-9, FR-51, FR-53
 Jiao, F.....MO-66
 Jiao, L.....FR-71
 Jiao, Z.....FR-25
 Jiménez-Galán, Á.....MO-56
 Jin, B.....WE-105
 Jin, C.....FR-23

Jin, D.....WE-105
 Jin, M.....WE-50, FR-21, FR-51, FR-53
 Jin, R.....FR-17, MO-37
 Jin, W.....TU-103
 Jochim, B.....TH-31
 Johnson,FR-142
 Jones, M.....FR-81
 Jonsell, S.....MO-67
 Jordan, I.....MO-31
 Jorge, A.....TH-116
 Joshi, F.....TU-91
 Joshipura, K.....TU-67, TU-79, TU-91
 Juhasz, Z.....MO-132
 Jun, Y.....FR-20
 Juodkazis, S.....TU-42
 Jureta, J.....MO-80
 Jusko, P.....TH-113

K

Kaastra, J.....MO-86
 Kabachnik, N.....MO-21
 Kaderiya, B.....TH-31, FR-52, FR-57
 Kadhane, U.....TU-132
 Kadokura, R.....TH-58
 Kadyrov, A.....WE-62, WE-136, WE-137, FR-108,
 FR-119, MO-96
 Kahl, E.....WE-28
 Kaida, M.....TU-13
 Kajita, M.....FR-2
 Kala, A.....TU-132
 Kaldun, A.....TH-3
 Kalinin, A.....MO-44, TU-04
 Källberg, A.....FR-15
 Kamińska, M.....TH-111, FR-15, FR-117, FR-118,
 MO-142
 Kämpfer, T.....MO-97
 Kanaka Raju, P.....TH-31

Kaneda, T.....TH-35
 Kaneyasu, T.....WE-19
 Kang, H.....MO-8, MO-16, TU-15
 Kanya, R.....WE-84
 Kartashov, D.....TH-7, TH-11
 Karthein, J.....TU-12
 Kastirke, G.....WE-45, WE-20, TH-21, TU-21,
 TU-04, TU-16
 Kato, D.....FR-72, FR-74, FR-76, FR-77, MO-63
 Kato, H.....TH-70, MO-99
 Katoh, M.....WE-19
 Kaur, J.....MO-89
 Kawachi, Y.....WE-40
 Kayani, A.....WE-134, MO-131
 Kazansky, A.....MO-21
 Keating, D.....WE-11
 Kedzierski, W.....WE-79
 Keil, M.....FR-122
 Keiling, M.....TU-08
 Keitel, C.....MO-25, MO-35
 Kellerbauer, A.....TH-98
 Kelley, M.....TH-77
 Kendrick, B.....TH-105
 Kester, O.....WE-111
 Kezerashvili, R.....FR-123
 Khalal, M.....WE-12
 Khan, A.....TH-99
 Khan, N.....MO-64
 Kheifets, A.....WE-8, TH-17, MO-2, MO-4, MO-5,
 MO-10, MO-11, MO-49
 Khreis, J.....FR-137
 Kibedi, T.....WE-32, MO-90
 Kiefer, D.....TH-106
 Kiefer, H.....TU-14
 Kilcoyne, A.....FR-5, TU-02
 Kilcoyne, D.....FR-52
 Killian, T.....TH-76, TH-85, TH-86
 Kim, B.....MO-84
 Kim, C.....MO-77
 Kim, E.....TU-114, TU-115

Kim, H.....	WE-44, TH-21, TU-09	Kothari, H.....	TU-67, TU-79
Kim, M.....	TH-88	Kotochigova, S.....	TH-105
Kimberg, V.....	FR-41	Kouchi, A.....	TU-40
Kimoto, Y.....	WE-118, WE-119	Kouchi, N.....	TH-24, TH-60, TU-13
Kimura, J.....	TU-111	Koushima, M.....	TU-103
Kimura, N.....	TH-87, FR-2	Kovacs, S.....	MO-132
King, F.....	WE-120, WE-121	Kovalenko, O.....	FR-97
Kino, Y.....	MO-67, MO-95	Kövér, Á.....	TH-58
Kircher, M.....	TH-21, FR-30, TU-16	Kozhedub, Y.....	FR-104, FR-110
Kirchner, T.....	WE-71, WE-126, TH-118, FR-113, FR-115, MO-128	Kozhina, A.....	MO-19
Kirian, R.....	TU-36	Kozhuharov, C.....	MO-87, MO-97
Kitajima, K.....	TU-110	Kozubek, R.....	TU-95, TU-98
Kitajima, M.....	TH-24, TH-60, TU-13	Kraemer, S.....	MO-109
Kitzler, M.....	WE-39, TH-7, TH-11, FR-43	Krantz, C.....	WE-64, TU-12
Kjær, C.....	TH-22	Krashennnikov, A.....	TU-95
Kjellsson, T.....	MO-57	Kreckel, H.....	TU-12
Klaiber, M.....	MO-35	Krems, R.....	TH-121
Kling, M.....	FR-27, FR-45, FR-63	Krishnakumar, E.....	TH-68, TU-52, TU-53
Klinker, M.....	FR-55	Kristiansson, M.....	FR-15
Klosowski, L.....	WE-68, WE-69, WE-70	Kroes, G.....	TU-106
Klumpp, S.....	FR-5, FR-29, TU-03	Krstic, P.....	TH-140, TU-96
Knie, A.....	TH-21, TH-24, MO-24, TU-07, TU-10, TU-11, TU-33	Krüger, M.....	TU-29
Kobayashi, Y.....	TH-92	Kruppa, K.....	FR-139
Koch, C.....	MO-29	Krušič, Š.....	MO-48
Koch, M.....	WE-39	Kubala-Kukuś, A.....	TU-113
Kočišek, J.....	TU-84, TU-85	Kübel, M.....	FR-63
Koike, F.....	WE-18, MO-63	Kubin, M.....	MO-33
Kojima, T.....	TU-111	Kudryavtsev, Y.....	FR-4
Kokoouline, V.....	FR-115	Kuehn, S.....	MO-109
Kolorenč, P.....	TU-08	Kuhls, A.....	TH-21
Komiyama, Y.....	TH-93	Kuhn, M.....	TH-59
Kono, H.....	WE-40	Kühn, S.....	FR-9, MO-10, MO-101
Kono, N.....	MO-134	Kukk, E.....	TU-37
Konomi, T.....	WE-19	Kulyk, K.....	MO-121, TU-99, TU-112
Kopyra, J.....	FR-140	Kuma, S.....	MO-28
Kornilov, O.....	MO-33	Kumagai, N.....	WE-18
Kostin, V.....	MO-36	Kumagai, Y.....	TU-13, TU-37
Kosugi, S.....	WE-18	Kumar, A.....	TH-131, FR-114
		Kumar, H.....	MO-118, MO-119, MO-141
		Kumar, N.....	WE-81

Kumar, S.....WE-57, WE-63, WE-104, FR-134,
MO-6
Kumara, N.....MO-131
Kumara, P.....WE-134
Kumarappan, V.....FR-52
Kunitski, M.....TH-36, MO-16, MO-17, MO-44,
TU-25
Küpper, J.....TU-35, TU-36
Kuroda, N.....FR-135, FR-22
Kurokawa, S.....TU-126
Kus, N.....TU-18
Kusakabe, T.....MO-127
Kushawaha, R.....FR-52
Kuzenov, V.....FR-136
Kwon, D.....WE-112

L

La Mantia, D.....WE-134, MO-131
Laarmann, T.....FR-32, TU-38
Laban, D.....FR-24
Lablanquie, P.....WE-12
Łabuda, M.....TH-115, TH-122
Lackner, F.....FR-116, MO-27
Lacourt, P.....TU-42
Lai, X.....TH-7, MO-42, MO-54
Lamicchane, B.....TH-124, FR-112
Lamour, E.....FR-114, TU-41, TU-116, TU-17
Lamprecht, S.....WE-111
Landers, A.....TU-05, TU-08
Lane, C.....TU-01
Lange, E.....FR-139
Langeland, J.....TU-14
Langer, C.....FR-107
Laoutaris, A.....WE-126, WE-127, WE-128
Lapicki, G.....WE-124
Lara-Astiaso, M.....WE-35, TH-41
Laricchia, G.....TH-58

Larimian, S.....WE-39, TH-11, FR-43
Larsson, M.....MO-121, TU-112
Lattouf, E.....MO-132
Laulan, S.....MO-50
Launoy, T.....TH-116, FR-118
Laux, M.....MO-35
Laws, B.....TH-42
Lazur, V.....WE-3
Lazzarino, L.....FR-32
Le Padellec, A.....TH-116, MO-120
Le, A.....FR-23
Le, T.....TH-116, MO-120
Lecesne, N.....FR-4
Lee, B.....WE-32, MO-90
Lee, H.....TH-82
Lei, X.....MO-9
Lei, Y.....FR-130
Lein, M.....TH-15
Lemell, C.....WE-108, TH-11, TH-15, TU-29,
TU-30
Leopold, T.....FR-124
Leredde, A.....WE-65
Lestinsky, M.....WE-64, MO-97
Leung, A.....MO-128
Lévy, A.....FR-114, TU-17, TU-41, TU-116
Lewenstein, M.....WE-41, WE-42, FR-45
Lewis, B.....TH-42
Li, B.....FR-84, TU-56
Li, H.....FR-35
Li, J.....TH-106, TH-108, FR-14, FR-17, MO-37
Li, M.....WE-110, TH-105, FR-66
Li, P.....WE-105, WE-43, MO-9
Li, Q.....FR-51
Li, R.....TH-91
Li, S.....FR-20, FR-21, FR-51, FR-53
Li, X.....TH-106, TH-108, FR-8, FR-90, FR-57,
MO-15, TU-44, TU-63
Li, Y.....TH-6, FR-84, TU-37
Li, Z.....WE-110
Liang, G.....MO-107

Libisch, F.....TU-29
 Liénard, E.....WE-65
 Liesen, D.....MO-97
 Light, P.....MO-26
 Limão-Vieira, P.....MO-81, MO-135, FR-139
 Limbachiya, C.....TH-51, TH-53, TH-71, TU-54,
 TU-59, TU-61
 Lin, C.....TH-3, FR-23
 Lin, J.....TU-23
 Lindahl, A.....MO-24
 Lindén, F.....TU-120
 Lindenblatt, H.....FR-63
 Lindinger, A.....TH-59
 Lindroth, E.....TH-18, MO-57
 Linnartz, H.....TH-59
 Lintuluoto, M.....TU-06
 Lion, J.....TU-12
 Lisak, D.....WE-68
 Litvinov, Y.....WE-122, FR-97, FR-106, FR-107,
 MO-97
 Litvinyuk, I.....TH-16, FR-24, MO-26, MO-49,
 TU-31, TU-32
 Liu, A.....TH-2
 Liu, H.....FR-53
 Liu, J.....WE-9, WE-130, FR-90, TU-20, TU-44
 Liu, L.....WE-143, MO-62, TU-20
 Liu, P.....MO-106
 Liu, Q.....TH-81
 Liu, X.....TH-7, TH-83, FR-35, MO-42, MO-100, MO-54
 Liu, Y.....WE-80, WE-94, TH-23, TH-25, FR-20,
 FR-63
 Liu, Z.....TH-46, TH-47, TH-64
 Llovet, X.....WE-104
 Loeser, M.....TH-106
 Löfgren, P.....FR-15
 Loh, Z.....MO-52
 Lohmann, S.....TU-12
 Lomsadze, R.....TH-124, FR-89, FR-123
 López, S.....MO-33
 Loreau, J.....TH-139

Lorenc, D.....FR-60, FR-61, FR-62
 Loreti, A.....TH-58
 Lötstedt, E.....WE-39
 Löttsch, R.....MO-97
 Loupas, A.....TH-52
 Lu, D.....WE-129, TH-49, FR-66, MO-78
 Lu, F.....MO-100
 Lu, H.....FR-138
 Lu, R.....WE-130
 Lucchese, R.....FR-47
 Luedde, H.....TH-118
 Luiten, A.....MO-26
 Luo, D.....MO-68
 Luo, S.....FR-59, MO-55
 Luo, Y.....WE-110
 Lv, H.....WE-50, WE-51
 Lv, Z.....FR-26
 Lyashchenko, K.....FR-101
 Lyman, N.....WE-15



Ma, J.....FR-70, FR-71
 Ma, R.....FR-37
 Ma, X.....TH-106, TH-108, TH-130, FR-103, FR-105,
 FR-110, MO-64, MO-64, MO-65, TU-56
 Ma, Y.....MO-75
 Maaza, M.....WE-103, WE-58
 MacDonald, M.....TH-44
 Macé, S.....FR-114, TU-41, TU-116, TU-17
 Machacek, J.....TH-62
 Madesis, I.....WE-126, WE-127, WE-128
 Madison, D.....WE-87, WE-88
 Madjet, M.....TU-24
 Madlener, T.....TU-29
 Madsen, L.....TH-4, TH-15
 Madugula, N.....TH-137
 Magrakvelidze, M.....TH-10

Magunia, A.....	MO-52	Masic, M.....	TH-40
Mahajan, T.....	TH-116	Mason, N.....	TH-68, TU-53, TU-45
Mai, S.....	FR-43	Massen-Hane, K.....	FR-119
Majety, V.....	MO-7	Masunaga, T.....	MO-139
Majima, T.....	FR-12, MO-143, TU-06, TU-110	Masuyama, T.....	TU-103
Makhoute, A.....	MO-79	Matejcek, S.....	FR-85, TU-86
Makrides, C.....	TH-105	Matoba, S.....	MO-105
Maksyuta, M.....	WE-114, FR-127, FR-128	Matsubara, M.....	MO-143, TU-103
Maltsev, I.....	FR-110, FR-111, MO-23	Matsuda, A.....	WE-40, TH-19
Man, Q.....	MO-72, MO-75	Matsuda, K.....	TU-37
Manakov, N.....	TH-4, MO-20	Matsumoto, J.....	TH-133, FR-102, MO-117, MO-134, MO-136, MO-141
Mandal, A.....	MO-4, MO-5	Mauracher, A.....	TH-59, TU-120
Mandal, K. S.....	FR-134	Mazza, T.....	MO-10, MO-21, MO-24
Manil, B.....	MO-97	McAcy, C.....	FR-31
Mannervik, S.....	TH-111, FR-15	Mcconkey, J.....	WE-79
Manson, S.....	WE-11, WE-13, MO-2, MO-4, MO-5, MO-11, TU-24	McCurdy, C.....	WE-17
Mao, L.....	TH-106, TH-108, FR-105, MO-64	McElwee-White, L.....	FR-138, FR-142
Mao, R.....	TH-106, TH-108	McKay, K.....	TU-114
Maquet, A.....	MO-56	Meckel, M.....	TU-09
Marangolo, M.....	TU-116	Mehta, N.....	TH-95
Marante, C.....	FR-55	Mei, X.....	WE-80
Marcus, G.....	MO-88	Meister, S.....	FR-63
Margitych, M.....	TU-92	Mendes, M.....	MO-81
Marinkovic, B.....	TH-40	Mendez, L.....	MO-123, MO-124
Markus, P.....	TH-27	Meng, C.....	FR-26
Marquetand, P.....	FR-43	Menk, S.....	MO-139
Martín, F.....	WE-34, WE-35, TH-59, TH-116, FR-46, FR-55, MO-56, TU-106	Meremianin, A.....	TH-4
Martin, N.....	MO-84	Mertens, K.....	FR-29
Martin, P.....	TU-41	Méry, A.....	WE-65, FR-114, MO-113, MO-117, MO-132
Märtin, R.....	MO-97	Metz, D.....	WE-20, TH-21
Martin, S.....	MO-122	Meyer, A.....	TH-116
Martinet, G.....	MO-120	Meyer, C.....	TU-12
Martinez, Y.....	FR-4	Meyer, M.....	WE-45, WE-24, FR-46, MO-10, MO-21, MO-24
Martini, L.....	WE-47	Mhamdi, A.....	TU-15
Martins, M.....	WE-5, FR-5, FR-29, TU-02, TU-03, TU-107	Mi, Y.....	MO-35
Martysh, Y.....	FR-128	Micke, P.....	FR-124, MO-109, MO-101
Masatsugu, M.....	FR-95	Midorikawa, K.....	FR-34

Mihelič, A.....MO-48
 Mika, A.....TH-134, TU-99, TU-122
 Miller, K.....TH-125
 Milne, B.....TH-22
 Milosavljevic, A.....TH-38
 Min, Q.....WE-25, WE-26, WE-27, FR-11
 Minowa, T.....TU-103
 Miron, C.....TH-32, TH-38, TU-37
 Mishra, P.....TU-12
 Misra, D.....TH-137
 Mita, M.....FR-77
 Miteva, T.....TU-05, TU-08
 Mitnik, D.....FR-120, FR-121, TU-22
 Mitroy, J.....FR-99
 Mityureva, A.....MO-19
 Miyamoto, Y.....MO-28
 Mizutani, S.....TU-110
 Modak, P.....TH-67
 Mogilevskyi, E.....FR-4
 Mohammadi, A.....TH-104
 Mohan, H.....FR-75
 Mohan, M.....MO-93
 Molkentin, T.....MO-83, MO-87
 Mondal, A.....FR-126, MO-111
 Monobe, M.....FR-76
 Monti, J.....TH-120, MO-125, MO-126
 Moradmand, A.....TU-08
 Mori, Y.....TH-60
 Moribayashi, K.....TU-97
 Morishita, T.....TH-19
 Moshhammer, R.....FR-63, MO-35, MO-45
 Mota-Furtado, F.....WE-36, WE-37
 Motomura, K.....TU-37
 Mozejko, P.....TU-82, TU-83
 Msezane, A.....WE-91, WE-92, WE-93, WE-13,
 FR-65
 Mueller, A.....FR-5, TU-02, TU-03
 Mukaiyama, T.....TH-103
 Mukhopadhyay, T.....MO-71
 Mukoyama, T.....WE-14, FR-83, FR-109

Mulin, D.....TH-113
 Mulkerin, B.....TH-83
 Müller, A.....WE-5, WE-64, TH-21, FR-89,
 FR-122, MO-83, MO-87, MO-106
 Müller, C.....WE-44, TU-04
 Müller, J.....WE-120, WE-121
 Müller, R.....FR-125
 Munitski, M.....TU-08
 Murakami, I.....FR-74, FR-77, MO-63
 Murata, S.....FR-73
 Murböck, T.....TH-1
 Murray, A.....WE-87, WE-88, WE-30, FR-68,
 FR-7, FR-81
 Musbat, L.....TH-22
 Mustary, M.....FR-24
 Muzas, A.....TU-106

N

Nabekawa, Y.....FR-34
 Nadarajan Achary, S.....TU-31, TU-32
 Nag, P.....WE-89, WE-90
 Nagata, Y.....TU-126
 Nagaya, K.....TU-37
 Nagele, S.....TH-3, FR-116
 Nagy, E.....WE-3
 Nagy, L.....WE-132, TH-73, FR-112, FR-116,
 MO-116, MO-18
 Naing, A.....WE-123, WE-133
 Najeeb, P. K.....TU-132
 Nakai, R.....TH-103
 Nakajima, K.....MO-28
 Nakajima, T.....FR-73
 Nakamura, N.....FR-73, FR-74, FR-76, FR-77,
 MO-63, MO-99
 Nakano, Y.....MO-139
 Nakayama, S.....TU-88
 Nakayama, W.....FR-10

Nalin, G.....TU-15, FR-141
 Nandi, D.....WE-89, WE-90
 Nandi, T.....FR-98, FR-100
 Nanos, S.....WE-127
 Nascimento, R.....FR-15, FR-117, FR-118
 Natsume, Y.....TU-111
 Nauta, J.....FR-9, FR-124
 Navarrete, F.....TH-124, FR-78, TU-127, TU-101
 Naviliat-Cuncic, O.....WE-65
 Neagu, L.....TU-37
 Neff, J.....TH-21
 Neill, P.....FR-15
 Neville, J.....TH-32
 Ngoko Djiokap, J.....TH-4
 Nguyen, T.....TU-49
 Ni, D.....TH-25
 Nicolas, C.....TH-32, TH-38, TU-17
 Ning, C.....WE-88
 Niozu, A.....TU-37
 Nishimura, H.....WE-118, WE-119
 Nishiyama, T.....TU-37
 Niu, B.....WE-105
 Niu, S.....TH-46, TH-47, TH-64
 Noda, K.....TU-06
 Nolden, F.....MO-97
 Noor, A.....MO-49
 Nörtershäuser, W.....TH-1
 Novotný, O.....WE-64, TU-12
 Numadate, N.....WE-138, WE-143

O

O'Connor, A.....TU-12
 Obaid, R.....FR-52
 Ochieng, A.....FR-82
 Odagiri, T.....TH-24, TU-13
 Ogawa, H.....FR-94, FR-95
 Ohae, C.....MO-28

Ohira, J.....WE-118, WE-119
 Ohmura, H.....FR-50
 Ohwada, S.....MO-28
 Ohyama-Yamaguchi, T.....TH-135
 Okada, K.....TH-87, TH-35, FR-2
 Okino, T.....FR-34
 Okumu, J.....FR-82
 Okumura, T.....TH-60
 Okunishi, M.....FR-47
 Oliveira, V.....TH-141
 O'Mahony, P.....WE-36, WE-37
 O'Mullane, M.....FR-88
 Ono, T.....TU-37
 Orimo, Y.....MO-53
 Országh, J.....FR-85, TU-86
 Osipov, T.....FR-52
 Ossenbrüggen, T.....TU-35
 O'Sullivan, G.....FR-84, FR-11
 Ott, C.....TH-3, MO-25, MO-52
 Ovcharenko, Y.....WE-45, MO-10, MO-21
 Ovsyannikov, V.....FR-89
 Owada, S.....TU-37
 Ozga, C.....TU-07, TU-11, TU-33

P

Pajek, M.....FR-109, TU-113
 Pal, S.....WE-81
 Palacios, A.....WE-34, WE-35, FR-46
 Palaudoux, J.....WE-12
 Palmer, A.....MO-26
 Pandiri, K.....FR-57
 Panigrahi, P.....TH-99
 Papagiannouli, I.....TU-17
 Pappas, D.....TU-114
 Paschen, T.....TU-29
 Pastega, D.....FR-139
 Patanen, M.....TH-32, TU-10, TU-17

Patel, U.....TU-67, TU-79
 Pathak, S.....FR-57
 Patoary, M.....WE-103, WE-58
 Paulus, G.....MO-6
 Pavlyukh, Y.....TH-26, TH-33, FR-32
 Pazourek, R.....TH-3
 Pearson, W.....FR-57
 Pedersen, B.....TH-22
 Pedregosa, J.....FR-124
 Penent, F.....WE-12
 Peng, L.....TH-8, TH-11
 Perez Rios, J.....TH-88
 Pérez-Hernández, J.....WE-42
 Perez-Rios, J.....TH-76, TH-82
 Perrot, L.....H-116, MO-120
 Pertot, Y.....MO-31
 Peshkov, A.....WE-4
 Petit, S.....TU-41
 Petridis, N.....MO-97
 Petrov, A.....TH-105
 Petrov, I.....TU-10
 Pfannkuche, D.....FR-29
 Pfeifer, T.....TH-3, FR-124, FR-63, MO-25,
 MO-35, MO-45
 Phung, V.....MO-120
 Pincelli, T.....TU-37
 Pino, T.....TH-116, MO-120
 Piot, J.....FR-4
 Piraux, B.....WE-36, WE-37
 Pitzer, M.....TH-21, TH-36, TU-04, TU-15
 Piwinski, M.....WE-68, WE-69, WE-70
 Plasil, R.....TH-113
 Plekan, O.....FR-46, MO-10, MO-21, MO-24
 Pleskacz, K.....WE-68
 Plunien, G.....FR-104, FR-110, TU-28
 Podlech, H.....WE-111
 Pohl, M.....TU-33
 Politis, M.....TH-45
 Pons, B.....WE-65, TH-116, FR-33
 Popov, R.....FR-110

Popov, Y.....WE-36, WE-37
 Porobic, T.....WE-65
 Postler, J.....TH-59
 Poštulka, J.....TU-84
 Pouilly, J.....MO-132
 Powell, J.....FR-57
 Pozdneev, S.....WE-74, WE-75, WE-76, WE-77
 Prabhudesai, V.....TH-68, TU-52, TU-53
 Prajapati, D.....TU-54
 Prajapati, S.....WE-63, WE-104
 Preval, S.....WE-21, FR-88
 Prigent, C.....FR-114, TU-41, TU-116, TU-17
 Prince, K.....TH-40, FR-46, MO-10, MO-21
 Prosmiiti, R.....TH-117, TH-123, TU-50, TU-124
 Przystawik, A.....FR-32
 Ptasinska, S.....TH-61
 Ptasińska-Denga, E.....TU-82
 Purkait, K.....FR-126
 Purkait, M.....FR-126, MO-110, MO-111
 Pursehouse, J.....WE-30
 Pyak, P.....FR-48
 Pysanenko, A.....TU-84

Q

Qian, D.....TH-130
 Qian, L.....WE-105
 Qian, Y.....MO-102
 Qiao, X.....MO-46
 Qin, C.....FR-36
 Quan, W.....MO-42
 Quemener, G.....WE-65
 Quint, W.....TH-1, MO-6
 Quinto, M.....TH-120, MO-125, MO-126, MO-137,
 MO-138, MO-140

R

Rabadan, I.....MO-123, MO-124
 Raeder, S.....FR-4
 Rafipoor, J.....MO-21
 Ragesh Kumar T P.....FR-143, FR-144
 Rahmanian, M.....WE-144, WE-145
 Rajput, J.....TH-31, MO-113, MO-118, MO-119
 Ralchenko, Y.....WE-133, FR-89
 Ralser, S.....TH-59
 Ramadhan, A.....FR-58
 Ramillon, J.....FR-114
 Randazzo, J.....MO-82
 Rangama, J.....FR-114, MO-113, MO-117, MO-132
 Raoult, M.....TH-102, TH-103, TH-104
 Rapp, L.....TU-42
 Räsänen, E.....TH-15, MO-29
 Rauch, C.....TU-04
 Rebholz, M.....MO-52
 Rebrov, O.....MO-121
 Recoules, V.....TU-41
 Reich, D.....MO-29
 Reifarh, R.....FR-107
 Rein, B.....TH-106
 Reinherd, P.....FR-15
 Reiß, P.....TU-33
 Ren, C.....MO-66
 Ren, J.....FR-130
 Ren, X.....TU-62, TU-63, TU-64, TU-65
 Renzler, M.....TH-59
 Repnow, R.....WE-64, TU-12
 Rescigno, T.....WE-17
 Richter, M.....MO-16, MO-17, TU-05
 Richter, R.....TH-37, TH-40, FR-46
 Ricz, S.....WE-5, FR-5, TU-02, TU-03
 Ringleb, S.....TH-1, MO-6
 Rios Rubiano, C.....TU-22
 Rist, J.....WE-20, TH-21, MO-16, MO-17, TU-08,
 TU-09, TU-16

Rittenhouse, S.....TH-95, TU-115
 Rivarola, R.....TH-120, MO-125, MO-126
 Robatjazi, S.....FR-57
 Robert, E.....TH-38
 Roberts, M.....MO-90
 Rocha, A.....TH-44
 Rode, A.....TU-36, TU-42
 Rodriguez, D.....WE-65
 Rodríguez, V.....MO-40, MO-41
 Rodríguez-Segundo, R.....TH-117
 Rohringer, N.....FR-41
 Roither, S.....TH-7, TH-11
 Rolles, D.....TH-31, FR-52, FR-57
 Ropars, F.....MO-117
 Rosén, S.....FR-15
 Rossi, G.....TU-37
 Roth, N.....TU-35, TU-36
 Roucka, S.....TH-113
 Rousseau, P.....TH-37, TH-134, FR-114, TU-99
 Roussel, E.....FR-46, MO-24
 Rozet, J.....FR-114, TU-41, TU-116, TU-17
 Ruan, F.....WE-130
 Rubinsky, I.....TU-35
 Rubo, A.....TH-22
 Rudenko, A.....TH-31, FR-52, FR-57, FR-63
 Rudolph, J.....MO-101
 Russakoff, A.....WE-39
 Ryding, M.....MO-121
 Ryszka, M.....TH-61
 Ryzhkov, S.....FR-136

S

Sa'adeh, H.....TH-40
 Sadeghpour, H.....TH-85, TU-114, TU-115
 Saenz, A.....MO-23
 Safarzade, Z.....WE-140
 Safavi-Naini, A.....TU-114

Safronova, M.	FR-73	Savajol, H.....	FR-4
Safronova, U.....	FR-73	Savelyev, E.....	FR-52
Safvan, C.....	TH-131, FR-134, MO-113, MO-114, MO-115, MO-117, MO-118, MO-119, MO-141, TU-132	Savin, D.....	WE-64, TH-125
Saha, B.....	WE-103, WE-58	Savin, S.....	FR-130
Saha, J.....	TH-69	Scarborough, T.....	FR-31
Saiba, R.....	FR-102	Scarlett, L.....	TH-63
Sairam, T.....	MO-114, MO-115, TU-132	Schaechter, L.....	WE-120
Saito, M.....	FR-12, MO-143, TU-06, TU-110	Scheier, P.....	TH-59
Saito, R.....	TH-103	Schippers, S.....	WE-117, WE-5, WE-64, FR-5, FR-89, FR-122, MO-83, MO-87, MO-106, TU-02, TU-03
Sakaamini, A.....	WE-87, WE-88, FR-68, FR-7	Schleberger, M.....	TU-95, TU-98
Sakaue, H.....	FR-74, FR-77, MO-63	Schlott, N.....	MO-1, MO-16, MO-17, TU-16
Sako, T.....	FR-49	Schmid, G.....	FR-63
Samanta, A.....	TU-35	Schmid, H.....	TU-14
Samel, M.....	TU-123	Schmidt, D.....	TU-21
Sanche, L.....	WE-107	Schmidt, H.....	TH-111, TH-112, TH-129, FR-15, FR-117, FR-118, MO-142, TU-112
Sanchez, M.....	FR-9	Schmidt, L.....	WE-121, WE-45, WE-20, TH-21, TH-36, MO-16, MO-17, MO-44, TU-21, TU-04
Sánchez-Claros, J.....	TU-109	Schmidt, P.....	TH-24, FR-124, TU-07, TU-11, TU-33
Sanderson, J.....	FR-58	Schmidt, R.....	TH-85
Sándor, B.....	WE-132	Schmidt, S.....	TH-1
Sang, R.....	TH-16, FR-24, MO-26, MO-49, TU-31, TU-32	Schmidt-Böcking, H.....	WE-44, TH-21, TH-30, TU-105, TU-09, TU-34
Sanjari, M.....	MO-97	Schmikt, L.....	TU-25
Sanjari, S.....	FR-106	Schmoeger, L.....	FR-124
Sann, H.....	WE-44, MO-16, TU-08, TU-09, TU-16	Schneider, D.....	WE-44, TU-09
Sansone, G.....	WE-24, MO-10	Schnorr, K.....	FR-63
Sant'Anna, M.....	TH-44	Schober, C.....	TH-21, TU-04
Santos, A.....	TH-141, TH-44	Schöffler, M.....	WE-39, WE-121, WE-44, WE-45, WE-20, WE-142, TH-21, TH-7, TH-36, FR-42, FR-43, MO-16, MO-17, MO-44, TU-21, TU-04, TU-08, TU-09, TU-25, TU-15, TU-16
Sarantseva, T.....	MO-20	Scholz, F.....	MO-24
Sartor, J.....	TU-05	Scholz, M.....	TH-34
Sasakawa, M.....	TH-103	Schößler, S.....	TU-21
Sasao, N.....	MO-28	Schramm, U.....	TH-106
Sato, S.....	TU-30	Schröter, C.....	FR-63
Sato, T.....	MO-27, MO-53		
Sato, Y.....	TU-37		
Satta, M.....	TH-27		
Saurabh, S.....	TU-12		
Savage, J.....	WE-95		

Schubert, K.....	TU-02	Sheil, J.....	MO-99
Schuch, R.....	WE-105	Shen, L.....	TU-56
Schueler, M.....	TH-33, FR-32	Shen, Y.....	FR-66, MO-78
Schuessler, H.....	TH-87	Sheng, L.....	FR-105
Schuler, M.....	TH-26	Shevchuk, I.....	MO-24
Schultz, D.....	WE-133	Shevelko, V.....	TU-118
Schultze, K.....	MO-97	Shi, Y.....	TH-47, FR-35, MO-100
Schulz, M.....	WE-71, TH-124, FR-112, FR-123	Shibata, K.....	TH-92, TH-93
Schussler, R.....	MO-109	Shields, D.....	TU-24
Schwalm, D.....	TU-12	Shigemasa, E.....	WE-18, WE-19, TH-35, FR-40, MO-28
Schwarz, M.....	FR-124	Shim, H.....	MO-77
Schweiger, C.	MO-109	Shimada, K.....	WE-138, WE-143
Schweikhard, L.....	TU-12	Shimizu, E.....	FR-74
Schwemlein, M.....	MO-97	Shiratori, T.....	TU-13
Schwenke, D.....	MO-130	Shiromaru, H.....	TH-133, FR-102, MO-117, MO-134, MO-136, MO-141
Schwestka, J.....	TU-95, TU-98	Shojaei Akbarabadi, F.....	WE-140
Schwingenschlogl, U.....	MO-102	Shojaei, F.....	WE-141, WE-144, WE-145
Scrinzi, A.....	MO-7	Shvetsov-Shilovski, N.....	TH-15
Sedlacek, J.....	TU-115	Si, R.....	FR-20
Segui, S.....	TU-101	Siebert, J.....	WE-45, TH-21, TU-21
Seidel, R.....	TU-33	Siebold, M.....	TH-106
Sels, S.....	FR-4	Sieradzka, A.....	TH-56
Seltmann, J.....	FR-5, MO-24	Sil, A.....	MO-73
Severjins, N.....	WE-65	Silkin, V.....	TU-22
Severt, T.....	TH-31	Silwal, R.....	FR-89
Shabaev, V.....	FR-104, FR-110, FR-111, MO-23, TU-28	Simionovici, A.....	MO-97
Shaffer, J.....	TU-115	Simon, A.....	WE-134, MO-131
Shafranyosh, I.....	TU-92	Simon, M.....	WE-44, WE-45
Shafranyosh, M.....	TH-57, TU-92	Simonsson, A.....	FR-15
Shah, C.....	MO-85, MO-86	Simpson, M.....	TH-59
Shan, X.....	TH-46, TH-47, TH-64, MO-133	Singh, A.....	WE-131
Shanker, R.....	WE-63, WE-104	Singh, B.....	WE-63, WE-63, WE-104, WE-104
Shao, C.....	WE-130, FR-90	Singh, C.....	FR-82
Shao, J.....	TU-119	Singh, G.....	WE-131
Sharma, D.....	TH-131	Singh, P.....	WE-83
Sharma, G.....	FR-134, TU-39, TU-117	Singh, V.....	TU-35
Sharma, P.....	FR-98, FR-100	Sinha, C.....	MO-91
Sharma, S.....	WE-125	Slaviček, P.....	TU-33, TU-84
Shaw, P.....	TU-130		

Slavkovska, Z.....FR-107
 Smale, L.....FR-92
 Smejkal, V.....TU-95
 Śmiatek-Telega, M.....TU-45
 Smirnov, V.....MO-19
 Sobota, D.....TU-113
 Sokell, E.....TH-26, MO-99
 Solanpää, J.....MO-29
 Somers, M.....TU-106
 Song, G.....WE-105
 Song, M.....WE-82
 Song, X.....MO-60
 Song, Z.....WE-105, WE-130
 Soulard, L.....TU-41
 Spencer, J.....FR-142
 Spieler, S.....TH-59
 Spillmann, U.....MO-97
 Spruck, K.....WE-64, TU-12
 Stabrawa, I.....TU-113
 Stallkamp, N.....TH-1, MO-6
 Starace, A.....TH-4, MO-20
 Starikov, E.....TU-06
 Stark, J.....FR-124
 Staroselskaya, E.....MO-39
 Staudte, A.....TH-7
 Steck, M.....MO-97
 Steinbruegge, R.....FR-9, MO-101, MO-85,
 MO-86
 Stevens, D.....TH-62
 Steydli, S.....FR-114, TU-41, TU-116, TU-17
 Stia, C.....TH-45
 Stiebing, K.....WE-120, WE-121
 Stockett, M.....TH-22, TH-129, FR-117, FR-118,
 TU-14
 Stoecklin, T.....TH-41
 Stöhlker, T.....WE-117, WE-122, TH-1, FR-97,
 FR-106, FR-110, MO-6, MO-87, MO-97, MO-101
 Stohner, J.....TU-25
 Stojanovic, N.....FR-63
 Stolte, W.....WE-23

Stooß, V.....TH-3, MO-25, MO-52
 Strakhova, S.....WE-24
 Stuchbery, A.....WE-32, MO-90
 Stumpf, V.....TU-05
 Stupavska, M.....FR-61
 Sturm, F.....WE-44, TU-09
 Sturm, S.....MO-109
 Su, M.....WE-25, WE-26, WE-27, FR-11
 Suarez, J.....MO-124
 Suárez, N.....WE-41, WE-42
 Sui, L.....FR-51
 Sukhoviya, M.....TU-92
 Sulik, B.....MO-132
 Sullivan, J.....TH-62
 Sun, D.....WE-25, WE-26, WE-27, FR-11
 Sun, J.....WE-9
 Sun, R.....MO-63
 Sun, X.....TU-35, TU-36
 Sunil Kumar, S.....TU-12
 Surzhykov, A.....FR-125, MO-85
 Suzuki, N.....WE-18
 Suzuki, R.....MO-134
 Svyda, Y.....TU-92
 Swadia, M.....TH-51, TH-53
 Swami, D.....FR-134
 Syshchenko, V.....WE-114
 Szabo, C.....MO-97
 Szmytkowski, C.....TU-82

T

Tachikawa, M.....TU-81
 Tagawa, M.....WE-118, WE-119
 Taïeb, R.....MO-56
 Tajima, M.....FR-132
 Takács, E.....FR-89
 Takada, Y.....TH-87
 Takadze, G.....FR-123

Takahashi, A.....	FR-95	FR-116, MO-96, TU-125	
Takahashi, K.....	TU-06	Tolstikhin, O.....	TH-19
Takahashi, M.....	TH-65, TH-66, TU-88	Tomita, S.....	TU-06
Takahasi, O.....	TH-39	Tong, X.....	FR-116, TU-30
Takanashi, T.....	TU-37	Tono, K.....	TU-37
Tamasaku, K.....	MO-28	Torizuka, Y.....	TH-24
Tan, J.....	WE-123, WE-133	Torny, T.....	MO-90
Tanabe, T.....	TU-06	Toshima, N.....	FR-116
Tanaka, A.....	TH-70	Tosic, S.....	TH-40
Tanaka, G.....	TH-92	Tóth, A.....	FR-54, MO-18
Tanaka, H.....	TH-70, TH-74	Tóth, I.....	TH-73
Tang, L.....	TH-84	Trabert, D.....	WE-45, TH-21, MO-44, TU-16
Tang, Y.....	TH-46, TH-47, TH-64	Tran, T.....	TH-113
Tang, Z.....	FR-14	Trassinelli, M.....	FR-114, MO-97, TU-41, TU-116, TU-17
Taniguchi, T.....	TU-13	Traykov, E.....	FR-4
Tanis, J.....	WE-134, MO-131, MO-132	Treusch, R.....	FR-63
Tanuma, H.....	WE-138, WE-143, TH-133, MO-134, MO-136	Tribedi, L.....	TH-119, TH-126, TH-137, TH-143, MO-129
Tarnovsky, A.....	WE-114	Trinter, F.....	WE-44, WE-20, TH-21, MO-17, MO-44, TU-04, TU-05, TU-08, TU-09, TU-15, TU-16
Tashenov, S.....	MO-85	Trojanowskaja, D.....	TU-25, TU-16
Tavernelli, I.....	WE-35	Tross, J.....	WE-44
Tayal, S.....	WE-59	Trotsenko, S.....	MO-97, MO-104
Telnov, D.....	MO-23	Tsuchida, H.....	FR-12, MO-143, TU-110
Tennyson, J.....	FR-115, TU-80	Tsuda, T.....	FR-74
Terekhin, P.....	MO-125, MO-126	Tsuru, S.....	FR-49
Teschmit, N.....	TU-35	Tu, B.....	WE-66, FR-66
Tey, M.....	TH-81	Tupitsyn, I.....	FR-104, FR-110
Thakar, Y.....	TH-54		
Thomas, J.....	WE-65, FR-4		
Thomas, R.....	TH-111, FR-15, MO-121		
Thompson, J.....	FR-15		
Thorman, R.....	FR-138, FR-142		
Threlfall, R.....	WE-96		
Thumm, U.....	TH-2, TU-26, TU-27, TU-43		
Tia, M.....	TH-21, TU-16		
Tielens, A.....	TH-59		
Togashi, T.....	MO-28, TU-37		
Tojo, S.....	TH-92, TH-93		
Toker, Y.....	TH-22		
Tókési, K.....	WE-108, TH-15, TH-141, FR-83,		

U

Uchikura, Y.....

WE-138, WE-143

Uddin, M.....

WE-103, WE-58

Ueda, K.....

WE-46, WE-24, TH-21, TH-28,
FR-28, FR-47, MO-10, MO-21, TU-37, TU-41

Ueltzhöffer, T.....

TU-33

U

Uchikura, Y.....	WE-138, WE-143
Uddin, M.....	WE-103, WE-58
Ueda, K.....	WE-46, WE-24, TH-21, TH-28, FR-28, FR-47, MO-10, MO-21, TU-37, TU-41
Ueltzhöffer, T.....	TU-33

Uggerud, E.....MO-121
 Uiterwaal, C.....FR-31
 Ullrich, J.....FR-124
 Ulrich, B.....TU-09
 Undurti, S.....TH-16, MO-49
 Unger, I.....TU-33
 Unlu, I.....FR-142, FR-144
 Urbain, X.....WE-29, TH-125, FR-118, MO-80
 Usachenko, V.....FR-48
 Uschmann, I.....MO-97
 Usenko, S.....FR-32

V

Valdés de Luxán, Á.....TU-50, TU-124
 Valdés, J.....TU-109
 Van Beveren, C.....FR-4
 Van den Bergh, P.....FR-4
 van der Burgt, P.....WE-98, WE-99
 Van Duppen,P.FR-4
 Van Gorp, S.....WE-65
 Varella, M.....TU-72
 Varga, K.....WE-39
 Vegvari, A.....TU-112
 Vela-Perez, I.....WE-45, TU-15
 Velic, D.....FR-60, FR-61, FR-62
 Verma, N.....MO-93
 Verma, P.....FR-134
 Vernhet, D.....FR-114, TU-41, TU-116, TU-17
 Versolato, O.....FR-124
 Vibók, Á.....FR-54
 Videau, L.....TU-41
 Viehhaus, J.....WE-5, WE-20, FR-5, MO-24
 Vig, S.....TU-132
 Vinitha M. V.....TU-132
 Vinodkumar, M.....TH-53, TH-71, TH-72,
 TU-54, TU-68, TU-91, TU-93
 Vinodkumar, P.....TH-71, TH-72, TU-54,

TU-68, TU-93
 Vizcaino, V.....MO-132
 Vogel, M.....TH-1, MO-6
 Vogel, S.....TU-12
 Voigtsberger, J.....WE-44, TU-04
 Voitkiv, A.....FR-101
 Volotka, A.....FR-125, TU-48
 von Hahn, R.....TU-12
 Vos, M.....WE-78, WE-32, MO-90
 Voss, S.....TU-09
 Vrakking, M.....MO-33
 Vuilleumier, R.....TH-45
 Vvedenskii, N.....MO-20, MO-36
 Vysotskii, V.....WE-114, FR-127, FR-128

W

Wachs, D.....MO-52
 Wachter, G.....TU-29, TU-30
 Wada, M.....TH-87
 Waitz, M.....WE-44, WE-45, TH-21, TU-04,
 TU-09, TU-16
 Wales, B.....FR-58
 Wallace, W.....MO-49
 Wallauer, R.....WE-44, TH-21, TU-04, TU-09
 Walter, C.....WE-15, FR-10
 Walter, P.....MO-24
 Walther, T.....TH-106
 Wan, C.....WE-105
 Wang, C.....FR-59, MO-30, MO-55
 Wang, D.....MO-112
 Wang, E.....TH-46, TH-47, TU-63
 Wang, F.....MO-37
 Wang, G.....MO-3, TU-19
 Wang, H.....TH-106, TH-108, TH-130, FR-103,
 FR-105, MO-64, MO-65
 Wang, J.....FR-129

Wang, J.....WE-15, WE-143, TH-83, FR-6,
FR-10, FR-96, MO-123

Wang, K.....WE-60, FR-20, TU-87

Wang, M.....TH-11

Wang, S.....MO-64

Wang, T.....TH-7

Wang, W.....WE-130, FR-90, TU-44

Wang, X.....WE-129, TH-9, TH-49, FR-23,
FR-26, FR-13, MO-66, MO-68, TU-130

Wang, X.....MO-49

Wang, Y.....WE-27, TH-59, FR-70,
FR-71, FR-130, FR-130

Watanabe, N.....TH-65, TH-66, TU-40

Watanabe, T.....FR-74

Weaver, C.....MO-84

Weber, G.....MO-97

Weber, T.....TU-05, TU-08

Wechselberger, N.....TH-21

Weck, P.....TU-114, TU-115

Wehlitz, R.....TH-44

Wehrhan, O.....MO-97

Wei, B.....WE-66, WE-129, WE-135, TH-49, MO-68

Wei, H.....TH-3, MO-107

Wei, L.....WE-105

Weller, M.....WE-44, WE-45, TH-21, TU-04,
TU-05, TU-16

Wen, W.....TH-106, TH-108, FR-105, MO-64,
MO-65

Wenzel, P.....TU-33

Wester, R.....TH-59, TH-109

Weyland, M.....TU-77

Whalen, J.....TH-76, TH-85

Wickramaratna, M.....WE-23

Wiegandt, F.....TH-21, TU-04

Wiesel, M.....TH-1

Wilhelm, R.....TU-95, TU-98

Williams, J.....TH-21, TU-04, TU-05, TU-08, TU-09

Winckler, N.....MO-97

Windberger, A.....FR-124

Winter, B.....TU-33

Winters, D.....TH-106, TH-108, MO-97

Winters, N.....MO-97

Wnuk, P.....FR-27

Woehl Jr., G.....TH-85

Wojtewicz, S.....WE-68

Wolf, A.....WE-64, TU-12

Wolf, M.....TH-112, TU-14, TU-112

Wolf, R.....MO-109

Wood, J.....FR-24

Worbs, L.....TU-35

Wörner, H.....MO-31

Wren-Little, K.....TU-80

Wu, B.....FR-105

Wu, C.....WE-31

Wu, J.....WE-44, WE-9

Wu, M.....MO-102

Wu, Y.....FR-129

Wu, Y.....FR-96, MO-123

Wu, Z.....FR-3

Wurth, W.....TU-107



Xi, W.....FR-90

Xia, G.....FR-81

Xia, J.....FR-105

Xiao, G.....FR-105, FR-130

Xiao, J.....WE-66, FR-66, MO-69, MO-78

Xie, L.....TH-107, FR-8, FR-13, MO-65, MO-66,
MO-72, MO-75, MO-100, TU-130

Xie, X.....WE-39, TH-7, TH-11, FR-43

Xiong, G.....MO-69

Xiong, H.....FR-52

Xiong, W.....TH-8

Xu, C.....WE-110

Xu, G.....FR-130

Xu, H.....WE-33, WE-50, WE-51, TH-16,
FR-105, MO-49

Xu, L.....TH-23, TH-25
 Xu, S.....MO-42, TU-56
 Xu, T.....MO-64
 Xu, W.....WE-80
 Xu, W.....MO-64
 Xu, X.....FR-84, MO-64
 Xu, Y.....TH-107
 Xue, J.....TH-100, TH-101, MO-46, MO-47
 Xue, Y.....WE-130, FR-90

Y

Yabana, K.....TU-30
 Yabashi, M.....MO-28, TU-37
 Yachi, K.....TU-13
 Yadav, H.....TH-71, TH-72, TU-68, TU-93
 Yagishita, A.....FR-49
 Yakaboylu, E.....MO-35
 Yamada, S.....TH-65
 Yamahira, S.....TH-39
 Yamanouchi, K.....WE-39, WE-84
 Yamashita, T.....MO-67
 Yamazaki, M.....TH-66, TU-88
 Yan, P.....TH-84
 Yan, S.....TH-130, TU-56
 Yan, Z.....TH-84, MO-102
 Yanagase, H.....TH-133
 Yang, A.....WE-113
 Yang, B.....WE-130, FR-90
 Yang, J.....TH-106, TH-108, TH-108, FR-105,
 FR-105, MO-63, MO-64, MO-69
 Yang, L.....WE-51, FR-90
 Yang, Y.....WE-66, FR-66, FR-44, MO-64,
 MO-78
 Yang, Z.....WE-105
 Yao, K.....WE-66, WE-129, MO-64, MO-69
 Yasuike, T.....TH-19
 Yavuz, I.....FR-45

Yin, H.....FR-35
 Yip, F.....WE-17
 Yokokawa, K.....MO-141
 Yokota, K.....WE-118, WE-119
 Yoshida, M.....MO-136
 Yoshida, S.....WE-1, TH-76, TH-11, TH-85,
 MO-143
 You, D.....WE-45, TU-37
 You, L.....TH-81
 Yu, D.....WE-130, FR-90, TU-44
 Yu, J.....FR-59, MO-55
 Yu, S.....TH-7, MO-54
 Yu, Y.....FR-14
 Yu, Z.....TH-75
 Yuan, J.....WE-9, FR-26, MO-14, TU-20
 Yuan, Y.....TH-106, TH-108, FR-105, MO-64
 Yue, X.....TH-114, TH-138
 Yukich, J.....FR-10

Z

Zadvornaya, A.....FR-4
 Zammit, M.....WE-95, WE-96, TH-63
 Zanuttini, D.....MO-117
 Zatsarinny, O.....WE-59, WE-60, WE-61, WE-2, WE-3
 Zawadzki, M.....TU-82, TU-84, TU-85
 Zaytsev, A.....TU-90
 Zaytsev, S.....TU-90
 Zeller, S.....TH-21, TH-36, TU-21, TU-09
 Zeng, D.....FR-17
 Zeng, J.....MO-106, MO-61, MO-108
 Zettergren, H.....TH-111, TH-112, TH-129, TH-134, FR-
 15, FR-117, MO-142, TU-99, TU-14, TU-112, TU-120
 Zhan, W.....FR-105
 Zhanbg, Y.....MO-68
 Zhang, A.....MO-46
 Zhang, B.....FR-56, MO-69
 Zhang, C.....FR-20

Zhang, D.....	TH-106, TH-107, TH-108, FR-26, FR-13, MO-66, MO-72, MO-75, MO-100, TU-130
Zhang, H.....	WE-105
Zhang, J.....	MO-69, MO-102
Zhang, K.....	TH-96
Zhang, L.....	TH-11, TU-19
Zhang, M.....	WE-130, FR-90, FR-103
Zhang, P.....	MO-37, TU-56, TU-89
Zhang, Q.....	WE-105, WE-51
Zhang, R.....	FR-103
Zhang, S.....	FR-129
Zhang, S.....	TH-130, FR-41, FR-96, FR-103, FR-105
Zhang, X.....	WE-1, MO-112, MO-46
Zhang, Y.....	WE-129, TH-9, TH-49
Zhao, D.....	TH-106, TH-108, TH-130, TU-56
Zhao, G.....	MO-107
Zhao, H.....	FR-105
Zhao, J.....	FR-26, MO-14, MO-62, TU-20
Zhao, L.....	WE-50, WE-51
Zhao, M.....	TH-64
Zhao, P.....	MO-3
Zhao, S.....	FR-23
Zhao, Y.....	FR-130
Zhao, Z.....	WE-9, FR-66, FR-26, MO-14, MO-62, TU-20
Zhou, F.....	TH-136
Zhou, X.....	WE-43, FR-23, FR-25, FR-105, FR- 130, MO-3, MO-9, TU-19
Zhou, Y.....	TH-81, FR-71
Zhu, J.....	TH-9, MO-7
Zhu, L.....	WE-80, TH-23, TH-25, TH-49, FR-1, MO-64
Zhu, X.....	TH-106, TH-108, TH-130, FR-90, FR-103, FR-105, MO-64, TU-56
Ziaee, F.....	TH-31, FR-52
Zikri, A.....	FR-79, FR-80
Zohrabi, M.....	TH-31, TU-08
Zou, Y.....	WE-66, WE-129, TH-49, FR-66, MO-68, MO-69, MO-78
Zouros, T.....	WE-126, WE-127, WE-128
Zubarev, R.....	TU-112
Zuin, L.....	TH-44
Zuo, W.....	WE-51
Zuo, Y.....	FR-25
Zymak, I.....	TH-113
Żywicka, B.....	TU-83



ICPEAC
2017

Cairns, Australia

XXX INTERNATIONAL CONFERENCE
ON PHOTONIC, ELECTRONIC
AND ATOMIC COLLISIONS



our sponsors



Looking to relax and unwind?
I know just the place

Queensland
AUSTRALIA



Mackay Cay, Tropical North Queensland



queensland.com

A truly global university

Curtin University is Western Australia's most preferred university and is widely recognised for its strong connections with industry, high-impact research and vast range of innovative courses. With campuses in Australia, Malaysia, Singapore and the United Arab Emirates, Curtin is an international university with a rapidly expanding global footprint.

Curtin continues to secure impressive rankings, including:

- Top 1% of universities worldwide ¹
- 2nd in the world and 1st in Australia for Mineral and Mining Engineering ²
- Top 100 in the world for Earth and Marine Sciences ²
- Top 150 in the world for Chemical, Civil and Structural Engineering ²
- 'Well above world standard' for Astronomical and Space Sciences, Physical Chemistry, Geochemistry, Geology, Crop and Pasture Production, and Electrical and Electronic Engineering ³

¹ QS World University Ranking 2017-18

² QS World University Rankings by Subject 2017

³ Excellence in Research for Australia (ERA) 2015

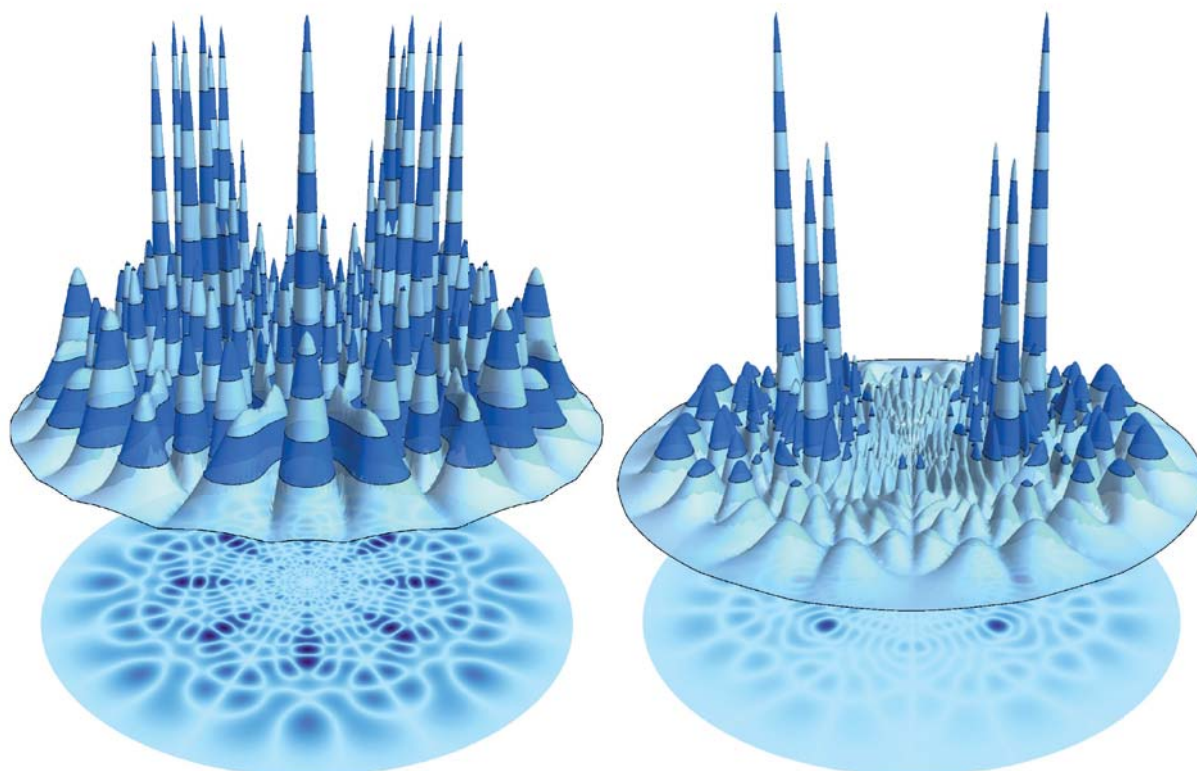
Find out more at scieng.curtin.edu.au



Make tomorrow better.



Curtin University



Journal of Physics B

Atomic, Molecular and Optical Physics

2015
IMPACT FACTOR
1.833

 iopscience.org/jphysb

Editor-in-Chief

Paul Corkum, NRC Steacie Institute for Molecular Sciences and University of Ottawa, Canada

Deputy Editor

Marc Vrakking, Max Born Institute for Nonlinear Optics and Short Pulse Spectroscopy, Germany

Publish with us to enjoy the following benefits:

- **Fast publication:** Receipt to first decision in 35 days. Articles can be published online within 24 hours of acceptance with IOP accepted manuscripts. Find out more at iopscience.org/page/acceptedmanuscripts
- **Article choices:** We publish Letters, regular research and special issue papers alongside Topical Reviews, Tutorials, and Invited papers
- **High visibility:** In 2016 JPhysB received more than 440k article downloads. Furthermore, selected research is regularly promoted on Twitter and our blog JPhys+.
- **High standards:** Rigorous peer review from IOP Publishing's global network of expert referees, with high-quality online production of published work.



Journal of Physics series
celebrates its 50th anniversary

Image: Symmetry-adapted orbitals for trilobite adiabatic potential energy curves (APECs) Ultracold molecular Rydberg physics in a high-density environment
Matthew TEILES et al. 2016 *J. Phys. B: At. Mol. Opt. Phys.* **49** 114005

IOP Publishing



**At Griffith University,
we are changing how
people view the world.**

We are a leading institution in quantum physics research with world class research in quantum information, quantum computing, attosecond science and ultra-fast Laser applications.

Our research is expanding the limits of what is possible.

griffith.edu.au/quantum



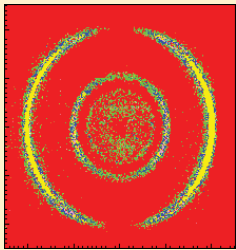
YOU MAKE US
#1 IN
AUSTRALIA

AND IN
THE WORLD
TOP 20



Australian
National
University

ANU.edu.au



RoentDek

Supersonic Gas Jets Handels GmbH
Detection Techniques
Data Acquisition Systems
Multifragment Imaging Systems

3D MOMENTUM IMAGING



Complete systems and custom made solutions:

The COLTRIMS reaction microscope for quantum mechanical systems is well known and successfully adopted in atomic physics and already applied in solid state physics and surface science

MCP-Detector Systems
Coincidence modules
Fast Data Acquisition
Gas Targets
Custom-Made Systems
Multi-Hit Particle Detection
Hardware & Software Solutions

www.roentdek.com

info@roentdek.com

TIME	TUESDAY, 25TH		WEDNESDAY, 26TH		THURSDAY, 27TH	
08:45-09:00			Hall A			
			ICPEAC Opening		Hall A	
09:00-10:00			Reinhard Kienberger		Henrik Cederquist	
10:00-10:30			Hall B Morning tea		Hall B Morning tea	
			Hall A	Room 1-2	Hall A	Room 1-2
			ANTI-MATTER	ATOMIC COLLISION	PHOTON STRONG FIELD	RINGS/TRAPS
10:30-11:00			Cassidy	Abdurakhmanov	Doblhoff-Dier	Pedersen
11:00-11:30			Fabrikant	Mukaiyama	Sato	Novotny
11:30-12:00			Nagashima	Kozhedub	Charalambidis	Litvinov
12:00-12:30			Green/Eriksson	Génévriez/Shah	Wu	Tu
12:30-13:00						General Meeting
13:00-14:00	Room 1-2		Lunch		Lunch	
	Student Tutorials		PHOTONS ULTRAFAST	ULTRACOLD	LEPTONS PLASMA	ION/MOLECULE
14:00-14:30	B. Schneider		Koch	Schmidt	Ralchenko	Domaracka
14:30-15:00			Staudte	Will	Preval	Wang Y
15:00-15:30	Pfeifer		Smirnova	Meyer	Hu	Rabadan
15:30-16:00			Litvinyuk	Whalen/Plasil	Huang/Nakamura	La Mantia/Eklund
16:00-16:30	Break		Hall B and Foyer Poster Session 1		Hall B and Foyer Poster Session 2	
16:30-17:00	Greene					
17:00-17:30						
17:30-18:00	Outdoor Plaza	TBA				
18:00-18:30	Welcome Reception	ExCom Meeting till late				
18:30-19:00						
19:00-19:30						
19:30-20:00				Hall A Public Lecture		

TIME	FRIDAY, 28TH		SATURDAY - SUNDAY, 29TH-30TH	MONDAY, 31ST		TUESDAY, 1ST	
08:45-09:00	<i>Hall A</i>			<i>Hall A</i>		<i>Hall A</i>	
09:00-10:00							
10:00-10:30							
				<i>Hall B and Foyer</i> Poster Session 3		<i>Hall B and Foyer</i> Poster Session 5	
10:30-11:00							
11:00-11:30	Linda Young						
11:30-12:00							
12:00-12:30				IUPAP Prize		Sheldon Datz & Business Meeting	
12:30-13:00							
13:00-14:00	Lunch		Lunch		Lunch		
	ORIENTATION	HEAVY/COLD					PHOTONS CONTROL
14:00-14:30	Murray	Truscott	van der Hart	Dorn	Schlathölter	Bolognesi	
14:30-15:00	Nahon	Deiglmayr	Dahlstrom	I. Schneider	Chen-yu	Travnikova	
15:00-15:30	Clayburn/Yoshida	Kjaergaard	Kling	Kossoski	Krems/Endo	Gryzlova	
15:30-16:00	Hall B Afternoon tea		Lackner/Zhang	Garcia	Hall B Afternoon tea		
	PHOTONS ULTRAFAST	LEPTONS/IMAGING	<i>Hall B and Foyer</i> Poster Session 4		PHOTONS SF/ATTO	LEPTONS/IMAGING	
16:00-16:30	Wörner	Centurion			Chang	Jones	
16:30-17:00	Gonzalez-Vazquez	Yamazaki			Biegert	Kumar	
17:00-17:30	Kim	Boyle			Ciappina	Smialek	
17:30-18:00	Patchkovskii	Nandi/Weller	Hall C-D Conference Dinner		Blättermann/Bray	Zawadzki/Laws	
18:00-18:30							
18:30-19:00							
19:00-19:30							
19:30-22:00							